Kaoru Nakata · Hiroya Sugisaki *Editors*

Impacts of the Fukushima Nuclear Accident on Fish and Fishing Grounds

Springer Open

Impacts of the Fukushima Nuclear Accident on Fish and Fishing Grounds

Kaoru Nakata • Hiroya Sugisaki
Editors

Impacts of the Fukushima Nuclear Accident on Fish and Fishing Grounds

Editors
Kaoru Nakata
Research Management Department
Fisheries Research Agency
Yokohama, Kanagawa, Japan

Hiroya Sugisaki
National Research Institute of Fisheries Sciences
Fisheries Research Agency
Yokohama, Kanagawa, Japan

ISBN 978-4-431-55536-0 ISBN 978-4-431-55537-7 (eBook)
DOI 10.1007/978-4-431-55537-7

Library of Congress Control Number: 2015939907

Springer Tokyo Heidelberg New York Dordrecht London

Printed on acid-free paper

Springer Japan KK is part of Springer Science+Business Media (www.springer.com)

Foreword

On March 11, 2011, the most disastrous earthquake and tsunami in modern Japanese history occurred in northeast Japan. They caused a great calamity for the people and industries on the Pacific coast of the Tohoku region of Japan, one of the most important regions for Japanese fisheries. The Fukushima Dai-ichi Nuclear Power Plant (FNPP) was covered by a 15-m-high tsunami, and the electric power supply to its four nuclear reactors was severed, resulting in hydrogen explosions and the meltdown of the core. This accident caused the elevation of the level of anthropogenic radioactivity in the marine environment in the western North Pacific from atmospheric fallout and direct discharges of highly radioactive waters. Security of food safety of marine products is a great concern for the people in the world and especially for the people involved in the fisheries industry.

The Fisheries Research Agency (FRA) has been conducting research and monitoring the radioactivity of fish and shellfish since the 1950s, when we were worried about the effect of nuclear arms tests in the ocean to marine environments and products. Because the FRA has enough experience and knowledge of research on the radioactivity of large quantities of specimens, we accepted the requests from the national government to analyze the radioactivity of marine products fished all over Japan and started to make a plan to monitor radioactivity of various marine products fished around Japan in cooperation with local governmental institutes just after the accident.

This book describes the results of the research on the effect of radioactivity to ocean and coastal ecosystems and various marine and freshwater fish caused by the FNPP accident of the huge magnitude of radioactivity on the ecosystems around Japan. This is the first report on the effect on the hydrosphere ecosystem from the point of view of marine ecology and fisheries oceanography. A scientifically precise description of the distribution and variation of radioactive elements in the ecosystem is presented in detail in this publication. Of course, this is the first step in revealing

the anthropological effect of radioactivity on the ecosystem, and we should continue the research. I trust that this book will contribute to overcoming the tragedy and enhance the culture of human beings in the world.

President of the Fisheries Research Agency Masanori Miyahara
Yokohama, Japan

Preface

On March 11, 2011, the Great East Japan Earthquake occurred. The earthquake itself and the resulting tsunami caused the Fukushima Daiichi Nuclear Power Plant (FNPP) accident. As a result, a large volume of radionuclides was released into the environment as fallout, which contaminated both freshwater and marine systems. On April 2, heavily contaminated water was released around the No. 2 reactor into the ocean. Several further leakages of water contaminated with radionuclides, as well as a release of low-level contaminated water by the Tokyo Electric Power Company (TEPCO), occurred around FNPP up until May 2011. This was the first time that heavily contaminated water originating from a nuclear power plant accident had been directly released into the ocean over a relatively short period. Since then, contaminated fish with relatively high radiocesium concentrations (higher than ca. 100 Bq/kg-wet) have often been caught in the coastal areas of Fukushima and in adjacent prefectures.

The Fisheries Research Agency (FRA) has monitored radioactive substances in marine organisms around Japan since 1954, when the H-bomb test was carried out on Bikini Atoll. Soon after the FNPP accident, the FRA began monitoring radionuclides in fisheries resources and their habitats. Decreasing trends of radiocesium concentration in small pelagic fish and demersal fish have been obvious since summer 2011 and winter 2012, respectively, based on intensive monitoring of radioactivity in fisheries products by local governments and the FRA (http://www.jfa.maff.go.jp/j/housyanou/kekka.html).

However, incidents that have worried the general public, including fishermen, have often occurred, including catches of cod with relatively high radiocesium concentrations in areas distant from Fukushima Prefecture, a catch of extremely highly contaminated fat greenlings, and continuing contamination of fish in some freshwater systems. Various questions have therefore been raised by the public, such as: When will the radiocesium concentrations of fish and fishing grounds recover to the level before the accident? Will the radiocesium in fish continue to be accumulated in fish via the food chain, like heavy metals and some kinds of chemicals? What is

the mechanism for the occurrence of extremely highly contaminated fish? Is the contamination of fish with radiocesium an ongoing phenomenon?

In order to restore trust in fisheries products from the Tohoku district, both abroad and among the Japanese people, it is important to answer these questions based on scientific data. Accordingly, the FRA has conducted research to clarify the impacts of the FNPP accident on fish and fishing grounds, and the dynamics of radionuclides through both marine and freshwater systems by in situ investigation, rearing experiments, and the use of simulation models.

Although our research is ongoing, the main body of our investigations was conducted from 2011 to 2013.

Yokohama, Japan

Tokio Wada
Kaoru Nakata
Hiroya Sugisaki

Contents

Chapter 1
Introduction: Overview of Our Research on Impacts of the Fukushima Dai-ichi Nuclear Power Plant Accident on Fish and Fishing Grounds

Kaoru Nakata and Hiroya Sugisaki

Abstract As a result of the Fukushima Dai-Ichi Nuclear Power Plant accident in March 2011, a large volume of radionuclides was released into the environment, thus contaminating marine and freshwater systems. The Fisheries Research Agency has conducted research beginning soon after the accident. Our research addressed the contamination processes of radionuclides (mainly radiocesium) through water, sediments, and food chains, in both marine and freshwater systems, based on a large volume of original in situ data. Our research has also provided important information on when and how marine fish have been contaminated. This chapter gives an overview of our research.

Keywords Fukushima • Radionuclides • Radiocesium • Marine and freshwater systems • Contamination process

1.1 Objectives of Our Research

As a result of the Great East Japan Earthquake on March 11, 2011, and the resulting tsunami, all power supplies to the No. 1 through No. 4 nuclear reactors at Tokyo Electric Power's Fukushima I Nuclear Power Plant (FNPP) were lost because of submergence and electrical discharge. As a result, core meltdowns occurred in the No. 1 to No. 3 reactors and hydrogen explosions sequentially occurred in No. 1, No. 3, and No. 4 nuclear reactors. By March 15, a large amount of radioactive materials had been released into the environment as fallout, which contaminated both marine

K. Nakata (✉)
Fisheries Research Agency, Queen's Tower B 15F, 2-3-3 Minato Mirai, Nishi-ku, Yokohama, Kanagawa 220-6115, Japan
e-mail: may31@affrc.go.jp

H. Sugisaki
National Research Institute of Fisheries Sciences, Fisheries Research Agency, 2-12-4, Fukuura, Yokohama, Kanagawa 236-8648, Japan

K. Nakata, H. Sugisaki (eds.), *Impacts of the Fukushima Nuclear Accident on Fish and Fishing Grounds*, DOI 10.1007/978-4-431-55537-7_1

and freshwater systems. On April 2, heavily contaminated water was found at an intake of the No. 2 reactor. In addition, several leakages of contaminated water around FNPP, as well as a release of low-level contaminated water by Tokyo Electric Power Company (TEPCO), had occurred by May 2011.

The Fisheries Research Agency (FRA) has conducted research to clarify the impacts of the FNPP accident on fish and fishing grounds since soon after the accident. Our research has mainly involved monitoring radionuclides in fish and their habitats and conducting studies to clarify the dynamics of radionuclides in both marine and freshwater systems. This book aims to introduce the results of our research, the bulk of which was conducted from 2011 to 2013. An overview of our results is given next.

1.2 Seawater and Plankton (Part I)

FNPP-derived radiocesium has accumulated in marine food webs via seawater intake and predator–prey interactions. Information on the spatiotemporal distribution of radiocesium concentration in seawater and plankters is therefore important for comprehending the accumulation and dynamics of radiocesium in pelagic ecosystems. Although a large amount of contaminated water was released into the ocean, by 2012 the ^{137}Cs concentrations in the surface seawater around Japan (Fig. 1.1), except for the waters off the Pacific coast of Tohoku district (Fig. 1.1), had dropped to levels seen before the accident (Table 1.1). The concentrations off the Pacific coast of Tohoku district in 2012 were still about ten times higher than those before the accident, but they had decreased to the level seen before the accident by late 2013 (FRA 2014).

Chapter 2 summarizes the dispersion process of FNPP-derived radioactive cesium (Cs) in seawater, based on observatory data and numerical simulation. A considerable amount of radioactive Cs from FNPP dispersed from the western North Pacific eastward to the central North Pacific during the first year after the accident. It then dispersed not only eastward but also northward and southward in the central North Pacific in the subsequent second and third years. Research by the FRA also shows transportation of the contaminated water into the subtropical zone beneath the Kuroshio Extension.

Chapter 3 shows the temporal variability of ^{137}Cs concentrations in zooplankters off the Joban coast and Sendai Bay, on the Pacific coast of the middle to southern Tohoku district. ^{137}Cs concentrations in both seawater and zooplankton have decreased during our research period since June 2011. However, the rate decrease in seawater was faster than in zooplankton, which resulted in a high apparent concentration ratio (aCR) for zooplankton (Chap. 3). We also show that the aCR value measured in zooplankton accurately describes the progress of ^{137}Cs contamination in zooplankton, from the beginning of the FNPP accident (dynamic nonequilibrium state) to the restoration phase (dynamic equilibrium state).

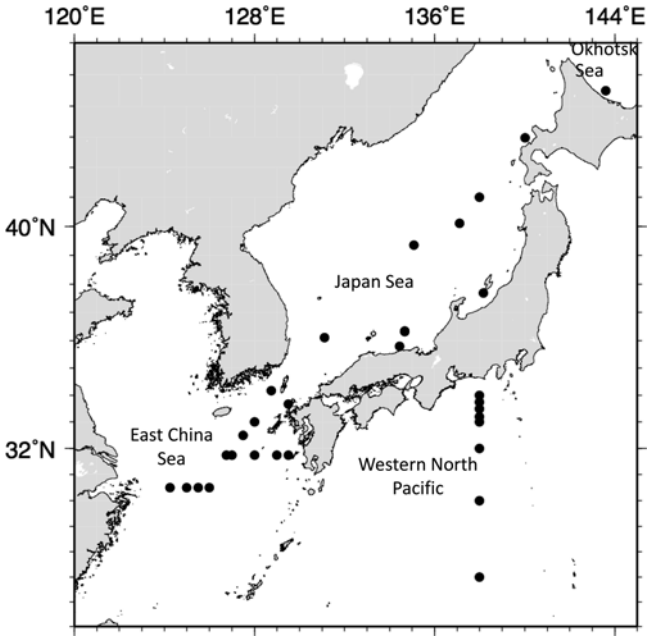

Fig. 1.1 Sampling points of surface water for analyzing the radiocesium concentrations around Japan

Table 1.1 Comparisons of ^{137}Cs concentration in surface waters around Japan between 2012 and periods before the accident at Fukushima Dai-ichi Nuclear Power Plant in March 2011

Sea area	Month surveyed (2012)	^{137}Cs concentration (mBq/kg)	
		2012	2001–2010
Sea of Okhotsk	Jun	1.9 ± 0.37	2.2–ND
Sea of Japan	Jun–Nov	2.4–2.0	2.9–ND
East China Sea	Jun–Oct	2.0–1.4	2.4–1.4
(Kuroshio)	Jan–Aug	2.7–1.2	3.8–ND

Source: http://www.fra.affrc.go.jp/eq/Nuclear_accident_effects/H24seika.pdf (in Japanese)

- Chapter 2. ^{134}Cs and ^{137}Cs in the Seawater Around Japan and in the North Pacific (H. Kaeriyama)
- Chapter 3. Temporal Changes in ^{137}Cs Concentration in Zooplankton and Seawater off the Joban–Sanriku Coast, and in Sendai Bay, After the Fukushima Dai-ichi Nuclear Accident (H. Kaeriyama)

1.3 Sediments and Benthos (Part II)

Intensive monitoring of radiocesium in marine organisms by the Fukushima Prefectural Fisheries Experimental Station showed that the radiocesium concentration in demersal fish was higher, and showed slower decline, compared with pelagic fish (Wada et al. 2013). This phenomenon might have been largely influenced by the distribution and dynamics of radiocesium in sediment. The FRA has investigated the spatial and temporal distribution of radiocesium concentrations in marine sediment, its translation from contaminated sediment to benthos, and the probable food of demersal fish. The results are summarized in Part II.

Chapter 4 shows the spatial distribution of the radiocesium concentration in the top 14 cm of sea sediment off the coast of northern Ibaraki to Fukushima, with 5-min horizontal resolution. There was a high concentration band along 100-m isobaths, where the concentration of ^{137}Cs reached a maximum of 1,240 Bq/kg-dry. When assessing radiocesium transportation from sea sediments to a marine demersal ecosystem, information is required not only on the concentration but also on the biological ingestibility of sea sediment radiocesium. To assess radiocesium transportation from sea sediments to a benthic ecosystem, radiocesium concentration in the organic fraction of sea sediments (Cs_{org}) was analyzed (Chap. 5), and showed horizontal distribution of Cs_{org} off the coast of northern Ibaraki to Fukushima and Sendai Bay. Cs_{org} of sea sediments was significantly higher than that of bulk sediments (Cs_{bulk}). We suggest that Cs_{org} can be used as an indicator of the potential effects of sediment radiocesium on the demersal ecosystem.

The FRA also monitored the behavior of particulate matter, which is closely related to that of sediment radiocesium, at a depth of 32 m off Iwaki, Fukushima, by automated observatory systems (Chap. 6). The behavior was largely influenced by waves, and particulate matter was resuspended and transported with water movement during high waves. We show that the combination of waves and currents resulting from meteorological disturbance is one of the important processes in the transport of suspended particle material off the Fukushima coast.

On the basis of the results from field investigations and rearing experiments using a benthic polychaete (*Perinereis aibuhitensis*) with highly contaminated sediment collected at the station 1 km off FNPP, the FRA estimated the transport of radiocesium from contaminated sediment to benthic organisms off the coast of Fukushima (Chap. 7). These results suggest that the intake of radiocesium through the benthic food web is limited for benthic organisms, even if the sediments are highly contaminated.

- Chapter 4. Three-Dimensional Distribution of Radiocesium in Sea Sediment derived from the Fukushima Dai-ichi Nuclear Power Plant (D. Ambe et al.)
- Chapter 5. Radiocesium Concentrations in the Organic Fraction of Sea Sediments (T. Ono et al.)
- Chapter 6. Bottom Turbidity, Boundary Layer Dynamics, and Associated Transport of Suspended Particulate Materials off the Fukushima Coast (H. Yagi et al.)

- Chapter 7. Investigation of Radiocesium Translation from Contaminated Sediment to Benthic Organisms (Y. Shigenobu et al.)

1.4 Marine Fish (Part III)

Off the Fukushima coast, the percentage of fish with a radiocesium concentration higher than 100 Bq/kg-wet (the standard value of radiocesium in foods) accounted for more than 90 % of the fish caught off Fukushima in April 2011. The percentage had declined to 0.6 % by October 2014, according to the Fukushima Prefectural Fisheries Experimental Station (2014). The concentration trend was different between pelagic and demersal fish. Part III describes the characteristics of the temporal variations of the concentration and their background mechanisms for small epipelagic fish (sardine and anchovy) and demersal fish (cod and flatfish).

In addition to the intrusion of the contaminated waters from FNPP, some radionuclides were delivered to marine fish and their habitat through the atmospheric pathway. Chapter 8 describes evidence of impacts via the atmospheric pathway on small epipelagic fish off the coast of southern Ibaraki and Chiba Prefectures, before the direct release of contaminated water into the ocean. After the release, fluctuations in the radiocesium concentration in fish muscles were synchronized with the decreasing concentration in the seawater near the fishing ground; the radiocesium concentration in fish muscles reached a maximum of 31 Bq/kg-wet in July 2011, after which it declined gradually (Chap. 9).

Decline of the radiocesium concentration in demersal fish seemed to be slower compared with pelagic fish, but this varied individually and across species. It is still unclear which species or individuals of demersal fish showed high radiocesium concentrations. Chapter 10 shows differences in radiocesium concentration in the Pacific cod (*Gadus microcephalus*) across year-classes and also suggests that the difference could be explained by ontogenetic changes in diet and seasonal changes in vertical distribution.

Chapter 11 describes three features of the contamination histories of the Japanese flounder (*Paralichthys olivaceus*) after the accident by analyzing the observed spatiotemporal changes in Cs concentration, a comparison of the dynamics of Cs concentration across year-classes, and simulation studies: (1) high Cs values with high variation in the first year after the accident, (2) low Cs values with their minimum values peaking around autumn 2011, and (3) lower Cs values observed for 2011 year-class and younger than 2010 year-class and older. A hypothesis on the background mechanisms is also discussed.

- Chapter 8. Detection of ^{131}I, ^{134}Cs, and ^{137}Cs Released into the Atmosphere from FNPP in Small Epipelagic Fishes, Japanese Sardine, and Japanese Anchovy, off the Kanto Area, Japan (T. Morita et al.)
- Chapter 9. Radiocesium Concentration of Small Epipelagic Fishes (Sardine and Japanese Anchovy) off the Kashima-Boso Area (K. Takagi et al.)

- Chapter 10. Why Do the Radionuclide Concentrations of Pacific Cod Depend on Body Size? (Y. Narimatsu et al.)
- Chapter 11. Radiocesium Contamination Histories of Japanese Flounder (*Paralichthys olivaceus*) after the 2011 Fukushima Nuclear Power Plant Accident (Y. Kurita et al.)

1.5 Mechanisms of Severe Contamination in Fish (Part IV)

Decreasing trends of radiocesium have generally been found for pelagic fish since summer 2011 and for demersal fish since winter 2012 (http://www.fra.affrc.go.jp/eq/Nuclear_accident_effects/H24seika.pdf). However, extremely contaminated fat greenlings (*Hexagrammos otakii*), with 25,800 Bq/kg-wet of radiocesium, which is the highest value except for fish collected in the FNPP port (Chap. 14), were caught off Ota River within a 20-km radius of FNPP. The FRA investigated the causes and mechanisms for the occurrence of the extremely contaminated fat greenlings.

Based on the radiocesium concentrations in 236 greenlings that had been collected off the coast of Fukushima after the accident, the probability of the occurrence of extremely contaminated fat greenlings was calculated assuming a normal distribution (Chap. 12). The probability was exceedingly low, at less than 2.794×10^{-6}, yet the concentration found was almost equivalent to that frequently observed for the greenlings caught in the FNPP port.

The contamination process for the extremely contaminated fat greenlings was also investigated by analyses of beta-ray emission from otoliths and using a biokinetic model; the results are shown in Chap. 13. Analyses of the beta-ray emission from the otoliths showed that the fat greenlings were in the highly contaminated environment in the period just after the FNPP accident. Simulation of the ^{137}Cs concentration in fat greenlings using the biokinetic model showed that the fat greenlings had their origin in the FNPP port just after the accident.

Contamination levels of fish caught in the FNPP port are summarized in Chap. 14, and radiocesium concentrations in fat greenlings, Japanese rockfish, and spotbelly rockfish are shown to be higher than in other species. Relationships among beta rays emitted from otoliths, ^{90}Sr, and radiocesium in the whole body without internal organs were confirmed for Japanese rockfish.

- Chapter 12. Evaluating the Probability of Catching Fat Greenlings (*Hexagrammos otakii*) Highly Contaminated with Radiocesium off the Coast of Fukushima (Y. Shigenobu et al.)
- Chapter 13. Analysis of the Contamination Process of the Extremely Contaminated Fat Greenling by Fukushima-Derived Radioactive Material (T. Watanabe et al.)
- Chapter 14. Contamination Levels of Radioactive Cesium in Fat Greenling Caught at the Main Port of the Fukushima Dai-ichi Nuclear Power Plant (K. Fujimoto et al.)

1.6 Freshwater Systems (Part V)

Contamination of freshwater systems by the FNPP accident was primarily caused by fallout from the FNPP. Part V describes factors affecting variation among freshwater systems, fish species, and individuals.

Contamination levels were compared across Lake Hayama, Lake Akimoto, and Lake Tagokura in Fukushima Prefecture (Chap. 15). Radiocesium concentrations of the lake water, bottom sediment, plankton, and fish were significantly correlated with the surface soil radiocesium content near the lake sites. In Lake Hayama, with the highest contamination level of the three lakes, factors affecting the radiocesium concentration level in several fish species were considered (Chap. 16). Body size and feeding habit seemed to influence the variation among fish species in Lake Hayama.

The radiocesium concentration level in ayu (*Plecoglossus altivelis*) was analyzed in five rivers in Fukushima Prefecture between summer 2011 and autumn 2013 (Chap. 17). The concentrations of radiocesium in ayu were shown to have decreased during the study period. Our research also shows a positive correlation between the concentrations of radiocesium in the internal organs and the muscle of ayu ($r = 0.746$, $p = 0.006$). However, the median concentration in the muscle was 14.5 % that of the median concentration in the internal organs, which shows that a small proportion (about 15 %) of the ingested food from the riverbed appears to be transferred to the muscle.

The contamination levels in salmonid fish were also investigated in Lake Chuzenji, central Honshu Island, Japan, in Tochigi Prefecture (160 km from the station) (Chap. 18). In Lake Chuzenji, substantial accumulations of radiocesium were confirmed in the muscle of hatchery-reared kokanee (*Oncorhynchus nerka*) and masu salmon (*Oncorhynchus masou*). Rearing experiments controlling for water and food radiocesium levels revealed that radiocesium contamination of fish is an ongoing process, and that radiocesium is accumulated in fish via the food chain (Chap. 19).

- Chapter 15. Comparison of the Radioactive Cesium Contamination Level of Fish and their Habitat Among Three Lakes in Fukushima Prefecture, Japan, After the Fukushima Fallout (K. Matsuda et al.)
- Chapter 16. Radiocesium Concentrations and Body Size of Freshwater Fish in Lake Hayama 1 Year After the Fukushima Dai-ichi Nuclear Power Plant Accident (K. Takagi et al.)
- Chapter 17. Spatiotemporal Monitoring of ^{134}Cs and ^{137}Cs in Ayu, *Plecoglossus altivelis*, a Microalgae-Grazing Fish, and in Their Freshwater Habitats in Fukushima (J. Tsuboi et al.)
- Chapter 18. Radiocesium Concentrations in the Muscle and Eggs of Salmonids from Lake Chuzenji, Japan, After the Fukushima Fallout (S. Yamamoto et al.)
- Chapter 19. Assessment of Radiocesium Accumulation by Hatchery-Reared Salmonids After the Fukushima Nuclear Accident (S. Yamamoto et al.)

References

Fukushima Prefectural Fisheries Experimental Station (2014) http://www.pref.fukushima.lg.jp/uploaded/attachment/930000.pdf. Accessed 27 Dec 2014. [in Japanese]

FRA (2014) http://www.fra.affrc.go.jp/eq/Nuclear_accident_effects/H25seika.pdf. Accessed 20 Nov 2014. [in Japanese]

Wada T, Nemoto Y, Shimamura S, Fujita T, Mizuno T, Sohtome T, Kamiyama K, Morita T, Igarashi S (2013) Effects of the nuclear disaster on marine products in Fukushima. J Environ Radioact 124:246–254

Part I
Seawater and Plankton

Chapter 2
^{134}Cs and ^{137}Cs in the Seawater Around Japan and in the North Pacific

Hideki Kaeriyama

Abstract Enormous quantities of radionuclides were released into the ocean via both atmospheric deposition and direct release as a result of the Fukushima Dai-ichi Nuclear Power Plant (FNPP) accident. The evaluation of FNPP-derived radioactive cesium (Cs) in the marine environment is important in addressing risks to both marine ecosystems and public health through consumption of fisheries products. Understanding the distribution patterns of radioactive Cs in the ocean throughout the water column is key in assessing its effects on marine ecosystems. This chapter summarizes the dispersion pattern of FNPP-derived radioactive Cs in the North Pacific and around Japan, based on our observational studies as follows: (1) eastward dispersion in surface seawater; (2) southwestward intrusion with mode water; and (3) background level ^{137}Cs without any detectable ^{134}Cs in the Japan Sea, East China Sea, Seto Inland Sea, and Bering Sea, along with highly radioactive Cs off the coast of East Japan.

Keywords Fukushima Dai-ichi Nuclear Power Plant accident • ^{134}Cs • ^{137}Cs • North Pacific • Kuroshio • Mode water

2.1 Fukushima Dai-ichi Nuclear Power Plant Accident

After the 9.0-magnitude Tohoku earthquake and the subsequent tsunami on March 11, 2011, loss of electric power at the Fukushima Dai-ichi Nuclear Power Plant (hereafter FNPP) resulted in overheated reactors and hydrogen explosions. Radioactive materials were then released into the ocean through atmospheric fallout as well as by direct release and leaking of the heavily contaminated coolant water (Chino et al. 2011; Buesseler et al. 2011). Because of its relatively long half-life (2.07 years for ^{134}Cs and 30.07 years for ^{137}Cs), evaluation of this radioactive Cs in the marine environment is important for addressing risks to both marine ecosystems

H. Kaeriyama (✉)
National Research Institute of Fisheries Sciences, Fisheries Research Agency,
2-12-4, Fukuura, Kanazawa, Yokohama, Kanagawa 236-8648, Japan
e-mail: kaeriyama@affrc.go.jp

K. Nakata, H. Sugisaki (eds.), *Impacts of the Fukushima Nuclear Accident on Fish and Fishing Grounds*, DOI 10.1007/978-4-431-55537-7_2

and public health through consumption of fisheries products. The Japanese government conducted intensive monitoring of ^{131}I, ^{134}Cs, and ^{137}Cs in the seawater offshore near the FNPP (Nuclear Regulation Authority 2014) and in fisheries products from a wide area around Japan (Fisheries Agency 2014). Although information on radioactive contamination covering a broad area of the North Pacific is still quite limited (Aoyama et al. 2013a, b), some model experiments have addressed the dispersion of FNPP-derived radioactive Cs (Kawamura et al. 2011; Bailly du Bois et al. 2012; Dietze and Kriest 2012; Tsumune et al. 2012; Miyazawa et al. 2012), and estimated amounts of ^{137}Cs discharged directly into the ocean ranged from 2.3 to 14.8 PBq, with considerable uncertainties (Masumoto et al. 2012). Although most studies have discussed the surface dispersion patterns of FNPP-derived radioactive Cs, understanding the ocean distribution patterns of radioactive Cs throughout the water column is key to assessing its effects on marine ecosystems.

2.2 Oceanic Background and ^{137}Cs in the North Pacific Before the FNPP Accident

The Kuroshio Current (KC) and its extension, Kuroshio Extension (KE), are the strongest eastward currents off the south and east coasts of Japan (Mizuno and White 1983). The KC and KE are important in the reproduction, dispersal, and migration of pelagic fish species (Sugisaki et al. 2010). Because the FNPP was located at 37°25.28′N, 141°02.02′E (north of KE), most of the radioactive Cs released directly to the ocean was believed to be dispersed eastward in the North Pacific by the KE because the KE is thought to act as a transport barrier against southward dispersion (Buesseler et al. 2011, 2012; Aoyama et al. 2013a, b; Kaeriyama et al. 2013). In the northern area off the coast near the FNPP, the subarctic Oyashio water flows southwardly, and the water masses off the coast of East Japan, including off the FNPP, revealed complex features with meso-scale eddies as a result of the mixing of the subarctic Oyashio water and subtropical Kuroshio water (Yasuda 2003). The largest ^{137}Cs deposition in the Pacific Ocean before the FNPP accident occurred in the early 1960s as a part of global fallout from atmospheric nuclear weapons testing (Povinec et al. 2004; Hirose and Aoyama 2003). In the North Pacific, the concentration of ^{137}Cs in surface water ranged from 1.5 to 2.0 Bq m^{-3}, decay-corrected in 2011, and displayed a horizontally homogeneous distribution (Hirose and Aoyama 2003). Southward transport of ^{137}Cs from the subarctic region (north of KE) to subtropical and tropical regions (south of KE) was observed at 20°N–165°E in 2002 (Aoyama et al. 2008). There were two ^{137}Cs concentration maxima, located at the density range of North Pacific Subtropical Mode Water (NPSTMW) and Lighter Central Mode Water (Aoyama et al. 2008). The winter mixed layer south of the KE, which forms the NPSTMW core layer, develops and reaches its deepest depth from February to March, and the newly formed NPSTMW south of the KE is subducted and advected southwestward by the Kuroshio recirculation (Aoyama et al. 2008). The NPSTMW then begins to appear

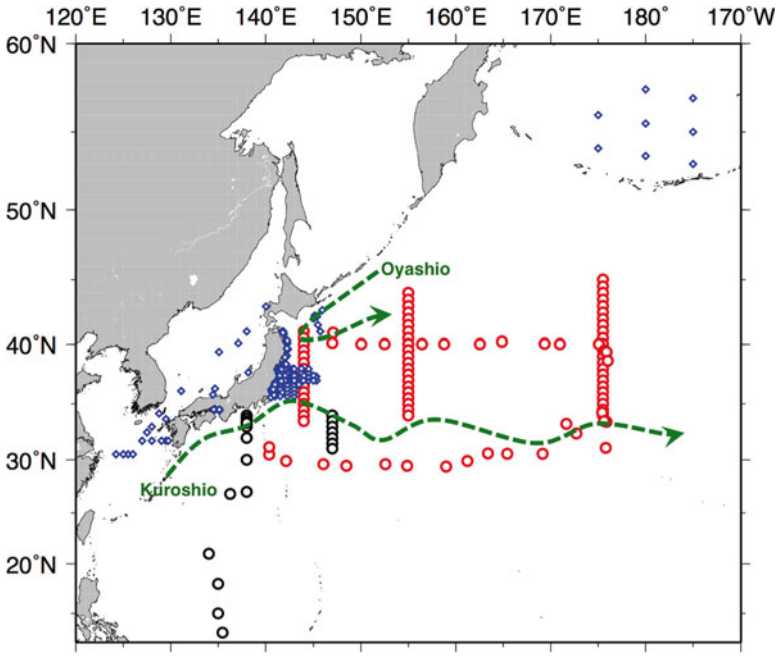

Fig. 2.1 Sampling locations of seawater for measurement of ^{134}Cs and ^{137}Cs described in Sect. 2.3 (*red open circles*), in Sect. 2.4 (*black open circles*), and in Sect. 2.5 (*blue open diamonds*). Schematic flows of Kuroshio and Oyashio are indicated as *green broken lines*

at the southernmost Japanese islands within a few months (Oka et al. 2007). The ^{137}Cs core waters observed at 20°N–165°E in 2002 were formed by the movement of mode waters between the 1960s and the 2000s (Aoyama et al. 2008).

This chapter consists of the following three descriptions concerning the distribution of ^{134}Cs and ^{137}Cs in seawater, based on our field observations after the FNPP accident (Fig. 2.1):

- Eastward dispersion of ^{134}Cs and ^{137}Cs in the western and central North Pacific (Kaeriyama et al. 2013, 2014c)
- Southwest intrusion of ^{134}Cs and ^{137}Cs with mode water (Kaeriyama et al. 2014a, c)
- ^{134}Cs and ^{137}Cs around the Japanese Islands (Kaeriyama et al. 2014b, d)

2.3 Eastward Dispersion in Surface Seawater

During the summer season, 3-year repeated observations were conducted along three north–south transects at 144°E, 155°E, and 175°30′E in 2011 and 2013. In October 2011, additional sampling was conducted around the area covering summer season observations.

In July 2011, the concentrations of ^{134}Cs and ^{137}Cs in surface seawater were highly elevated, with values exceeding 10 Bq m^{-3} and up to 140 Bq m^{-3} and 153 Bq m^{-3} at the northern end of the Kuroshio Extension (KE) along with 144°E and at all stations at 155°E (Fig. 2.2a). At 38°30′N–144°00′E, ^{134}Cs was not detected (<1.4 Bq m^{-3}), and ^{137}Cs concentration was lower than that detected at adjacent stations, despite being located at the north of the KE (Fig. 2.3). The concentrations of ^{137}Cs in the central North Pacific (175°30′E transect) ranged from 3.2 to 9.3 Bq m^{-3} and were lower than those in the western part of the studied area (144°E and 155°E transects) but still higher than background level (~2.0 Bq m^{-3}; Hirose and Aoyama 2003). In the northern section of the KE, an east–west gradient of ^{134}Cs and ^{137}Cs was observed in the surface water at the stations around 40°N in October 2011 (Fig. 2.2b). More than 10 Bq m^{-3} of ^{134}Cs and ^{137}Cs was observed between 147°E and 175°05′E, and the highest concentrations were observed at 152°31′E. On the other hand, in the southern area of the KE, concentrations of ^{137}Cs were relatively lower than those in the northern KE. A slight increase in ^{137}Cs was observed at the eastern stations (31°N–34°N, around 175°30′E). ^{134}Cs was not detected at almost any station located in the southern KE, mainly because of the short measurement time; the detection limit for ^{134}Cs was 3–4 Bq m^{-3} with 7,200 s counting. After 1 year from the observation in July 2011, ^{134}Cs and ^{137}Cs were drastically decreased at the 144°E and 155°E transects (Fig. 2.2c), and the concentrations of ^{134}Cs and ^{137}Cs at the 175°E transect between the 2 years were similar or slightly increased in July 2012 compared to July 2011. In July 2013, the concentrations of ^{137}Cs were almost the same as background level at the 144°E and 155°E transects, and ^{134}Cs was only detected at 41°30′N–155°E (1.9 Bq m^{-3}). On the other hand, ^{134}Cs was still detected at most stations (1.5–5.8 Bq m^{-3}), and the concentrations of ^{137}Cs were slightly higher than those measured before the FNPP accident at the 175°30′E transect (Fig. 2.2d).

During the 3-year observations, FNPP-derived Cs was high in the northern KE and low in the southern KE. The low concentration of radioactive Cs in the southern KE was also confirmed by field observations of seawater (Buesseler et al. 2011, 2012; Aoyama et al. 2012) and simulation models (Masumoto et al. 2012). Thus, the majority of radioactive Cs directly released to the ocean from the FNPP was not dispersed south of the KE near the east coast of Japan in 2011; rather, the detection of ^{134}Cs at three stations along with the 175°30′E transect and station located south of the KE (35°N–144°E) in July 2011 and stations around 30°N in October 2011 may indicate the effect of atmospheric deposition. Atmospheric deposition occurred mostly in March 2011 (Chino et al. 2011), and most of the direct discharge occurred during late March and early April 2011 (Tsumune et al. 2012). Aoyama et al. (2013b) reported a high radioactive Cs concentration area around the International Date Line in April–July 2011. The eastward speed of the radioactive plume was estimated to be 8 cm s^{-1}. Moreover, atmospheric deposition of radioactive Cs and ^{131}I south of the KE near the east coast of Japan was strongly indicated by numerical simulations (Kawamura et al. 2011; Kobayashi et al. 2013). Thus, the highly radioactive Cs area observed in the central North Pacific in July 2011 and south of the KE near the east coast of Japan may have originated from atmospheric deposition.

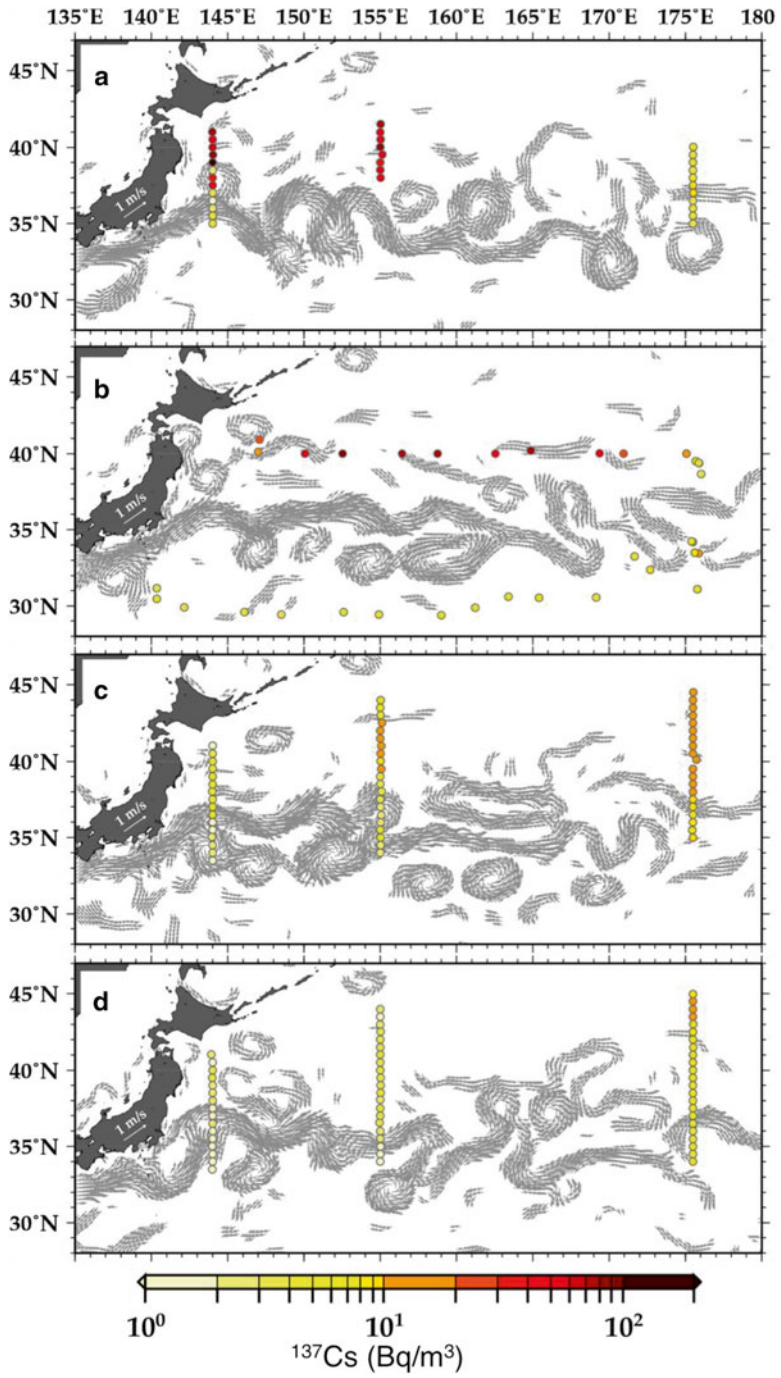

Fig. 2.2 Sampling locations for surface seawater in the western and central North Pacific. *Closed circles* indicate the sampling stations. *Color* of the *closed circles* indicates the concentration of ^{137}Cs in the surface seawater. *Gray arrows* indicate the estimated temporal mean velocity vectors for the period between June 30 and July 29, 2011 (**a**), October 14 and November 7, 2011 (**b**), July 2 and August 1, 2012 (**c**), and July 2–31, 2013 (**d**). (Modified from Kaeriyama et al. 2013)

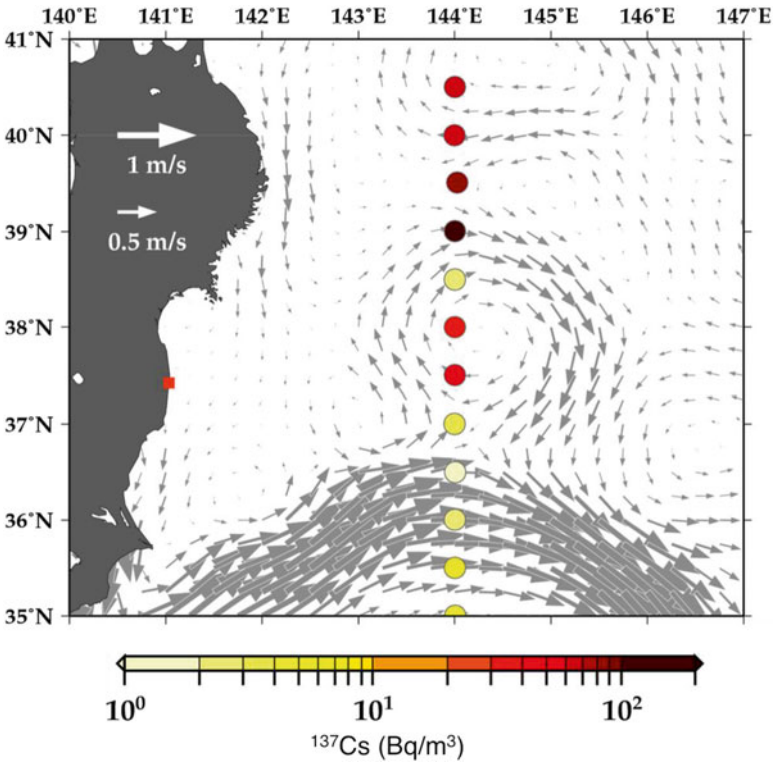

Fig. 2.3 Sampling locations for surface seawater around the anti-cyclonic eddy observed in July 2011. *Color* of the *closed circles* indicates concentration of ^{137}Cs in the surface seawater. *Gray arrows* indicate the estimated temporal mean velocity vectors for the period between June 30 and July 29, 2011 (Modified from Kaeriyama et al. 2013)

Some patchy distribution of radioactive Cs was also observed; local minima of ^{137}Cs and ^{134}Cs were observed at 38°30′N–144°E, whereas the adjacent stations had higher concentrations in July 2011 (Fig. 2.3). Judging from the sea surface velocity field, 38°30′N–144°E was located at the edge of an anti-cyclonic eddy (Fig. 2.3). Because the surface water of anti-cyclonic eddies originates from the KE (Itoh and Yasuda 2010a; Yasuda et al. 1992), the water at 38°30′N–144°E would not contain much water derived from the FNPP. As there are many meso-scale eddies that originate from both the KE and Oyashio in the western Kuroshio–Oyashio transition area (Itoh and Yasuda 2010b), the concentration of radioactive Cs should be patchy corresponding to eddies there. An area with high concentration (more than 50 Bq m^{-3}) of ^{137}Cs was distributed around 40°N between 150°E and 170°E in October 2011 (Fig. 2.2b). As Isoguchi et al. (2006) showed the existence of two quasi-stationary jets that flow northeastward from the KE to the subarctic front between 150°E and 170°E, radioactive Cs from the FNPP might have dispersed along these jets around the time of this observation period.

The concentrations of radioactive Cs at the 144°E and 155°E transects in July 2012 were much less than those in the previous year (July 2011). These differences strongly suggest that the water with a high concentration of radioactive Cs had been transported eastward by 16 months after the FNPP accident. In contrast, the concentrations of radioactive Cs at the 175°30′E transect were similar between the 2 years. The concentration of radioactive Cs observed at the 175°30′E transect in July 2012 would have been a result of dilution processes that occurred in the western North Pacific during the 16 months since the FNPP accident. Because the KE jet weakens eastward and its streamline spreads northward or southward by 175°E (see fig. 1 of Qiu and Chen 2011), the highly radioactive Cs waters would be stagnant around the central Pacific and would disperse not only eastward but also slowly northward and southward. Actually, ^{134}Cs was still detected at the 175°30′E transect, but it was not detected at the 144°E and 155°E transects, except for that at 41°30′N, 155°E in 2013.

A considerable amount of radioactive Cs from the FNPP was dispersed eastward from the western North Pacific to the central North Pacific during the first year after the FNPP accident. In addition, it dispersed not only eastward but also northward and southward in the central North Pacific for 2 to 3 years after the FNPP accident (Kaeriyama et al. 2013).

2.4 Southwest Intrusion with Mode Water

A repeat observation was conducted four to five times per year between 27°N and 34°N along 138°E during August 2011 and March 2013. As the 138°E transect lies across the Kuroshio Current (KC), the water samples were collected north of the KC, in the KC, and south of the KC. In September 2012, additional sampling was conducted at five stations located far south of Japan between 13°N and 26°50′N around 135°E. In October 2011 and November 2012, seawater samples were also collected between 30°30′N and 36°30′N along 147°E near the Kuroshio Extension (KE) (Fig. 2.1).

2.4.1 Transect Across the Kuroshio Current

For the nine observations along the 138°E transect, the concentration of ^{137}Cs at all sampling depths ranged from 1.3 to 3.7 Bq m^{-3} at 34°N (north of the KC), and from 1.2 to 2.6 Bq m^{-3} in the KC. No ^{134}Cs was detected except at 100 m in the KC in January 2012. The vertical distribution pattern of ^{137}Cs at the stations north of and in the KC was relatively uniform throughout the water column between 0 and 500 m, whereas ^{137}Cs concentrations south of the KC had significant peaks (2.3–12 Bq m^{-3}) at subsurface depths (100–500 m), especially after April 2012 (Fig. 2.4). We also detected ^{134}Cs at the subsurface peak of ^{137}Cs (mostly at 300 m), which

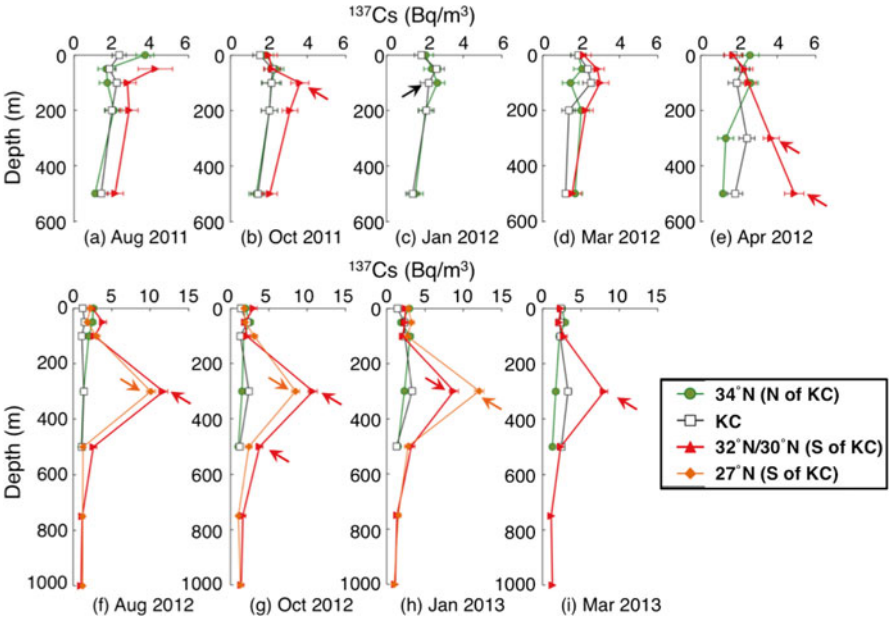

Fig. 2.4 Vertical profiles of ^{137}Cs at three to four stations along the 138°E line during August 2011 and March 2013. *Arrows* indicate the detection of ^{134}Cs. *Error bars* indicate counting error (±1σ). When ^{137}Cs was under the detection limit (<3σ), the detection limit was plotted (Adopted with permission from Kaeriyama et al. 2014a. Copyright (2014) American Chemical Society)

varied from 1.8 to 6.8 Bq m^{-3} south of the KC. The concentration of ^{137}Cs in deeper water (≥750 m) was lower than 1.6 Bq m^{-3}, and no ^{134}Cs was detected. Thus, the subsurface peak of ^{134}Cs and ^{137}Cs was observed between 100 and 500 m south of the KC. Further south of the 138°E transect, ^{134}Cs was also detected at 300 m, and ^{137}Cs ranged from 1.2 to 14 Bq m^{-3} between 0 and 500 m in September 2012 between 18°N and 26°49′N around 135°E. The ^{137}Cs concentration was relatively low and vertically homogenized, and ^{134}Cs was not detectable at 14°59′N or 13°N on the same cruise (Fig. 2.5). The ^{137}Cs inventories were nearly the same level, between 630 ± 180 and 1,160 ± 190 Bq m^{-2}, both north of the KC and in the KC during the entire study period (Fig. 2.6a). South of the KC, the inventories were comparable with those found north of the KC and in the KC during August 2011 and February 2012 (1,000–1,350 Bq m^{-2}) and then markedly increased to 3,260 ± 410 Bq m^{-2} after April 2012 (Fig. 2.6a). The inventories of ^{137}Cs ranged from 800 ± 300 to 3,460 ± 560 Bq m^{-2} and decreased traveling southward between 13°00′N and 26°49′N around 135°E in September 2012 (Fig. 2.6b).

Because water usually circulates along the isopycnal layer below the subsurface, the density range of the subsurface peak of ^{134}Cs and ^{137}Cs gives information about what water mass transported FNPP-derived radioactive Cs. Although the subsurface peaks were found at the isopycnals from 25.0 to 25.5 σ_θ and from 26.0 to 26.5 σ_θ at 34°46′N, 148°52′E in February 2012 (Kumamoto et al. 2013), the present study

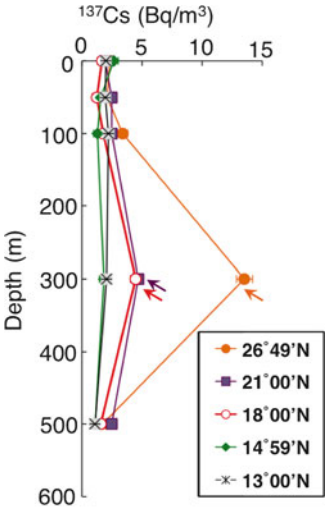

Fig. 2.5 Vertical profiles of ^{137}Cs at five stations around 135°E in September 2012. *Arrows* indicate the detection of ^{134}Cs. *Error bars* indicate counting error (±1σ). When ^{137}Cs was below the detection limit (<3σ), the detection limit was plotted (Adopted with permission from Kaeriyama et al. 2014a. Copyright (2014) American Chemical Society)

shows that ^{134}Cs south of the KC along 138°E and around 135°E was observed at a density range from 23.9 to 25.7 σ_θ, with a sharp peak around 25.3 σ_θ (Fig. 2.7). The ^{134}Cs peak at 25.3 σ_θ suggests that core waters with high ^{134}Cs and ^{137}Cs levels derived from the FNPP accident are distributed in the North Pacific Subtropical Mode Water (NPSTMW). The predominant temperature (16.4 °–17.9 °C) and salinity (34.6–34.7 psu) ranges of ^{134}Cs and ^{137}Cs are present within the NPSTMW (Oka 2009). In the present study, the radioactive Cs detected in the southern region was thought to contain the atmospheric fallout from the FNPP to the sea surface south of the KE during mid-March and early April 2011 (Sect. 2.3; Chino et al. 2011; Rypina et al. 2013; Honda et al. 2012; Kobayashi et al. 2013).

Using dissolved oxygen data (apparent oxygen utilization, AOU) (Ebbesmeyer and Lindstrom 1986), we examined whether the subsurface water was ventilated with highly radioactive Cs at the surface in March 2011 as oxygen in the NPSTMW gradually decreases after its subduction (Suga and Hanawa 1995). The detected ^{134}Cs south of the KC in April 2012 and in January 2013 did in fact originate from atmospheric deposition and was ventilated in March 2011 (Kaeriyama et al. 2014a). The inventory of ^{137}Cs south of the KC along the 138°E transect increased from 1,100 to 3,210 Bq m^{-2} between February and August 2012 (Fig. 2.6a), suggesting that the newly formed NPSTMW brought more FNPP-derived radioactive Cs to the south of the KC. Alternatively, the inventories of ^{137}Cs north of the KC and in the KC along the 138°E transect varied from 650 to 1,410 Bq m^{-2} throughout the study period (Fig. 2.6a), which is almost comparable with the water column inventories of ^{137}Cs detected in the North Pacific before the FNPP accident (almost 1,000 Bq m^{-2}) Aoyama et al. 2008; Povinec et al. 2004). These data may indicate that the water north of and in the KC was mostly unaffected by the FNPP-derived radioactive Cs. In September 2012, ^{134}Cs was detected at 18°N, but not at 14°59′N (Fig. 2.5). The inventories of ^{137}Cs at 13°N and 14°59′N (Fig. 2.6b) were comparable with those in

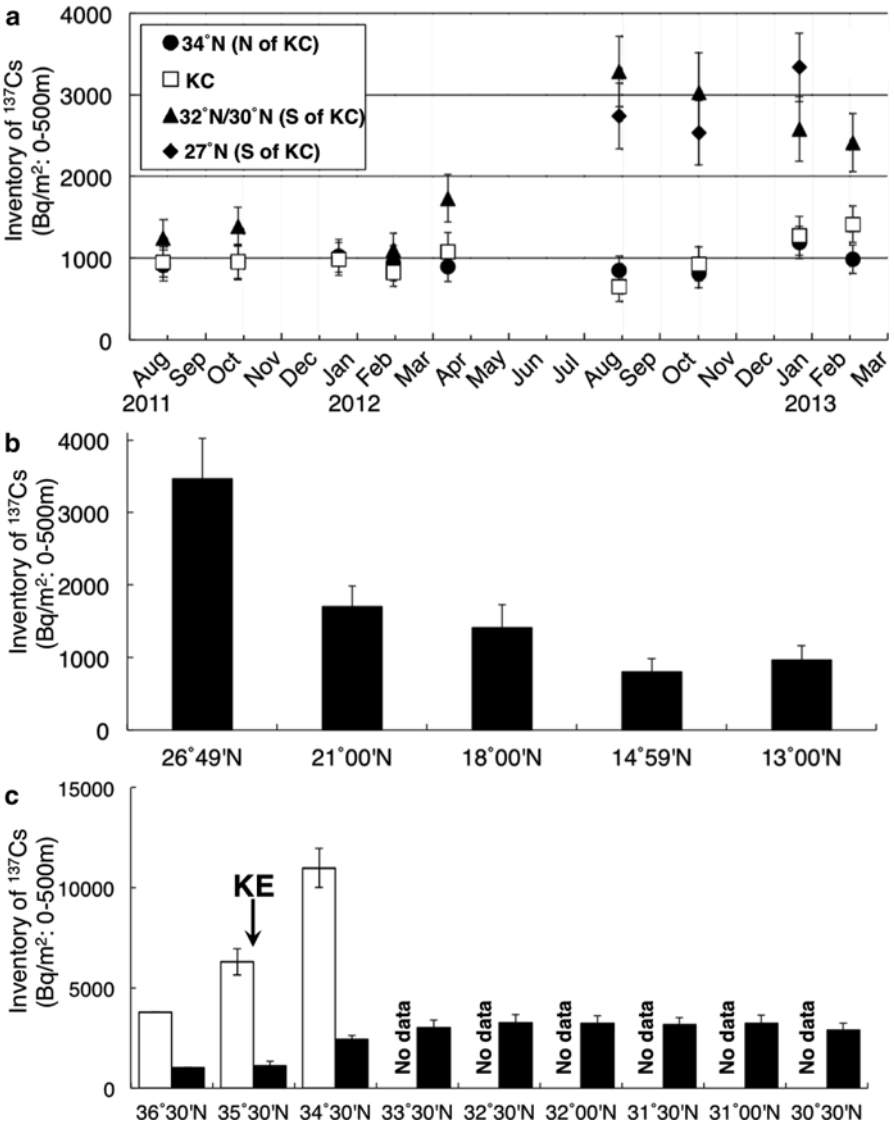

Fig. 2.6 Water column inventories of ^{137}Cs between 0- and 500-m depth along the 138°E transect from August 2011 to March 2013 (**a**), around 135°E in September 2012 (**b**), and along l47°E in October 2011 (*open bars*) and November 2012 (*closed bars*) (**c**). When ^{137}Cs was under the detection limit (<3σ), the detection limit was used for calculation (Adopted with permission from Kaeriyama et al. 2014a. Copyright (2014) American Chemical Society)

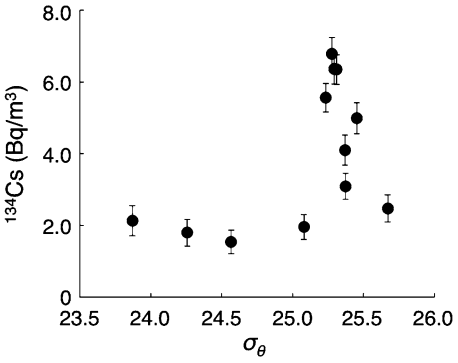

Fig. 2.7 Relationship between subsurface (≥100 m depth) ^{134}Cs concentration and potential density (σ_θ) south of the Kuroshio Current (KC) along the 138°E transect (Adopted with permission from Kaeriyama et al. 2014a. Copyright (2014) American Chemical Society)

the North Pacific before the FNPP accident (Aoyama et al. 2008; Povinec et al. 2004). These results suggest the FNPP-derived radioactive Cs core water had dispersed southward to at least 18°N by 19 months after the FNPP accident. Nakano and Povinec (2012) reported long-term simulations of FNPP-derived ^{137}Cs dispersion in the global oceans with a grid size of 2 × 2 and 15 layers of vertical direction. The vertical distribution pattern of FNPP-derived ^{137}Cs with subsurface peaks between 100 and 300 m at 20°N–130°E is in agreement with our results at 21°N–134°E from September 2012 (Fig. 2.5). However, the timing of the appearances and concentrations of subsurface ^{137}Cs peaks are very different from our results. Their model results revealed the first appearance of a subsurface peak of FNPP-derived ^{137}Cs was in 2014 and the peak depth concentration was estimated as 0.5 Bq m^{-3}. However, our results showed a subsurface peak concentration of 2.1 Bq m^{-3} for FNPP-derived ^{134}Cs at 20°N–130°E in September 2012, that is, 2 years earlier than the model result. These differences between the modeled result of Nakano and Povinec (2012) and our direct observation may be the result of limitations such as uncertainties regarding the amount of ^{137}Cs released from the FNPP and the resolution of the velocity field. Nakano and Povinec (2012) mentioned that the KC and the KE were weaker in their model than the ARGO drifters predicted.

2.4.2 *Transect Across the Kuroshio Extension*

In October 2011, concentrations of ^{134}Cs and ^{137}Cs in excess of 20 Bq m^{-3} were observed in surface waters and at 50-m depth north of the KE at 147°E (Fig. 2.8). Alternatively, the subsurface peak of radioactive Cs was observed in the KE and south of the KE (Fig. 2.8). The concentrations of ^{137}Cs drastically decreased after 1 year at all three stations and were distributed uniformly between 1.3 and 4.3 Bq m^{-3}, which were observed north of and in the KE in November 2012 (Fig. 2.8). In contrast, the subsurface peak of ^{137}Cs was observed at 9 to 12 Bq m^{-3} south of the KE, with ^{134}Cs detected in the KE and south of the KE in November 2012 (Fig. 2.8). Southeast of the FNPP, ^{137}Cs inventories north of the KE, in the KE, and south of the KE in October 2011 were calculated to be 3,840 ± 660, 6,370 ± 2,060, and 10,990 ± 3,870 Bq m^{-2},

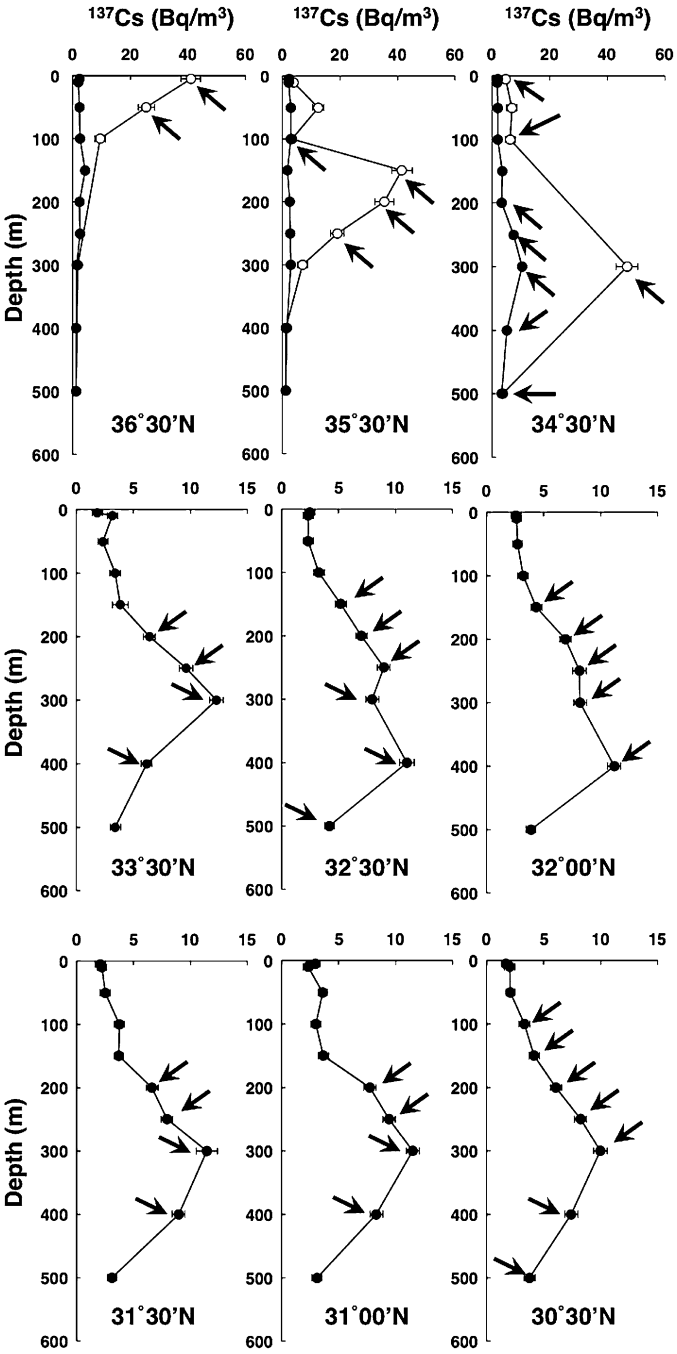

Fig. 2.8 Vertical profiles of ^{137}Cs north of the Kuroshio Extension (KE) (36°30′N), in the KE (35°30′N), and south of KE (30°00′N-34°30′N). *Open circles* represent values recorded in October 2011. *Closed circles* represent values recorded in November 2012. *Arrows* indicate the detection of ^{134}Cs. *Error bars* indicate counting error (±1σ). When ^{137}Cs was under the detection limit (<3σ), the detection limit was plotted

respectively (Fig. 2.6c); those from November 2012 were 1,030 ± 280, 1,150 ± 370, and between 2,440 and 3,300 Bq m^{-2}, respectively (Fig. 2.6c).

In shallow water (0 and 50-m depth), high concentrations of ^{134}Cs and ^{137}Cs were observed north of the KE, but low concentrations were observed in the KE and south of the KE, which is consistent with previous studies showing that the KE prevented the southward dispersion of radioactive Cs from the FNPP in the surface water (Sect. 2.3; Aoyama et al. 2013a, b; Buesseler et al. 2012). Our results showed that deeper intrusion of FNPP-derived radioactive Cs occurred at 34°30′N and 35°30′N in October 2011 before the first winter after the FNPP accident. In October 2011, the subsurface peak of ^{134}Cs was observed from 24.0 to 26.5 σ_θ. Observations at 34°30′N in November 2012 were between 25.1 and 26.1 σ_θ with a peak at 25.3 σ_θ. The difference in the density of subsurface ^{134}Cs waters may indicate that different water masses of FNPP-derived radioactive Cs existed during these 2 years. The large spatial variation of the FNPP-derived radioactive Cs around the KE was also discussed with data obtained at 34°46′N–148°52′E in February 2012 (Kumamoto et al. 2013). Rypina et al. (2013) reported model results of FNPP-derived radioactive Cs in the area of 34°N–37°N, 142°E–147°E during March and June 2011. The three-dimensional (3-D) model results (fig. 9 of Rypina et al. 2013) suggested that FNPP-derived ^{137}Cs occasionally penetrated to 300–400 m in depth north of the KE during April and June 2011 as a consequence of the spatial heterogeneity of mixed-layer depth and the existence of strong downwelling regions. Furthermore, Oikawa et al. (2013) showed data obtained near the FNPP during March 2011 and February 2012, which were part of the monitoring program initiated by the Ministry of Education, Culture, Sports, Science and Technology (MEXT). They concluded that the depth of σ_t isopycnals of 25.5–26.5 waters increased with time and transported the FNPP-derived radioactive Cs to deep water from the FNPP-proximal coastal waters between May and December 2011. Taking into account the monitoring data of MEXT (Oikawa et al. 2013), the observational data from February 2012 (Kumamoto et al. 2013), and model results (Rypina et al. 2013), it has been suggested that the subsurface peak of radioactive Cs observed south of and in the KE in October 2011 may have been transported from the coastal area off the FNPP without subduction.

2.4.3 *Amount of ^{134}Cs in Subsurface Core Waters in the Southern Area*

We estimated the amount of ^{134}Cs in subsurface core waters south of both the KC and the KE from our observational data collected in September 2012, when the southernmost detection of ^{134}Cs was observed at 18°N–135°E (Fig. 2.5). Results suggest that the FNPP-derived radioactive Cs was taken into the NPSTMW and then transported southwestward by the Kuroshio recirculation (Suga and Hanawa 1995). As a first step, the amount of ^{134}Cs in the entire area of the NPSTMW was estimated. The average concentration of ^{134}Cs in the NPSTMW (26°49′N–34°30′N), decay-corrected on March 11, 2011, was 11 ± 1.7 Bq m^{-3}. Suga et al. (2008) estimated the total volume of the NPSTMW as 1×10^6 km^3. Therefore, the amount of

^{134}Cs in the entire area of the NPSTMW would be estimated as 11 ± 1.7 PBq. Kumamoto et al. (2014) reported ^{134}Cs in the area around the center of the NPSTMW during January and February 2012, estimating the total inventory of ^{134}Cs in the NPSTMW to be 6 PBq. These estimates may indicate that 6 PBq of ^{134}Cs intruded into the NPSTMW during March and April 2011, as observed in January and February 2012 (Kumamoto et al. 2014), and 3.3–6.7 PBq additional ^{134}Cs had intruded into the NPSTMW during the 2011–2012 winter season, observed in September 2012 (this study). Because the vertical resolution of this study was low (seven layers between the surface and 1,000 m), and the study area was limited to the western part of the NPSTMW, considerable uncertainty should have been taken into account. The second estimate was limited to the peak depth of radioactive Cs around the western part of the NPSTMW. Contours of acceleration potential on an isopycnal surface indicate isopycnal streamlining in September 2012 based on ARGO float data. The shape of the closed contour line of 19 m^2 s^{-2} is similar to the Kuroshio recirculation as described by Suga and Hanawa (1995), and the area was defined as the western part of the NPSTMW (Fig. 2.9a).

The ^{134}Cs concentration was estimated for the observationally sparse area in the western part of the NPSTMW by Gaussian averaging (Fig. 2.9b). The thickness of the NPSTMW core was estimated as the difference between the depths of isopycnal surfaces 25.2 σ_θ and 25.4 σ_θ (Fig. 2.9c). The horizontal inventory of ^{134}Cs in the western part of the NPSTMW core was estimated using the product of the concentration and thickness listed above (Fig. 2.9d). Then, the amount of ^{134}Cs in the core of the western part of the NPSTMW in September 2012 was estimated to be 1.07 PBq, which accounts for 7–47 % of the total amount of ^{134}Cs released directly into the ocean from the FNPP (2.3–14.8 PBq of ^{137}Cs; ^{134}Cs/^{137}Cs ratio assumed to be 1.0 Masumoto et al. 2012), or 10 % of the total deposition including direct release and atmospheric surface deposition (11 PBq ^{134}Cs; Kobayashi et al. 2013). Although the estimation includes enormous uncertainties, it should be noted that a considerable amount of the FNPP-derived radioactive Cs had been dispersed in the southwestern portion of the North Pacific across the KC, which was considered to act as a barrier against the southward dispersion of FNPP-derived radionuclides (Sect. 2.3, Aoyama et al. 2013a, b; Buesseler et al. 2012). To clarify and improve the amount of FNPP-derived radioactive Cs in the southwestern portion of the North Pacific, future studies should include not only collection of observational data, but also an improved model with a comprehensive understanding of FNPP-derived Cs dispersion in the oceanic environment.

Fig. 2.9 (continued) (**b**) Estimated spatial distribution of ^{134}Cs concentration (Bq m^{-3}) at the core water of the western part of the NPSTMW, which is estimated by Gaussian averaging with a 1,000-km e-folding scale applied to the ^{134}Cs data collected during September and November 2012 and decay-corrected on March 11, 2011. The *black line* indicates acceleration potential of 19 m^2 s^{-2}. (**c**) Spatial distribution of water thickness between the isopycnal surfaces 25.2 σ_θ and 25.4 σ_θ based on the Argo data. (**d**) Estimated inventory of ^{134}Cs in the core water of the western part of the NPSTMW in September 2012, which is estimated by the ^{134}Cs concentration (Bq m^{-3}) and the water column thickness. The *black line* indicates acceleration potential of 19 m^2 s^{-2}

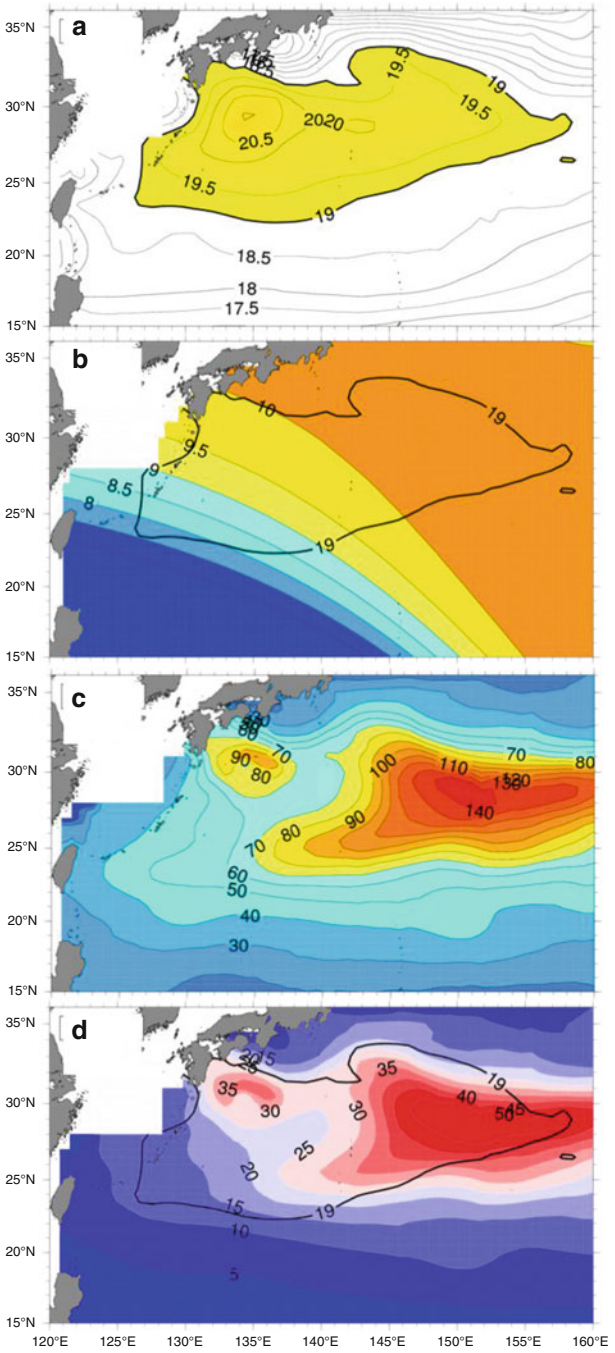

Fig. 2.9 (**a**) Acceleration potential on isopycnal surface 25.3 σ_θ referred to 1,000 dbar based on the quality-checked Argo data (resolutions: horizontal 1° × 1°, vertical 25 layers from surface to 2,000-m depth) during September 2012, which were obtained from http://www.jamstec.go.jp/ARGO/argo_web/argo/index.html. The area with acceleration potential >19 m^2 s^{-2} is colored in *yellow*.

2.5 ^{134}Cs and ^{137}Cs Around Japan Islands

The seawater samples for measurement of ^{134}Cs and ^{137}Cs were collected between May 2011, 2 months after the FNPP accident, and March 2014 (Fig. 2.1). In the Japan Sea, the East China Sea, the Seto Inland Sea, and the Bering Sea, only ^{137}Cs was detected at background levels (<2.0 Bq m^{-3}), without any detectable ^{134}Cs (Fig. 2.10). Inoue et al. (2012), Wu et al. (2012), and Kim et al. (2012) reported ^{134}Cs at trace levels in the Japan Sea, the East China Sea, and around the Korean

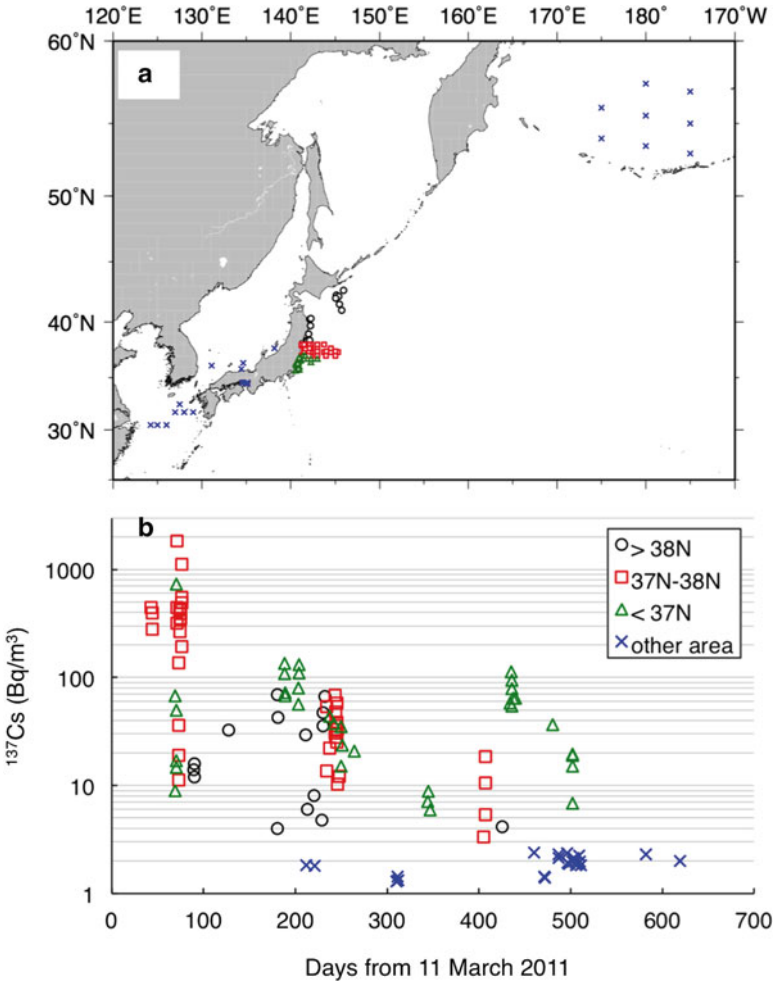

Fig. 2.10 Sampling locations of surface seawater (**a**), and temporal variations of ^{137}Cs in the western North Pacific (**b**), in the area north of 38°N (*open circles*), 37°N–38°N (*open squares*), south of 37°N (*open triangles*), and in other areas, including the Japan Sea, the Seto Inland Sea, the East China Sea, and the Bering Sea (*cross*) (Modified from Kaeriyama et al. 2014b)

Peninsula, respectively. These results demonstrated that FNPP-derived radioactive Cs slightly affected the Japan Sea, the East China Sea, the Seto Inland Sea, and the Bering Sea.

In contrast, a high level of radioactive Cs was observed off the coast of East Japan in the western North Pacific (Fig. 2.10). In May 2011, a high concentration of ^{137}Cs, in excess of 200 Bq m^{-3}, was observed in the area 36°20′N–38°N, but concentrations were lower than 100 Bq m^{-3} south of 36°20′N (Fig. 2.11). In the area south of 36°20′N, more than 500 Bq m^{-3} ^{137}Cs was observed in June 2011, 1 month after our observation (Buesseler et al. 2012). Aoyama et al. (2012) reported temporal variation of radioactive Cs at Hasaki (35°50.4′N–140°45.6′E), 180 km south of the FNPP site, during April and December 2011. The peak of radioactive Cs at Hasaki observed in June 2011 represented a delay of 2 months from the appearance of the peak of radioactive Cs at the FNPP site in April 2011. The meso-scale eddy existed in mid-latitudes between FNPP and Hasaki, and its center is located at 36°30′N–141°24′E. This eddy may have prevented the southward transport of FNPP-derived radioactive Cs to Hasaki until the end of May 2011 (Aoyama et al. 2012). The difference in the horizontal distribution of ^{137}Cs between May and June 2011 (Fig. 2.11) also clearly indicates that the warm core eddy inhibited the southward dispersion of FNPP-derived radioactive Cs along the east Japan coast until the end of May 2011. North of the FNPP, the meso-scale eddy also affected the local

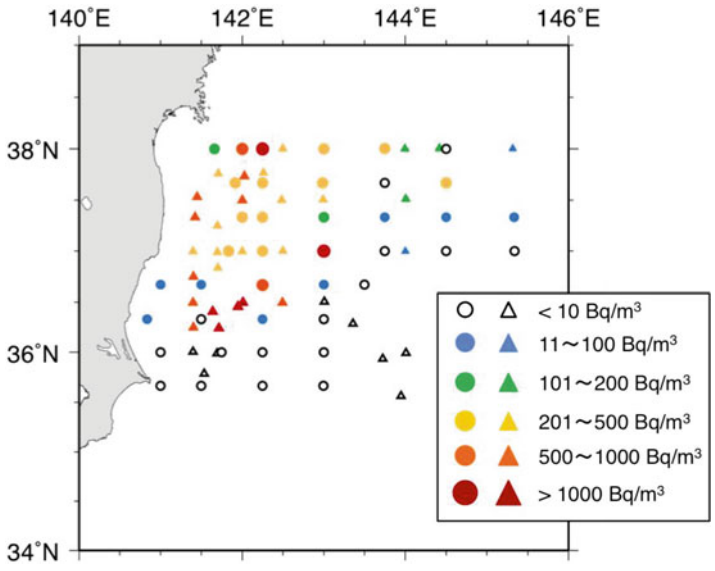

Fig. 2.11 Sampling locations of surface seawater and ^{137}Cs concentration in May (*circles*) and June (*triangles*) 2011. The data for June 2011 were obtained from Buesseler et al. (2012). *Colors* of the *closed* and *open symbols* indicate the concentrations of ^{137}Cs (Modified from Kaeriyama et al. 2014b)

distribution of FNPP-derived Cs (Kofuji and Inoue 2013). The patchy distribution of radioactive Cs was also observed around the meso-scale eddy just north of the KE (as shown in Sect. 2.3). To comprehensively understand the patchy distribution of radioactive Cs released from the FNPP, meso-scale-resolved models should be developed.

Figure 2.12 shows temporal variations of ^{137}Cs off the coast of East Japan based on selected data sets (Aoyama et al. 2012; Buesseler et al. 2011; Kaeriyama et al. 2014b, d; Kaeriyama, unpublished data). To compare the decreasing trend of FNPP-derived radioactive Cs within these data sets, the data of Aoyama et al. (2012) and Buesseler et al. (2011) were plotted from the timing of the observed peak concentration. Exponential decrease was observed in each data set. During the first year from the FNPP accident, drastic decreases of ^{137}Cs were observed off the east coast of Japan. On the other hand, after 1 year from the FNPP accident, the decay rate seemed to be slower than that of the first year (Fig. 2.12), which may imply that the extremely high radioactive Cs released during March and April 2011 was quickly dispersed from the coastal area to the open ocean within 1 year from the FNPP accident in this area. The weakened decreasing trend apparent after 1 year from the FNPP accident would be affected by new inputs of FNPP-derived radioactive Cs, such as continuing release from the FNPP site, even though continued release was more than four orders of magnitude less than the direct discharge that occurred during March and April 2011 (Kanda 2013). Furthermore, river-borne waters and sediments should have been considered as a long-term source of FNPP-derived radioactive Cs to the ocean. The concentration of ^{137}Cs obtained from very near coast (off the coast of Onahama; Fig. 2.12) were higher than that of offshore stations (off the east Japan coast and Sendai Bay; Fig. 2.12), possibly caused by the fluvial input of terrestrial FNPP-derived radioactive Cs. Nagao et al. (2013) reported the transport of FNPP-derived radioactive Cs from a contaminated watershed in Fukushima Prefecture to the coastal ocean area during July and December 2011; they estimated the export flux of ^{134}Cs and ^{137}Cs after the heavy rain event (Typhoon Roke in September 2011) as roughly $0.74–2.6 \times 10^{10}$ Bq day^{-1} for the rivers of Fukushima Prefecture. These values account for 30–50 % of the export of radioactive Cs for the 10 months of March 11–December 31, 2011 in these rivers (Nagao et al. 2013). In the future, secondary dispersion of FNPP-derived radioactive Cs through rivers, as considered in Nagao et al. (2013), and through groundwater should be studied to understand the long-term effects of the FNPP accident in the coastal area of East Japan.

Fig. 2.12 (continued) (Kaeriyama et al. 2014b), near the coast of Onahama (*open triangles*) (Kaeriyama, unpublished data), near the coast of Hasaki (*purple open diamonds*) (Aoyama et al. 2012), and near the coast of Iwasawa (*blue open diamonds*) (Buesseler et al. 2011)

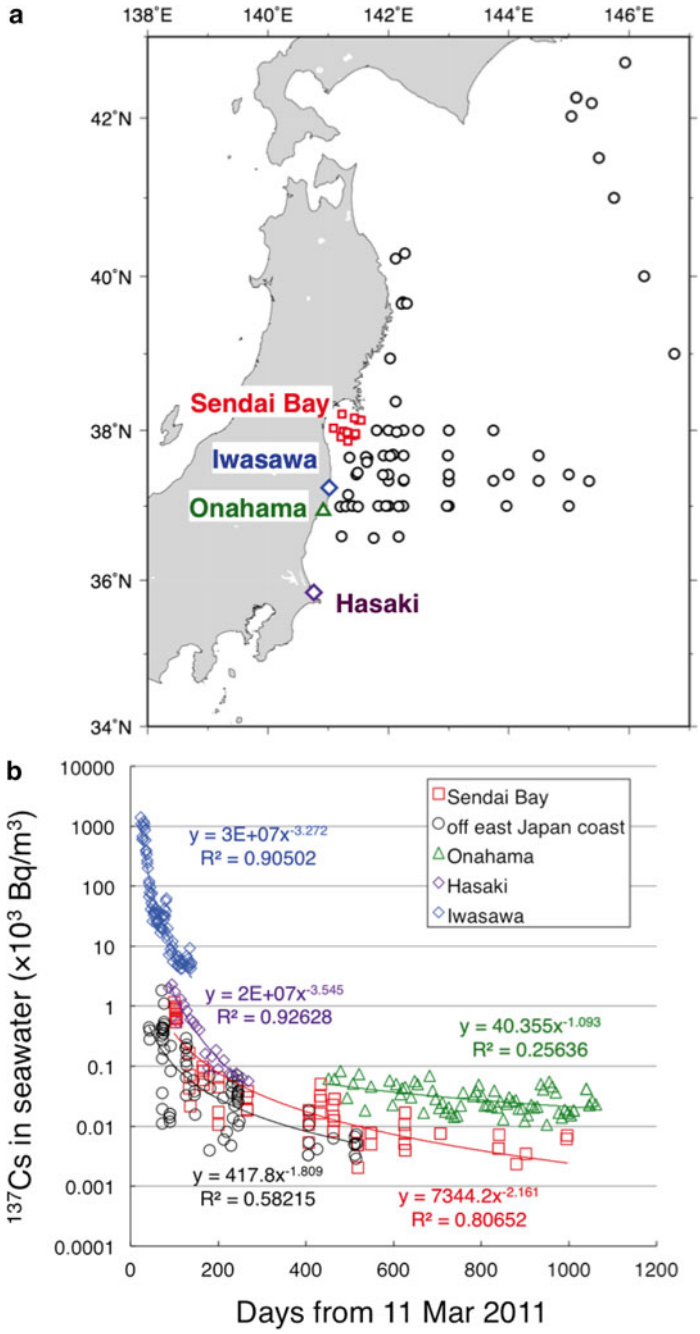

Fig. 2.12 Sampling locations of surface seawater (**a**) and temporal variations of ^{137}Cs (**b**) in Sendai Bay (*open squares*) (Kaeriyama et al. 2014d), off the coast of east Japan (*open circles*)

References

Aoyama M, Hirose K, Nemoto K, Takatsuki Y, Tsumune D (2008) Water masses labeled with global fallout ^{137}Cs formed by subduction in the North Pacific. Geophys Res Lett 35. doi:10.1029/2007GL031964

Aoyama M, Tsumune D, Uematsu M, Kondo F, Hamajima Y (2012) Temporal variation of ^{134}Cs and ^{137}Cs activities in surface water at stations along the coastline near the Fukushima Dai-ichi Nuclear Power Plant accident site. Geochem J 46:321–325

Aoyama M, Tsumune D, Hamajima Y (2013a) Distribution of ^{137}Cs and ^{134}Cs in the North Pacific Ocean: impacts of the TEPCO Fukushima-Daiichi NPP accident. J Radioanal Nucl Chem 296:535–539

Aoyama M, Uematsu M, Tsumune D, Hamajima Y (2013b) Surface pathway of radioactive plume of TEPCO Fukushima NPP1 released ^{134}Cs and ^{137}Cs. Biogeosciences 10:3067–3078

Bailly du Bois P, Laguionie P, Boust D, Korsakissok I, Didier D, Fiévet B (2012) Estimation of marine source-term following Fukushima Dai-ichi accident. J Environ Radioact 114:2–9

Buesseler KO, Aoyama M, Fukasawa M (2011) Impacts of the Fukushima nuclear power plants on marine radioactivity. Environ Sci Technol 45:9931–9935

Buesseler KO, Jayne SR, Fisher NS, Rypina II, Baumann H, Baumann Z, Breier CF, Douglass EM, George J, Madonald AM, Miyamoto H, Nishikawa J, Pike SM, Yoshida S (2012) Fukushima-derived radionuclides in the ocean and biota off Japan. Proc Natl Acad Sci U S A 109:5984–5988

Chino M, Nakayama H, Nagai H, Terada H, Katata G, Yamazawa H (2011) Preliminary estimation of release amount of ^{131}I and ^{137}Cs accidentally discharged from the Fukusima Daiichi nuclear power plant into the atmosphere. J Nucl Sci Technol 48:1129–1134

Dietze H, Kriest I (2012) ^{137}Cs off Fukushima Dai-ichi, Japan: model-based estimates of dilution and fate. Ocean Sci 8:319–332

Ebbesmeyer CC, Lindstrom EJ (1986) Structure and origin of 18°C water observed during the POLYMODE local dynamics experiment. J Phys Oceanogr 16:443–453

Fisheries Agency (2014) Results of the monitoring on radioactivity level in fisheries products. http://www.jfa.maff.go.jp/e/inspection/index.html (referred at 20 October 2014)

Hirose K, Aoyama M (2003) Present background levels of surface ^{137}Cs and ^{239,240}Pu concentrations in the Pacific. J Environ Radioact 69:53–60

Honda MC, Aono T, Aoyama M, Hamajima Y, Kawakami H, Kitamura M, Masumoto Y, Miyazawa Y, Takigawa M, Saino T (2012) Dispersion of artificial caesium-134 and -137 in the western North Pacific one month after the Fukushima accident. Geochem J 46:e1–e9

Inoue M, Kofuji H, Nagao S, Yamamoto M, Hamajima Y, Yoshida K, Fujimoto K, Takada T, Isoda Y (2012) Lateral variation of ^{134}Cs and ^{137}Cs concentrations in surface seawater in and around the Japan Sea after the Fukushima Dai-ichi Nuclear Power Plant accident. J Environ Radioact 109:45–51

Isoguchi O, Kawamura H, Oka E (2006) Quasi-stationary jets transporting surface warm waters across the transition zone between the subtropical and the subarctic gyres in the North Pacific. J Geophys Res 111, C10003. doi:10.1029/2005JC003402

Itoh S, Yasuda I (2010a) Water mass structure of warm and cold anticyclonic eddies in the western boundary region of the subarctic North Pacific. J Phys Oceanogr 40:2624–2642

Itoh S, Yasuda I (2010b) Characteristics of mesoscale eddies in the Kuroshio-Oyashio extension region detected from the distribution of the sea surface height anomaly. J Phys Oceanogr 40:1018–1034

Kaeriyama H, Ambe D, Shimizu Y, Fujimoto K, Ono T, Yonezaki S, Kato Y, Matsunaga H, Minami H, Nakatsuka S, Watanabe T (2013) Direct observation of ^{134}Cs and ^{137}Cs in surface seawater in the western and central North Pacific after the Fukushima Dai-ichi nuclear power plant accident. Biogeosciences 10:4287–4295

Kaeriyama H, Shimizu Y, Ambe D, Masujima M, Shigenobu Y, Fujimoto K, Ono T, Nishiuchi K, Taneda T, Kurogi H, Setou T, Sugisaki H, Ichikawa T, Hidaka K, Hiroe Y, Kusaka A, Kodama T, Kuriyama M, Morita H, Nakata K, Morinaga K, Morita T, Watanabe T (2014a) Southwest intrusion of ^{134}Cs and ^{137}Cs derived from the Fukushima Dai-ichi nuclear power plant accident in the western North Pacific. Environ Sci Technol 48:3120–3127

Kaeriyama H, Ambe D, Shigenobu Y, Fujimoto K, Ono T, Nakata K, Morita T, Watanabe T (2014b) ^{134}Cs and ^{137}Cs in seawater around Japan after the Fukushima Daiichi nuclear power plant accident. Oceanogr Jpn 23:127–146 (in Japanese with English abstract)

Kaeriyama H, Ambe D, Shigenobu Y, Fujimoto K, Ono T, Watanabe T, Morita T (2014c) Oceanic dispersion of radioactive cesium in the western North Pacific: eastward dispersion in surface water and southward intrusion with mode water. In: Extended abstract of Third International Conference on Radioecology and Environment Radioactivity, OP089, Barcelona, Spain, September 2014.

Kaeriyama H, Fujimoto K, Ambe D, Shigenobu Y, Ono T, Tadokoro K, Okazaki Y, Kakehi S, Ito S, Narimatsu Y, Nakata K, Morita T, Watanabe T (2014d) Fukushima-derived radionuclides ^{134}Cs and ^{137}Cs in zooplankton and seawater samples collected off the Joban-Sanriku coast, in Sendai Bay, and in the Oyashio region. Fish Sci. doi:10.1007/s12562-014-0827-6

Kanda J (2013) Continuing ^{137}Cs release to the sea from the Fukushima Dai-ichi Nuclear Power Plant through 2012. Biogeosciences 10:6107–6113

Kawamura H, Kobayashi T, Furuno A, In T, Ishikawa Y, Nakayama T, Shima S, Awaji T (2011) Preliminary numerical experiments on oceanic dispersion of ^{131}I and ^{137}Cs discharged into the ocean because of the Fukushima Daiichi Nuclear Power Plant disaster. J Nucl Sci Technol 45:1349–1356

Kim CK, Byun JI, Chae JS, Choi HY, Choi SW, Kim DJ, Kim YJ, Lee DM, Park WJ, Yim AJ, Yun JY (2012) Radiological impact in Korea following the Fukushima nuclear accident. J Environ Radioact 111:70–82

Kobayashi T, Nagai H, Chino M, Kawamura H (2013) Source term estimation of atmospheric release due to the Fukushima Dai-ichi Nuclear Power Plant accident by atmospheric and oceanic dispersion simulations. J Nucl Sci Technol 50:255–264

Kofuji H, Inoue M (2013) Temporal variations in ^{134}Cs and ^{137}Cs concentrations in seawater along the Shimokita Peninsula and the northern Sanriku coast in northeastern Japan, one year after the Fukushima Dai-ichi Nuclear Power Plant accident. J Environ Radioact 124:239–245

Kumamoto Y, Murata A, Kawano T, Aoyama M (2013) Fukushima-derived radiocesium in the northwestern Pacific Ocean in February 2012. Appl Radiat Isot 81:335–339

Kumamoto Y, Aoyama M, Hamajima Y, Aono T, Kouketsu S, Murata A, Kawano T (2014) Southward spreading of the Fukushima-derived radiocesium across the Kuroshio extension in the North Pacific. Sci Rep 4:4276–4285

Masumoto Y, Miyazawa Y, Tsumune D, Tsubono T, Kobayashi T, Kawamura H, Estournel C, Marsaleix P, Lanerolle L, Mehra A, Garraffo ZD (2012) Oceanic dispersion simulations of ^{137}Cs released from the Fukushima Daiichi nuclear power plant. Elements 8:207–212

Miyazawa Y, Masumoto Y, Varlamov SM, Miyama T (2012) Transport simulation of the radionuclide from the shelf to open ocean around Fukushima. Cont Shelf Res 50-51:16–29

Mizuno K, White WB (1983) Annual and interannual variability in the Kuroshio current system. J Phys Oceanogr 13:1847–1867

Nagao S, Kanamori M, Ochiai S, Tomihara S, Fukushi K, Yamamoto M (2013) Export of ^{134}Cs and ^{137}Cs in the Fukushima river systems at heavy rains by Typhoon Roke in September 2011. Biogeosciences 10:6215–6223

Nakano M, Povinec PP (2012) Long-term simulations of the ^{137}Cs dispersion from the Fukushima accident in the world ocean. J Environ Radioact 111:109–115

Nuclear Regulation Authority (2014) Monitoring information of environmental radioactivity level. http://radioactivity.nsr.go.jp/en/ (referred at 20 October 2014)

Oikawa S, Takata H, Watabe T, Misono J, Kusakabe M (2013) Distribution of the Fukushima-derived radionuclides in seawater in the Pacific coast of Miyagi, Fukushima, and Ibaraki Prefectures, Japan. Biogeosciences 10:5031–5047

Oka E (2009) Seasonal and interannual variation of North Pacific Subtropical Mode Water in 2003–2006. J Oceanogr 65:151–164

Oka E, Talley LD, Suga T (2007) Temporal variability of winter mixed layer in the mid- to high-latitude North Pacific. J Oceanogr 63:293–307

Povinec PP, Hirose K, Honda T, Ito T, Scott EM, Togawa O (2004) Spatial distribution of ^{3}H, ^{90}Sr, ^{137}Cs and ^{239,240}Pu in surface waters of the Pacific and Indian Oceans: GLOMARD database. J Environ Radioact 76:113–137

Qiu B, Chen S (2011) Effect of decadal Kuroshio Extension Jet and eddy variability on the modification of North Pacific Intermediate Water. J Phys Oceanogr 41:503–515

Rypina II, Jayne SR, Yoshida S, Macdonald AM, Douglass E, Buesseler KO (2013) Short-term dispersal of Fukushima-derived radionuclides off Japan: modelling efforts and model–data intercomparison. Biogeosciences 10:4973–4990

Suga T, Hanawa K (1995) Subtropical Mode Water south of Honshu, Japan in the spring of 1988 and 1989. J Oceanogr 51:1–19

Suga T, Aoki Y, Saito H, Hanawa K (2008) Ventilation of the North Pacific subtropical pycnocline and mode water formation. Prog Oceanogr 77:285–297

Sugisaki H, Nonaka M, Ishizaki S, Hidaka K, Kameda T, Hirota Y, Oozeki Y, Kubota H, Takasuka A (2010) Status and trends of the Kuroshio region. In: McKinnel SM et al (eds) PICES special publication 4. Marine ecosystem of the North Pacific Ocean, 2003–2008. North Pacific Marine Science Organization, Sydney, B.C, pp 330–359

Tsumune D, Tsubono T, Aoyama M, Hirose K (2012) Distribution of oceanic ^{137}Cs from the Fukushima Dai-ichi Nuclear Power Plant simulated numerically by a regional ocean model. J Environ Radioact 111:100–108

Wu JW, Zhou KB, Dai MH (2012) Impacts of the Fukushima nuclear accident on the China Seas: evaluation based on anthropogenic radionuclide ^{137}Cs. Chin Sci Bull. doi:10.1007/s11434-012-5426-2

Yasuda I (2003) Hydrographic structure and variability in the Kuroshio–Oyashio transition area. J Oceanogr 59:389–402

Yasuda I, Okuda K, Hirai M (1992) Evolution of a Kuroshio warm-core ring variability of the hydrographic structure. Deep-Sea Res 39(suppl 1):S131–S161

Chapter 3
Temporal Changes in ^{137}Cs Concentration in Zooplankton and Seawater off the Joban–Sanriku Coast, and in Sendai Bay, After the Fukushima Dai-ichi Nuclear Accident

Hideki Kaeriyama

Abstract The Fukushima Dai-ichi Nuclear Power Plant (FNPP) accident following the Great East Japan Earthquake in 2011 resulted in the release of enormous quantities of anthropogenic radionuclides into the ocean off the east Japanese coast, especially radioactive cesium (^{134}Cs and ^{137}Cs). FNPP-derived radioactive Cs might have consequently accumulated within marine food webs via seawater intake and predator–prey interactions. This study provides evidence of temporal variability in ^{137}Cs concentrations in seawater and zooplankton samples collected off the Joban–Sanriku coast and in Sendai Bay between June 2011 and December 2013. In Sendai Bay, seawater ^{137}Cs concentration was more than 1 Bq/kg in June 2011 and rapidly decreased over the study period. ^{137}Cs concentration in zooplankton was also measured to be as high as high 23 Bq/kg-wet in June 2011, and this concentration decreased at a slower rate than seawater concentrations. The difference in the rate of decrease of ^{137}Cs concentration between seawater and zooplankton resulted in an elevated apparent concentration ratio (aCR) for zooplankton. The observed relationship between ^{137}Cs in seawater and the aCR of zooplankton reflected the progression of ^{137}Cs contamination in zooplankton from the beginning of the FNPP accident to the restoration phase.

Keywords Fukushima Dai-ichi Nuclear Power Plant accident • ^{134}Cs • ^{137}Cs • Zooplankton • Seawater • Dynamic equilibrium • Concentration ratio

H. Kaeriyama (✉)
National Research Institute of Fisheries Sciences, Fisheries Research Agency,
2-12-4, Fukuura, Kanazawa, Yokohama, Kanagawa 236-8648, Japan
e-mail: kaeriyama@affrc.go.jp

K. Nakata, H. Sugisaki (eds.), *Impacts of the Fukushima Nuclear Accident on Fish and Fishing Grounds*, DOI 10.1007/978-4-431-55537-7_3

3.1 Introduction

After the magnitude 9.0 Great East Japan Earthquake and subsequent tsunami on March 11, 2011, a loss of electric power at the Fukushima Dai-ichi Nuclear Power Plant (hereafter FNPP) resulted in an overheated reactor and hydrogen explosions. Enormous quantities of radionuclides were then released into the ocean through atmospheric fallout as well as direct release and leaking of the heavily contaminated coolant water (Chino et al. 2011; Buesseler et al. 2011). Because of its relatively long half-life (2.07 years for ^{134}Cs and 30.07 years for ^{137}Cs), evaluation of this radioactive Cs in the marine environment is important for addressing risks both to marine ecosystems and to public health through consumption of fisheries products. The Japanese government conducted intensive monitoring of ^{131}I, ^{134}Cs, and ^{137}Cs concentrations in seawater offshore near the FNPP (Nuclear Regulation Authority 2014) and in fisheries products in a wide area around Japan to ensure the safety of fishery products (Fisheries Agency 2014). In the western North Pacific, the dispersion pattern of FNPP-derived radioactive cesium from just after the FNPP accident was studied by means of direct observations and simulation models (see Chap. 2). The FNPP-derived radioactive Cs was dispersed eastward in the surface seawater in a wide area of the northern Kuroshio Extension, and a part of the FNPP-derived radioactive Cs contamination intruded into the southern area of the Kuroshio Extension with mode water and was transported westward far south of the Japan Islands (see Chap. 2).

Wada et al. (2013) demonstrated the temporal change in ^{134}Cs and ^{137}Cs concentrations as total radioactive cesium (^{134}Cs + ^{137}Cs), which is limited to 100 Bq/kg-wet by Japanese authorities, in numerous species of marine organisms collected around Fukushima Prefecture and clarified the difference in the decrease rate of radioactive cesium among species. The decrease in rates of radioactive Cs in demersal fish was slower than that of pelagic fish (Wada et al. 2013; Iwata et al. 2013; Buesseler 2012), mainly because of a high concentration of FNPP-derived radioactive cesium in the marine sediments offshore near the FNPP (Kusakabe et al. 2013; Chap. 4). Even though temporal changes of many fisheries products were clarified from the monitoring data, the mechanism controlling the concentrations of radioactive Cs in each marine organism is still unknown (Wada et al. 2013; Iwata et al. 2013; Buesseler 2012). One of the most important factors controlling the amount of radioactive Cs in marine organisms is the uptake of radioactive Cs through food (Yoshida and Kanda 2012). Unfortunately, information concerning FNPP-derived radioactive Cs in the prey of fisheries products such as zooplankton and benthos is limited to those of zooplankton collected from the open ocean after the FNPP accident (Buesseler et al. 2012; Kitamura et al. 2013). Before the FNPP accident, several studies reported the concentration of ^{137}Cs in zooplankton around the Japanese coast (Tateda 1998; Kaeriyama et al. 2008a). Kaeriyama et al. (2008a) reported that the concentration of ^{137}Cs in zooplankton collected before the FNPP accident off the coast of Aomori Prefecture ranged from 0.01 to 0.02 Bq/kg-wet.

The concentration ratio (CR) (concentration in organisms relative to that in media) under equilibrium conditions is a useful environmental parameter, used in

mathematical models to estimate the level of radionuclides present in the organisms in comparison to the surrounding environment such as soil, sediments, water, or air (IAEA 2004; Tagami and Uchida 2013; Howard et al. 2013). The recommended CR values for ^{137}Cs in marine zooplankton, fish, and crustaceans are 40, 100, and 50, respectively (IAEA 2004). In this chapter, we did not calculate CR under equilibrium conditions; therefore, the CR value was referred to as the "apparent CR (aCR)" and was compared to the pre-FNPP CR.

In June 2011, only 3 months after the FNPP accident, the Fisheries Research Agency initiated a monitoring program to measure the environmental concentration of FNPP-derived radioactive Cs in different marine ecosystems, such as seawater, sediments, zooplankton, benthos, and fishes, in the most severely affected area off the coasts of Fukushima, Miyagi, and Ibaraki Prefectures (hereafter Joban–Sanriku coast) and in Sendai Bay (Fig. 3.1). In this chapter, we describe temporal changes in the concentrations of ^{137}Cs in seawater and zooplankton off the Joban–Sanriku coast and in Sendai Bay that occurred from June 2011 to December 2013 based on data from Kaeriyama et al. (2014). Although ^{134}Cs was also determined, the decreasing trend of ^{134}Cs during more than 2 years was strongly affected by the physical decay of ^{134}Cs. Thus, only ^{137}Cs is presented (^{134}Cs data were reported in

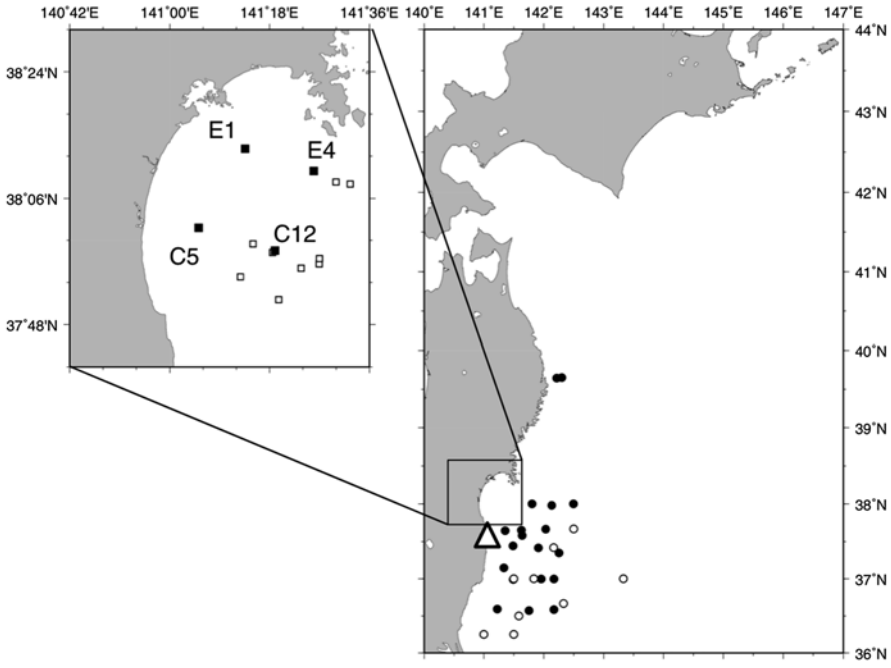

Fig. 3.1 Seawater and zooplankton sampling locations. *Filled and open circles* indicate sampling locations off the Joban–Sanriku coast in 2011 and in 2012, respectively. *Filled and open squares* indicate the repeated sampling stations (E1, E4, C5, C12) and other stations, mostly observed in June 2011 in Sendai Bay. The Fukushima Dai-ichi Nuclear Power Plant is shown as an *open triangle* in the *right panel* (Modified from Kaeriyama et al. 2014)

Kaeriyama et al. 2014). The fate of FNPP-derived radioactive Cs in seawater and zooplankton is also discussed in regard to the atomic ^{137}Cs/stable Cs ratio and the relationship between ^{137}Cs in seawater and ^{137}Cs aCR of zooplankton.

3.2 Temporal Changes of ^{137}Cs in Seawater and Zooplankton

After the FNPP accident, environmental ^{137}Cs concentrations increased in seawater and zooplankton in the area off the Joban–Sanriku coast and in Sendai Bay. Off the Joban–Sanriku coast, the concentration of ^{137}Cs decreased drastically by one order of magnitude between 2011 and 2012 (Fig. 3.2a). Generally, the behavior of cesium is thought to be conservative. Cesium is a soluble substance (<1 % is attached to marine particles) (Buesseler et al. 2011), and it is dispersed primarily by ocean currents. In fact, FNPP-derived radioactive Cs was dispersed eastward rapidly in the North Pacific, with an estimated speed of 8 cm/s, following predominant water currents (Aoyama et al. 2013). According to Kaeriyama et al. (2013), ^{134}Cs and ^{137}Cs concentrations in surface seawaters at 144°E decreased by one or two orders of magnitude between July 2011 and July 2012. The fate of ^{137}Cs off the Joban–Sanriku coast also mainly depends on seawater dilution. In Sendai Bay, the ^{137}Cs monthly average value measured in seawater drastically decreased from 770 mBq/kg in June to 30 mBq/kg in December 2011. Subsequently, the decreasing trend continued, although moderately, until the concentration reached 7 mBq/kg in November–December 2013 (Fig. 3.2a). The residence time of seawater in Sendai Bay has been estimated to be 40 days (Kakehi et al. 2012) even for calm ocean conditions; therefore, the rapid decrease in ^{137}Cs observed during the first year following the FNPP accident might have been influenced by the level of water exchange in this bay. ^{137}Cs peaked in surface waters between June and September 2011 at the E1, E4, and C5 sampling stations, although the vertical differences in ^{137}Cs concentrations were not obvious in December 2011 for the same stations (Fig. 3.3). The depth of the seasonal mixed layer may also influence the seasonal variation observed in the seawater ^{137}Cs vertical profile. In April 2012, the differences observed in ^{137}Cs concentrations between the surface and the middle or bottom waters were reduced in comparison with the differences observed during June and September 2011. During 2011–2012, winter mixing led to a homogeneous vertical distribution of ^{137}Cs in this bay.

In contrast to the rapid decrease of FNPP-derived radioactive Cs measured in seawater, the concentration of ^{137}Cs in zooplankton showed only a gradual decrease over the course of this study. ^{137}Cs concentration in zooplankton ranged from 0.21 to 23 Bq/kg-wet (Fig. 3.2b). Off the Joban–Sanriku coast, the median ^{137}Cs concentration in zooplankton decreased from 1.4 to 0.39 Bq/kg-wet between July–August 2011 and August 2012 (Fig. 3.2b). Although these data varied considerably among stations, the ^{137}Cs concentrations in zooplankton differed significantly between July–August 2011 and August 2012 (Wilcoxon rank-sum test, $p<0.05$). In Sendai Bay, ^{137}Cs concentrations in zooplankton did not differ significantly between zoo-

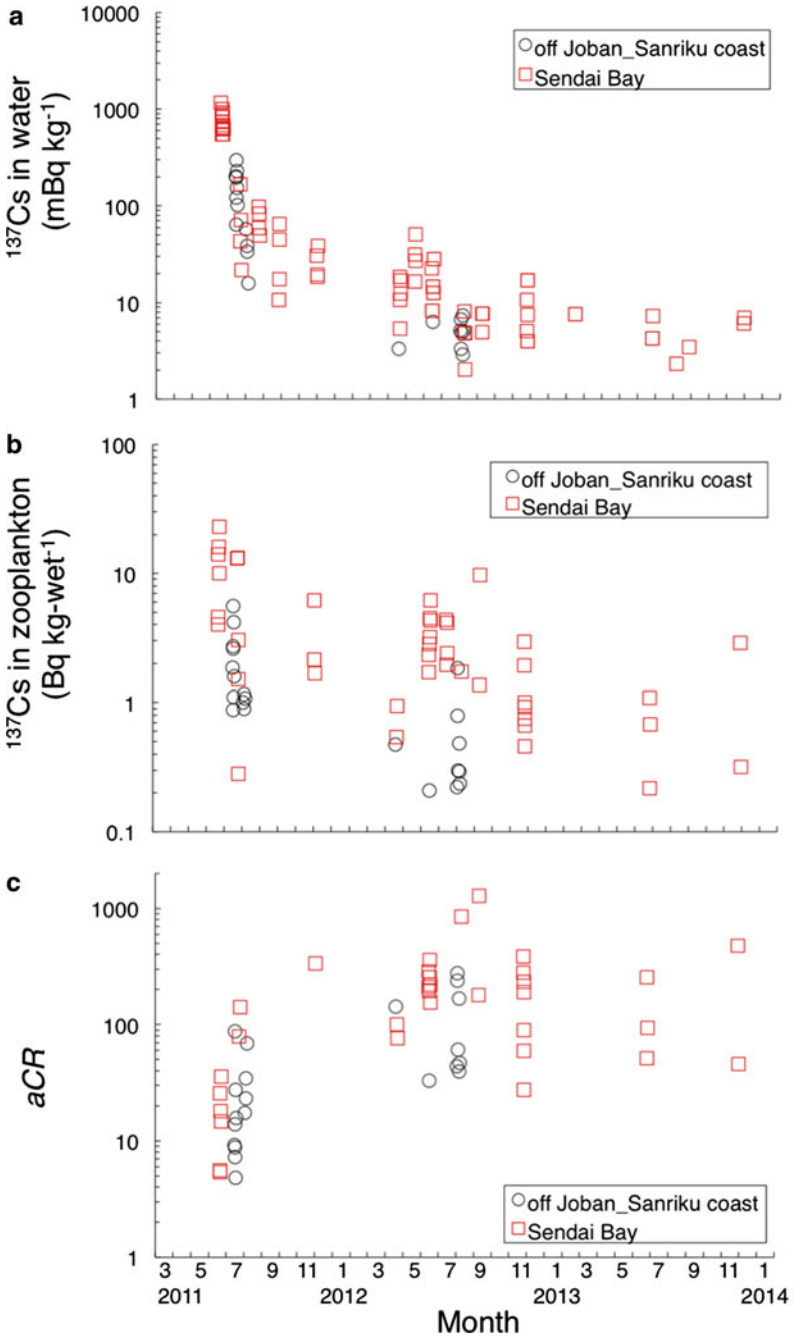

Fig. 3.2 Temporal changes in the concentration of ^{137}Cs in seawater (average value of two or three depth strata) (**a**) and in zooplankton (**b**), and the apparent concentration ratio (*aCR*) for zooplankton (**c**). *Black open circles and red squares* indicate data obtained off the Joban–Sanriku coast and in Sendai Bay, respectively (Modified from Kaeriyama et al. 2014)

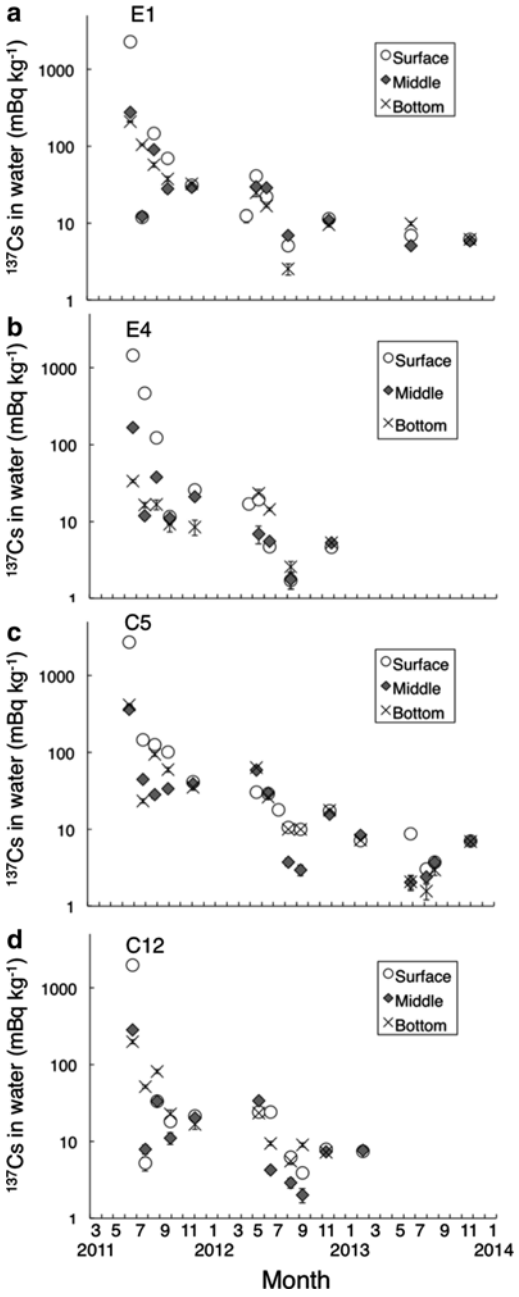

Fig. 3.3 Temporal changes in ^{137}Cs concentration in seawater at E1 (**a**), E4 (**b**), C5 (**c**), and C12 (**d**) in Sendai Bay. *Open circles, filled diamonds, and crosses* indicate the concentration of ^{137}Cs in surface, middle, and bottom waters, respectively (Modified from Kaeriyama et al. 2014)

plankton collected using a Bongo net and a sledge net (Wilcoxon rank-sum test, $p > 0.05$). The temporal change in the ^{137}Cs concentration of zooplankton, in terms of the median value calculated for each sampling period, clearly decreased from June 2011 to April 2012, slightly increased and fluctuated between June and September 2012, and then decreased again between September 2012 and June 2013 (Fig. 3.2b). The median ^{137}Cs value measured in zooplankton in November 2013 was 13 % of that measured in June 2011.

The concentration of radioactive Cs in marine organisms is mainly influenced by the rate of excretion of the organism and its intake of radioactive Cs from the prey and the surrounding seawater. Iwata et al. (2013) estimated the "ecological half-life" (T_{eco}) for marine organisms collected off the Fukushima prefecture. T_{eco} is defined as the time required for the radionuclides concentration to decline by 50 % in a natural population. This value is influenced by both abiotic factors (such as temporal changes in the concentration of radioactive Cs in seawater, extension of the contaminated area, temperature, and salinity) and biotic factors (such as life stages, feeding habitat, and population migration range). The T_{eco} for the zooplankton samples collected in Sendai Bay and off the Joban–Sanriku coast was estimated to be 263 ± 48 days ($T_{eco} \pm$ SE, $p < 0.0001$) and 178 ± 31 days ($p < 0.0001$), respectively. The difference in T_{eco} values between Sendai Bay and the Joban–Sanriku coast may result from the difference in the decreasing rate of ^{137}Cs in the surrounding seawater. The time required for a 50 % decline of ^{137}Cs in seawater in Sendai Bay (122 ± 10 days, $p < 0.0001$) was longer than that of the Joban–Sanriku coast (85 ± 8 days, $p < 0.0001$). The ratios of T_{eco} of zooplankton to the time required for 50 % decline in seawater in Sendai Bay and off the Joban–Sanriku coast are almost comparable (2.2 vs. 2.1), suggesting that the decreasing rate of ^{137}Cs in zooplankton was strongly affected by the decreasing rate of ^{137}Cs in ambient seawater.

3.3 Dynamic Equilibrium of Radioactive Cs Between Zooplankton and Seawater

The concentration of radioactive Cs in marine organisms is mainly influenced by the rate of uptake of radioactive Cs from prey and the surrounding seawater and the excretion rate from the organism, which comes down to the dynamic equilibrium of radioactive Cs between organisms and the surrounding seawater. The atomic ratio of radioactive Cs and stable Cs in organisms and seawater is a good indicator of whether dynamic equilibrium between the organism and seawater has been reached (Tateda and Koyanagi 1994, 1996; Tateda 1998). The range of stable Cs concentrations in this study (16–190 ng/g-dry; Table 3.1) is comparable to the reported values of zooplankton collected around the Japan Islands before the FNPP accident (12–447 ng/g dry; Kaeriyama et al. 2008b; Masuzawa et al. 1988; Marumo et al. 1998; Tateda 1998). The atomic ^{137}Cs/Cs ratio in zooplankton ($0.063–5.1 \times 10^{-7}$; Table 3.1) was one or two order of magnitudes higher than previously reported ($2.7 \pm 2.0 \times 10^{-9}$ (Tateda 1998). Furthermore, the atomic ^{137}Cs/Cs ratio fluctuated with time, and high

Table 3.1 Concentrations of ^{137}Cs and stable Cs in zooplankton and the atomic ^{137}Cs/Cs ratios in zooplankton and seawater

Station ID	Latitude	Longitude	Sampling date	Days from March 11 2011	^{137}Cs (Bq/kg-wet)	Stable Cs (ng/g-dry)	Atomic ^{137}Cs/Cs ratio	
							Zooplankton ($\times 10^{-7}$)	Seawater[a] ($\times 10^{-9}$)
Off Joban–Sanriku coast								
F250	37°34.8′N	141°38.37′E	2012/4/19	405	0.47	154	0.063	3.5
F250	37°34.8′N	141°38.37′E	2012/6/16	463	0.21	63	0.10	6.6
SY20	37°00.0′N	141°30.0′E	2012/8/3	511	1.8	34	1.1	3.4
SY21	37°00.0′N	141°50.0′E	2012/8/3	511	0.79	34	0.66	6.9
SY22	37°00.0′N	143°50.0′E	2012/8/4	512	0.30	27	0.45	5.1
SY16	36°15.0′N	141°00.0′E	2012/8/6	514	0.29	34	0.17	3
SY17	36°15.0′N	141°30.0′E	2012/8/6	514	0.49	79	0.18	7.7
F250	37°34.8′N	141°38.37′E	2012/8/7	515	0.24	41	0.092	5.3
Sendai Bay								
C16	37°56.6′N	141°26.9′E	2011/7/22	133	0.28	34	0.18	NS[b]
C10	37°59.5′N	141°15.0′E	2011/12/3	267	1.7	53	0.62	NS
E1	38°13.1′N	141°13.1′E	2012/4/22	408	0.95	54	0.25	13
E4	38°09.9′N	141°26.0′E	2012/6/15	462	2.3	16	5.1	8.5
C5	38°01.8′N	141°05.2′E	2012/6/18	465	6.2	126	2.0	29

C5	38°01.8′N	141°05.2′E	2012/7/14	491	4.3	64	1.8	NS
C10	37°59.5′N	141°15.0′E	2012/7/14	491	2.4	42	2.1	NS
C16	37°56.6′N	141°26.9′E	2012/7/15	492	4.1	35	3.1	NS
C22	37°53.6′N	141°39.0′E	2012/7/15	492	2.0	30	1.6	NS
E4	38°09.9′N	141°26.0′E	2012/8/10	518	1.7	127	0.32	2.2
C5	38°01.8′N	141°05.2′E	2012/9/9	548	1.4	33	1.3	7.9
C5	38°01.8′N	141°05.2′E	2012/9/10	549	9.7	77	3.4	7.9
E1	38°13.1′N	141°13.1′E	2012/11/10	610	3.0	71	1.8	1.8
E4	38°09.9′N	141°26.0′E	2012/11/10	610	1.9	179	0.37	1.8
C5	38°01.8′N	141°05.2′E	2012/11/10	610	1.0	69	0.65	11
C5	38°01.8′N	141°05.2′E	2012/11/10	610	0.46	72	0.28	5.3
E1	38°13.1′N	141°13.1′E	2013/6/15	827	0.68	58	0.28	4.4
C5	38°01.8′N	141°05.2′E	2013/6/15	827	1.1	75	0.35	4.4
C5	38°01.8′N	141°05.2′E	2013/6/15	827	0.22	42	0.12	7.6
E1	38°13.1′N	141°13.1′E	2013/11/15	980	2.9	189	0.50	7.3
C5	38°01.8′N	141°05.2′E	2013/11/15	980	0.32	49	0.26	6.3

Source: Modified from Kaeriyama et al. (2014)

[a]The concentration of stable Cs in seawater was assumed to be 0.29 μg/l (Tateda and Koyanagi 1996)

[b]*NS* no sample

values were observed between June and November 2012 (Table 3.1). According to Tateda and Koyanagi (1996), the mean concentration of stable Cs in Japanese coastal waters was 0.29 μg/l. From this value and the ^{137}Cs concentration in seawater obtained in this study, the atomic ^{137}Cs/Cs ratio of seawater was also calculated (Table 3.1). The geometric mean of the atomic ^{137}Cs/Cs ratio in seawater was 5.6×10^{-9} with a range of $2.2–29 \times 10^{-9}$. The geometric mean is comparable with that obtained before the FNPP accident ($3.5–6.9 \times 10^{-9}$; Tateda and Koyanagi 1996). A high atomic ^{137}Cs/Cs ratio of seawater ($11–29 \times 10^{-9}$) was observed at station E1 in April 2012 and at station C5 in June and November 2012. One of the possible explanations for the temporal and spatial variations in the atomic ^{137}Cs/Cs ratios of seawater and zooplankton may be the pulse input of FNPP-derived ^{137}Cs from land to ocean caused by heavy rain during the typhoon season or ice melt during thaw season. Actually, Nagao et al. (2013) reported that the export flux of ^{137}Cs from land to ocean during the heavy rain season (September 2011) through rivers located in the Fukushima Prefecture contributed 50 % of their annual export flux in 2011 (see also Sect. 2.5). The input of FNPP-derived ^{137}Cs from land to ocean is one of the most important processes affecting the coastal environment and needs further investigation to understand the long-term effects of the FNPP accident on the coastal region. Another possible input source of FNPP-derived radioactive Cs is continuing release from the FNPP harbor; the estimated average release rate of ^{137}Cs was 93 GBq day^{-1} in the summer of 2011 and 8.1 GBq day^{-1} in the summer of 2012 (Kanda 2013). However, as this radioactive Cs would be diluted offshore near the FNPP harbor, the elevation of radioactive Cs concentration in seawater and zooplankton would be almost negligible within the present study area. Judging from the atomic ^{137}Cs/Cs ratio, which was higher than before the FNPP accident in zooplankton but constant in seawater, ^{137}Cs dynamic equilibrium between zooplankton and the surrounding seawater was not attained during the study period.

In contrast to T_{eco} (see Sect. 3.2), the biological half-life (T_b) of zooplankton was reported as 13 days (Vives i Batlle et al. 2007). The T_b of zooplankton strongly suggests that dynamic equilibrium should have been attained during this study. Because the zooplankton samples contained multiple species (such as copepods, euphausiids, amphipods, chaetognath), including those with gut contents, the concentration of radioactive Cs in zooplankton may have been affected by interspecies variability in radioactive Cs concentrations in this study. The species-specific difference in stable Cs content was less than one order of magnitude (Kaeriyama et al. 2008b; Masuzawa et al. 1988; Marumo et al. 1998). Thus, the difference in species composition should not be a major factor influencing radioactive Cs in zooplankton. The gut contents of zooplankton may contain suspended particles and/or clay particles; clay particles have higher radioactive Cs than organic particles such as phytoplankton (Kusakabe et al. 2013). In addition, high concentrations of ^{134}Cs and ^{137}Cs were observed in fecal pellets of zooplankton soon after the Chernobyl accident (Fowler et al. 1987). The stable Cs contents in this study were almost comparable with previous studies based on samples containing gut contents (Kaeriyama et al. 2008b). Thus, the high radioactive Cs in gut contents likely did not affect the concentration of radioactive Cs in zooplankton. At present, it is difficult to determine the reason

for the slow decrease in the rate of ^{137}Cs in zooplankton observed in this study. Laboratory experiments on the uptake and excretion of radioactive Cs by zooplankton under unstable conditions, such as radioactive Cs in seawater/prey that increases/decreases with time, would provide insights on the time-dependent concentration of radioactive Cs in seawater and the corresponding time-dependent concentration of radioactive Cs in zooplankton.

3.4 Temporal Changes of the ^{137}Cs Apparent Concentration Ratio (aCR) of Zooplankton

The ^{137}Cs aCR in zooplankton collected off the Joban–Sanriku coast varied from 5 to 276, and the median value increased with time from 12, measured in July 2011, to 29, measured in August 2011, and to 115, measured in August 2012 (Fig. 3.2c). In Sendai Bay, the aCR varied between 5 and 1,280 throughout the study period. Because of the large variation in ^{137}Cs concentrations among zooplankton samples, aCR also varied within each sampling period in Sendai Bay. The aCR monthly median value increased from 16, measured in June 2011, to 335 in December 2011 and fluctuated by more than 80, up to 854 in August 2012 and 730 in September 2012. The ^{137}Cs aCR of zooplankton increased over time, although it varied significantly between months (Fig. 3.2c). In November–December 2013, the median aCR value (262) was more than one order of magnitude higher than *CR* values obtained before the FNPP accident, which ranged from 6 to 14 (Kaeriyama et al. 2008a). The increase in aCR was mainly associated with differences in the rate of decrease of ^{137}Cs in seawater and zooplankton, as was clearly observed in Sendai Bay. The continuous uptake of ^{137}Cs by zooplankton may lead to a slow rate of decrease of ^{137}Cs in zooplankton.

Figure 3.4a conceptually shows the temporal change in ^{137}Cs expected in seawater and zooplankton following a release of large quantities of ^{137}Cs, similar to the FNPP accident. The concentration of ^{137}Cs in seawater is expected to increase soon after the release, and the increase in ^{137}Cs in zooplankton is observed after that (phase I). A sharp peak of ^{137}Cs is observed in seawater samples, followed by an exponential decrease with time (phase II). On the other hand, the maximum concentration of ^{137}Cs in zooplankton is expected to be delayed from the peak of ^{137}Cs concentration in seawater and to gradually decrease with time (phase III). A time lag in the ^{137}Cs concentration between seawater and zooplankton leads to temporal changes in aCR observed in zooplankton (Fig. 3.4b). Eventually, the rate of decrease of ^{137}Cs in seawater and zooplankton equalizes, and the zooplankton aCR reaches the same level as the CR before the release of ^{137}Cs to the environment (phase IV). The dynamic equilibrium of ^{137}Cs between zooplankton and the surrounding seawater is attained during phase IV. Figure 3.4c shows the relationship between seawater ^{137}Cs and aCR in zooplankton resulting from the temporal changes shown in Fig. 3.4a, b. The relationship between seawater ^{137}Cs concentration and ^{137}Cs zooplankton aCR in this study along with those obtained from previous studies con-

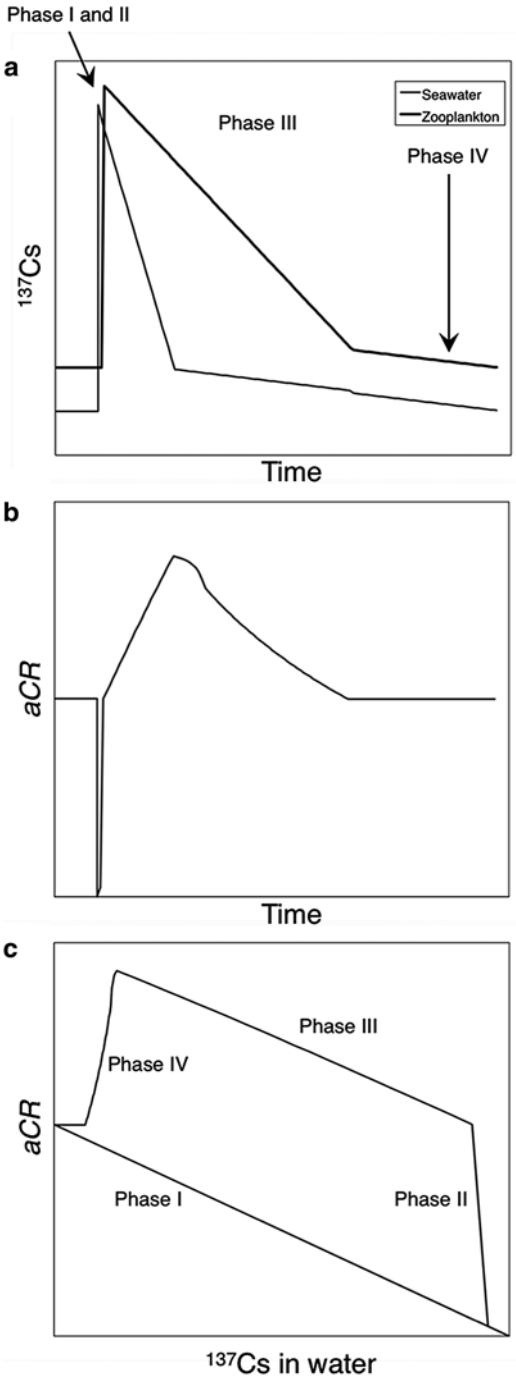

Fig. 3.4 Conceptual temporal variation in ^{137}Cs concentration in seawater (*thin lines*) and in zooplankton (*bold lines*) (**a**), *aCR* for zooplankton (**b**), and a *scatter plot* between ^{137}Cs concentrations in seawater and *aCR* for zooplankton (**c**). The temporal variation of ^{137}Cs is defined as the time-course phase from I to IV (Modified from Kaeriyama et al. 2014)

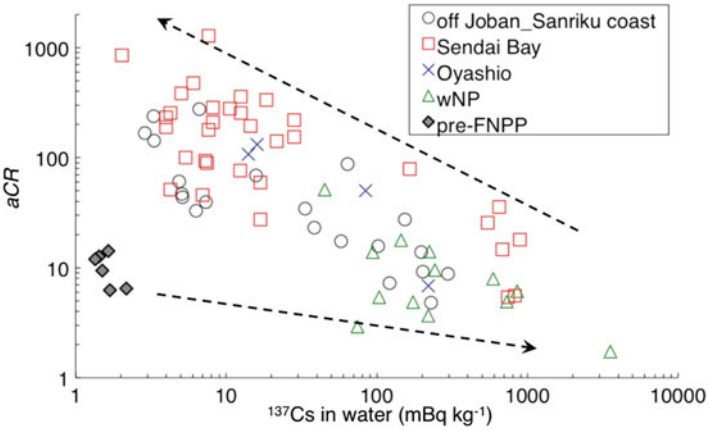

Fig. 3.5 Scatter plot between ^{137}Cs concentration in seawater and *aCR* for zooplankton off the Joban–Sanriku coast (*black open circles*) and in Sendai Bay (*red open squares*) from this study compared to those obtained in June 2011 in the western North Pacific (wNP) (*green open triangles*; Buesseler et al. 2012). The scatter plot between ^{137}Cs concentrations in seawater and the concentration ratio (*CR*) for zooplankton collected off Aomori Prefecture during October 2005 and June 2006, before the FNPP accident, is shown as *black filled diamonds* (data from Kaeriyama et al. 2008a). *Arrows* indicate flow of time (Modified from Kaeriyama et al. 2014)

ducted off the east of Japan in June 2011 (Buesseler et al. 2012) revealed that the pattern observed in Fig. 3.4c corresponds with the aCR increasing phase under dynamic nonequilibrium conditions (phase III; Fig. 3.5). Figure 3.5 also shows data obtained under dynamic equilibrium conditions before the FNPP accident (Kaeriyama et al. 2008a). The time lag expected during the elevation phase (phase I and II) should have occurred during the few months following the FNPP accident; however, this phase is not shown in Fig. 3.5 because these data were not available. On the other hand, the fate of the FNPP-derived ^{137}Cs in seawater and zooplankton varied throughout the 3 years between the FNPP accident and this study, which resulted in the negative correlation shown in Fig. 3.5. Although the ^{137}Cs aCR in zooplankton has steadily increased, the concentration of ^{137}Cs in seawater has remained nearly constant since before the FNPP accident (Fig. 3.5; 1–2 mBq/kg). If no more ^{137}Cs is added to the environment, the aCR in zooplankton would reach the decreasing phase (phase IV), and ^{137}Cs concentration in zooplankton would reach pre-FNPP accident levels in the near future. Based on the T_{eco} of zooplankton off the Joban–Sanriku coast, the ^{137}Cs concentration in zooplankton will reach the pre-FNPP accident level (0.015 Bq/kg-wet) after 2.6 years. Although the data were limited, the observed relationship between ^{137}Cs concentration in seawater and the aCR value measured in zooplankton accurately describes the progression of ^{137}Cs contamination in zooplankton from the beginning of the FNPP accident (dynamic nonequilibrium state) to the restoration phase (dynamic equilibrium state).

3.5 Possible Application of the Relationship Between Seawater ^{137}Cs and aCR to Pelagic Fishes

The concept just mentioned could also be applicable to other marine organisms, in particular to pelagic fishes that prey on zooplankton. Figure 3.6a shows the temporal changes in ^{137}Cs concentration in pelagic fish collected from Sendai Bay and off the Miyagi Prefecture (Fisheries Agency 2014) compared to the seawater and zooplankton concentrations in Sendai Bay shown in Fig. 3.2a, b. The two planktivorous fishes, the sand lance *Ammodytes personatus* and the Japanese anchovy *Engraulis japonica*, together with two carnivorous fishes, the chub mackerel *Scomber japonicus* and the Japanese sea bass *Lateolabrax japonicas*, were selected for this analysis. Figure 3.6b shows the scatter plots between ^{137}Cs in seawater and the aCRs of four fish species in relationship to the ^{137}Cs concentrations measured in zooplankton from Sendai Bay. The concentrations of radioactive Cs in fish published by the Fisheries Agency in 2011 were the total of two radionuclides, ^{134}Cs and ^{137}Cs. The activity ratio of ^{134}Cs to ^{137}Cs just after the FNPP accident is considered to be approximately 1.0 (Chino et al. 2011; Buesseler et al. 2011), and the concentrations of ^{137}Cs, including physical decay, in fish in 2011 were estimated from this ratio. To calculate the ^{137}Cs aCR in fish, the concentration of ^{137}Cs in seawater was estimated from the exponential relationship between the concentrations of ^{137}Cs measured in Sendai Bay and the days since March 11, 2011 (Fig. 3.6a).

The concentration of ^{137}Cs and aCR of planktivorous fishes, sand lance, and Japanese anchovy were similar to those measured for zooplankton. On the other hand, Japanese sea bass showed a higher concentration of ^{137}Cs and aCR than other fish and zooplankton. The species-specific difference in utilization of the environment, both for pelagic and benthic food webs and those from brackish environments in the case of the Japanese sea bass (Kosaka 1969), may have led to the observed difference in ^{137}Cs concentrations and aCRs for the Japanese sea bass and other fish and zooplankton. At present, understanding of the relationship between ^{137}Cs in seawater and the aCR in fish and their change with time is limited. Further analysis that includes ^{137}Cs data from prey items such as benthic organisms and seawater samples covering broader areas is required to completely understand the evolution of ^{137}Cs concentrations in food webs. In addition, ecological/biological features of target fish species, including spatiotemporal distribution, life cycles, and feeding habitats, would provide further insights regarding the effect of the FNPP accident on pelagic ecosystems in coastal areas off the FNPP.

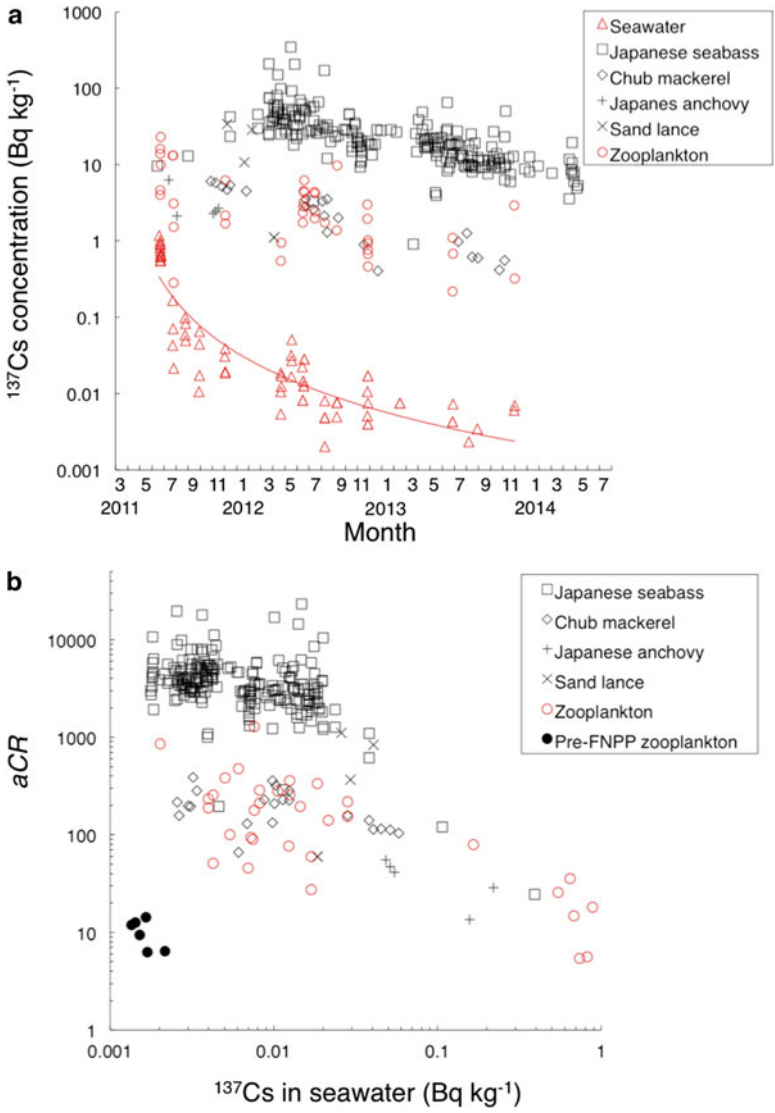

Fig. 3.6 (**a**) Temporal changes in ^{137}Cs concentrations in seawater (*red open triangles*), zooplankton (*red open circles*), sand lance (*black crosses*), Japanese anchovy (*black plus symbols*), chub mackerel (*black open diamonds*), and Japanese sea bass (*open squares*) in Sendai Bay and off the coast of the Miyagi prefecture (Fisheries Agency 2014). (**b**) *Scatter plots* showing the relationship between ^{137}Cs concentration in Sendai Bay seawater and the *aCR* in zooplankton (*red open circles*), sand lance (*black crosses*), Japanese anchovy (*black plus symbols*), chub mackerel (*black open diamonds*), and Japanese sea bass (*black open squares*) in Sendai Bay and off the coast of Miyagi Prefecture. The scatter plot between ^{137}Cs concentration in seawater and the *CR* for zooplankton off Aomori Prefecture, obtained during October 2005 and June 2006 before the FNPP accident, is also shown as *filled circles* (data from Kaeriyama et al. 2008a) (Modified from Kaeriyama et al. 2014)

References

Aoyama M, Uematsu M, Tsumune D, Hamajima Y (2013) Surface pathway of radioactive plume of TEPCO Fukushima NPP1 released ^{134}Cs and ^{137}Cs. Biogeosciences 10:3067–3078

Buesseler KO (2012) Fishing for answers off Fukushima. Science 338:480–482

Buesseler KO, Aoyama M, Fukasawa M (2011) Impacts of the Fukushima nuclear power plants on marine radioactivity. Environ Sci Technol 45:9931–9935

Buesseler KO, Jayne SR, Fisher NS, Rypina I, Baumann H, Baumann Z, Brier CF, Douglass EM, George J, Macdonald AM, Miyamoto H, Nishikawa J, Pike SM, Yoshida S (2012) Fukushima-derived radionuclides in the ocean and biota off Japan. Proc Natl Acad Sci U S A 109:5984–5988

Chino M, Nakayama H, Nagai H, Terada H, Katata G, Yamazawa H (2011) Preliminary estimation of release amounts of ^{131}I and ^{137}Cs accidentally discharged from the Fukushima Daiichi nuclear power plant into the atmosphere. J Nucl Sci Technol 48:1129–1134

Fisheries Agency (2014) Results of the monitoring on radioactivity level in fisheries products. http://www.jfa.maff.go.jp/e/inspection/index.html. Referred at Oct 20, 2014

Fowler SW, Buat-Menard P, Yokoyama Y, Ballestra S, van Holm E, Nguyen H (1987) Rapid removal of Chernobyl fallout from Mediterranean surface waters by biological activity. Nature (Lond) 329:56–58

Howard BJ, Beresford NA, Copplestone D, Telleria D, Proehl F, Fesenko S, Jeffree RA, Yankovich TL, Brown JE, Higley K, Johansen MP, Mulye H, Vandenhove H, Gashchak S, Wood MD, Takata H, Andersson P, Dale P, Ryan J, Bollhofer A, Doering C, Barnett CL, Wells C (2013) The IAEA handbook on radionuclide transfer to wildlife. J Environ Radioact 121:55–74

IAEA (2004) Sediment distribution coefficients and concentration factors for biota in the marine environment. Technical reports series no. 422. IAEA, Vienna

Iwata K, Tagami K, Uchida S (2013) Ecological half-lives of radiocesium in 16 species in marine biota after the TEPCO's Fukushima Daiichi Nuclear Power Plant accident. Environ Sci Technol 47:7696–7703

Kaeriyama H, Watabe T, Kusakabe M (2008a) ^{137}Cs concentration in zooplankton and its relation to taxonomic composition in the western North Pacific Ocean. J Environ Radioact 99:1838–1845

Kaeriyama H, Watabe T, Kusakabe M (2008b) The concentration of ^{137}Cs and stable Cs in zooplankton in the western North Pacific in relation to their taxonomic composition. In: Proceedings of the 16th Pacific Basin Nuclear Conference, paper ID P16P1197, Aomori, Japan, October 2008

Kaeriyama H, Ambe D, Shimizu Y, Fujimoto K, Ono T, Yonezaki S, Kato Y, Matsunaga H, Minami H, Nakatsuka S, Watanabe T (2013) Direct observation of ^{134}Cs and ^{137}Cs in the western and central North Pacific after the Fukushima Dai-ichi Nuclear Power Plant accident. Biogeosciences 10:4287–7295

Kaeriyama H, Fujimoto K, Ambe D, Shigenobu Y, Ono T, Tadokoro K, Okazaki Y, Kakehi S, Ito S, Narimatsu Y, Nakata K, Morita T, Watanabe T (2014) Fukushima-derived radionuclides ^{134}Cs and ^{137}Cs in zooplankton and seawater samples collected off the Joban-Sanriku coast, in Sendai Bay, and in the Oyashio region. Fish Sci. doi:10.1007/s12562-014-0827-6

Kakehi S, Ito S, Yagi H, T Wagawa (2012) Estimation of the residence time of fresh and brackish water in Sendai Bay. J Jpn Soc Civ Eng Ser B2 (Coastal Engineering) 68:951–955 (in Japanese with English abstract)

Kanda J (2013) Continuing ^{137}Cs release to the sea from the Fukushima Dai-ichi Nuclear Power Plant through 2012. Biogeosciences 10:6107–6113

Kitamura M, Kumamoto Y, Kawakami H, Cruz EC, Fujioka K (2013) Horizontal distribution of Fukushima-derived radiocesium in zooplankton in the northwestern Pacific Ocean. Biogeosciences 10:5729–5738

Kosaka M (1969) Ecology of the common sea bass, *Lateolabrax japonicas* in Sendai Bay. J Coll Mar Sci Technol Tokai Univ 3:67–85 (in Japanese with English abstract)

Kusakabe M, Oikawa S, Takata H, Misono J (2013) Spatiotemporal distributions of Fukushima-derived radionuclides in nearby marine surface sediments. Biogeosciences 10:5019–5030

Marumo K, Ishii T, Ishikawa Y, Ueda T (1998) Concentration of elements in marine zooplankton from coastal waters of Boso Peninsula, Japan. Fish Sci 64:185–190

Masuzawa T, Koyama M, Terazaki M (1988) A regularity in trace element contents of marine zooplankton species. Mar Biol 97:587–591

Nagao S, Kanamori M, Ochiai S, Tomihira S, Fukui K, Yamamoto M (2013) Export of ^{134}Cs and ^{137}Cs in the Fukushima river systems at heavy rains by Typhoon Roke in September 2011. Biogeosciences 10:6215–6223

Nuclear Regulation Authority (2014) Monitoring information of environmental radioactivity level. http://radioactivity.nsr.go.jp/en/. Referred at Oct 20, 2014

Tagami K, Uchida S (2013) Marine and freshwater concentration ratios (CRwo-water): review of Japanese data. J Environ Radioact 126:420–426

Tateda Y (1998) Concentration factor of ^{137}Cs for zooplankton collected from the Misaki coastal water. Fish Sci 64:176–177

Tateda Y, Koyanagi T (1994) Concentration factors for ^{137}Cs in marine algae from Japanese coastal waters. J Radiat Res 35:213–221

Tateda Y, Koyanagi T (1996) Concentration factors for ^{137}Cs in Japanese coastal fish (1984–1990). J Radiat Res 37:71–79

Vives i Batlle J, Wilson RC, McDonald P (2007) Allometric methodology for the calculation of biokinetic parameters for marine biota. Sci Total Environ 388:256–269

Wada T, Nemoto Y, Shimamura S, Fujita T, Mizuno T, Sohtome T, Kamiyama K, Morita T, Igarashi S (2013) Effects of the nuclear disaster on marine products in Fukushima. J Environ Radioact 124:246–254

Yoshida N, Kanda J (2012) Tracking the Fukushima radionuclides. Science 336:1115–1116

Part II
Sediments and Benthos

Chapter 4
Three-Dimensional Distribution of Radiocesium in Sea Sediment Derived from the Fukushima Dai-ichi Nuclear Power Plant

Daisuke Ambe, Hideki Kaeriyama, Yuya Shigenobu, Ken Fujimoto, Tsuneo Ono, Hideki Sawada, Hajime Saito, Mikiko Tanaka, Shizuho Miki, Takashi Setou, Takami Morita, and Tomowo Watanabe

Abstract This section introduces results of an investigation for radiocesium (^{134}Cs and ^{137}Cs) in sea sediment. The three-dimensional spatial distributions of radiocesium in sea sediment to a 14-cm core depth were surveyed from off the northern part of Ibaraki Prefecture to off Fukushima Prefecture with 5-min horizontal resolution in July 2012, approximately 16 months after the Fukushima Dai-ichi Nuclear Power Plant (FNPP) accident. A high concentration band was observed along the 100-m isobaths where the

D. Ambe (✉) • H. Kaeriyama • Y. Shigenobu • K. Fujimoto • T. Ono
M. Tanaka • S. Miki • T. Setou
National Research Institute of Fisheries Sciences, Fisheries Research Agency,
2-12-4, Fukuura, Kanazawa, Yokohama, Kanagawa 236-8648, Japan
e-mail: Ambe@affrc.go.jp

H. Sawada
National Research Institute of Fisheries Engineering, Fisheries Research Agency,
7620-7, Hasaki, Kamisu, Ibaraki 314-0408, Japan

Maizuru Fisheries Research Station, Field Science Education and Research Center,
Kyoto University, Nagahama, Maizuru, Kyoto 625-0086, Japan

H. Saito
National Research Institute of Fisheries Engineering, Fisheries Research Agency,
7620-7, Hasaki, Kamisu, Ibaraki 314-0408, Japan

Agriculture, Forestry, and Fisheries Council, Agriculture, Forestry and Fisheries Research Council, 1-2-1, Kasumigaseki, Chiyoda-ward, Tokyo 100-8907, Japan

T. Morita
National Research Institute of Fisheries Sciences, Fisheries Research Agency,
2-12-4, Fukuura, Kanazawa, Yokohama, Kanagawa 236-8648, Japan

Fisheries Agency, 1-2-1, Kasumigaseki, Chiyoda-ward, Tokyo 100-8907, Japan

T. Watanabe
Tohoku National Fisheries Research Institute, Fisheries Research Agency,
3-27-5, Shinhama, Shiogama, Miyagi 985-0001, Japan
e-mail: wattom@affrc.go.jp

K. Nakata, H. Sugisaki (eds.), *Impacts of the Fukushima Nuclear Accident on Fish and Fishing Grounds*, DOI 10.1007/978-4-431-55537-7_4

concentration of the ^{137}Cs reached 1,240 Bq/kg-dry at the maximum and where vertical profiles of the concentration generally had an exponential-type decline with depth. The concentrations were very low at the area shallower than 100 m of depth north from the FNPP, where vertical concentration peaks often occurred in deeper layers. These horizontal and vertical distribution patterns are suggested to be mainly determined by the supplied amount of radiocesium from the radiocesium-contaminated bottom seawater and the ability of radiocesium adsorption as dependent on the grain size of the sediment.

Keywords Radiocesium • Sea sediment • Grain size • Organic matter • Bottom seawater

4.1 Introduction

The Fukushima Dai-ichi Nuclear Power Plant (FNPP) accident associated with the Great Earthquake and ensuing tsunami that occurred east of Japan on March 11, 2011 caused a serious discharge of anthropogenic radionuclides directly into the sea environment from that site. Although a large part of the FNPP-derived radiocesium (^{134}Cs and ^{137}Cs) released directly into the ocean, which was one of the main discharged radionuclides (TEPCO 2012), was transported and diffused to the open ocean by ocean currents (Buesseler et al. 2011; Aoyama et al. 2012; Tsumune et al. 2012; Kaeriyama et al. 2013, 2014), the radiocesium remained with relatively high concentration levels in sea sediment off East Japan (Kusakabe et al. 2013).

Because ^{134}Cs and ^{137}Cs have long half-lives, about 2.06 years and 30.17 years, respectively, these isotopes are of concern about their affects on the marine benthic ecosystems. A report of marine organism monitoring (Wada et al. 2013) indicated that the radiocesium concentrations in demersal fishes tended to have a higher and slower decline than those in pelagic fish. Therefore, evaluation of the impact of the radiocesium in the sea bottom environment on marine benthic ecosystems is strongly and socially required, but detailed distribution of the radiocesium on the sea bottom and its features had been unclear. In this chapter, the three-dimensional distribution of the radiocesium concentration in sea sediment on July 2012, which was reported by Ambe et al. (2014), is introduced. They revealed the detailed spatial distribution of radiocesium in sediments off the northern part of Ibraki Prefecture to Fukushima Prefecture, with 5-min horizontal resolution (Fig. 4.1). Furthermore, they also obtained the vertical structures of radiocesium in sediment to a 14-cm depth from the sea bottom by tube-type sediment core sampling (Fig. 4.2). (For details of the collecting and analyses for the sediment samples, please see the original article.) The discussion by Amber et al. for formative factors of the distribution of radiocesium in sediment is also introduced here.

4.2 Horizontal Distribution of Radiocesium

Figure 4.3 shows the obtained distributions of ^{134}Cs and ^{137}Cs concentrations in the 0–1, 1–2, 2–4, 4–6, 6–10, and 10–14 cm layers on July 2012 by Ambe et al. (2014). The ^{134}Cs concentrations were detected at all sampled locations to the 2–4 cm layer,

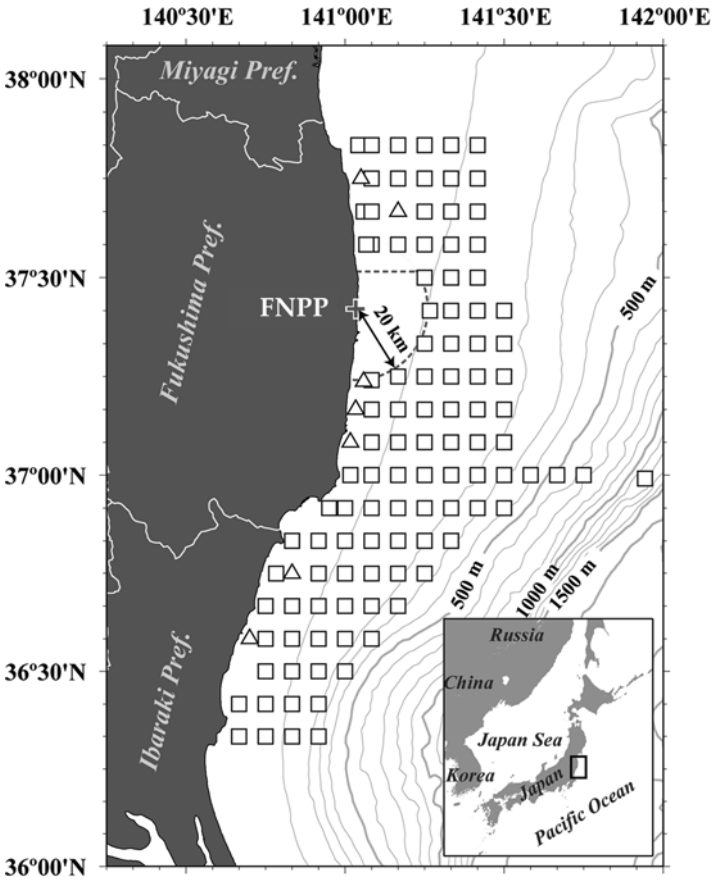

Fig. 4.1 Location of survey for radiocesium concentration in sea sediment in July 2012. Sediments were sampled with a tube-type core sampler (*squares*) and a Smith–McIntyre grab sampler (*triangles*). *Contour lines* indicate water depth at an interval of 100 m. *Cross* indicates the location of the Fukushima Dai-ichi Nuclear Power Plant (FNPP). *Dotted line* indicates a caution zone that had been established during the survey period by the Japanese government

Fig. 4.2 Photographs of collecting sea sediment by a tube-type core sampler

indicating that radioactive contamination reached this depth by 16 months after the FNPP accident. Although the obtained data were sparse in the deeper layer because of the absence of sediment samplings, they indicated some interesting features of horizontal patterns of radiocesium concentration throughout those sediment layers.

One point is that sediments with relatively high concentrations were distributed along and near the coast and and in 100-m isobaths. For example, concerning the ^{137}Cs concentrations in the 0–1 cm sediment layer (Fig. 4.3g), where the geometric mean of the concentration value was 100 Bq/kg-dry in the whole area with a value

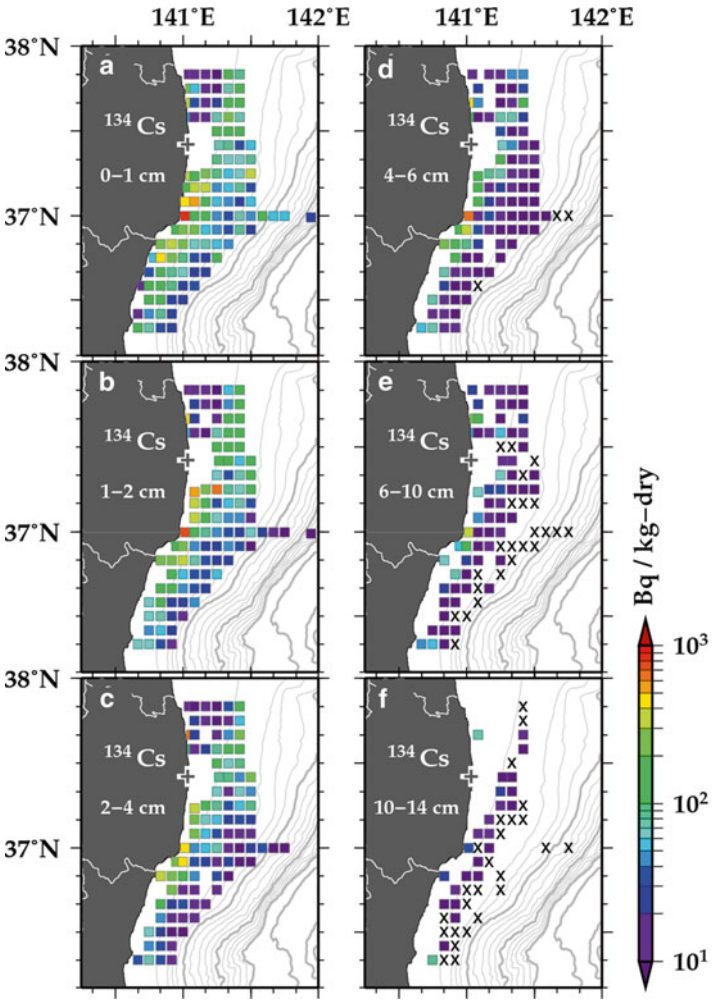

Fig. 4.3 Spatial distributions of ^{134}Cs (**a**–**f**) and ^{137}Cs (**g**–**l**) concentrations in sediment in July 2012. The respective nuclide and layer are indicated at the *upper left side* of each map. "X" mean that radiocesium was not detected (concentration was less than the lower limit of detection, which was from 0.63 to 3.0 Bq/kg-dry). *Blank tiles* mean data missing where no sample was collected. *Contour lines* indicate water depth at an interval of 100 m. *Cross* indicates the location of the FNPP

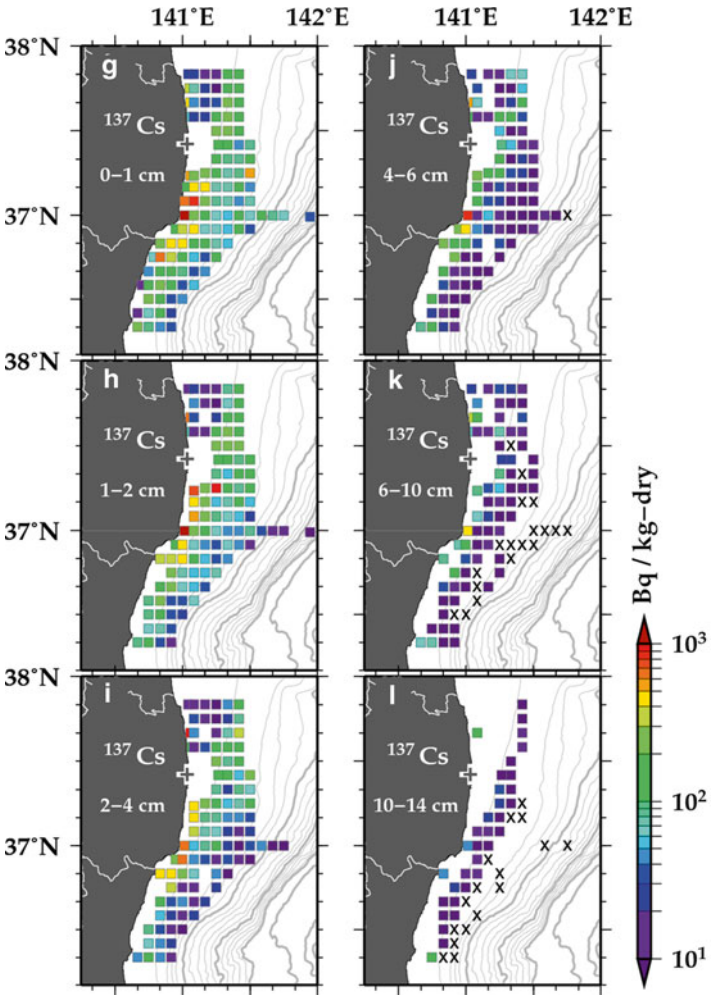

Fig. 4.3 (continued)

range from 8.8 to 1,240 Bq/kg-dry, most of the concentrations higher than 150 Bq/kg-dry were distributed in these areas. It can be also seen that the high-concentration bands were divided into two in the northern part of Fukushima Prefecture, associated with the 100-m isobath that goes away from the coast there.

Another significant feature is that sediments with relatively low concentrations were found between the two high-concentration bands in the northern part of Fukushima Prefecture. The concentration value less than approximately 20 Bq/kg-dry was locally concentrated in this area. Furthermore, a narrow minimal concentration band of 30–60 Bq/kg-dry in the 0–1 cm sediment layer also seemed to exist near the 200-m isobaths in about 20–30 km east from the high-concentration band in the south of the FNPP. Because this low band did not quite range over plural grid points from east to west, the band width was probably less than 15 km (for instance,

a longitudinal 5-min grid interval is approximately 7.4 km at 37°N). These results indicate that radiocesium concentration does not simply decrease toward offshore.

4.3 Vertical Distribution of Radiocesium

Figure 4.4 shows all the acquired vertical profiles of the ^{137}Cs concentrations in the sea sediment in July 2012. Although the ^{137}Cs concentration values ranged widely over two orders of magnitude in each layer, the values from the 25 to 75 percentiles ranged less than one order of magnitude. The median value was the highest in the uppermost layer from the surface (0–1 cm), and generally exponentially decreased in deeper layers; the median values were 102, 78.3, 46.8, 19.3, 13.1, and 6.54 Bq/kg-dry in the 0–1, 1–2, 2–4, 4–6, 6–10, and 10–14 cm layers, respectively. Cases wherein the highest concentration was found in the surfacemost layer occupied 53 % of all the profiles. In the remaining cases, the concentration peaks were found in layers deeper than 0–1 cm.

To detect areas with concentration peaks in the deeper layers, all the ^{137}Cs concentration data were converted to relative ratios to ^{137}Cs concentration in the 0–1 cm layer at each location (Fig. 4.5). It can be seen that relatively high ratios were found near the coast. Ambe et al. (2014) suggested resuspension and redeposition pro-

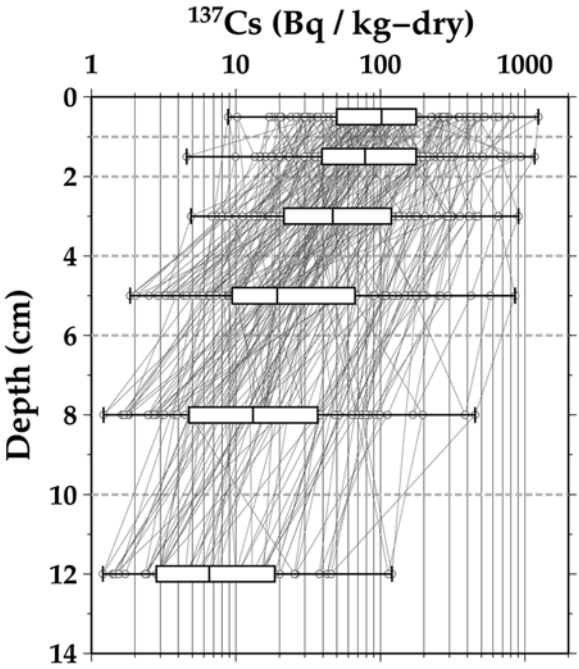

Fig. 4.4 All obtained vertical profiles (*gray lines with circles*) of ^{137}Cs concentration in July 2012. The *box-and-whisker plot* shows the minimum value, the 25th, 50th, and 75th percentiles, and the maximum value, respectively, in each layer

cesses of sediment as possible causes for this factor; that is, in the coastal region, the sea bottom is easily disturbed by ocean waves and bottom currents in general. Therefore, sediment contaminated by radiocesium at the surface and that uncontaminated in deep layers can be mixed or overturned. However, they also suggested another process can operate at the area north of the FNPP where the radiocesium concentrations were very low (Fig. 4.3); the relative ratios were especially high in the deeper layers there. In this regard, a possible factor is introduced with the grain size of sea sediment in the following section.

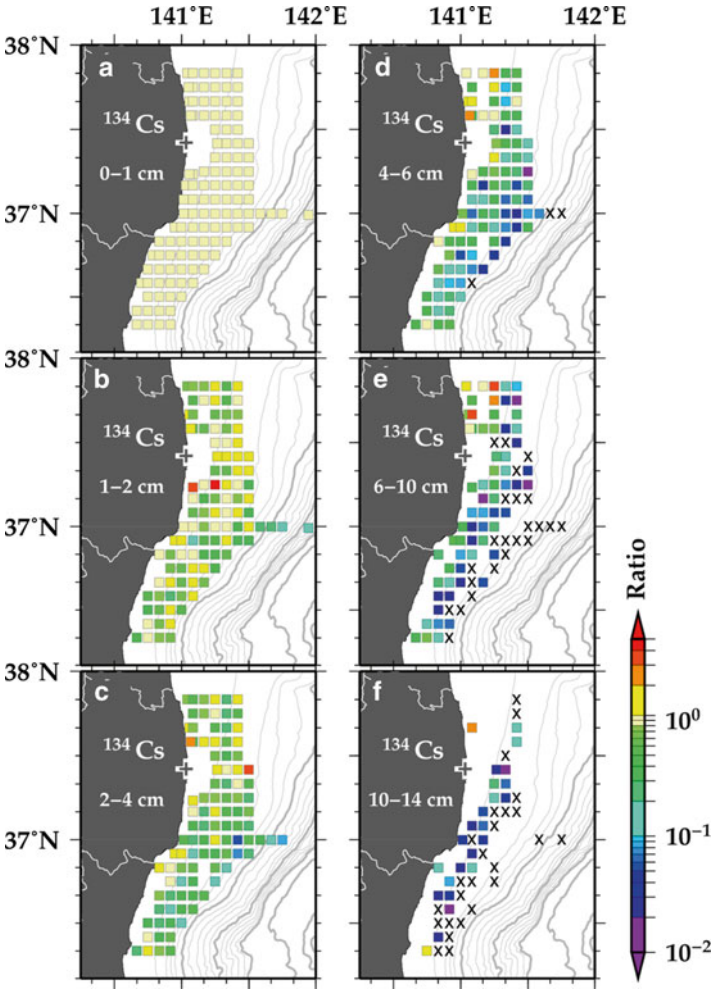

Fig. 4.5 Relative magnitude of ^{134}Cs (**a–f**) and ^{137}Cs (**g–l**) concentration compared with in the surface-most (0–1 cm) sediment at each location in July 2012. The respective layer is indicated at the *side* of each map

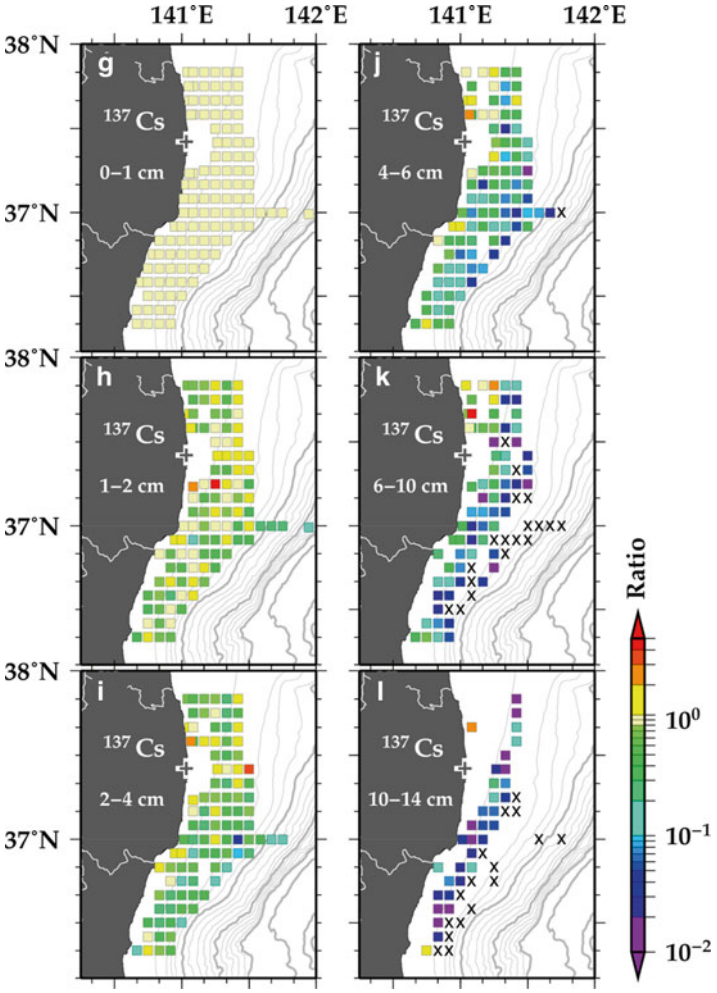

Fig. 4.5 (continued)

4.4 Grain-Size Distribution and Relationship with Radiocesium Concentrations in Sediment

Figure 4.6 shows the horizontal distribution of the median grain sizes of sediments in the surface layer (0–1 cm). Relatively large grain sizes were distributed in the north of the FNPP where the radiocesium concentrations were very low (Fig. 4.3), whereas a band of very small grain sizes, less than 100 μm diameter, was found around the 100-m isobaths where the radiocesium concentrations were high (Fig. 4.3). Ambe et al. (2014) further showed a significant correlation between ^{137}Cs

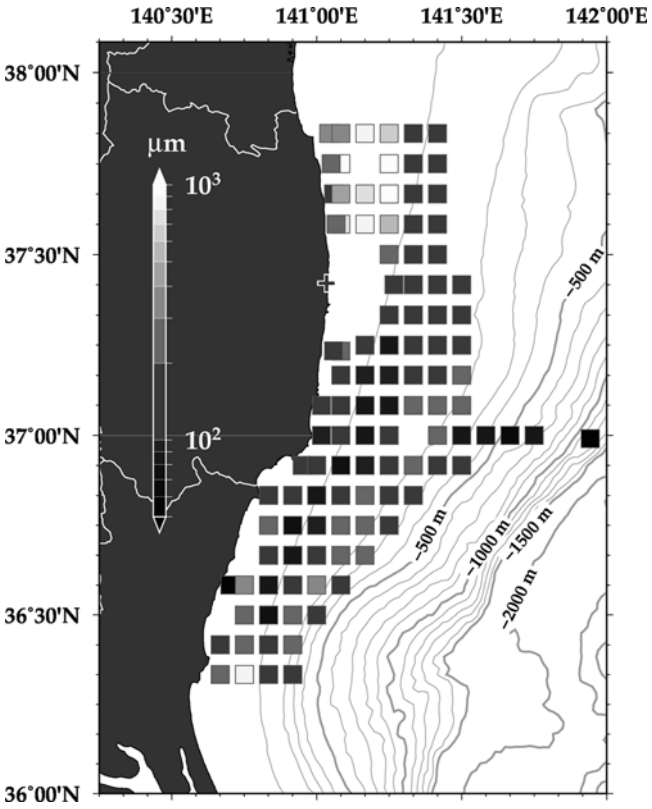

Fig. 4.6 Spatial distribution of median particle grain size of the surface-most sediment in July 2012

concentration and median grain size: the correlation coefficient is −0.38 ($p<0.01$) (Fig. 4.7a). It is well known that Cs has strong affinity with fine minerals, especially illite minerals (Børrentzen and Salbu 2012; Comans et al. 1991; Comans and Hockley 1992; Sakuma and Kawamura 2011). Indeed, by sieving and dividing the surface sediment samples into three grain-size fractions (<106, 106–250, and >250 μm), we also obtained similar results, that is, the finer-size fraction of the sediment samples had higher radiocesium concentrations than the bulk sediment in most cases (Fig. 4.8). Thus, the probable grain size-dependent adsorption capability of cesium is strongly suggested as one of the factors that determines the spatial distribution pattern of radiocesium concentration. In addition, as the proportional relationship between the permeability and grain size of sediment is also well known (Shepherd 1989), dissolved radiocesium can migrate downward with seawater through large-grained sediments. Therefore, it can be considered that higher radiocesium concentrations than those in the surface sediment existed in deeper layers at the area north from the FNPP, as indicated in the previous section.

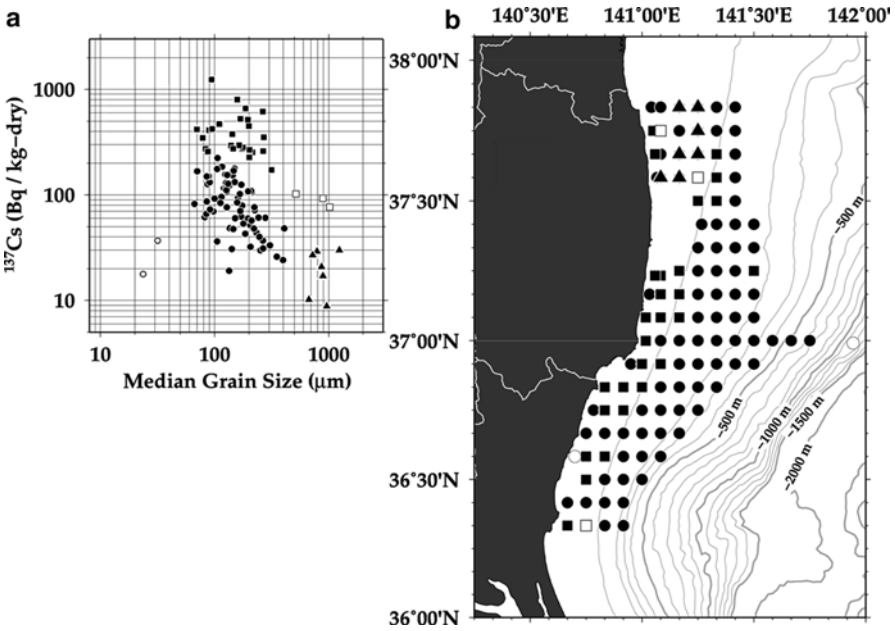

Fig. 4.7 (**a**) Comparison between ^{137}Cs concentration and median grain size in the most-surface sediment. The *symbols* for the scatter plot show the clusters segmented into five types by the group average method; the corresponding locations of those types are projected in (**b**)

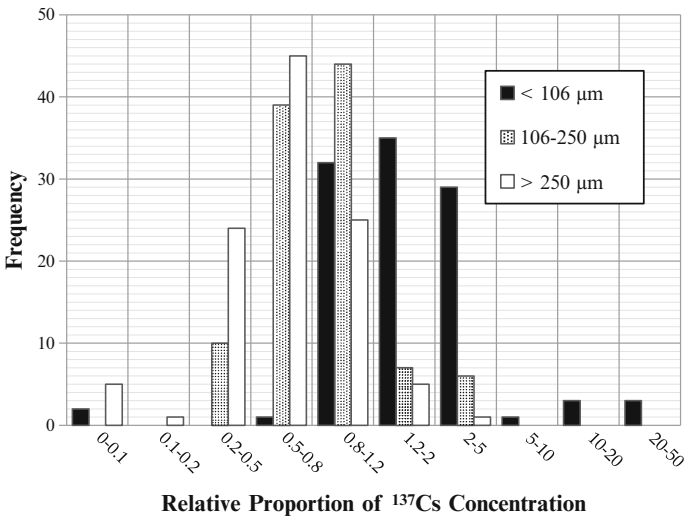

Fig. 4.8 Histograms of relative magnitude of ^{137}Cs concentration in each diameter class of the surface-most sediment compared with the concentration in bulk sediment. Diameter classes are indicated at *upper right*

Ambe et al. (2014) also indicated that the quantity of radiocesium supplied to the sea bottom from seawater is another factor to determine the distribution of the radiocesium concentration in sea sediment. The concentrations ranged over more than one order of magnitude in each similar grain-size class, but the samples could be divided into five clusters (symbols in Fig. 4.7a) by cluster analysis based on the group average method (Romesburg 2004), using the distance on the coordinate between the median grain size and ^{137}Cs concentration. Accordingly, three types of clusters by geographic dependence were detected (Fig. 4.7b): (1) large grain sizes and low radiocesium concentrations, distributed at depths shallower than 100 m in the region north from the FNPP (indicated by filled triangles in the figure); (2) small grain sizes with high radiocesium concentrations, distributed mainly at depths shallower than 100 m, excepting the area of cluster (1) (indicated by filled squares); and (3) small grain sizes with low radiocesium concentrations, mainly in the area deeper than 100 m (filled circles). The division of cluster (1) from others can be attributed mainly to the low adsorption capability of large-grain-size sediment for cesium, as already mentioned. On the other hand, the radiocesium concentration in bottom seawater could be more than twice or one order higher in the area shallower than 100 m than in the area at 100–300 m depth by monitoring data (Oikawa et al. 2013) and numerical study (Bailly du Bois et al. 2014), for division between the clusters (2) and (3).

4.5 Organic Matter Content and Relationship with Radiocesium Concentration in Sediment

Ambe et al. (2014) also investigated the horizontal distribution of the organic matter content in the surface sediment (as shown in Fig. 4.9a). Although notably higher values, up to almost 10 %, existed along the 100-m isobaths where the radiocesium concentrations were very low, the content was relatively low north of the FNPP where the radiocesium concentrations were high. These patterns highly corresponded to those of the median grain size. Therefore, the organic matter content also was correlated with the ^{137}Cs concentration ($r = 0.38$, $p < 0.01$) and the median grain size ($r = -0.76$, $p < 0.01$) (Fig. 4.9b). This result seems superficially to indicate that organic content also can determine radiocesium concentration. However, a report for radiocesium concentration in the coastal area of Ibaraki Prefecture after the FNPP accident (Otosaka and Kobayashi 2013) indicated that the lithogenic fraction contained most of the ^{137}Cs in the sediment. The contribution of organic matter to the radiocesium concentration in sea sediment is also small by chemical leaching for the samples of Ambe et al. (2014) (as seen in the next chapter). Thus, the organic matter might not be the constitutive factor that determines radiocesium concentration in sea sediment more than 1 year after the FNPP accident. The grain size of sediment could determine the distributions of both the ^{137}Cs concentration and the organic matter content in sediment.

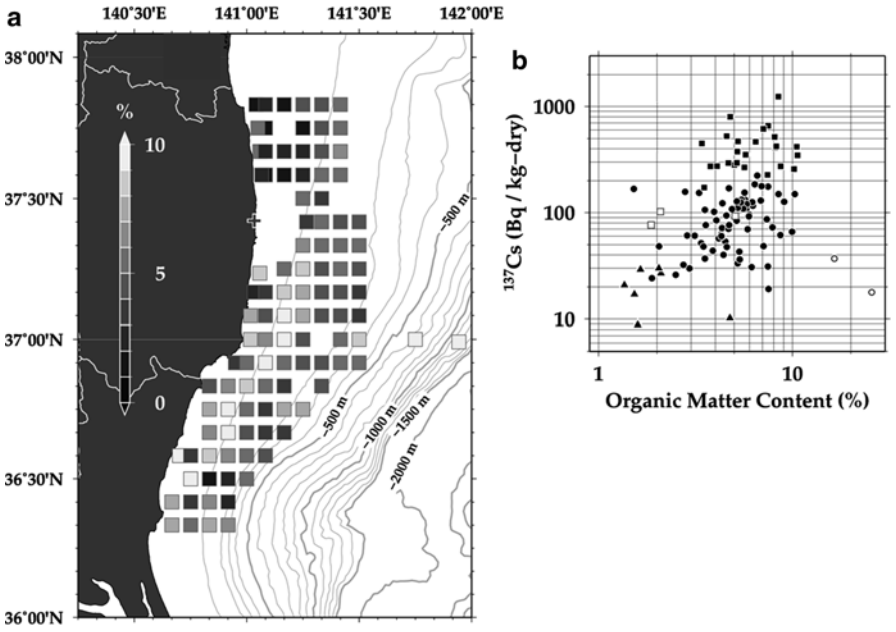

Fig. 4.9 (**a**) Spatial distribution of organic matter content of the surface-most sediment in July 2012. (**b**) Comparison between ^{137}Cs concentration and organic matter content in the surface sediment. Symbols correspond to the result of cluster analysis in Fig. 4.7a

Acknowledgments This study was supported by the Fisheries Agency, Ministry of Agriculture, Forestry and Fisheries, Japan.

References

Ambe D, Kaeriyama H, Shigenobu Y, Fujimoto K, Ono T, Sawada H, Saito H, Miki S, Setou T, Morita T, Watanabe T (2014) Five-minute resolved spatial distribution of radiocesium in sea sediment derived from the Fukushima Dai-ichi Nuclear Power Plant. J Environ Radioact 138:264–275. doi:10.1016/j.jenvrad.2014.09.007

Aoyama M, Tsumune D, Uematsu M, Kondo F, Hamajima Y (2012) Temporal variation of ^{134}Cs and ^{137}Cs activities in surface water at stations along the coastline near the Fukushima Dai-ichi Nuclear Power Plant accident site, Japan. Geochem J 46(4):321–325

Bailly du Bois P, Garreau P, Laguionie P, Korsakissok I (2014) Comparison between modelling and measurement of marine dispersion, environmental half-time and ^{137}Cs inventories after the Fukushima Daiichi accident. Ocean Dyn 64(3):361–383. doi:10.1007/s10236-013-0682-5

Børrentzen P, Salbu B (2012) Fixation of Cs to marine sediments estimated by a stochastic modeling approach. J Environ Radioact 61:1–20

Buesseler K, Aoyama M, Fukasawa M (2011) Impacts of the Fukushima Nuclear Power Plants on marine radioactivity. Environ Sci Technol 45:9931–9935

Comans RNJ, Hockley D (1992) Kinetics of cesium sorption on illite. Geochim Cosmochim Acta 56:1157–1164

Comans RNJ, Haller M, DePreter P (1991) Sorption of cesium on illite: non-equilibrium behavior and reversibility. Geochim Cosmochim Acta 55:433–440

Kaeriyama H, Ambe D, Shimizu Y, Fujimoto K, Ono T, Yonezaki S, Kato Y, Matsunaga H, Minami H, Nakatsuka S, Watanabe T (2013) Direct observation of ^{134}Cs and ^{137}Cs in the western and central North Pacific after the Fukushima Dai-ichi Nuclear Power Plant accident. Biogeosciences 10:4287–7295

Kaeriyama H, Shimizu Y, Ambe D, Masujima M, Shigenobu Y, Fujimoto K, Ono T, Nishiuchi K, Taneda T, Kurogi H, Setou T, Sugisaki H, Ichikawa T, Hidaka K, Hiroe Y, Kusaka A, Kodama T, Kuriyama M, Morita H, Nakata K, Morinaga K, Morita T, Watanabe T (2014) Southwest intrusion of ^{134}Cs and ^{137}Cs derived from the Fukushima Dai-ichi Nuclear Power Plant accident in the western North Pacific. Environ Sci Technol 48:3120–3127

Kusakabe M, Oikawa S, Takata H, Misonoo J (2013) Spatiotemporal distributions of Fukushima-derived radionuclides in nearby marine surface sediments. Biogeosciences 10:5019–5030. doi:10.5194/bg-10-5019-2013

Oikawa S, Takata H, Watabe T, Misonoo J, Kusakabe M (2013) Distribution of the Fukushima-derived radionuclides in seawater in the Pacific off the coast of Miyagi, Fukushima, and Ibaraki prefectures, Japan. Biogeosciences 10:5031–5047. doi:10.5194/bgd-10-4851-2013

Otosaka S, Kobayashi T (2013) Sedimentation and remobilization of radiocesium in the coastal area of Ibaraki, 70 km south of the Fukushima Dai-ichi Nuclear Power Plant. Environ Monit Assess 185:5419–5433. doi:10.1007/s10661-012-2956-7

Romesburg HC (2004) Cluster analysis for researchers. Lulu Press, Morrisville

Sakuma H, Kawamura K (2011) Structure and dynamics of water on Li^+-, Na^+-, K^+-, Cs^+-, H_3O^+-exchanged muscovite surfaces: a molecular dynamics study. Geochim Cosmochim Acta 75:63–81

Shepherd RG (1989) Correlations of permeability and grain size. Ground Water 27:633–638. doi:10.1111/j.1745-6584.1989.tb00476.x

TEPCO (Tokyo Electric Power Co.) (2012) TEPCO news press releases. http://www.tepco.co.jp/en/press/corp-com/release/2012/1204659_1870.html

Tsumune D, Tsubono T, Aoyama M, Hirose K (2012) Distribution of oceanic ^{137}Cs from the Fukushima Dai-ichi Nuclear Power Plant simulated numerically by a regional ocean model. J Environ Radioact 111:100–108. doi:10.1016/j.jenvrad.2011.10.007

Wada T, Nemoto Y, Shimamura S, Fujita T, Mizuno T, Sohtome T, Kamiyama K, Morita T, Igarashi S (2013) Effects of the nuclear disaster on marine products in Fukushima. J Environ Radioact 124:246–254. doi:10.1016/j.jenvrad.2013.05.008

Chapter 5
Radiocesium Concentrations in the Organic Fraction of Sea Sediments

Tsuneo Ono, Daisuke Ambe, Hideki Kaeriyama, Yuya Shigenobu, Ken Fujimoto, Kiyoshi Sogame, Nobuya Nishiura, Takashi Fujikawa, Takami Morita, and Tomowo Watanabe

Abstract Sequential chemical extraction of radiocesium was performed on 22 surface sediment samples to assess radiocesium concentration in the organic fraction of sea sediments (Cs_{org}). Our results showed that Cs_{org} of sea sediments was significantly larger than that of bulk sediments (Cs_{bulk}). The concentration factor of radiocesium in organic fraction against the bulk concentration (CF) varied from 3 to 50 off the Fukushima continental margin and showed a proportional relationship with median grain size and an inversely proportional relationship with organic content (OC) of the sediment. By using these relationships, the regression equation of Cs_{org} based on median grain size, organic content, and Cs_{bulk} was determined to construct a two-dimensional (2-D) distribution of Cs_{org} along the continental margin off the Fukushima region. The resultant map showed that the continental margin north of Fukushima Dai-ichi Nuclear Power Plant (FNPP) had moderate Cs_{org} values despite very low Cs_{bulk}. On the other hand, sediments sampled at the mouth of Abukuma River showed extremely low CF, which might have been caused by the existence of river-derived sediment particles.

Keywords Sediment • Radiocesium • Organic fraction

T. Ono (✉) • D. Ambe • H. Kaeriyama • Y. Shigenobu
K. Fujimoto • T. Morita
National Research Institute of Fisheries Sciences, Fisheries Research Agency,
2-12-4, Fukuura, Kanazawa, Yokohama, Kanagawa 236-8648, Japan
e-mail: tono@affrc.go.jp

K. Sogame • N. Nishiura • T. Fujikawa
KANSO Technos, 3-1-1 Higashikuraji, Katano, Osaka 576-0061, Japan

T. Watanabe
Tohoku National Fisheries Research Institute, Fisheries Research Agency,
3-27-5, Shinhama, Shiogama, Miyagi 985-0001, Japan
e-mail: wattom@affrc.go.jp

K. Nakata, H. Sugisaki (eds.), *Impacts of the Fukushima Nuclear Accident on Fish and Fishing Grounds*, DOI 10.1007/978-4-431-55537-7_5

5.1 Introduction

In the assessment of radiocesium transportation from sea sediments to a marine demersal ecosystem, information is required not only on the concentration but also on biological ingestibility of sea sediment radiocesium. Although IAEA has provided a standard concentration factor of radiocesium from sea sediments in marine organisms (e.g., 1×10^2 for fish; IAEA 2004), its actual value may vary according to sediment properties such as grain size and chemical composition. Radiocesium concentration in the organic fraction of sediments (Cs_{org}) is an important factor because the transport of radiocesium from sediment to demersal ecosystem occurs primarily through the feeding/ingestion of carbon sediments by benthos. With regard to the FNPP accident, a large amount of data is available on the spatiotemporal distribution of radiocesium concentration in sea sediments (Cs_{bulk}) off the Fukushima Prefecture (Otosaka and Kobayashi 2012; Kusakabe et al. 2013; Otosaka and Kato 2014; Ambe et al. 2014). Unfortunately, insufficient data are available on the spatiotemporal distribution of Cs_{org}. To address this issue, we conducted sequential chemical leaching experiments for 21 sea sediments sampled in July 2012 at 5′×5′ grid stations off Fukushima Prefecture (Ambe et al. 2014; see Fig. 5.1 for station map) to measure Cs_{org} of these sediments. For details of sampling stations and experimental procedures, see Ono et al. (2015).

5.2 Cs_{org} and Its Relationship with Cs_{bulk}

Estimated radiocesium concentrations in organic fraction (Cs_{org}) and bulk sediment (Cs_{bulk}) in 21 grid samples are listed in Table 5.1. Cs_{bulk} ranged from 31 to 910 Bq/kg-dry and Cs_{org} ranged from 345 to 3,390 Bq/kg-org-dry. Concentration factor (CF) and inventory ratio (IR) of radiocesium in organic fraction against bulk sediment were then calculated by the following equation:

$$CF = Cs_{org} / Cs_{bulk} \tag{5.1}$$

$$IR = \left(Cs_{org} \cdot OC\right) / Cs_{bulk} \tag{5.2}$$

where OC represents the organic content of the sediment (Table 5.1).

CF values vary from 3 to 50, clearly illustrating that radiocesium concentration in the organic fraction of sea sediments is always several times larger than that of bulk sediment in areas off Fukushima. Despite these high CF values, IR showed relatively low values, ranging from 2.4 % to 13.9 %, reflecting low organic content in open ocean sediments.

Land sediments and soils have highly selective, nonexchangeable cesium adsorption capacity, up to 1×10^{-11} mol/kg-dry, because of the frayed edge sites in illite particles (Nakao et al. 2012). In marine environments, however, such nonexchangeable adsorption sites are occupied by stable cesium ($\sim 2 \times 10^{-9}$ mol/l in seawater) and potassium ($\sim 1 \times 10^{-2}$ mol/l in seawater). Newly supplied radiocesium from the accident, therefore, can only be bound to nonselective, exchangeable sorption sites, with the distribution coefficient of radiocesium estimated to be

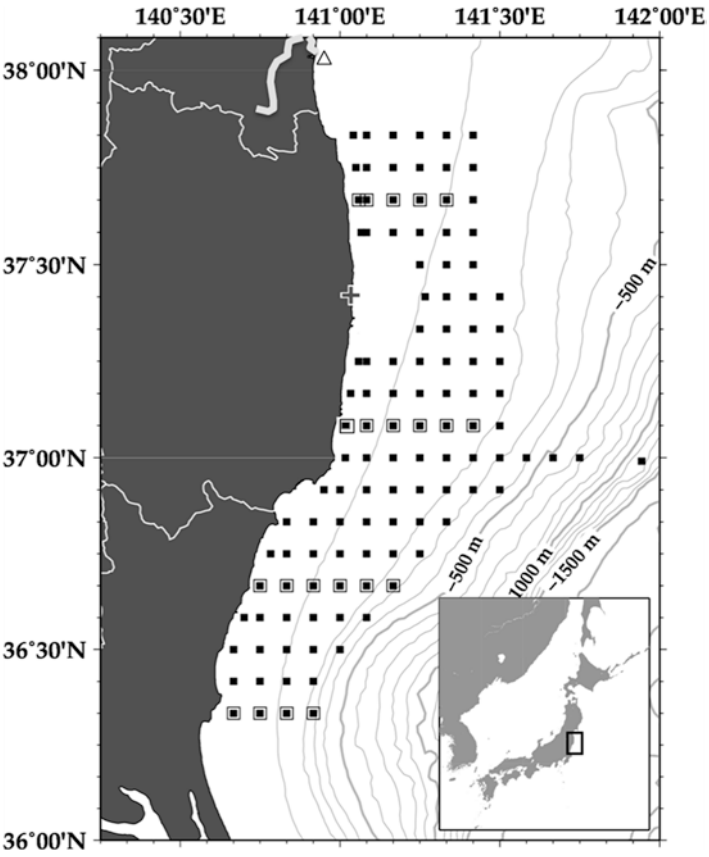

Fig. 5.1 Map of the location of the samples used in this study. *Thick gray line* denotes Abukuma River (only lower reaches are shown). *Open squares* denote the samples used for the bulk extraction experiment (Table 5.1), and *open triangles* denote the location of the off-Abukuma station (Table 5.2). Sampling stations of Ambe et al. (2014) are overlaid as *solid squares*

300–4,000 l/kg-dry (IAEA 2004). Organic substances in the sediments also have nonselective sorption sites for cesium, but so far little is known about the distribution coefficient of cesium between marine organic matter and seawater. On land, several observations have indicated that the distribution coefficient of cesium for organic substances in soils is of the order of 10^2–10^3 l/kg-dry (Bunzl and Schimmack 1991; Nakamaru et al. 2007). If we assume that marine organic substances have the same distribution coefficient of cesium as land soils, we can consider that mineral and organic substances in the off-Fukushima sediments have the same order of preference as FNPP-derived radiocesium. The apparent preference of radiocesium in organic substances further increases when the surface of mineral particles is covered by organic substances (Keil et al. 1994; Mayer 1994; 1999). Mayer (1999), for example, found that even 0.5 % (w/w) of organic carbon can cover more than 10 % of total sediment surface area. In this case, with the assumption that organic carbon and mineral surfaces have the same preference with cesium, the observed CF of radiocesium increases to more than 20.

Table 5.1 Specifications and measurement results of grid samples

Station no.	Sampling date	Latitude [N]	Longitude [E]	Bottom depth (m)	Median grain size (μm)	OC (%)	Cs_{bulk} (Bq/kg-dry)	Cs_{org} [Bq/kg-org-dry]	CF	IR [%]
S1	2012.7.11	36° 20′	140° 55′	257	142	0.8	49±5.5	350	7	5.8
S2	2012.7.11	36° 20′	140° 50′	120	136	0.7	78±6.6	1,440	19	12.0
S3	2012.7.11	36° 20′	140° 45′	59	889	0.4	153±9.7	2,440	16	5.9
S4	2012.7.11	36° 20′	140° 40′	33	201	1.0	310±20	1,090	4	3.4
S20	2012.7.12	36° 40′	141° 10′	261	233	0.6	103±6.3	520	5	3.0
S21	2012.7.12	36° 40′	141° 05′	144	265	0.5	60±4.7	850	14	7.0
S22	2012.7.12	36° 40′	141° 00′	133	161	1.0	180±13	1,330	7	7.3
S23	2012.7.12	36° 40′	140° 55′	111	87	1.6	180±14	960	6	8.9
S24	2012.7.12	36° 40′	140° 50′	70	116	1.0	270±21	1,300	5	4.9
S25	2012.7.12	36° 40′	140° 45′	33	no data	0.3	69±5.9	490	7	2.4
S59	2012.7.13	37° 05′	141° 25′	177	247	0.6	83±5.4	470	6	3.2
S60	2012.7.13	37° 05′	141° 20′	151	225	0.6	104±6.3	2,360	23	13.9
S61	2012.7.13	37° 05′	141° 15′	140	85	1.3	101±7.6	600	6	7.4
S62	2012.7.13	37° 05′	141° 10′	120	87	1.6	440±27	1,200	3	4.5
S63	2012.7.12	37° 05′	141° 05′	72	158	1.6	690±32	1,840	3	4.2
S64	2012.7.12	37° 05′	141° 01′	25	167	0.9	910±32	3,120	3	3.2
S92	2012.7.15	37° 40′	141° 03.5′	24	118	1.0	710±28	3,390	5	4.9
S93	2012.7.15	37° 40′	141° 05′	28	407	0.2	82±5.9	1,270	16	4.0
S94	2012.7.15	37° 40′	141° 10′	37	723	0.1	31±3.4	780	25	3.2
S95	2012.7.15	37° 40′	141° 15′	59	1,240	0.1	47±4.1	2,330	50	5.0
S96	2012.7.15	37° 40′	141° 20′	100	146	0.7	230±16	2,080	9	6.5

All data are reproduced from Ono et al. (2015)

Note: For definitions of Cs_{bulk}, Cs_{org}, OC, CF, and IR, see the text

5.3 Horizontal Distribution of Cs_{org} in off-Fukushima Continental Margin

CF is roughly proportional to median grain size and inversely proportional to OC (Fig. 5.2), suggesting that either or both of these properties are the main control factors of CF, although detailed analysis by Ono et al. (2015) concluded that OC is a major control factor and median grain size is minor. Using this information, we applied dual-parameter regression, appropriate for CF, against median grain size and combustion loss as follows:

$$\mathrm{CF} = 0.0255\mu + 20.08 / \mathrm{IL} - 0.69 \left(r^2 = 0.736, \rho < 0.01 \right) \tag{5.3}$$

where μ and IL represent median grain size in μm (micrometers) and ignition loss in percentage, respectively. We chose IL instead of OC as an explanatory variable because the latter parameter was not measured for all samples reported by Ambe et al. (2014). Although IL somewhat overestimated the actual OC, we confirmed the linearity of IL against OC before the derivation of Eq. (5.3). We applied this equation to 113 surface stations observed by Ambe et al. (2014), and the calculated CF was multiplied by Cs_{bulk} in each station (Fig. 4.3 in Chap. 4) to obtain Cs_{org}. The results are shown in Fig. 5.3. A high Cs_{org} band exists just offshore south of FNPP, within which the highest Cs_{org} value of 10,300 Bq/kg-org-dry was obtained. In this area, the typical range of Cs_{bulk} south of FNPP was 2,000–7,000 Bq/kg-org-dry for the area with a bottom depth shallower than 100 m, and 500–1,500 Bq/kg-org-dry

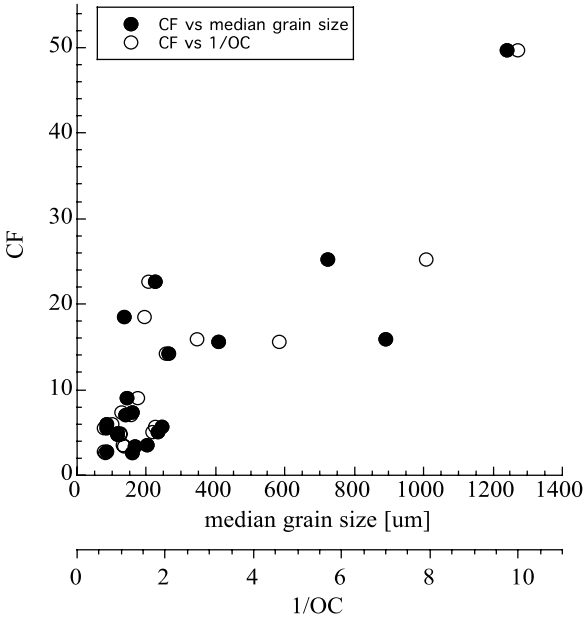

Fig. 5.2 Plot of concentration factor (CF) versus median grain size (*solid circles*) and 1/organic content (OC) (*open circles*) for 21 off-Fukushima samples

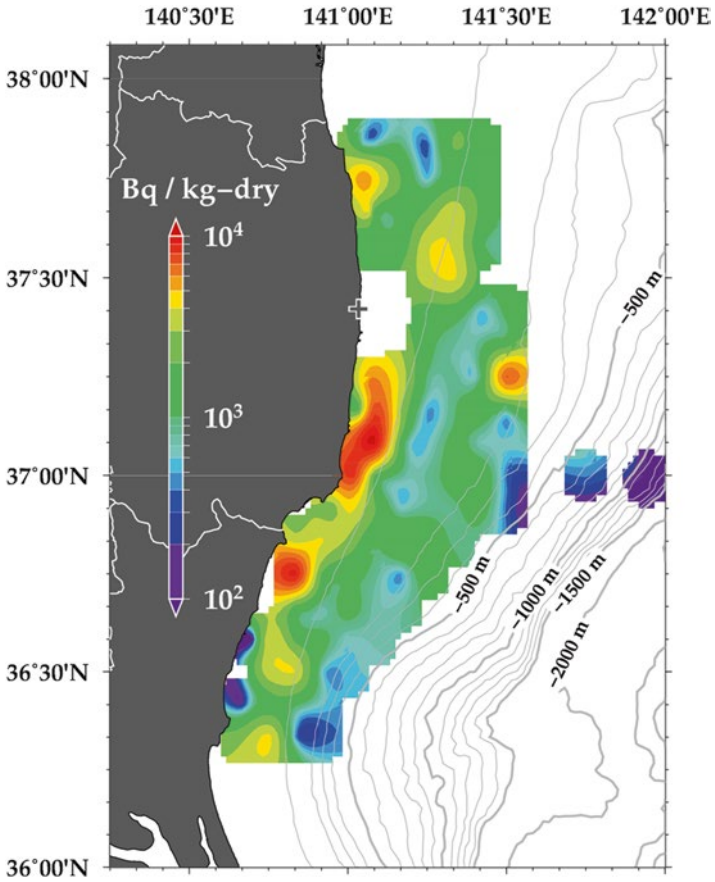

Fig. 5.3 Distribution of calculated Cs_{org} (organic cesium) in the off-Fukushima continental margin area. Contours are drawn from the Cs_{org} value estimated by Eq. (5.3) for each station of Ambe et al. (2014)

for the area with bottom depth ranging from 100 to 200 m. In the station north of FNPP, Cs_{org} showed medium concentrations (~300–3,600 Bq/kg-org-dry) for the area with a bottom depth shallower than 100 m, and Cs_{bulk} values were extremely low (~10–100 Bq/kg-dry; see Ambe et al. 2014 and previous chapter); this is because the sediments of the mid-depth area (~30–100 m) north of FNPP consist mainly of large particles with low organic carbon content, which, using Eq. 5.3, leads to very high CF values. This result implies that the potential effect of sea sediment radiocesium on benthos would not be too different between the area south of FNPP with a bottom depth ranging from 100 to 200 m and north of FNPP with a bottom depth shallower than 100 m, despite a significant Cs_{bulk} difference between these areas. Wada et al. (2013) detected similar radiocesium level of demersal fishes between these two areas after 2012. These findings suggest that Cs_{org} can be used as an indicator of the potential effect of sediment radiocesium on the demersal ecosystem.

Table 5.2 Specifications and measurement results of off-Abukuma patch

Station no.	Sampling date	Latitude [N]	Longitude [E]	Bottom depth (m)	Median grain size (μm)	OC (%)	Cs_{bulk} (Bq/kg-dry)	Cs_{org} (Bq/kg-org-dry)	CF	IR (%)
ABK-A	2013.8.22	38° 2.4′	140° 56.4′	13	No data	16	5,600 ± 75	7,882	1.4	23

5.4 Cs_{org} and CF in off-Abukuma River Sediments

As the sediments described in the former sections are sampled from the continental margin, organic materials contained in these sediments are thought to be produced in the ocean. However, sediments in some local areas such as river mouths contain lithogenic particles, which were produced within freshwater or on land and then transported to the seafloor after the FNPP accident. For such sediments, CF can be considerably low because the nonexchangeable adsorption sites of mineral particles were not occupied by stable cesium or potassium at the time of the accident. To assess the CF value for such sediments, we performed additional Cs_{org} measurements for sediments taken from the local high radiocesium patch recently discovered by the Nuclear Regulation Office (NRA 2014), located just outside of the Abukuma River mouth, with a horizontal scale of about 900 × 400 m width.

Differing from the foregoing grid samples, Cs_{org} in the off-Abukuma patch showed significantly low CF values (~1.4; Table 5.2), possibly because of the significantly high OC value in the sample. Hence, a high-OC sediment tends to have a low CF value (Fig. 5.2). Another reason might be that the sediments in this patch contain a significant amount of lithogenic particles derived from the Abukuma River (Yamashiki et al. 2014). Although the observed Cs_{bulk} in this patch is the highest among the oceanic stations we observed, a low CF in the sediments causes the Cs_{org} value to be at the same level as the average value of off-Fukushima sediments. The monitoring results for marine products for the off-Miyagi prefecture region did not detect any local increase in the occurrence of high-Cs fishes in off-Abukuma regions (JFA 2014), despite the existence of a high-Cs patch in sediments. A significantly low CF in the off-Abukuma sediment patch may explain these observation results. Again, our results showed that not only Cs_{bulk} but also Cs_{org} are essential for accurately assessing the potential effect of sediment radiocesium on the demersal ecosystem in each region.

5.5 Summary

Our study clarifies that radiocesium concentration in the organic fraction of sea sediments is always larger than that in the organic fraction of bulk sediments. This result indicates that the transport efficiency of radiocesium from the organic fraction of sediments to the marine benthos is extremely low, because the radiocesium

concentration in marine benthos is of the order of 10^1 Bq/kg-wet (see Chap. 7). The details of the physiological mechanism that results in such low transport efficiency is an important topic for future study.

Based on Cs_{org}, we assessed that the sediments in the off-Fukushima continental margin north of the FNPP have moderate potential to transport radiocesium to benthic ecosystems, despite the low Cs_{bulk} observed in this region. However, sediments off Abukuma River have less potential to transport radiocesium than the level inferred from its Cs_{bulk} value.

References

Ambe D, Kaeriyama H, Shigenobu Y, Fujimoto K, Ono T, Sawada H, Saito H, Miki S, Setou T, Morita T, Watanabe T (2014) A high-resolved spatial distribution of radiocesium in sea sediment derived from Fukushima Dai-ichi Nuclear Power Plant. J Environ Radioact 138:264–275

Bunzl K, Schimmack W (1991) Kinetics of the sorption of ^{137}Cs, ^{85}Sr, ^{57}Co, ^{65}Zn, and ^{109}Cd by the organic horizons of a forest soil. Radiochim Acta 54:97–102

IAEA (2004) Sediment distribution coefficients and concentration factors for biota in the marine environment. IAEA technical reports series No.422. IAEA, Vienna

JFA (2014) Results of the monitoring on radioactivity level in fisheries products. http://www.jfa.maff.go.jp/e/inspection/index.html

Keil RG, Montlucon DB, Prahl FG, Hedges JI (1994) Sorptive preservation of labile organic matter in marine sediments. Nature (Lond) 370:549–552

Kusakabe M, Oikawa S, Takata H, Misonoo J (2013) Spatiotemporal distributions of Fukushima-derived radionuclides in nearby marine surface sediments. Biogeosciences 10:5019–5030. doi:10.5194/bg-10-5019-2013

Mayer LM (1994) Surface area control of organic carbon accumulation in continental shelf sediments. Geochim Cosmochim Acta 58:1271–1284

Mayer LM (1999) Extent of coverage of mineral surfaces by organic matter in marine sediments. Geochim Cosmochim Acta 63:207–215

Nakamaru Y, Ishikawa N, Tagami K, Uchida S (2007) Role of soil organic matter in the mobility of radiocesium in agricultural soils common in Japan. Colloid Surf A 306:111–117. doi:10.1016/j.colsurfa.2007.01.014

Nakao A, Funakawa S, Takeda A, Tsukada H, Kosaki T (2012) The distribution coefficient for cesium in different clay fractions in soils developed from granite and Paleozoic shales in Japan. Soil Sci Plant Nutr 58:397–403. doi:10.1080/00380768.2012.698595

NRA (2014) FY2013 Report of NRA survey for distribution of radioactive nuclides in marine environment (in Japanese) http://radioactivity.nsr.go.jp/ja/contents/10000/9423/24/report_20140613.pdf

Ono T, Ambe D, Kaeriyama H, Shigenobu Y, Fujimoto K, Sogame K, Nishiura N, Fujikawa T, Morita T, Watanabe T (2015) Concentration of radiocesium bonded to organic fraction of sediment off Fukushima, Japan. Geochem J 49. doi: 10.2343/geochemj.2.0351

Otosaka S, Kato Y (2014) Radiocesium derived from the Fukushima Daiichi Nuclear Power Plant accident in seabed sediments: initial deposition and inventories. Environ Sci Processes Impacts 16:978–990. doi:10.1039/C4EM00016A

Otosaka S, Kobayashi T (2012) Sedimentation and remobilization of radiocesium in the coastal area of Ibaraki, 70 km south of the Fukushima Dai-ichi Nuclear Power Plant. Environ Monit Assess 185:5419–5433. doi:10.1007/s10661-012-2956-7

Wada T, Nemoto Y, Shimamura S, Fujita T, Mizuno T, Sahtome T, Kamiyama K, Morita T, Igarashi S (2013) Effects of the nuclear disaster on marine products in Fukushima. J Environ Radioact 124:246–254. doi:10.1016/j.jenvrad.2013.05.008

Yamashiki Y, Onda Y, Smith HG, Blake WH, Wakahara T, Igarashi Y, Matsuura Y, Yoshimura K (2014) Initial flux of sediment-associated radiocesium to the ocean from the largest river impacted by Fukushima Daiichi Nuclear Power Plant. Sci Rep 4:3714. doi:10.1038/srep03714

Chapter 6
Bottom Turbidity, Boundary Layer Dynamics, and Associated Transport of Suspended Particulate Materials off the Fukushima Coast

Hiroshi Yagi, Kouichi Sugimatsu, Shigeru Kawamata, Akiyoshi Nakayama, and Toru Udagawa

Abstract Long-term monitoring and intensive field experiments for the bottom layer off the Fukushima coast were performed from October 2012 to November 2014 to understand the bottom processes, which are closely related to the spatial distribution and temporal variations of radiocesium in sea sediment. In this section, focusing on autumn 2012, we examine the bottom processes for a 32-m depth site (Sta. B) off Iwaki, Fukushima. Observational results showed that the bottom shear stresses from waves generally dominated over those from currents in this depth region, and the bottom turbidity increased in high wave conditions. Stepwise and significant southward cumulative transports of bottom turbidity were observed when high waves with long periods (LPW) coming from an E–ENE direction were superimposed on the southward current flow that has a periodicity of 5 days; both phenomena are influenced by successive passages of low pressure systems and the associated spatial distribution of atmospheric pressure. The combination of waves and currents caused by meteorological disturbance is a key process in the transport of suspended particulate material off the Fukushima coast.

Keywords Turbidity • Bottom boundary layer • Low period waves • Low pressure system

H. Yagi (✉)
Department of Civil and Environmental Engineering, National Defense Academy, 1-10-20, Hashirimizu, Yokosuka, Kanagawa 239-8686, Japan
e-mail: yagih@nda.ac.jp

K. Sugimatsu • S. Kawamata • A. Nakayama • T. Udagawa
National Research Institute of Fisheries Engineering, Fisheries Research Agency, 7620-7, Hasaki, Kamisu, Ibaraki 314-0408, Japan

K. Nakata, H. Sugisaki (eds.), *Impacts of the Fukushima Nuclear Accident on Fish and Fishing Grounds*, DOI 10.1007/978-4-431-55537-7_6

6.1 Introduction

More than 3 years have passed since the accident at the Fukushima Dai-ichi Nuclear Power Plant (FNPP) associated with the Great Earthquake east of Japan on March 11, 2011. Concentrations of seawater radionuclides are decreasing, but the bottom sediment still has appreciable levels of radionuclides that could be incorporated in the benthic ecosystem. Therefore, it is important to understand the details of the spatial distribution and temporal variations of radionuclide concentrations included in the bottom sediment. Several studies have investigated the spatial distribution of radiocesium in the seabed (Otosaka and Kobayashi 2013; Kusakabe et al. 2013; Thornton et al. 2013; Ambe et al 2014); however, to understand the formation mechanism of the measured spatial distributions and temporal variations of sea bottom radiocesium, the characteristics of suspended sediment transport in the Fukushima coastal sea area must be known. These characteristics are closely related to the movement of sediment and suspended particulate radiocesium. In this section, we introduce the characteristics of bottom turbidity, boundary layer dynamics, and associated bottom turbidity transport off the Fukushima coast, based on the field measurement results reported by Yagi et al. (2013).

6.2 Outline of Field Measurements for Bottom Processes off the Fukushima Coast

We performed two kinds of field measurements to understand the bottom processes off the Fukushima coast: one was the long-term monitoring of coastal bottom environments focusing on basic parameters (current, wave, turbidity, temperature, salinity), and the other was an intensive field survey aimed at understanding the details of bottom boundary layer dynamics and associated sediment transport processes. For long-term monitoring, three monitoring sites were deployed off Iwaki, the southern part of the Fukushima coast (stations B, C, and D at depths of 32, 80, and 130 m, respectively), and one site (Sta. A at a depth of 30 m) off Ooarai on the Ibaraki coast (see Fig. 6.1). Bottom-mounted and bottom-moored instrument platforms were installed with an ADCP (acoustic Doppler current profiler, Telendy RDI), OBS (optical back-scatter sensor for turbidity, Infinity-CLW, JEF-advantec), and salinity–temperature sensors (Infinity-CTW, JEF-advantec) (Fig. 6.2a); mooring systems to measure the surface and middle layer conditions (temperature, salinity, and turbidity) were also deployed for stations A and B. Measurements began in mid-October 2012 and continued for 2 years until early November 2014. The intensive survey focusing on the bottom boundary layer involved the installation of a bottom tripod (Fig. 6.2b) equipped with a vertical array of OBSs, a 3-D acoustic Doppler velocimeter (ADV-Vector, Nortec), and an in-situ laser particle size analyzer (LISST-100x, Sequoia Sci) at Sta. B (32 m depth) (Fig. 6.1). Three field campaigns were conducted: BBL-Exp. I (15 October to 20 November 2012), BBL-Exp. II (13 February to 25 March 2013), and BBL-Exp. III (1 November to 15 December 2013).

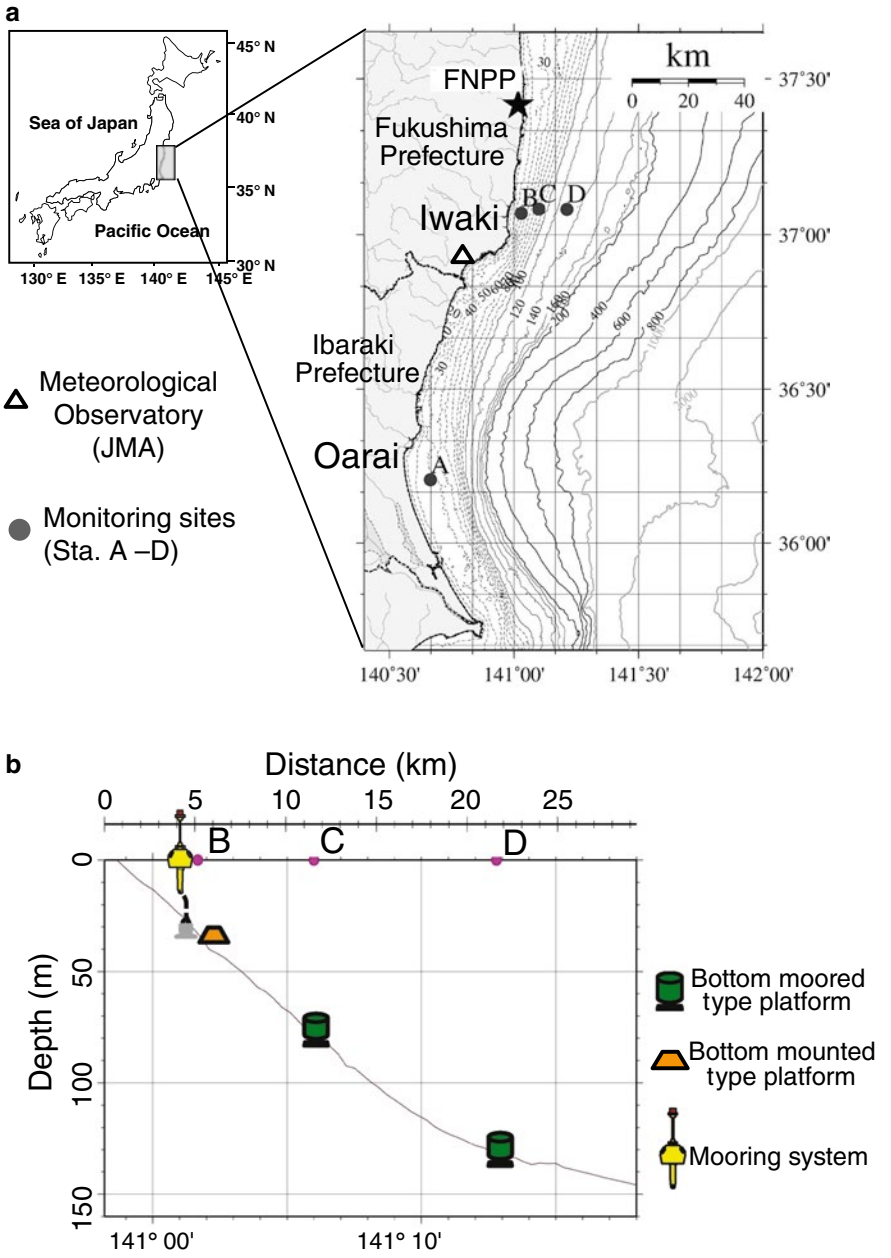

Fig. 6.1 (**a**) Map of study area. Topography and locations of monitoring station A off Oarai of Ibaraki Prefecture, and stations B, C, and D off Iwaki of Fukushima Prefecture. *FNPP* marks the location of the Fukushima Dai-ichi Nuclear Power Plant. (**b**) On- to offshore topography changes around the monitoring sites off Iwaki and locations of stations B, C, and D

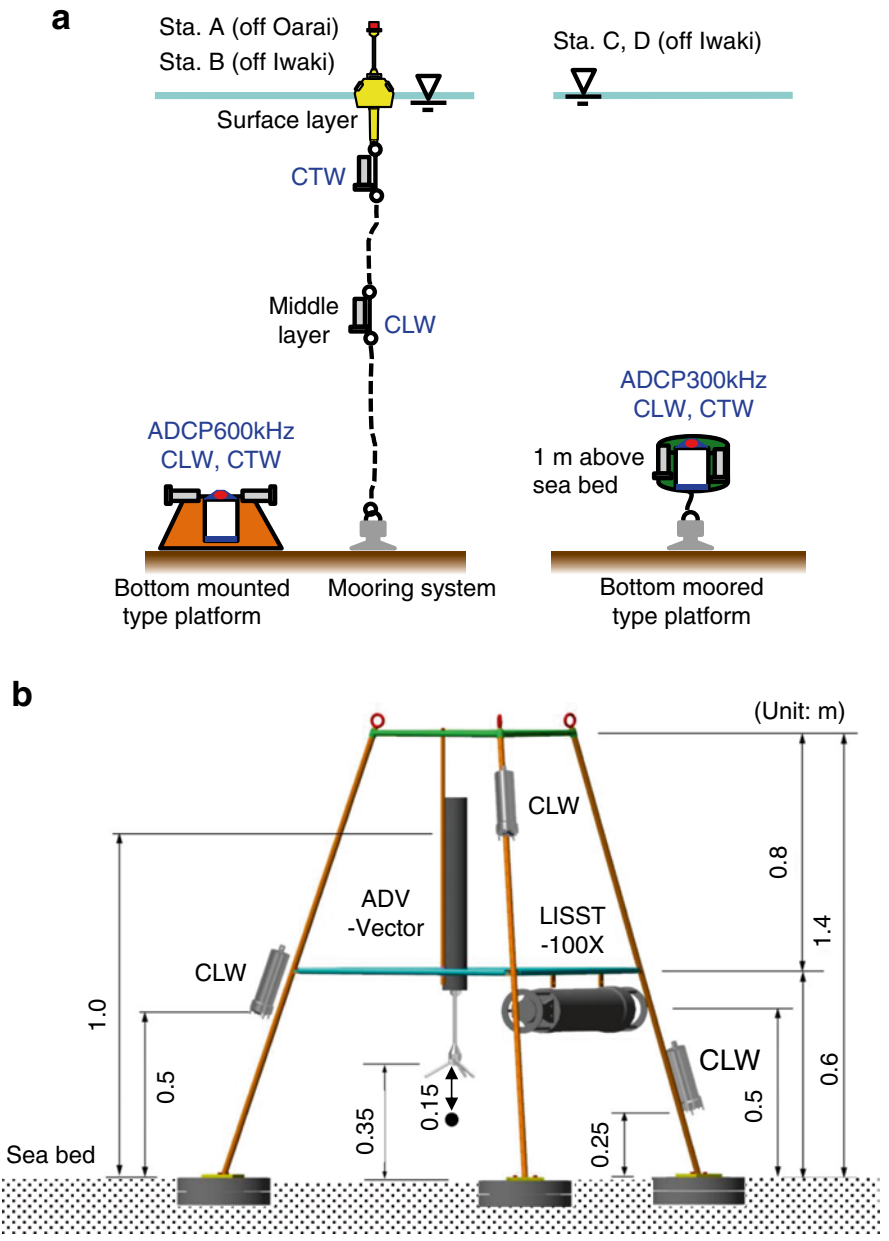

Fig. 6.2 Schematics of the monitoring systems. (**a**) Deployed experimental setup of the instrument platform (bottom-mounted and -moored types) and mooring system at stations A–D. (**b**) Bottom tripod for bottom boundary layer experiment and instrumentation layout. CLW shows OBS (optical back-scatter sensor for turbidity) and CTW shows a salinity-temperature sensor

Of all the data from these measurements, we focused first on the bottom boundary layer experiment for the 32-m depth site (Sta. B) and the corresponding long-term monitoring in autumn 2011. The fundamental characteristics of bottom processes off the Fukushima coast for this period are discussed in the following subsections.

6.3 Bottom Turbidities and Boundary Layer Characteristics off the Fukushima Coast in Autumn 2012

Measurement results in autumn 2012 revealed that temporal variations in turbidity in the inner-shelf and mid-shelf bottom layers off the Fukushima coast have different characteristics (Fig. 6.3). The bottom turbidities at the inner-shelf site

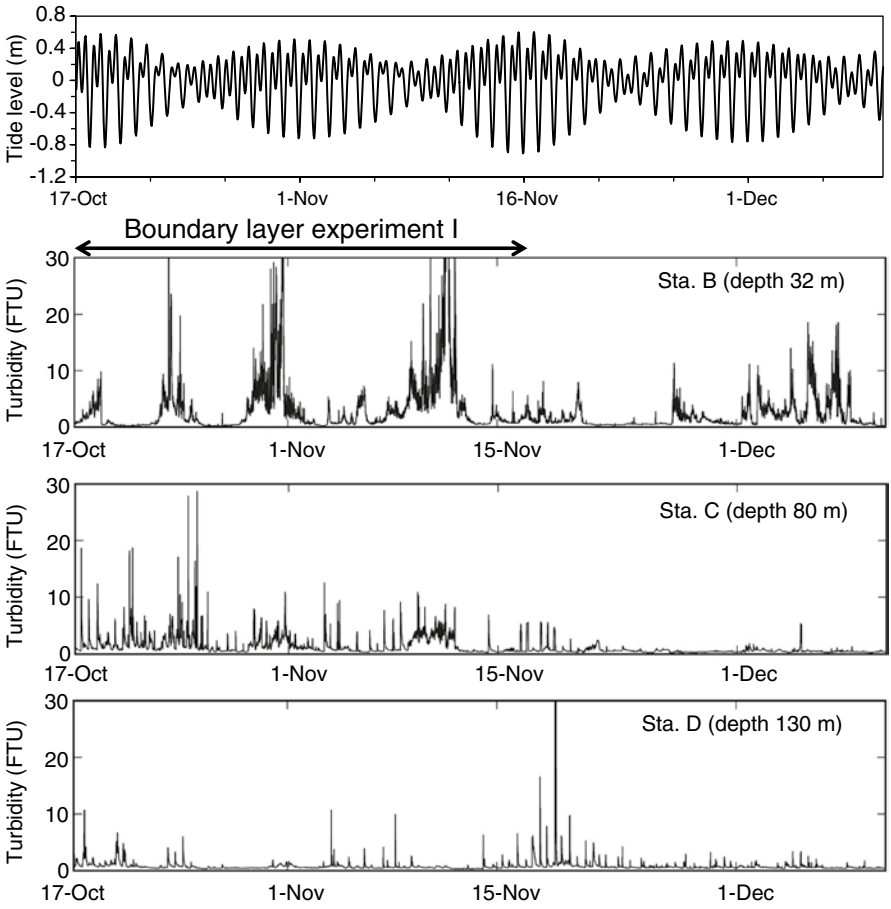

Fig. 6.3 Bottom turbidities at stations B, C, and D with tidal elevations in autumn 2012. The turbidity data are given in FTUs (Formazin turbidity units)

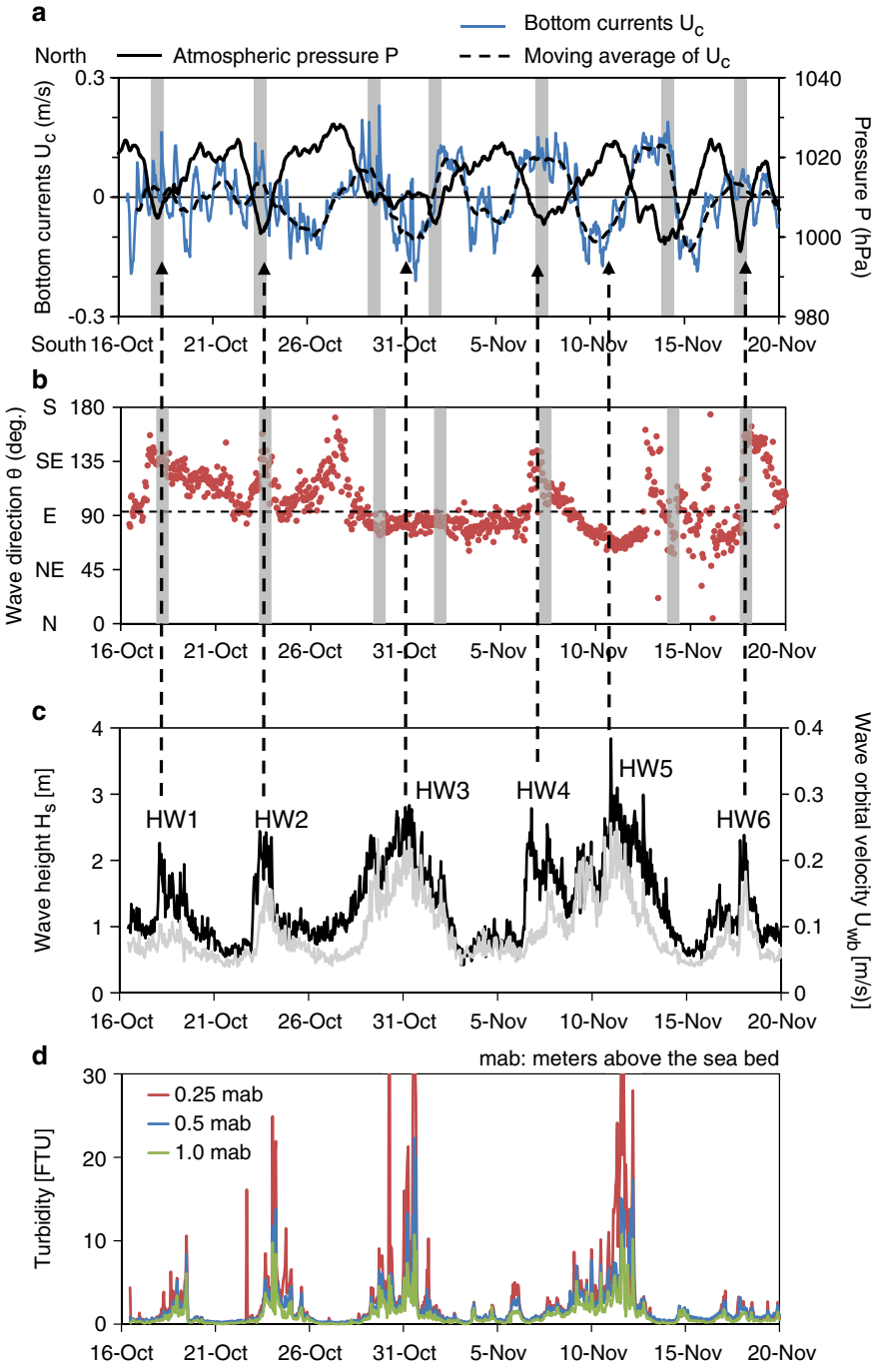

Fig. 6.4 Measurement results for the bottom boundary experiment: bottom currents and atmospheric pressure (**a**), wave direction (**b**), significant wave heights (H_s, *black trace*) and wave orbital

(32-m depth; Sta. B) were generally larger than those at the mid-shelf site (130-m depth; Sta. D), and Sta. B saw high turbidity conditions over several days. In contrast, turbidity at the mid-shelf site (Sta. D) showed temporal variations with high frequencies. The intermediate depth site (80-m depth; Sta. C) combined the bottom turbidity features observed at the inner- and mid-shelf sites.

Focusing on the inner-shelf bottom layer, we examined the details of boundary layer characteristics (currents, waves, bottom shear stress) and the relationships with bottom turbidities (Fig. 6.4). The bottom currents (Fig. 6.4a) showed temporal variations with a period of around 5 days, which were well correlated with low pressure system passages over the study area (shown by the gray hatching in this figure) associated with temporal variations of local atmospheric pressure. These periodic and subtidal current fluctuations off the Fukushima coast were also observed by Kubota et al. (1981) and were thought to be shelf waves in the forcing region caused by periodic meteorological disturbances (Kubota 1982). In contrast, waves observed in high wave conditions showed two distinct sets of characteristics. (1) High waves during low pressure passages had relatively shorter wave periods and an ESE–SSE wave direction (type 1: corresponding to the high wave periods HW1, HW2, HW4, and HW6 in Fig. 6.4c, and indicated as type 1 in Fig. 6.5a). (2) High waves occurring in the intervals between low pressure passages had longer wave periods and an E–ENE wave direction (type 2: corresponding to the high wave periods HW3 and HW5 in Fig. 6.4c, and indicated as type 2 in Fig. 6.5a). These different characteristics were the result of the different wave generation systems, in that type 1 was induced by the passage of a low pressure system over the study area (Fig. 6.5b, left panel) and type 2 developed off the east part of the main island of Japan (Fig. 6.5b, right panel) and propagated into the study region from an E–ENE direction with longer periods.

Bottom shear stress from currents and waves (τ_c and τ_w) can be evaluated by the following equations (Soulsby 1997):

$$\tau_c = \rho U_c^2 \Big/ \left[\frac{1}{\kappa}\ln\left(\frac{z}{z_0}\right)\right]^2 \text{ and} \tag{6.1}$$

$$\tau_w = \rho \frac{1}{2} f_w U_w^2, \tag{6.2}$$

where U_c is the current velocity at z (elevation above the sea bed), κ is the von Karman constant, ρ is the density of seawater, z_0 is the bed roughness length, U_w is

Fig. 6.4 (continued) velocities (U_{wb}, *gray trace*) (**c**), and turbidities (**d**) at 0.25, 0.5, and 1 m above the seabed. Timing of low pressure passages over the study area, which were defined from local atmospheric pressure data and synoptic-scale information on atmospheric pressure (weather map) from the JMA (Japan Meteorological Agency), is shown by the *gray hatching* in (**a**) and (**b**). (**c**) HW 1–6 are high wave periods during the observation period. HW1, -2, -4, and -6 occurred during the low pressure passage; HW3 and -5 in intervals between low pressure passages are shown by *dotted arrows*

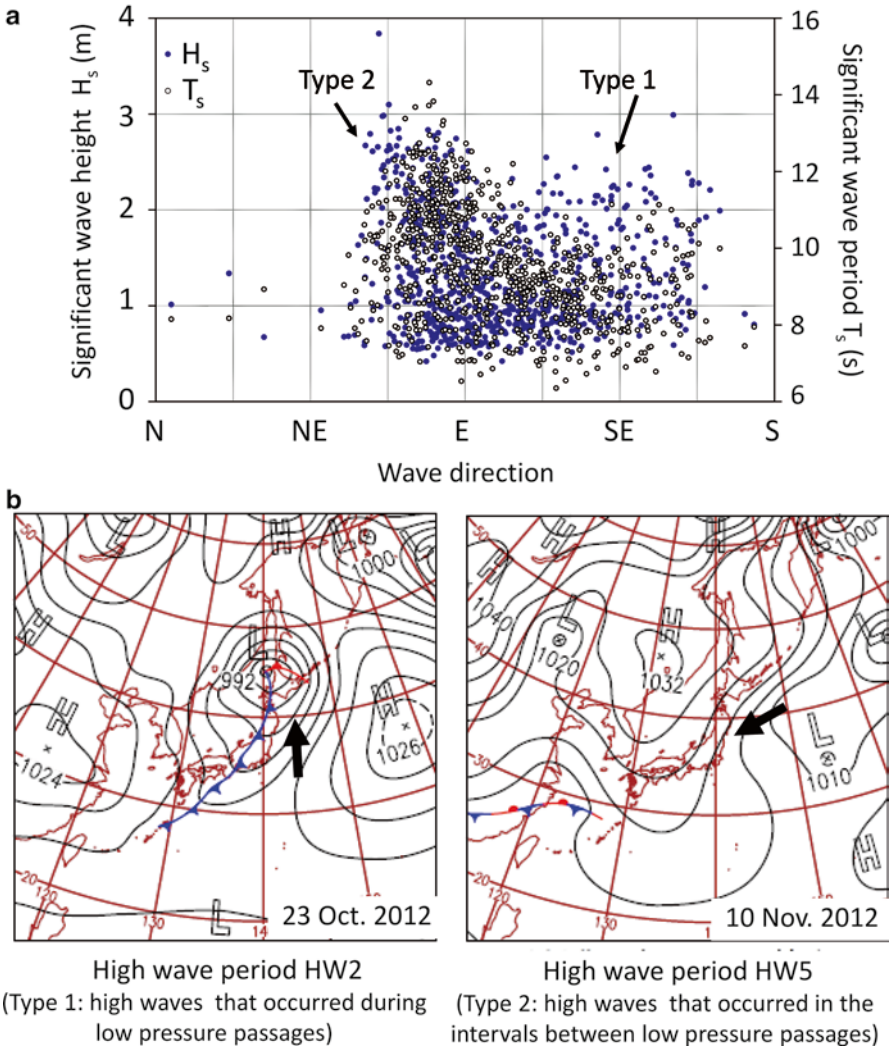

Fig. 6.5 (**a**) Relationship between wave direction, significant wave heights, and wave periods for autumn 2012. (**b**) Weather map by the JMA for two high wave periods: *left*, high wave period HW2 (type 1); *right*, high wave period HW5 (type 2). Wave directions are illustrated based on the wave map by the JMA

the bottom wave orbital velocity, and f_w is the bottom friction coefficient caused by waves (Soulsby 1997). By substituting the measured ADCP velocity at the lowest layer (z=2.12 m) for U_c, and RMS wave orbital velocities by the ADV-Vector for U_w, we can obtain the bottom shear stresses.

The estimated bottom shear stress caused by waves (τ_w) generally dominated over that caused by currents (τ_c) in autumn 2012 and showed larger values in type 2 high wave conditions (HW3 and HW5 in Fig. 6.6a). Furthermore, τ_w correlates well

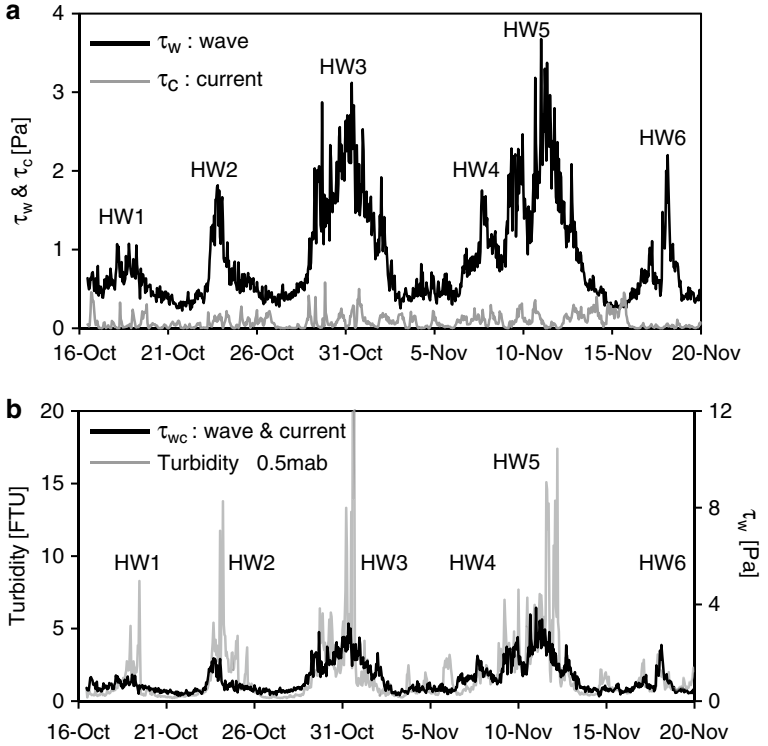

Fig. 6.6 (**a**) Temporal variations in estimated bottom shear stresses caused by waves (τ_w) and currents (τ_c). (**b**) Temporal variations in bottom turbidities (0.5 mab) and τ_w for autumn 2012. HW 1–6 in the figure are as defined for Fig. 6.4c

with the observed turbidities, meaning high turbidity conditions occurred simultaneously with the larger bottom shear stresses (Fig. 6.6b). These observational results demonstrate that the larger bottom turbidities are induced by the high wave conditions in the intervals between low pressure passages (type 2), which showed longer wave periods and larger bottom shear stresses.

6.4 Near-Bottom Turbidity Transport off Fukushima Coast Under the Condition of Successive Low Pressure Passages

To understand the characteristics of near-bottom turbidity transport off the Fukushima coast, which are closely related to the movement of suspended sediment and particulate radiocesium, we evaluated the turbidity transport rates from the estimated vertical distributions of turbidity and velocity in the bottom layer. Measured

bottom turbidities at three different depths (0.25, 0.5, and 1 m above the seabed) were approximated with the exponential function

$$C(z) = C_{be} \cdot \exp[-\alpha \cdot z] \tag{6.3}$$

where $C(z)$ is estimated turbidity and z is the distance above the seabed. C_{be} (reference bottom turbidity) and α (shape factor) are time-varying parameters decided by regression analysis of the measured bottom turbidities. Additionally, the vertical profile of bottom current velocities can be approximated using a well-known logarithmic law of the wall for a sea bottom boundary layer (Soulsby 1997) as follows:

$$u(z) = \frac{\ln z - \ln z_0}{\ln z_{ADCP} - \ln z_0} u_{ADCP} \tag{6.4}$$

where $u(z)$ is estimated bottom velocity (north–south or east–west component), u_{ADCP} is the velocity of the lowest layer of ADCP (north–south or east–west component), and z_{ADCP} is the distance above the seabed for the lowest layer of ADCP (2.12 m above the seabed). Horizontal turbidity flux is calculated as the product of Eqs. (6.3) and (6.4) and integrated over the bottom layer to evaluate the bottom turbidity transport rate q_b as follows:

$$q_b = \int_0^{z_b} C(z) \cdot u(z) \cdot dz \tag{6.5}$$

where z_b is the thickness of the bottom layer. defined here as 2 m.

The estimated temporal and vertical distribution of bottom turbidity (Fig. 6.7a) shows that significant turbidity variation occurred predominantly below 2 m above the seabed in autumn 2012. The cumulative transport rate q_b (Fig. 6.7b) demonstrates that southward transport dominated and occurred stepwise during type 2 high wave periods (HW3 and HW5 in Fig. 6.7b), which have longer wave periods and larger bottom shear stresses, as shown in Figs. 6.5a and 6.6a. In contrast, as discussed, the bottom currents represent temporal variations with a periodicity around 5 days, and southward currents occurred in the intervals between low pressure atmospheric events. As a result, significant southward bottom turbidity transport was induced during high wave periods HW3 and HW5 (Fig. 6.7b), in the interval between low pressure events when higher bottom turbidities and southward bottom currents co-occurred. From these observational results, it is revealed that successive low pressure passages and the associated spatial distributions of atmospheric pressure influenced both the current and wave fields, and that significant southward bottom turbidity transports were induced by the co-occurrence of high waves coming from E–ENE with longer periods (favorable for high bottom turbidity) and southward bottom currents in the interval between low pressure passages (Fig. 6.8). The relationship between waves and currents through atmospheric conditions is an important influence on bottom processes off the Fukushima coast.

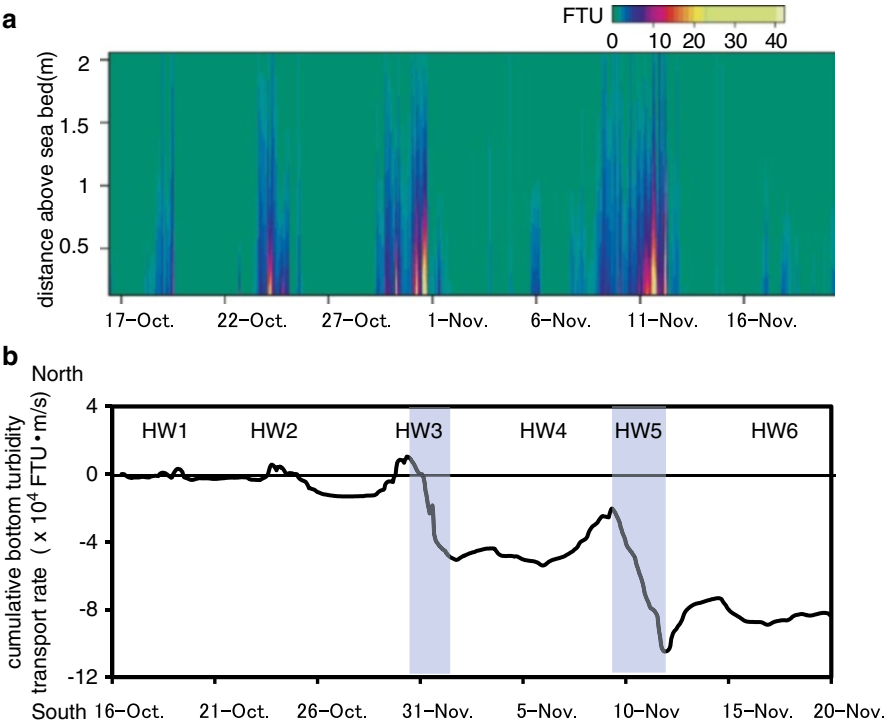

Fig. 6.7 (**a**) Temporal and vertical distribution of turbidity estimated by Eq. (6.3). (**b**) Temporal variation of the cumulative value of the bottom turbidity transport rate found by Eq. (6.5) (north–south direction). HW1–6 in **b** as defined for Fig. 6.4c

In the bottom boundary layer experiment in autumn 2012, a sediment trap was also installed at the inner-shelf site (32-m depth, Sta. B) to measure the sinking flux and radiocesium concentration of suspended particulate material in the bottom layer (Kaeriyama et al. 2013). The measurement results showed a significant correlation between bottom turbidities and the sinking fluxes of particulate radiocesium (Yagi et al. 2014), which fact suggests that sediment or particulate radiocesium movements are closely related to the transport processes of the bottom turbidity examined here.

6.5 Conclusions

In this section, fundamental characteristics of bottom turbidity, bottom boundary layer dynamics, and associated bottom turbidity transport off the Fukushima coast were examined based on field measurement results in autumn 2012, focusing on the inner-shelf bottom layer (32-m depth, Sta. B). Observational results showed that the bottom shear stresses from waves generally dominated those caused by currents, and the bottom turbidity increased in high wave conditions. In particular, significant

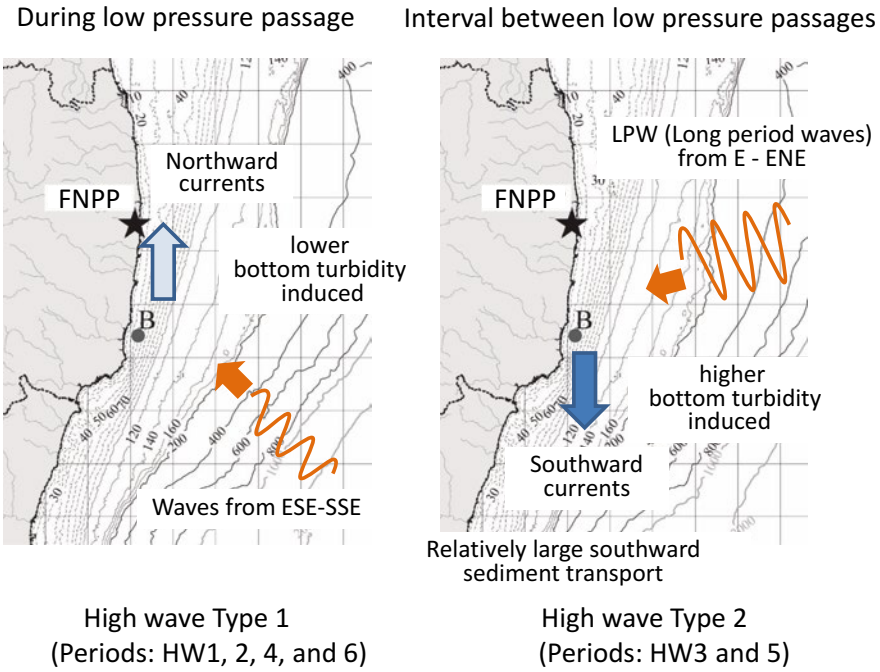

Fig. 6.8 Schematic illustrations of bottom turbidity transport processes for type 1 and type 2 high wave events

and stepwise southward cumulative transport of bottom turbidity was observed when southward currents and high waves coming from an E–ENE direction with longer periods co-occurred. This combination of bottom current variations with a periodicity of several days and high wave conditions with longer wave periods (LPW), both of which are influenced by the successive passage of periodic low pressure systems and the associated spatial distribution of atmospheric pressure, affects the transport of suspended particulate material in the bottom layer. The results of this study highlight the importance of the relationship between atmospheric conditions and trends in waves and currents in understanding the bottom processes off the Fukushima coast.

Acknowledgments We appreciate the extensive support from Mr. A. Suzuki, Mr. M. Hosono, and Mr. M. Kobayashi of International Meteorological & Oceanographic Consultants Co. Ltd, and from Mr. Y. Nishi of Alpha Hydraulic Engineering Consultants Co., Ltd. This study was financially supported by the Fisheries Research Agency of Japan.

References

Ambe D, Kaeriyama H, Shigenobu Y, Fujimono K, Ono T, Sawada H, Saito H, Miki S, Setou T, Morita T, Watanabe T (2014) A high-resolved spatial distribution of radiocesium in sea sediment derived from Fukushima Dai-ichi nuclear power plant. J Environ Radioact 136:218–228

Kaeriyama H, Ambe D, Ono T, Yagi H, Sugimatsu K, Kawamata S, Udagawa T, Nakayama T, Watanabe T (2013) Sinking flux of particle radioactive cesium near sea bottom off the coast of Fukushima prefecture. In: Fall Meeting of the Oceanographic Society of Japan, Sapporo, Hokkaido, Japan, 17–21 Sept 2013, 316, p. 162 (in Japanese)

Kubota M (1982) Continental shelf waves off the Fukushima coast. Part II: theory of their generation. J Oceanogr Soc Jpn 38:323–330

Kubota M, Nakata K, Nakamura Y (1981) Continental shelf waves off the Fukushima coast. Part I: observations. J Oceanogr Soc Jpn 37:267–278

Kusakabe M, Oikawa S, Takata H, Misonoo J (2013) Spatiotemporal distributions of Fukushima-derived radionuclides in nearby marine surface sediments. Biogeosciences 10:5019–5030

Otosaka S, Kobayashi T (2013) Sedimentation and remobilization of radiocesium in the coastal area of Ibaraki, 70 km south of the Fukushima Dai-ichi Nuclear Power Plant. Environ Monit Assess 185(7):5419–5433

Soulsby R (1997) Dynamics of marine sands. Thomas Telford, London, p 249

Thornton B, Ohnishi S, Ura T, Odano N, Fujita T (2013) Continuous measurement of radionuclide distribution off Fukushima using a towed sea-bed gamma ray spectrometer. Deep-Sea Res I 79:10–19

Yagi H, Sugimatsu K, Nishi Y, Kawamata S, Nakayama A, Udagawa T, Suzuki A (2013) Field measurements of bottom boundary layer and suspend particle materials on Jyoban coast in Japan. Journal of Japan Society of Civil Engineers, Ser B2 (Coastal Engineering) 69(2): 1046–1050 (in Japanese)

Yagi H, Sugimatsu K, Kawamata S, Nakayama A, Udagawa T, Kaeriyama H, Ono T, Ambe D (2014) Estimation of horizontal flux of particulate radiocesium in the bottom layer off Joban coast. In: Spring Meeting of the Oceanographic Society of Japan, Tokyo, Japan, 26–30 March 2014, 201, p. 59 (in Japanese)

Chapter 7
Investigation of Radiocesium Translation from Contaminated Sediment to Benthic Organisms

Yuya Shigenobu, Daisuke Ambe, Hideki Kaeriyama, Tadahiro Sohtome, Takuji Mizuno, Yuichi Koshiishi, Shintaro Yamasaki, and Tsuneo Ono

Abstract We estimated the radiocesium translation from contaminated sediments to benthic organisms off the coast of Fukushima. We conducted field investigations and an experiment with a benthic polychaete (*Perinereis aibuhitensis*) reared on highly contaminated sediments collected from a station 1 km off the Fukushima Dai-ichi Nuclear Power Plant. Results of the field investigations revealed that radiocesium contamination in benthic organisms depended on their feeding habitat. The radiocesium concentration in carnivore or herbivore feeder polychaetes was higher than that in deposit feeders. Radiocesium concentrations of all benthic organism specimens were lower than that in sediments collected from the same sampling point. Results of the rearing experiment showed that the concentration ratio (CR) of ^{137}Cs for *P. aibuhitensis* and contaminated sediments (wet/wet) was less than 0.10. Moreover, 4 days after separation from the contaminated sediments, the ^{137}Cs concentrations in *P. aibuhitensis* rapidly decreased. Based on the results of our field investigations and rearing experiment, we conclude that the intake of radiocesium through the benthic food web is limited for benthic organisms, despite the high contamination of the surrounding sediments.

Y. Shigenobu (✉) • D. Ambe • H. Kaeriyama • Y. Koshiishi • T. Ono
National Research Institute of Fisheries Sciences, Fisheries Research Agency,
2-12-4, Fukuura, Kanazawa, Yokohama, Kanagawa 236-8648, Japan
e-mail: yshig@affrc.go.jp

T. Sohtome • T. Mizuno
Fukushima Prefectural Fisheries Experimental Station,
13-2, Matsushita, Onahama, Iwaki, Fukushima 970-0316, Japan

S. Yamasaki
National Research Institute of Fisheries Engineering, Fisheries Research Agency,
7620-7, Hasaki, Kamisu, Ibaraki 314-0408, Japan

K. Nakata, H. Sugisaki (eds.), *Impacts of the Fukushima Nuclear Accident on Fish and Fishing Grounds*, DOI 10.1007/978-4-431-55537-7_7

Keywords Benthic organisms • Contaminated sediment • Rearing experiment • Concentration ratio (CR)

7.1 Introduction

The Fukushima Dai-ichi Nuclear Power Plant (FNPP) accident in March 2011 released a large amount of anthropogenic radionuclides into the marine environment. Although most of the short-lived radionuclides soon decayed to a level below the detection limit, two isotopes of radiocesium (^{134}Cs and ^{137}Cs), which have relatively long half-lives (2.07 years and 30.1 years, respectively), have been continually detected in the environment. Tsumune et al. (2012) estimated that $3.5 \pm 0.7 \times 10^{15}$ Bq of ^{137}Cs was released directly into the ocean from 26 March 2011 to the end of May 2011. The discharged radiocesium from the FNPP gradually associated with suspended material and settled to the sea bottom around Fukushima. Ambe et al. (2014) reported that the radiocesium concentrations in the surface sediment layer (0–1 cm) collected off the coast of Fukushima in 2012 and 2013 were mainly in the range of dozens to several hundred Bq/kg-dry (see Sect. 2.1). Moreover, the particularly highly contaminated (^{137}Cs concentration = 40,152 ± 3,998 Bq/kg-wet) area that is extremely small, encompassing only a few square meters of the seafloor, was confirmed near the FNPP in February 2013 (Thornton et al. 2013). It is thought that demersal fish and benthic organisms take in radiocesium from highly contaminated sediments through the benthic food web (Buesseler 2012; Tateda et al. 2013; Sohtome et al. 2014). High radiocesium concentrations were detected from some sedentary demersal fish species, such as fat greenling (*Hexagrammos otakii*), marbled flounder (*Pseudopleuronectes yokohamae*), slime flounder (*Microstomus achne*), and Japanese rockfish (*Sebastes cheni*), off the coast of Fukushima (Wada et al. 2013).

The radiocesium concentrations in benthic organisms off the coast of Fukushima range from several to dozens Bq/kg-wet (Sohtome et al. 2014). According to a previous experimental study on the concentration ratio (CR) of ^{137}Cs between contaminated sediments and marine polychaetes (CR = 0.179) (Ueda et al. 1977), this level of contamination in benthic organisms off the coast of Fukushima is reasonable. However, the current transfer efficiency of radiocesium from contaminated sediments to the benthic organisms along the sea bottom off the coast of Fukushima is unclear. In this section, we discuss the results of our measurements of radiocesium concentrations in benthic organisms caught off the coast of Fukushima in October 2013 and the results of experiments rearing a benthic polychaete (*Perinereis aibuhitensis*) on highly contaminated sediments collected at the station 1 km off the FNPP in August 2013 (Fig. 7.1). Through our field investigations and the rearing experiment, we estimated the radiocesium translation from contaminated sediments to benthic organisms off the coast of Fukushima.

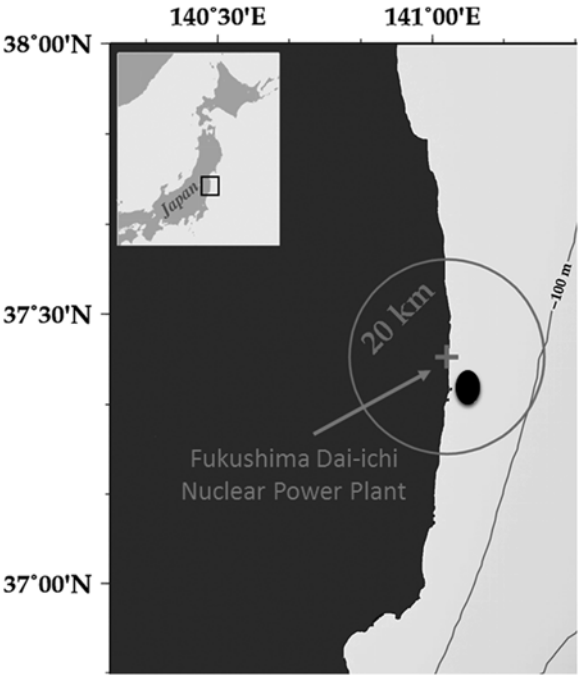

Fig. 7.1 Sampling point (*black spot*) of benthic organisms off the coast of Fukushima in October 2013. *Gray circle* indicates a 20-km radius around the Fukushima Dai-ichi Nuclear Power Plant

7.2 Radiocesium Concentrations in Benthic Organisms off the Coast of Fukushima

Benthic organisms in the southern coastal waters of Fukushima were collected using a dredge on the R/V *Taka-maru* of the Fisheries Research Institute of Fisheries Engineering in October 2013 (Fig. 7.1). We sorted benthic organisms into major taxonomic groups and measured radiocesium concentrations of whole-body specimens, which included digestive system contents (Fig. 7.2). The specimens were packed tightly in plastic cylindrical containers, and specific gamma rays of ^{134}Cs (605 and 796 keV) and ^{137}Cs (662 keV) were measured with a high-purity germanium (HPGe) semiconductor detector (ORTEC, GEM30-70-LB-C, 1.85 Kev/1.33 MeV of resolution) with a multichannel analyzer.

Radiocesium concentrations in all benthic organisms were lower than that in the sediments (216 Bq/kg-wet) collected from the same sampling point. Radiocesium concentrations in benthic organisms ranged from not-detected (N.D.) to 99.4 Bq/kg-wet. Although a low level of radiocesium contamination was detected in crustacean specimens, radiocesium concentrations in polychaete specimens varied among taxonomic groups (Table 7.1).

The radiocesium concentrations in benthic organisms were typically measured for whole-body specimens, which contained the contaminated sediments within and

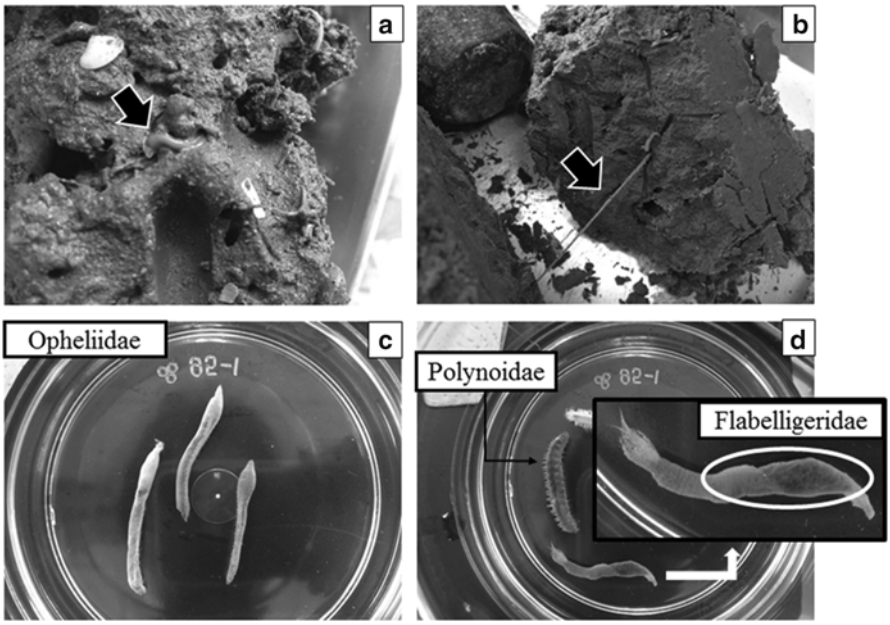

Fig. 7.2 Polychaetes collected off the coast of Fukushima in October 2013. We selected several species of polychaetes from sea sediments (**a**, **b** and **c**). *White oval* in **d** indicates the internal sediments in Flabelligeridae specimens

Table 7.1 Radiocesium concentrations in benthic organisms off the coast of Fukushima in October 2013

Taxonomic group of benthic organisms		$^{134}Cs + {}^{137}Cs$ concentrations (Bq/kg-wet)	Concentration ratios between sea sediments[a] and benthic organisms
Polychaeta	Glyceridae	N.D. (<2.89)	—
	Eunicidae	11.2	0.0519
	Flabelligeridae	99.4	0.460
	Terebellidae	30.2	0.140
	Opheliidae	N.D. (<6.56)	—
	Polynoidae	12.1	0.0560
Crustacea	Crangonidae	1.09	0.00505
	Paradorippe granulata	4.37	0.0202
Asteroidea	*Philyra syndactyla*	3.58	0.0166
	Luidia quinaria	2.65	0.0123
	Asterias amurensis	N.D. (<2.47)	—

[a]Radiocesium concentration of sea sediment at the sampling point was 216 Bq/kg-wet

around their body. Ono et al. (in press, 2015) reported that organic matter in marine sediments had a higher radiocesium concentration than did mineral substances. Therefore, it is thought that the feeding habitats of benthic organisms influence radiocesium concentrations within the organisms. In this investigation, we observed internal sediments in the Flabelligeridae specimens, which had the highest radiocesium concentration. Species belonging to Flabelligeridae, Terebellidae, and Opheliidae are categorized as filter feeders or surface deposit feeders (Fauchald and Jumars 1979). Except for the Opheliidae specimens, radiocesium concentrations in deposit feeder polychaetes were comparatively higher than in other benthic organisms. In contrast, species with low radiocesium concentration (Glyceridae, Eunicidae, and Polynoidae) are categorized as carnivore or herbivore feeders. The reason for low contamination levels in Opheliidae specimens was unclear. Additional and continuous investigations are required to reveal the relationship between radiocesium contamination and feeding habitats of benthic organisms off the coast of Fukushima.

7.3 Rearing Experiments of the Marine Polychaete (*Perinereis aibuhitensis*) Using Highly Contaminated Sediment from Near the FNPP

Contaminated sediments from near the FNPP (37°24.850′N–141°02.330′E) were collected using a Smith-Mclntyre grab sampler on the R/V *Takusui* of the Fukushima Prefectural Fisheries Experimental Station in August 2013. After removing impurity particles using a 2-mm sieve, we agitated the contaminated sediment for equalization. Before initiating the rearing experiments, we confirmed noncontamination of the marine polychaete (*Perinereis aibuhitensis*) specimens with an HPGe semiconductor detector. The specimens of *P. aibuhitensis* were reared for 5 weeks in four tanks (450 mm × 300 mm × 330 mm) with the contaminated sediments, and then *P. aibuhitensis* were reared for 2 weeks without sediments (seawater only). The ^{137}Cs concentrations of living *P. aibuhitensis* in plastic cylindrical containers were measured with an HPGe semiconductor detector, and then the specimens were returned to the rearing tank. The sediment samples were dried at 60 °C for 7 days, and the dry weight was converted into wet weight concentrations using the percentage of lost water content. Because organic matter in contaminated sediments has a high preference for radiocesium (Ono et al. in press, 2015), an ignition loss test was employed to determine the sediment content in each of the four tanks. The sediment samples were heated in a muffle furnace at 750 °C for 1 h.

Figure 7.3 shows the time-series trends of ^{137}Cs concentrations for contaminated sediments and *P. aibuhitensis* in each tank. At the start of the rearing experiment, the ^{137}Cs concentration in the contaminated sediments was 1,250 Bq/kg-wet. However, ^{137}Cs concentrations in the contaminated sediments fluctuated with time. During the rearing period with contaminated sediments, the geometric mean of ^{137}Cs concentration for sediments in tank 1, tank 2, tank 3, and tank 4 were 1,500 Bq/kg-wet,

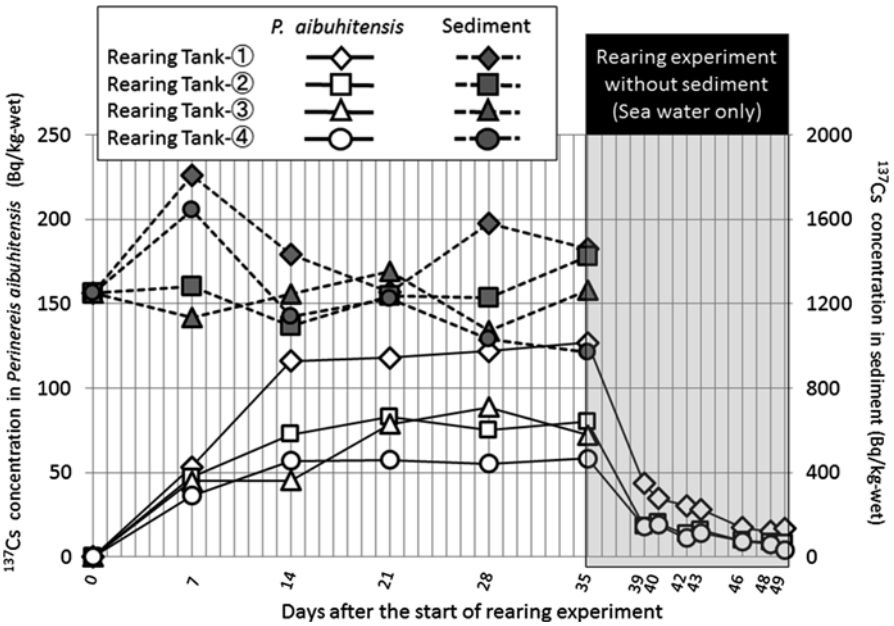

Fig. 7.3 Temporal trends of ^{137}Cs concentrations in *Perinereis aibuhitensis* and sediments

Table 7.2 Temporal trend of organic matter contents (%) in sediments for each rearing tank

Tank		Days after the start of rearing experiment				
		7 days	14 days	21 days	28 days	35 days
Rearing tank-①	Initial value 5.9	5.1	5.1	4.9	4.5	5.1
Rearing tank-②		4.2	4.8	4.7	4.6	4.5
Rearing tank-③		5.3	5.4	5.8	4.4	4.3
Rearing tank-④		4.9	4.7	5.5	4.4	4.9

1,250 Bq/kg-wet, 1,210 Bq/kg-we,t and 1,180 Bq/kg-wet, respectively. Insufficient agitation of the initial contaminated sediments and the burrowing activity of *P. aibuhitensis* could have caused the variation of ^{137}Cs concentration among the tanks. In contrast, the organic matter content in the contaminated sediments for each tank was approximately equal during the rearing period (Table 7.2).

The ^{137}Cs concentrations of *P. aibuhitensis* reached the maximum value after approximately 2 weeks, and conspicuous fluctuations were not observed during the next 3 weeks. On the 35th day after the start of the experiment, the CR for ^{137}Cs between *P. aibuhitensis* and sediments (wet/wet) was less than 0.10 (tank 1 = 0.087, tank 2 = 0.056, tank 3 = 0.057, tank 4 = 0.060). Meanwhile, the ^{137}Cs concentrations in *P. aibuhitensis* varied among the tanks. On the 14th day after the start of the experiment, the ^{137}Cs concentrations in tank 1, tank 2, tank 3, and tank 4 were 116 Bq/kg-wet, 72.5 Bq/kg-wet, 45.1 Bq/kg-wet, and 56.8 Bq/kg-wet, respectively. Four days after separation from the contaminated sediments, the ^{137}Cs concentration

in *P. aibuhitensis* rapidly decreased, to 23–34 % of the concentration on the 35th day. The ^{137}Cs concentration in *P. aibuhitensis* eventually decreased to less than 20 Bq/kg-wet in all tanks. These results suggest that the ^{137}Cs concentrations in *P. aibuhitensis* are associated with the sediment contamination level in each tank. We assumed that the observed radiocesium concentration in *P. aibuhitensis* include measurements of contaminated sediments in their digestive systems.

Our rearing experiments determined that the CR for radiocesium between *P. aibuhitensis* and contaminated sediments (wet/wet) was less than 0.10. Otosaka and Kobayashi (2013) calculated that the amount of bioavailable ^{137}Cs in the surface sediment layer (0–3 cm) off the coast of Ibaraki Prefecture (approximately 70 km south of the FNPP) was only about 20 % of the total sedimentary ^{137}Cs because more than 75 % of the ^{137}Cs was incorporated into lithogenic fractions that were not bioavailable to marine products. Therefore, most of the sedimentary radiocesium in the digestive system of benthic organisms would be excreted with their wastes. Moreover, the ability of osmoconformation in invertebrates would influence the rapid excretion of internally absorbed radiocesium. The results of our study indicate that the intake of radiocesium through the benthic food web is limited for benthic organisms and demersal fish species, despite high contamination of the surrounding sediments.

Acknowledgments We are grateful to Satoshi Igarashi for the sorting of benthic organisms. We also thank Takami Morita and Ken Fujimoto for their valuable discussions and information. We appreciate the captains and crews of the R/V *Takusui* and *Taka-maru* for sampling contaminated sediments and benthic organisms.

References

Ambe D, Kaeriyama H, Shigenobu Y, Fujimoto K, Ono T, Sawada H, Saito H, Miki S, Setou T, Morita T, Watanabe T (2014) Five-minute resolved spatial distribution of radiocesium in sea sediment derived from the Fukushima Dai-ichi Nuclear Power Plant. J Environ Radioact 138:264–275

Buesseler KO (2012) Fishing for answers off Fukushima. Science 338:480–482

Fauchald K, Jumars PA (1979) The diet of worms: a study of polychaete feeding guilds. Oceanogr Mar Biol Annu Rev 17:193–284

Ono T, Ambe D, Kaeriyama H, Shigenobu Y, Fujimoto K, Sogame K, Nishiura N, Fujikawa T, Morita T, Watanabe T (2015) Concentration of ^{134}Cs + ^{137}Cs bonded to the organic fraction of sediments offshore Fukushima, Japan. Geochem J 49 (in press)

Otosaka S, Kobayashi T (2013) Sedimentation and remobilization of radiocesium in the coastal area of Ibaraki, 70 km south of the Fukushima Dai-ichi Nuclear Power Plant. Environ Monit Assess 185:5419–5433

Sohtome T, Wada T, Mizuno T, Nemoto Y, Igarashi S, Nishimune A, Aono T, Ito Y, Kanda J, Ishimaru T (2014) Radiological impact of TEPCO's Fukushima Dai-ichi Nuclear Power Plant accident on invertebrates in the coastal benthic food web. J Environ Radioact 138:106–115

Tateda Y, Tsumune D, Tsubono T (2013) Simulation of radioactive cesium transfer in the southern Fukushima coastal biota using a dynamic food chain transfer model. J Environ Radioact 124:1–12

Thornton B, Ohnishi S, Ura T, Odano N, Sasaki S, Fujita T, Watanabe T, Nakata K, Ono T, Ambe D (2013) Distribution of local ^{137}Cs anomalies on the seafloor near the Fukushima Dai-ichi Nuclear Power Plant. Mar Pollut Bull 74:344–350

Tsumune D, Tsubono T, Aoyama M, Hirose K (2012) Distribution of oceanic ^{137}Cs from the Fukushima Dai-ichi nuclear power plant simulated numerically by a regional ocean model. J Environ Radioact 111:100–108

Ueda T, Nakamura R, Suzuki Y (1977) Comparison of influence of sediments and sea water on accumulation of radionuclides by worms. J Radiat Res 18:84–92

Wada T, Nemoto Y, Shimamura S, Fujita T, Mizuno T, Sohtome T, Kamiyama K, Morita T, Igarashi S (2013) Effects of the nuclear disaster on marine products in Fukushima. J Environ Radioact 124:246–254

Part III
Marine Fish

Chapter 8
Detection of ^{131}I, ^{134}Cs, and ^{137}Cs Released into the Atmosphere from FNPP in Small Epipelagic Fishes, Japanese Sardine and Japanese Anchovy, off the Kanto Area, Japan

Takami Morita, Kaori Takagi, Ken Fujimoto, Daisuke Ambe, Hideki Kaeriyama, Yuya Shigenobu, Shizuho Miki, Tsuneo Ono, and Tomowo Watanabe

Abstract The artificial radionuclides ^{131}I, ^{134}Cs, and ^{137}Cs released from FNPP were detected in Japanese sardine (*Sadinopes melanostictus*) and Japanese anchovy (*Engraulis japonicus*) off the Kanto area of Japan. In the research period from 24 March 2011 to 13 July 2011, the maximum concentrations of ^{131}I, ^{134}Cs, and ^{137}Cs were detected in the internal organs of Japanese anchovy collected on 24 March 2011. The concentration of ^{131}I in the internal organs tended to be higher than that in muscle and the whole body, although no clear tendency was observed for ^{134}Cs and ^{137}Cs; it was thought that that was caused by ^{131}I of the planktonic contents in the internal organs. These radionuclides detected in sardine and anchovy would be derived through the atmospheric pathway from FNPP to off the Kanto area, because these radionuclides were detected before the direct release of contaminated water into the ocean from FNPP.

Keywords Radioiodine • Diocesium • Epipelagic fish • Atmosphere

T. Morita (✉) • K. Fujimoto • D. Ambe • H. Kaeriyama
Y. Shigenobu • S. Miki • T. Ono
National Research Institute of Fisheries Sciences, Fisheries Research Agency,
2-12-4, Fukuura, Kanazawa, Yokohama, Kanagawa 236-8648, Japan
e-mail: takam@affrc.go.jp

K. Takagi
Marine Biological Research Institute of Japan Co., LTD,
4-3-16, Yutaka, Shinagawa, Tokyo 142-0042, Japan

T. Watanabe
Tohoku National Fisheries Research Institute, Fisheries Research Agency,
3-27-5, Shinhama, Shiogama, Miyagi 985-0001, Japan
e-mail: wattom@affrc.go.jp

K. Nakata, H. Sugisaki (eds.), *Impacts of the Fukushima Nuclear Accident on Fish and Fishing Grounds*, DOI 10.1007/978-4-431-55537-7_8

8.1 Introduction

Large amounts of artificial radionuclides such as ^{131}I, ^{134}Cs, and ^{137}Cs, were released into the environment by the Fukushima Dai-ichi Nuclear Power Plant (FNPP) accident, which was caused by the Great East Japan Earthquake and tsunami on 11 March 2011. Tokyo Electric Power Company (TEPCO) estimated that 4.7×10^{15} Bq of radioactive materials including ^{131}I, ^{134}Cs, and ^{137}Cs were released directly into the ocean from the FNPP Unit 2 reactor during April 1–6 in 2011 (Nuclear Emergency Response Headquarters 2011), although it was reported that the direct release to the ocean had already occurred on 26 March 2011, and showed the estimation that the total amount of ^{137}Cs directly released was $3.5 \pm 0.7 \times 10^{15}$ Bq from March 26 to the end of May 2011 (Tsumune et al. 2012). The total quantity of ^{131}I and ^{137}Cs released into the atmosphere between 12 March 2011 and 1 May 2011 was estimated to be approximately 2.0×10^{17} Bq and 1.3×10^{16} Bq, respectively. Furthermore, the quantities of ^{131}I and ^{137}Cs deposited on the ocean surface from the atmosphere were estimated as 9.9×10^{16} Bq and 7.6×10^{15} Bq, respectively (Kobayashi et al. 2013).

Monitoring research detected ^{131}I, ^{134}Cs, and ^{137}Cs in marine organisms (Fisheries Agency 2014). The source of the ^{131}I and ^{134}Cs detected in marine organisms clearly originated from FNPP because of the short physical half-lives, 8.02 days for ^{131}I and about 2.06 years for ^{134}Cs. However, it has been unclear whether the radionuclides were released into the atmosphere or directly into the ocean from FNPP. In this report, we focus on the detection of ^{131}I, ^{134}Cs, and ^{137}Cs in small epipelagic fishes, sardine and anchovy, off the Kanto area of Japan. Our results indicate that the ^{131}I, ^{134}Cs, and ^{137}Cs detected in small epipelagic fishes was released into the atmosphere from FNPP.

8.2 Experimental Procedure

Fish samples were commercially collected from 24 March 2011 to 13 July 2011 at regions shown in Fig. 8.1. An individual fish sample contain only small amounts of ^{131}I, ^{134}Cs, and ^{137}Cs, so to determine the concentrations we used multiple fish samples for each measurement specimen. Therefore, we prepared the specimen for measurement consisting of muscle, internal organs, and whole body from multiple samples, a total of 5–10 kg individuals. The previous report showed ^{134}Cs and ^{137}Cs concentrations in most of the fish samples obtained from raw measurement specimens (Takagi et al. 2014). In this report, those samples were re-measured after ashing. On the other hand, ^{131}I concentrations were obtained from the measurement using a raw measurement specimen. For preparation of the ashed measurement specimen, raw samples were dried in an oven at 105 °C for 72–120 h, carbonized in a gas furnace at 350–400 °C for approximately 6 h, and ashed in an electric furnace at 450 °C for 48–72 h. The ashed samples were ground to a fine powder, transferred to a plastic cup, and pressed using a hand press. The concentrations of ^{131}I, ^{134}Cs, and ^{137}Cs were measured using a high-purity germanium (HpGe) semiconductor

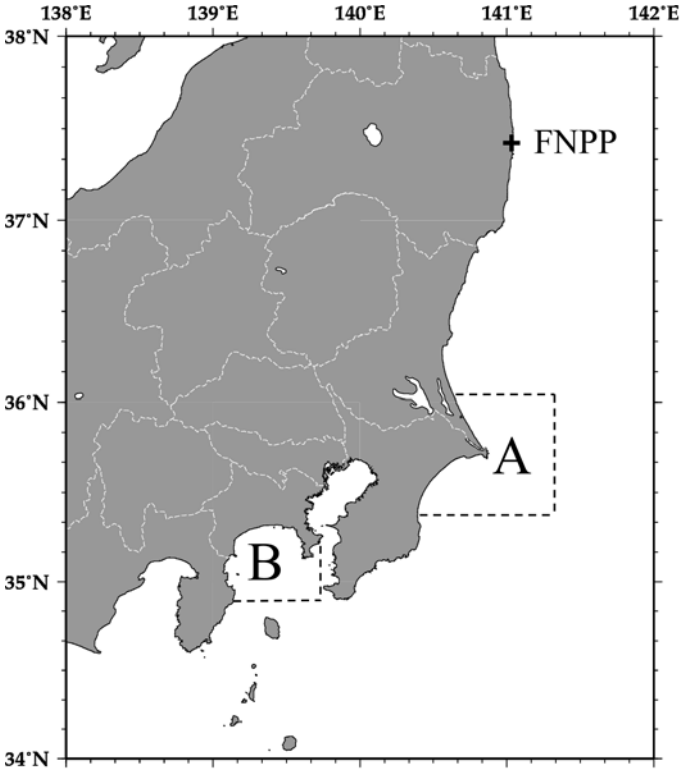

Fig. 8.1 Location of the Fukushima Dai-ichi Nuclear Power Plant (*FNPP*) and sampling regions (*A* and *B*). Respective sampling regions are surrounded by *dashed lines* indicating shorelines

detector with a multichannel analyzer (Seiko EG & G; ORTEC, Oak Ridge, TN, USA). This HpGe semiconductor detector has a resolution of 1.44 keV at a peak of 662.15 keV (^{137}Cs). The counting efficiency of the Ge semiconductor detector was calibrated using volume standard sources (MX033U8PP; Japan Radioisotope Association, Tokyo, Japan). Coincidence summing effects of ^{134}Cs were corrected with ^{134}Cs standard solutions (CZ005; Japan Radioisotope Association, Tokyo, Japan). The counting times were about 7,200 s for the raw specimen and from about 3,000 s to about 7,200 s for ashed specimens. All radionuclide concentrations were corrected for decay from the respective sampling date. The concentration of three standard deviations (σ) from counting error was defined as the detection limit.

8.3 Concentrations of ^{131}I, ^{134}Cs, and ^{137}Cs in Sardine and Anchovy

There was no difference in the ^{134}Cs/^{137}Cs concentration ratio between sardine and anchovy and among the respective measurement specimens. Considering that the half-life for ^{134}Cs is 2.1 years, the ^{134}Cs/^{137}Cs concentration ratio in these small

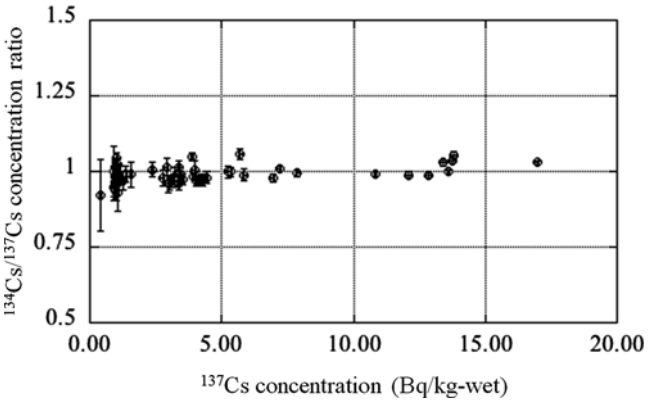

Fig. 8.2 Relationship between ^{134}Cs/^{137}Cs concentration ratio and concentration of ^{137}Cs detected in this study. The ^{134}Cs/^{137}Cs concentration ratio was calculated from the data decay corrected on 11 March 2011

epipelagic fishes was close to 1.0 (Fig. 8.2, Table 8.1). This ratio is consistent with the ^{134}Cs/^{137}Cs concentration ratio already reported in seawater and marine organisms (Aoyama et al. 2012; Wada et al. 2013). The ratio indicated that the ^{134}Cs and most of the ^{137}Cs detected in these small epipelagic fishes originated from the FNPP accident. The concentration of ^{137}Cs in muscle and whole bodies without internal organs of sardines collected off the Kanto area in 2010, before the FNPP accident, was 0.052 ± 0.0038 Bq/kg-wet and 0.030 ± 0.0044 Bq/kg-wet, respectively (Fisheries Research Agency 2012).

The previous report showed the summed concentration of ^{134}Cs and ^{137}Cs in raw measurement specimens for muscle of sardine and anchovy (Takagi et al. 2014). These concentrations were 61.0 % to 155.9 % of the sum concentration of ^{134}Cs and ^{137}Cs in the ashed measurement specimen consisting of the same samples as the raw measurement specimen. Figure 8.3 shows the temporal variation of ^{131}I and ^{137}Cs concentrations in the internal organs of sardine and anchovy. The maximum concentrations of ^{131}I, ^{134}Cs, and ^{137}Cs were 309.08 ± 2.06 Bq/kg-wet, 61.01 ± 0.52 Bq/kg-wet, and 59.63 ± 0.39 Bq/kg-wet, respectively, in the internal organs of anchovy collected 24 March 2011 (Fig. 8.3, Table 8.1). There was no detection of ^{131}I on 26 April 2011 because of the short physical half-life, 8.02 days. The concentrations of ^{131}I in the internal organs of sardine and anchovy until 26 April 2011 decreased to half by 4.4 and 4.6 days, respectively.

The respective concentrations in fishes collected in region B were obviously lower than those in region A. It was clear that the reason was the distance from FNPP to each sampling region. The concentration of ^{131}I in the internal organs tended to be higher than those in other measurement specimens, although no clear tendency was observed for ^{134}Cs and ^{137}Cs (Table 8.1). Although the concentration factor of iodine in fish is from 9 to 10, the factor of iodine in phytoplankton and zooplankton is from 800 to 1,000 (IAEA 2004). The measurement specimen from the internal organs of sardine and anchovy, which are plankton feeders, could include some plankton. Therefore, the higher concentrations of ^{131}I would be detected in the internal organ specimens from sardine and anchovy.

Table 8.1 Concentrations of ^{131}I, ^{134}Cs and ^{137}Cs in sardine and Japanese anchovy

Region	Sampling Date	Internal organs			Muscle			Whole body		
		^{131}I	^{137}Cs	^{134}Cs	^{131}I	^{137}Cs	^{134}Cs	^{131}I	^{137}Cs	^{134}Cs
Sardine										
A	2011/3/28	84.06±1.55[a]	13.75±0.12	13.34±0.09	7.90±0.42	3.04±0.05	2.88±0.04	24.47±0.77	3.96±0.09	3.93±0.07
A	2011/4/6		6.96±0.11	6.53±0.08	5.77±0.35	3.55±0.05	3.37±0.04	3.50±0.16	2.90±0.06	2.88±0.05
A	2011/4/11	13.22±0.20	3.69±0.09	3.58±0.07	2.00±0.22	3.36±0.06	3.32±0.04	6.20±0.28	5.24±0.08	5.10±0.06
A	2011/4/13	6.73±0.29	3.43±0.09	3.23±0.07	0.99±0.17	3.41±0.06	3.29±0.04	3.25±0.23	2.75±0.06	2.62±0.04
A	2011/4/25	1.78±0.30	2.28±0.07	2.12±0.05	<0.75	4.28±0.06	3.99±0.04	<0.73	3.39±0.06	3.13±0.04
A	2011/4/26	0.86±0.25			0.74±0.21			0.57±0.15		
A	2011/5/5	<0.79	<0.79		<0.53			<0.59		
A	2011/5/9	<0.69	<0.69		<0.52			<0.56		
A	2011/5/16	<0.60	1.66±0.05	1.52±0.04	<0.56	3.91±0.04	3.64±0.03	<0.59	3.23±0.09	3.00±0.06
A	2011/5/20	<0.64	2.25±0.07	2.11±0.06	<0.56	5.70±0.08	5.67±0.06	<0.54	3.88±0.04	3.83±0.03
A	2011/5/25	<0.61	1.33±0.07	1.12±0.05	<0.60			<0.61	3.15±0.05	2.88±0.03
A	2011/6/2	2.19±0.48	50.20±0.28	44.78±0.20	<0.72	12.86±0.10	11.80±0.07	<0.82	12.09±0.11	11.12±0.08
A	2011/6/4	1.16±0.25	8.64±0.16	8.14±0.12	<0.68	4.25±0.06	3.84±0.05	<0.59	4.44±0.07	4.04±0.05
A	2011/6/22	<0.85	13.37±0.15	12.57±0.12	<0.63	13.42±0.10	12.64±0.08	<0.61		
A	2011/6/29	<0.77	12.92±0.17	12.01±0.13	<0.81	13.78±0.10	13.22±0.08	<0.70	13.76±0.11	12.96±0.08
B	2011/4/11	2.39±0.33	1.15±0.05	1.07±0.03	<0.57	0.94±0.02	0.86±0.02	0.89±0.24	0.92±0.03	0.85±0.02
B	2011/6/6	<0.58	2.29±0.07	2.07±0.05	<0.65			<0.62	1.26±0.03	1.13±0.02
Japanese anchovy										
A	2011/3/24	309.08±2.06	61.01±0.52	59.63±0.39	14.30±0.35			117.46±1.27		
A	2011/4/7	12.05±0.40	8.80±0.18	8.72±0.13	2.20±0.35	2.38±0.04	2.34±0.03			
A	2011/4/14	3.61±0.39			<0.67			2.34±0.28		
A	2011/4/18	1.75±0.09	6.22±0.11	5.95±0.08	<0.54	4.01±0.05	3.77±0.04	1.20±0.16	2.95±0.07	2.74±0.05

(continued)

Table 8.1 (continued)

Region	Sampling Date	Internal organs			Muscle			Whole body		
		^{131}I	^{137}Cs	^{134}Cs	^{131}I	^{137}Cs	^{134}Cs	^{131}I	^{137}Cs	^{134}Cs
A	2011/4/26	2.42 ± 0.38			<0.51			1.10 ± 0.17		
A	2011/5/12	<0.72	13.31 ± 0.20	13.16 ± 0.15	<0.79	16.96 ± 0.08	16.54 ± 0.06	<0.75		
A	2011/5/18	<0.65	8.29 ± 0.11	7.60 ± 0.08		13.61 ± 0.07	12.82 ± 0.05	<0.61		
A	2011/5/26	<0.58	8.92 ± 0.11	8.59 ± 0.08	<0.67	10.84 ± 0.06	10.06 ± 0.04	<0.55	7.88 ± 0.07	7.34 ± 0.05
A	2011/5/26	<0.68	8.51 ± 0.12	7.79 ± 0.08	<0.59			<0.69	6.93 ± 0.07	6.34 ± 0.05
A	2011/7/13	<0.57	3.49 ± 0.05	3.06 ± 0.04	<0.70	7.18 ± 0.05	6.52 ± 0.04	<0.57	5.31 ± 0.06	4.77 ± 0.05
B	2011/3/16	18.56 ± 0.60	2.37 ± 0.16	2.37 ± 0.12	2.62 ± 0.13	1.07 ± 0.05	1.00 ± 0.04	4.88 ± 0.22	0.40 ± 0.04	0.37 ± 0.03
B	2011/3/29	13.65 ± 0.70	3.25 ± 0.08	3.23 ± 0.06	1.46 ± 0.35	1.39 ± 0.03	1.35 ± 0.02	4.82 ± 0.34	1.56 ± 0.05	1.52 ± 0.04
B	2011/6/6	<0.77	2.34 ± 0.13	2.11 ± 0.11	<0.50	5.87 ± 0.09	5.38 ± 0.07			

[a]Value shows 1 σ counting error

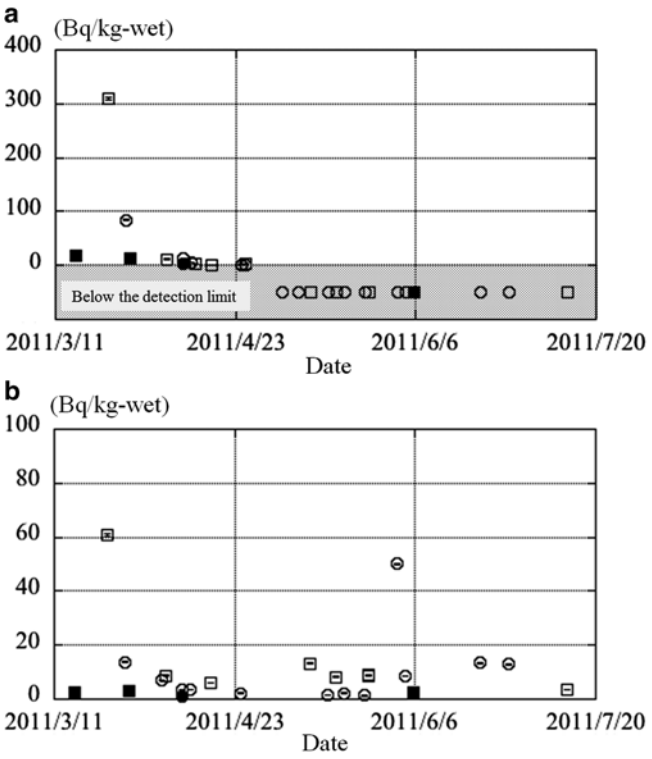

Fig. 8.3 Temporal variation in the concentration of ^{131}I (**a**) and ^{137}Cs (**b**) in internal organs of sardine and anchovy. *Circles* and *square symbols* indicate data for sardine and anchovy, respectively. *Open* and *closed symbols* indicate data for samples collected in regions *A* and *B*, respectively. *Error bar* shows 1 σ value derived from counting statistics. Errors for many of the data are too small to show an error bar

8.4 Detection of ^{131}I, ^{134}Cs, and ^{137}Cs Released into the Atmosphere from FNPP

The ^{137}Cs concentration in sardine gradually decreased until the end of May in 2011, but the concentration suddenly increased in the first week of June in 2011 (Fig. 8.3b, Table 8.1). It was considered that this sudden increase was caused by the disappearance on 30 May 2011 of a warm water eddy, the center of which was located off Iwaki between Onahama and Hasaki from the middle of May (Takagi et al. 2014; Fig. 9.4 in Chap. 9). The warm water eddy prevented the seawater, including ^{131}I, ^{134}Cs, and ^{137}Cs, from moving southward to sampling region A (Aoyama et al. 2012). In this time, ^{131}I was again detected in the internal organs of sardine, although there had come to be no detection of ^{131}I on 26 April 2011. This detection of ^{131}I also could indicate the southward movement of contaminated seawater.

^{134}Cs and ^{137}Cs were detected in sardine and anchovy collected in sampling region A before the southward movement of contaminated seawater. According to the previous report, the reason for these detections was considered to be that the contaminated sardine and anchovy migrated southward to the region earlier than the southward movement of contaminated seawater (Takagi et al. 2014). It is well known that the radioactively contaminated fishes are able to migrate from a contaminated area to a noncontaminated area. Radionuclides were transported from Russia to Japan by walleye pollock and from Japan to the United States of America by Pacific bluefin tuna (Morita et al. 2007; Madigan et al. 2012). However, in the large amount of ^{131}I, ^{134}Cs, and ^{137}Cs deposited on the ocean surface off the Kanto area (Kobayashi et al. 2013), it would be difficult to distinguish between directly released and atmospheric pathway radionuclides.

The ^{131}I/^{137}Cs concentration ratio in the internal organs of sardine and anchovy that were collected during from 16 March 2011 to 29 March 2011 in regions A and B was from 4.2 to 7.8. The ^{131}I/^{137}Cs concentration ratio of the radionuclides that were released directly from FNPP to 30 km offshore from 26 March to 6 April 2011 agreed with the radioactive decay curve of ^{131}I (Tsumune et al. 2012). However, it was unclear whether this agreement applied to the region A. In addition, the ^{131}I/^{137}Cs concentration ratio shows variations during atmospheric transport (Kinoshita et al. 2011) because of differences in the wet deposition rate depending on the size of particles (Hirose et al. 1993), whereas the simulation estimated that the ^{131}I/^{137}Cs ratio deposited in the ocean during 22 March 2011 to 24 March 2011 around region A was 6.7–40.4 (T. Kobayashi, personal communication). Therefore, it was also difficult to determine the route (as direct release or via the atmospheric pathway) of these radionuclides by the ^{131}I/^{137}Cs concentration ratio because of the range variation in the estimated ratio and the difference in incorporation rate into the internal organs between ^{131}I and ^{137}Cs. On the other hand, it was estimated that the direct release of the contaminated water from FNPP into the ocean occurred from 26 March 2011 (Tsumune et al. 2012). We detected ^{134}Cs and ^{137}Cs in Japanese anchovy collected on 24 March 2011 in region A and on 16 March 2011 in region B. Consequently, it was clear that these radionuclides were released into the atmosphere from FNPP; these would deposit on the surface water in this region through the atmospheric pathway. In addition, we also detected ^{134}Cs and ^{137}Cs in sardines collected on 28 March 2011 in region A and in both sardine and anchovy collected on 29 March 2011 in region B. Considering the distance between the FNPP and these sampling regions, these radionuclides were clearly released into the atmosphere from FNPP.

Acknowledgments We thank Dr. Takuya Kobayashi of the Japan Atomic Energy Agency (JAEA) for helpful discussion. We appreciate the great help from the staff members of the radioecology group, research center for fisheries oceanography and marine ecosystem, National Research Institute of Fisheries Science. This study was supported financially by the Fisheries Agency of Japan.

References

Aoyama M, Tsumune D, Uematsu M, Kondo F, Hamajima Y (2012) Temporal variation of ^{134}Cs and ^{137}Cs activities in surface water at stations along the coastline near the Fukushima Dai-Ichi Nuclear Power Plant accident site, Japan. Geochem J 46:321–325

Fisheries Agency (2014) Results of the monitoring on radioactivity level in fisheries products. http://www.jfa.maff.go.jp/e/inspection/index.html. Referred to on 30 Oct 2014

Fisheries Research Agency (2012) Annual reports of environmental radioactivity research for 2010. The Ministry of Agriculture, Forestry and Fisheries of Japan, Tokyo

Hirose K, Takatani S, Aoyama M (1993) Wet deposition of long-lived radionuclides derived from the Chernobyl accident. J Atmos Chem 17:61–73

IAEA (2004) Sediment distribution coefficients and concentration factors for biota in the marine environment. Technical reports series no. 422. IAEA, Vienna

Kinoshita N, Sueki K, Sasa K, Kitagawa J, Ikarashi S, Nishimura T, Wong Y, Satou Y, Honda K, Takahashi T, Sato M, Yamagata T (2011) Assessment of individual radionuclide distributions from the Fukushima nuclear accident covering central-east Japan. Proc Natl Acad Sci U S A 108:19526–19529

Kobayashi T, Nagai H, Nagai H, Terada H, Chino M, Kawamura H (2013) Source term estimation of atmospheric release due to the Fukushima Dai-ichi Nuclear Power Plant accident by atmospheric and oceanic dispersion simulations. J Nucl Sci Technol 50:255–264

Madigan D, Baumann Z, Fisher N (2012) Pacific bluefin tuna transport Fukushima-derived radionuclides from Japan to California. Proc Natl Acad Sci U S A 109:9483–9486

Morita T, Fujimoto K, Minamisako Y, Yoshida K (2007) Detection of high concentrations of ^{137}Cs in walleye pollock collected in the Sea of Japan. Mar Pollut Bull 60:1287–1306

Nuclear Emergency Response Headquarters (2011) Report of Japanese government to the IAEA ministerial conference on nuclear safety: the accident at TEPCO's Fukushima nuclear power station. http://www.kantei.go.jp/foreign/kan/topics/201106/iaea_houkokusho_e.html. Referred at 30 Oct 2014

Takagi K, Fujimoto K, Watanabe T, Kaeriyama H, Shigenobu Y, Miki S, Ono T, Morinaga K, Nakata K, Morita T (2014) Radiocesium concentration of small epipelagic fishes (sardine and Japanese anchovy) off Kashima-Boso area. Nippon Suisan Gakkaishi 80:786–791 (in Japanese with English abstract)

Tsumune D, Tsubono T, Aoyama M, Hirose K (2012) Distribution of oceanic ^{137}Cs from the Fukushima Dai-ichi Nuclear Power Plant simulated numerically by a regional ocean model. J Environ Radioact 111:100–108

Wada T, Nemoto Y, Shimamura S, Fujita T, Mizuno T, Sohtome T, Kamiyama K, Morita T, Igarashi S (2013) Effects of the nuclear disaster on marine products in Fukushima. J Environ Radioact 124:246–254

Chapter 9
Radiocesium Concentration of Small Epipelagic Fishes (Sardine and Japanese Anchovy) off the Kashima-Boso Area

Kaori Takagi, Ken Fujimoto, Tomowo Watanabe, Hideki Kaeriyama, Yuya Shigenobu, Shizuho Miki, Tsuneo Ono, Kenji Morinaga, Kaoru Nakata, and Takami Morita

Abstract After the Fukushima Dai-ichi Nuclear Power Plant (FNPP) accident, which occurred in March of 2011, the National Research Institute of Fisheries Science (NRIFS) undertook emergent radioactivity monitoring of 63 samples of small epipelagic fishes (such as sardine and Japanese anchovy) collected by commercial fishery boats off the Kashima-Boso area (located to the south of the Fukushima coast) from 24 March 2011 to 21 March 2013. Fluctuations in the radiocesium concentration in fish muscles synchronized with the decreasing concentration from seawater near the fishing ground; the radiocesium concentration in fish muscles reached a maximum of 31 Bq/kg-wet in July 2011, after which it declined gradually. From 2012 to 2013, the radiocesium concentrations in fish muscles were low (0.58–0.63 Bq/kg-wet). Compared to the ^{137}Cs concentration before the FNPP accident, ^{137}Cs concentration in fish muscles in 2013 was still about 10 times higher, whereas it was about 4.5 times higher in seawater near the fishing ground in 2012.

K. Takagi (✉)
Marine Biological Research Institute of Japan Co., LTD,
4-3-16, Yutaka, Shinagawa, Tokyo 142-0042, Japan

K. Fujimoto • H. Kaeriyama • Y. Shigenobu
S. Miki • T. Ono • K. Morinaga • T. Morita
National Research Institute of Fisheries Sciences, Fisheries Research Agency,
2-12-4, Fukuura, Kanazawa, Yokohama, Kanagawa 236-8648, Japan
e-mail: takam@affrc.go.jp

T. Watanabe
Tohoku National Fisheries Research Institute, Fisheries Research Agency,
3-27-5, Shinhama, Shiogama, Miyagi 985-0001, Japan
e-mail: wattom@affrc.go.jp

K. Nakata
Fisheries Research Agency Headquarters,
2-3-3, Minatomirai, Nishi, Yokohama, Kanagawa 220-6115, Japan

K. Nakata, H. Sugisaki (eds.), *Impacts of the Fukushima Nuclear Accident on Fish and Fishing Grounds*, DOI 10.1007/978-4-431-55537-7_9

Keywords Japanese anchovy • Off the Kashima-Boso area • Pacific Ocean • Radiocesium • Sardine • Seawater

9.1 Introduction

Artificial radionuclides were released into the environment as a result of the Tokyo Electric Power Company (TEPCO) Fukushima Dai-ichi Nuclear Power Plant (FNPP) accident that occurred in March of 2011. TEPCO (2012) has estimated that radiocesium (^{134}Cs and ^{137}Cs) at approximately 10 PBq for both ^{134}Cs and ^{137}Cs was released into the atmosphere in March 2011. In addition, it was estimated that ^{134}Cs was released into the atmosphere and the ocean from the port of the nuclear power plant from March to September 2011 at a level of 3.5 PBq and that the level of ^{137}Cs was 3.6 PBq. Some of the released radiocesium was taken into the bodies of marine organisms through the surrounding water and their prey, and an investigation into radioactive substances in marine products, conducted by Fisheries Agency (FA), showed that a relatively high radiocesium concentration (compared to the concentration before the FNPP accident) was detected in some of the fish of the northwest Pacific Ocean (Fisheries Agency 2012, 2013). These results indicate that there is a possibility of long-term residual radiocesium in organisms with strong regional characteristics, including bottom fish (Buesseler 2012). The mechanisms of radioactive substance migration in marine ecosystems need to be understood (Yoshida and Kanda 2012), but this would entail an analysis of the radioactive substance transfer mechanism corresponding to ecological characteristics related to each component of the marine ecosystem. The National Research Institute of Fisheries Science (NRIFS), Fisheries Research Agency (FRA) cooperated with the radioactive substance investigation and conducted an intensive survey of marine products caught in the Kanto region for approximately 6 months immediately after the FNPP accident.

Some of the species of fish that were present during the high fishing season off the Pacific Ocean coast after the FNPP accident included small migratory epipelagic fishes, namely, sardine (*Sardinops melanostictus*) and Japanese anchovy (*Engraulis japonicus*). Sardine and Japanese anchovy actively eat plankton, and they are preyed upon by whales and large fishes, which gives them an important ecological niche in the Pacific Ocean coastal areas of the Tohoku region. Each year, from winter/spring to summer, sardine and Japanese anchovy migrate to Kashima-Boso, temporarily remaining in the area to create a fishing ground, and they are fished in large- to medium-scale round-haul fisheries (Uchiyama 1998; Yasumi 2008; Kubota 2012). Thus, this chapter contains an analysis of fluctuations in the radiocesium concentration of these small epipelagic fishes caught in the fishing grounds off the Kashima-Boso area.

9.2 Collection of Fish and Radioactivity Measurement

NRIFS prepared 63 specimens for radioactivity measurement for each fish species for each sampling date for adult sardine and Japanese anchovy caught mainly in a large- to medium-scale round-haul fishery off the Kashima-Boso area (Fig. 9.1)

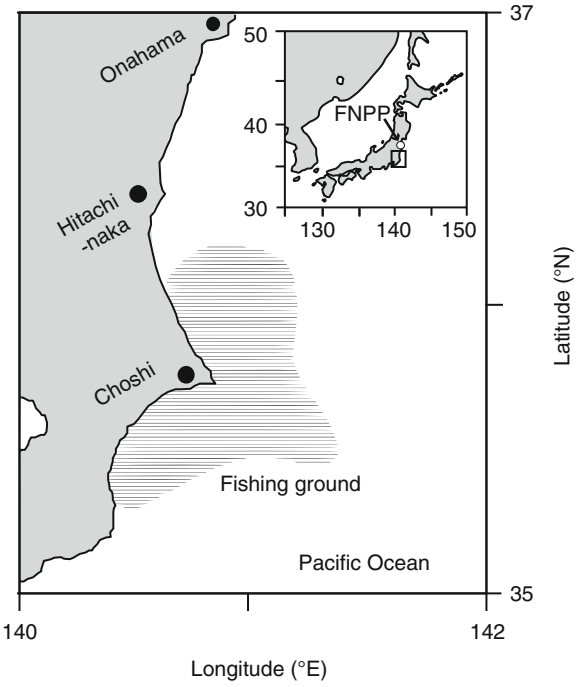

Fig. 9.1 Locations of the Fukushima Dai-ichi Nuclear Power Plant (FNPP), and fishing grounds of fish sampled (sardine and Japanese anchovy) in this chapter (*shaded area*)

from 24 March to 3 November 2011; 27 June and 20 August 2012; and 18 February 2013. Muscles were chosen as the measurement sample for this study. For small epipelagic fishes collected in 2011, 60 raw specimens were prepared, and for small epipelagic fishes collected in 2012 and 2013, 3 ashed specimens were prepared, assuming that the radiocesium concentration would be quite low.

To measure radiocesium concentrations, a germanium semiconductor detector (EG ORTEC Solid-State Photon Detector) and a pulse-height analyzer (SEIKO EG MCA 7600 Multichannel Analyzer) were used. The resolution of the germanium semiconductor detector [full width at half-maximum (FWHM)] was 1.80 keV (^{60}Co, 1,333 keV), and the relative efficiency was 33.0 %. The standard source was the quasi-gamma-ray volume source standard MX033SPS prepared by Japan Radioisotope Association (a special order was placed to obtain source heights of 5, 10, 20, 30, and 50 mm), and the MX033U8PP type prepared by the Association. Nuclides that were objects of measurement were ^{134}Cs (605, 796 keV; without summing the effect correction) and ^{137}Cs (662 keV). For calculation of the targeted nuclide concentrations, we followed the directive 'The gamma-ray spectrometry by germanium semiconductor detector' (Ministry of Education, Culture, Sports, Science and Technology 1992), and we calculated using the Covell method. Sixty specimens of epipelagic fishes collected in 2011 were used as raw samples for 7,200-s measurements, and three specimens of epipelagic fishes collected in 2012 and 2013 were ashed under the assumption that the radiocesium concentration is

quite low; they were analyzed by carrying out 40,000-s measurements or longer. Radiocesium data (both ^{134}Cs and ^{137}Cs) were obtained by making attenuation corrections to the sample of small epipelagic fishes for the sampling date.

9.3 Tracking the 2010 Year-Class Fish

We first introduce the distribution ecology based on the fluctuation in catch volumes for both sardine and Japanese anchovy. From March to August 2011, the sardine haul was more than that of Japanese anchovy, and the sardine haul in Chiba Prefecture during this period (66,000 tons) was twice that of Japanese anchovy (33,000 tons) (National Research Institute of Fisheries Science 2011). As for which sardine haul is relatively larger, the main target of the round-haul fishery is the southward migrating group of sardine during winter and spring, but during summer, the target changes to the northward migrating group composed of age 2 fish and older as usual (Fisheries Agency and Fisheries Research Agency 2011). However, in the fishing season of 2011, the 2010 year-class had the highest amount of recruitment to the sardine stock since 2002 (Kawabata et al. 2012). Furthermore, during the fishing seasons from winter/spring to the summer of 2011, the 2010 year-class was widespread in the Boso area. Thus, only a small number of age 2 fish and older (which are older than the 2010 year class) were mixed among the catch (Fisheries Agency and Fisheries Research Agency 2011).

Before preparing the radioactivity measurement samples, ten specimens were randomly selected, and the standard length (SL, mm) was measured to calculate the average length of each sample. The average values of SL of small epipelagic fish samples were 132–200 and 99–124 mm for sardine and Japanese anchovy, respectively (Fig. 9.2). The average length of fishes used as samples generally matched the mode of length composition of the catch in the Joban-Boso area from March to August 2011 (National Research Institute of Fisheries Science 2011). Thus, it was determined that both the sardine and Japanese anchovy used for this study were the results of continuously tracking the temporal fluctuations in radiocesium concentration of age 1 fish (the 2010 year-class) in the surveyed area in the ocean. It was also determined from the average length of the sample that we tracked the 2010 year-class until August 2012, and the February 2013 sample was the result of tracking age 1 fish from the 2012 year-class. Whitebait (Japanese anchovy) of coastal areas off Fukushima Prefecture is known as an example of the turnover of fish schools affecting the fluctuations of radiocesium concentration in fish (Wada et al. 2013), but it was considered to be fluctuation of radiocesium concentration in the 2010 year-class sardine that was tracked during 2011 in this chapter. Subsequently, the main catch for Japanese anchovy during April to June was age 1 fish (the 2010 year-class) (Fisheries Agency and Fisheries Research Agency 2011), similar to sardine.

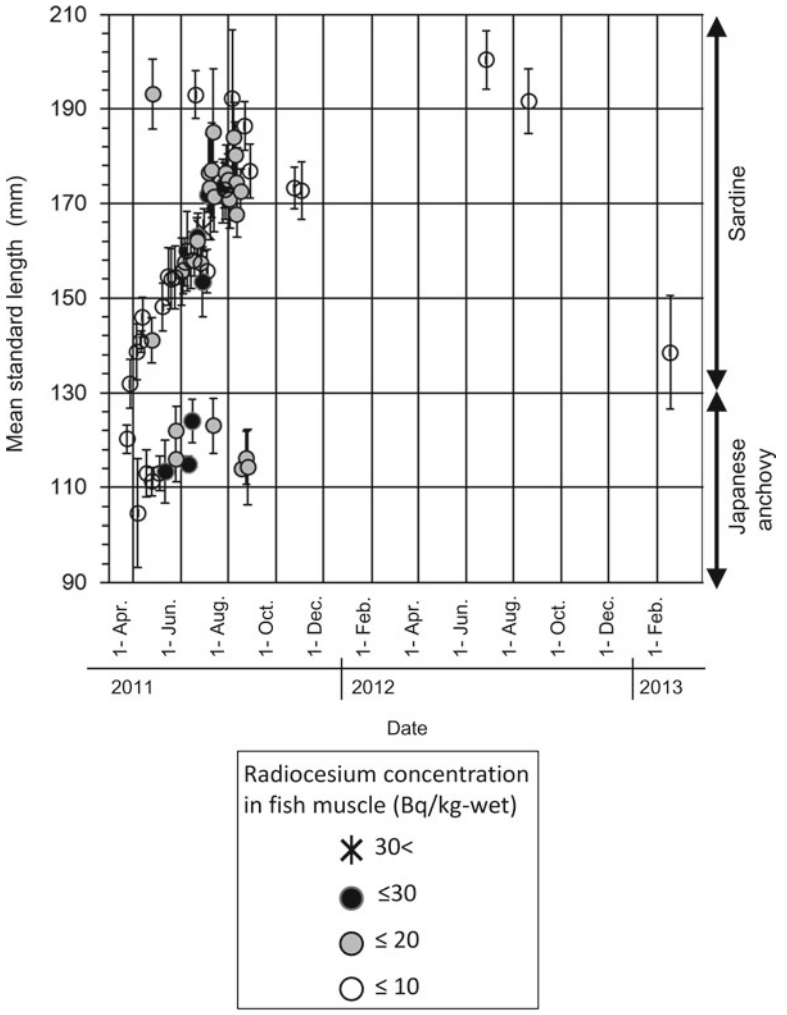

Fig. 9.2 Mean standard length of fish samples (sardine and Japanese anchovy) used in this chapter. *Vertical bar* indicates standard deviation

9.4 Temporal Fluctuations in Radiocesium Concentration of Small Epipelagic Fishes

Because there was no significant difference between radiocesium concentrations of sardine and Japanese anchovy collected during the research period (Fig. 9.3), these two species were considered together as 'small epipelagic fishes' for the analysis. From March to May 2011, the radiocesium concentration in the muscle of small epipelagic fishes exhibited relatively high concentrations on certain occasions, such as 13 Bq/

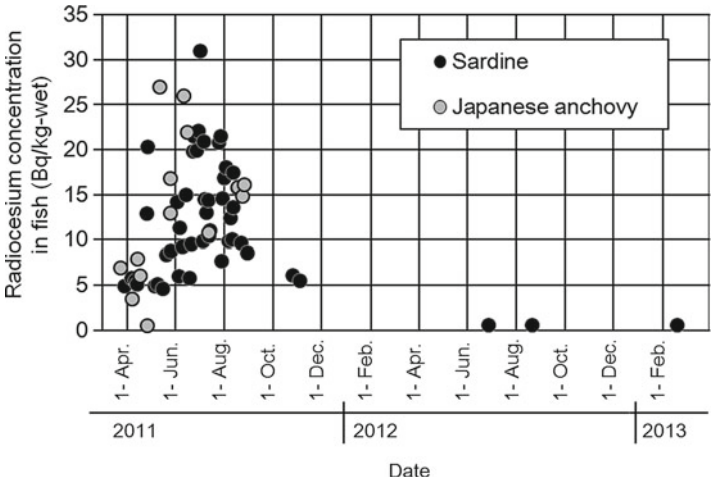

Fig. 9.3 Temporal variations of radiocesium ($^{134}Cs + {}^{137}Cs$) concentration in small epipelagic fish (sardine and Japanese anchovy) caught off the Kashima-Boso area

kg-wet on 25 April, 21 Bq/kg-wet on 26 April, and 27 Bq/kg-wet on 12 May; however, the concentrations generally remained at 9 Bq/kg-wet or lower (Fig. 9.3). Concentrations mostly ranged from 9 to 22 Bq/kg-wet from June to August (Fig. 9.3), and these values were significantly higher than the concentrations detected from March to May (Mann–Whitney U test, $p < 0.01$). After detecting the maximum value of 31 Bq/kg-wet in early July, none of the specimens had a value greater than 20 Bq/kg-wet in August, and 6 and 5.5 Bq/kg-wet were recorded on 25 October and 3 November, respectively, which was after the summer fishing season (Fig. 9.3). Concentrations have continued to decrease since 2012, and levels as low as 0.58–0.63 Bq/kg-wet were detected (Fig. 9.3).

9.5 Decreasing Trend of Radiocesium Concentration of Small Epipelagic Fishes

Measurement results of small epipelagic fishes by NRIFS used in this research were mainly conducted until August 2011. To complete the time-series data, data for 200 specimens collected in the same area (Fig. 9.4a) as this study were referenced from radiocesium concentration data (for both ^{134}Cs and ^{137}Cs) of sardine and Japanese anchovy reported on the FA website from 24 March 2011 to 21 March 2013 (Fig. 9.4b) (Fisheries Agency 2012, 2013). These data were mostly obtained as raw samples through 7,200-s measurements by local municipalities in the same manner as the NRIFS data. However, information regarding the length of fish from which samples were taken was not made public. In addition to muscle samples, samples prepared from the whole fish are included in the measurement samples (in this chapter, whitebait and samples that are labeled as processed goods were excluded).

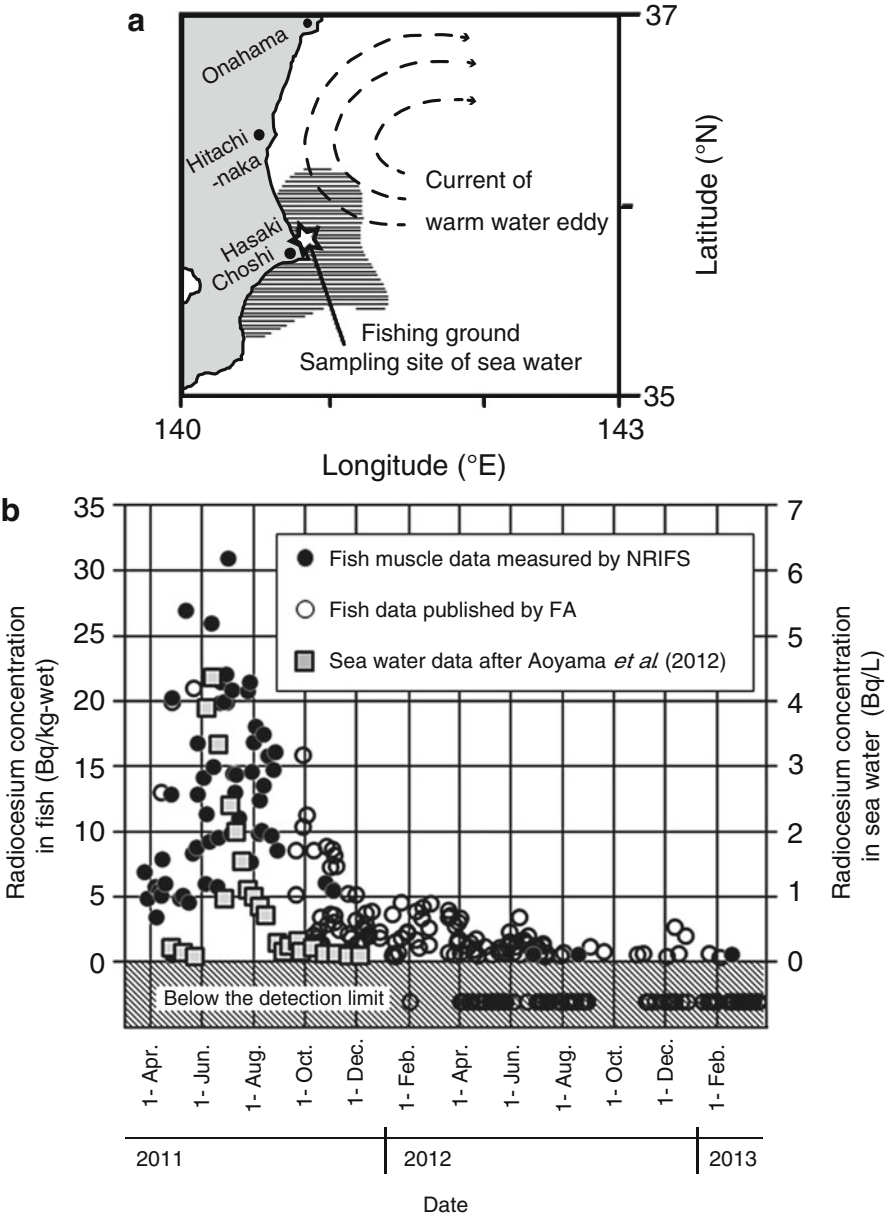

Fig. 9.4 (**a**) Locations of fishing grounds of fish sampled (sardine and Japanese anchovy) in this chapter (*shaded area*), and sampling site of seawater (*star*) (after Aoyama et al. 2012). *Thin curved arrows* indicate current of warm water eddy (after Aoyama et al. 2012). (**b**) Temporal variations of radiocesium ($^{134}Cs + {}^{137}Cs$) concentration in small epipelagic fish (sardine and Japanese anchovy) caught off the Kashima-Boso area and seawater (after Aoyama et al. 2012). The National Research Institute of Fisheries Science (NRIFS) measured radiocesium concentration of fish muscle. Data from the Fisheries Agency (FA) indicate radiocesium concentrations of both muscle and whole body in fish. Plot below the *x*-axis indicates the existence of data indicating a radiocesium concentration below the detection limit

The published data on the aforementioned FA website do not state the collection date; thus, in this study we substituted the published date as the collection date for each datum. According to this, even after August 2011, the gradual decreasing trend of the concentration continued. After December 2011, the concentration decreased below 5.0 Bq/kg-wet, and by April 2012, many specimens had concentrations below the lower limit of detection. The detection limit value since April 2012 was 0.54 Bq/kg-wet on average for ^{137}Cs (range, 0.29–0.76). The concentrations of ^{137}Cs obtained from the measurement of ashed samples by NRIFS in June 2012, August 2012, and February 2013 were 0.38, 0.42, and 0.42 Bq/kg-wet, respectively, which were lower than the aforementioned average detection limit values.

9.6 Radiocesium Concentration in Seawater of the Fishing Ground

Aoyama et al. (2012) measured the radiocesium concentration (Fig. 9.4b) of the seawater collected in Hasaki (Fig. 9.4a) near the fishing ground from 25 April to 5 December 2011 after the FNPP accident. According to these results, the radiocesium concentration of seawater was less than 1.0 Bq/l from April to May 2011, and then it suddenly increased in June, reaching an average of 3.9 Bq/l in early June. After attaining the maximum value of 4.4 Bq/l in mid-June, concentration gradually decreased in late June to an average of 3.4 Bq/l. The concentration continued to decrease and reached an average of 1.1 Bq/l in late July, and in late August the average concentration was less than 1.0 Bq/l (Fig. 9.4b) (Aoyama et al. 2012). Differing from the fluctuations in the radiocesium concentration of small epipelagic fishes in the same marine area (Figs. 9.3 and 9.4b), the radiocesium concentration of seawater spiked in June, showing values significantly higher than the concentrations in April to May and July to August (Mann–Whitney U test, $p<0.05$). Aoyama et al. (2012) analyzed this situation as a reflection of the temporary inhibition of southward flow of the seawater (strongly affected by the FNPP accident) because of the presence of a warm eddy (Fig. 9.4a) and its arrival to Hasaki in early June. According to the survey conducted by FRA in August 2012, it has been found that the radiocesium concentration near the fishing ground (36°15′N–141°00′E) has decreased to 16 mBq/l (10 mBq/l for ^{137}Cs only) (Fisheries Research Agency 2013).

9.7 Fluctuations of Radiocesium Concentration of Small Epipelagic Fishes Associated with Their Migration Patterns

Compared to spiking fluctuations of the radiocesium concentration of the seawater, the radiocesium concentration in the muscle of small epipelagic fishes showed a relatively mild increase and decrease (Fig. 9.4b). Because radiocesium is

incorporated into the bodies of fish from the environment and remains there for some time, the radiocesium concentration of small epipelagic fishes gradually decreased following the fluctuations of radiocesium concentration in seawater. However, because samples were prepared from the catch for this study, fluctuations in concentration in the bodies of fish might be affected by the distribution condition of small epipelagic fishes in the fishing ground. Sardine and Japanese anchovy are widespread in the Sanriku-Boso area during winter and spring, and wintering age 0 fish are known to migrate southward from Sanriku to Boso (Uchiyama 1998; Yasumi 2008; Kubota 2012). From the coast off Hokota City, which is located just to the north of Kashima City, to the coast off Kitaibaraki City, the concentrations detected from April to May 2011 for sardine and Japanese anchovy were 40 and 30–170 Bq/kg-wet, respectively (Fisheries Agency 2012). Based on these results, the reason that the radiocesium concentration of small epipelagic fishes increased before the concentration in the seawater of Hasaki increased, and showed some variability, may be that the school of fish from the northern ocean with a radiocesium concentration higher than that of Hasaki has migrated into the fishing ground off the Kashima-Boso area.

9.8 Comparison of Situations Before and After the FNPP Accident

From ^{134}Cs and ^{137}Cs released as a result of the FNPP accident, we will use the ^{137}Cs nuclide with a relatively long half-life (30.1 years), which can be compared to the pre-FNPP accident conditions, to continue this discussion.

Measurement values from May to November 2011 (for which radiocesium concentration data of seawater in Hasaki are complete from the early part of a month to the later part) were used to compare the fluctuations in ^{137}Cs concentration of seawater and small epipelagic fishes in 2011 for monthly average values (Fig. 9.5). The average concentrations in small epipelagic fishes were 6.1 ± 4.3, 8.8 ± 3.8, 8.9 ± 3.9, and 7.9 ± 2.0 Bq/kg-wet for May, June, July, and August, respectively; the August average value was close to those of June and July, but it had relatively small deviations (Fig. 9.5). The values decreased to approximately half the value recorded in May by October and November at 3.2–3.4 Bq/kg-wet. In comparison, the concentrations in seawater were 0.07 ± 0.02 Bq/l in May, with a maximum value of 1.65 ± 0.77 Bq/l in June. It then decreased to 0.95 ± 0.30 Bq/l in July, and the decreasing trend continued; by November, the value was similar to that from May at 0.07 ± 0.01 Bq/l. As these results show, seawater concentrations quickly decreased after peaking in June, but the concentrations of small epipelagic fishes remained relatively high until August. Thus, this clearly indicates a delayed decreasing trend compared to the seawater. Assuming that the small epipelagic fishes and environmental water are in equilibrium, we calculated the concentration coefficient (biological concentration/seawater concentration) of ^{137}Cs in the muscle of small pelagic fish from the average monthly values of radiocesium concentration already

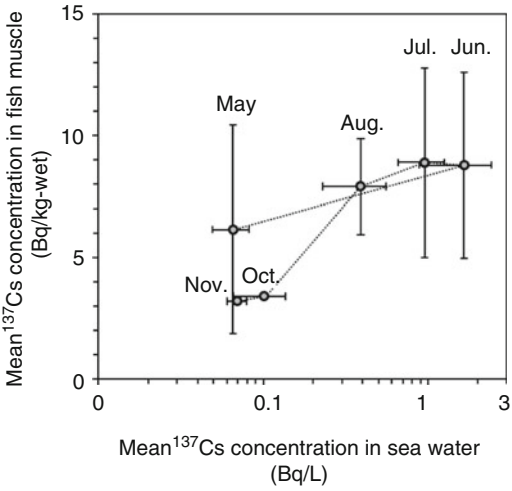

Fig. 9.5 Relationship in mean ^{137}Cs concentration per month between seawater (after Aoyama et al. 2012) and small epipelagic fish (sardine and Japanese anchovy) measured by National Research Institute of Fisheries Science (NRIFS) during May to November 2011. *Horizontal and vertical bars* indicate standard deviation

described. The results showed that the coefficient varied from 5 to 94 in 2011, with October and November having values of 34 and 46, respectively. Based on the survey results by FRA (2013), the concentration coefficient of ^{137}Cs of seawater concentration near the fishing ground in August 2012 was obtained, and the result was 42. The concentration coefficient of ^{137}Cs before the FNPP accident was 10–100 for all types of fishes, but 20–40 for sardine (Yoshida 1999); thus, the concentration coefficient of small epipelagic fishes collected in the target marine area since the fall of 2011 appears to be returning to this range. In contrast to the ^{137}Cs concentration in the muscles of sardine collected in the same marine area in June 2009, 0.038 Bq/kg-wet (Ministry of Agriculture, Forestry and Fisheries Agriculture 2011), concentrations approximately 10 times higher than those from before the FNPP accident (0.42 Bq/kg-wet) were detected in August 2012 and February 2013 during the course of this study. Meanwhile, as the ^{137}Cs concentration in seawater was 2.2 mBq/l in June 2009 (Japan Coastal Guard 2010), the value in August 2012 was approximately 4.5 times higher than that from before the FNPP accident. Therefore, it has been indicated that the seawater concentration decreases before the radiocesium concentration of small epipelagic fishes decreases. Based on these results, although the rapid fluctuations in radiocesium concentrations are decreasing, the radiocesium concentration still remains higher than that before the FNPP accident. It is necessary to continue long-term monitoring to track the decreasing process of radiocesium in small epipelagic fishes and analyze the behaviour of radiocesium in marine ecosystems.

Acknowledgments This chapter was written based on Takagi et al. (2014). As emergent radioactivity monitoring of marine organisms immediately after the Tohoku Region Pacific Coast Earthquake, fishes were dissected with great cooperation from everyone at National Research Institute of Fisheries Science, for which we hereby express our sincere gratitude. In particular, the contract staffs from Radioecology Group of the Marine Ecology Research Centre have continued to dissect and measure the fishes for radioactive content. We wish to extend our most sincere

thanks to Dr. Satoshi Honda of Fisheries Research Agency headquarters, who gave us valuable advice on the fishing situations and resource conditions of the Pacific stock of sardine. In addition, this study was conducted under the 2011–2013 Fisheries Agency Commissioned Project 'Radioactive Material Impact Investigation Research Project.'

References

Aoyama M, Tsumune D, Uematsu M, Kondo F, Hamajima Y (2012) Temporal variation of ^{134}Cs and ^{137}Cs activities in surface water at stations along the coastline near the Fukushima Dai-ichi Nuclear Power Plant accident site, Japan. Geochem J 46:321–325

Buesseler KO (2012) Fishing for answers off Fukushima. Science 338:480–482

Fisheries Agency, Fisheries Research Agency (2011) To understand the current condition of aquatic resources around Japan—Forecasting of fishing and oceanographic conditions (updated 29th July, 2011). http://abchan.job.affrc.go.jp/koshin_2.html. Referred at 8 Jan 2014 (in Japanese)

Fisheries Agency (2012) The results of a radioactivity survey for marine products in each prefecture (30th March, 2012). http://www.jfa.maff.go.jp/j/housyanou/kekka.html. Referred at 5 Jun 2013 (in Japanese)

Fisheries Agency (2013) The results of a radioactivity survey for marine products in each prefecture (29th March, 2013). http://www.jfa.maff.go.jp/j/housyanou/kekka.html. Referred at 5 Jun 2013 (in Japanese)

Fisheries Research Agency (2013) [fiscal year] 2012 report on the radioactive material impact investigation project (March 2013). http://www.fra.affrc.go.jp/eq/Nuclear_accident_effects/index.html. Referred at 2 Oct 2013 (in Japanese)

Japan Coastal Guard (2010) Radioactivity survey report (2009 survey results). Oceanographic Information Department, Japan Coast Guard, Tokyo (in Japanese)

Kawabata A, Honda S, Watanabe C, Kubota H (2012) [fiscal year] 2012 Fishery resource evaluation of waters surrounding Japan. Resource evaluation of 2012 Pacific group sardine, Fisheries Agency, Tokyo, pp 15–44 (in Japanese)

Kubota H (2012) Ecological characteristics estimated by long-term resource fluctuations in the Pacific group of Japanese anchovy. Fish Biol Oceanogr Kuroshio 13:27–32 (in Japanese)

Ministry of Agriculture, Forestry and Fisheries (2011) [fiscal year] 2009 Ministry of Agriculture, Forestry and Fisheries related radioactivity survey research annual report, Tokyo (in Japanese)

Ministry of Education, Culture, Sports, Science and Technology (1992) Radioactivity Measurement series 7 Gamma-ray spectrometry by germanium semiconductor detector (1992 revised edition). Tokyo

National Research Institute of Fisheries Science (2011) [fiscal year] 2011 2nd Pacific Ocean fishing and oceanographic condition prediction conference on Sardine, Horse Mackerel, Cub and Spotted Mackerel — fishing condition related materials. National Research Institute of Fisheries Science, Fisheries Research Agency, Yokohama, 20–21 Dec (in Japanese)

Takagi K, Fujimoto K, Watanabe T, Kaeriyama H, Shigenobu Y, Miki S, Ono T, Morinaga K, Nakata K, Morita T (2014) Radiocesium concentration of small epipelagic fishes (sardine and Japanese anchovy) off Kashima–Boso area. Nippon Suisan Gakkaishi 80:786–791 (in Japanese)

Tokyo Electric Power Company (2012) For an estimation of the amount of radioactive substances released into the atmosphere and the ocean accompanying the FNPP accident due to the impact of the Tohoku Region Pacific Coast Earthquake (evaluated as of May 2012). http://www.tepco.co.jp/cc/press/2012/1204619_1834.html. Referred at 30 May, 2013 (in Japanese)

Uchiyama M (1998) Immature fish during the wintering season. In: Watanabe Y, Wada T (eds) Changes in resources and ecology of sardine, Fisheries science series 119. Kouseisha-Kouseikaku Corporation, Tokyo, pp 103–113 (in Japanese)

Wada T, Nemoto Y, Shimamura S, Fujita T, Mizuno T, Sohtome T, Kamiyama K, Morita T, Igarashi S (2013) Effects of the nuclear disaster on marine products in Fukushima. J Environ Radioact 124:246–254

Yasumi N (2008) Biological properties of sardine during the low resource season. Kaiyo Mon 40:189–194 (in Japanese)

Yoshida K (1999) Biological transport of Cs-137 to the deep-sea—regarding *Coryphaenoides yaquinae*. Aquabiology 122:210–218 (in Japanese)

Yoshida N, Kanda J (2012) Tracking the Fukushima radionuclides. Science 336:1115–1116

Chapter 10
Why Do the Radionuclide Concentrations of Pacific Cod Depend on the Body Size?

Yoji Narimatsu, Tadahiro Sohtome, Manabu Yamada, Yuya Shigenobu, Yutaka Kurita, Tsutomu Hattori, and Ryo Inagawa

Abstract We examined year-class-related differences in radiocesium concentrations in Pacific cod (*Gadus macrocephalus*) and evaluated the potential factors affecting the differences after the release of large amounts of radionuclides from Fukushima Dai-ichi Nuclear Power Plant (FNPP) in March 2011. The concentration of radiocesium was highest in the 2009 and earlier year-classes (yc) (≤2009 yc), followed by the 2010 yc, and was rarely detected in the 2011 yc. Trawl surveys throughout the year revealed that a proportion of Pacific cod born in or before 2009 and 2010 were distributed in the coastal area from winter to early summer, whereas all individuals were on the upper continental slope from early summer to winter. The concentration of radiocesium decreased more rapidly in the 2010 yc than in the ≤2009 yc. The diet of cod changed ontogenetically and spatiotemporally. The organisms preyed upon on the upper continental slope by cod of all year-classes and in the coastal area by the 2010 yc contained very low concentrations of radiocesium. However, some food items ingested in the coastal area by the ≤2009 yc had relatively

Y. Narimatsu (✉) • T. Hattori
Hachinohe Laboratory, Tohoku National Fisheries Research Institute, Fisheries Research Agency, 25-259, Shimomekurakubo, Samemachi, Hachinohe, Aomori 031-0841, Japan
e-mail: nary@affrc.go.jp

T. Sohtome • M. Yamada
Fukushima Prefectural Fisheries Experimental Station,
13-2, Matsushita, Onahamashimokajiro, Iwaki, Fukushima 970-0316, Japan

Y. Shigenobu
National Research Institute of Fisheries Sciences, Fisheries Research Agency,
2-12-4, Fukuura, Kanazawa, Yokohama, Kanagawa 236-8648, Japan

Y. Kurita
Tohoku National Fisheries Research Institute, Fisheries Research Agency,
3-27-5, Shinhama-cho, Shiogama-city, Miyagi, 985-0001, Japan

R. Inagawa
Hachinohe Laboratory, Tohoku National Fisheries Research Institute, Fisheries Research Agency, 25-259, Shimomekurakubo, Samemachi, Hachinohe, Aomori 031-0841, Japan

Kushiro Laboratory, Hokkaido National Fisheries Research Institute, Fisheries Research Agency, 116 Katsurakoi, Kushiro, Hokkaido 085-0802, Japan

K. Nakata, H. Sugisaki (eds.), *Impacts of the Fukushima Nuclear Accident on Fish and Fishing Grounds*, DOI 10.1007/978-4-431-55537-7_10

high radiocesium levels. These results suggest that Pacific cod primarily accumulated radiocesium during the first few months after the FNPP accident. Age- and body size-dependent differences in growth, metabolic rate, and diet, as well as seasonal migration patterns, also affected the rate of decrease in radiocesium levels, which likely led to the differences we observed between year-classes.

Keywords Pacific cod • Nuclear Power Plant accident • Radiocesium • Year-class • Seasonal migration • Ontogenetic shift of diet

10.1 Introduction

Huge amounts of radionuclides were released from the devastated Fukushima Daiichi Nuclear Power Plant following the Great East Japan Earthquake on 11 March 2011. The radionuclides contaminated the air, land, and ocean both directly and indirectly. Model estimates suggest that 3.5 ± 0.7 PBq radiocesium 137 was emitted directly to the ocean (Tsumune et al. 2012). A number of marine organisms ingested radionuclides into their body via the water and their diet. As a result, high concentrations of radiocesium were detected in almost all fish that inhabit the coast of Fukushima Prefecture within a year after the tsunami (Buesseler 2012). The level of contamination has decreased over time, and has now stabilized at a low level in pelagic fish species and invertebrates (Wada et al. 2013; Sohtome et al. 2014). In contrast, the decline in radionuclide levels has occurred more slowly in demersal fishes, resulting in food safety problems.

Pacific cod (*Gadus macrocephalus*) are one of the most important species in the upper continental slope ecosystem for commercial fishermen in the North Pacific off northern Japan (Tohoku area). The concentration of radiocesium in demersal fishes such as bighand thornyhead (*Sebastolobus macrochir*) and threadfin hakeling (*Laemonema longipes*) that inhabit the upper continental slope was low and stable even soon after the Fukushima Daiichi Power Plant (FNPP) accident (MAFF 2014). Despite occupying a similar spatial niche as these species, the radiocesium levels in some Pacific cod individuals were higher than allowable values in Japan ($^{134}Cs + {}^{137}Cs$, 100 Bq/kg-wet). Additionally, the majority of demersal fishes that had radiocesium levels exceeding this standard were clustered in Fukushima and neighboring prefectures. In contrast, unsafe levels of radiocesium were measured in Pacific cod over a much wider area in 2011 and 2012, including five prefectures in the Tohoku district.

Commercial fishing or landing of cod was prohibited for 8 months after the shipment of cod was regulated in May 2012 in Miyagi Prefecture. The cod fishery was partially restarted in September 2012 when small cod (<1 kg) were approved for harvest, because high levels of radiocesium were only detected in large fish ($\geq$1 kg). Therefore, the concentration of radiocesium in Pacific cod appears to be a

function of age and body length. Our objective was to evaluate the relationship between age, body size, and radiocesium concentrations in Pacific cod following the FNPP accident. We documented the seasonal change in the distribution of fish of two age classes. Additionally, we evaluated the feeding ecology of Pacific cod in two regions to document ontogenetic shifts in diet. We measured radiocesium concentrations in the primary diet items of Pacific cod. Based on these data, we estimated when and how radiocesium was taken up by Pacific cod and the rate of decrease. We then used these results to predict conditions in the near future.

10.2 Radiocesium Concentration of Pacific Cod

We recorded the standard length and body weight of Pacific cod that were captured from April 2011 to March 2014 off Fukushima Prefecture and then removed the sagittal otoliths. One of the sagittal otoliths was cut into slices with hard resin and used for age determination following the method of Hattori et al. (1992). We determined the birth year-class of all specimens. Muscle tissue samples were removed from the vertebrae and skin to measure radiocesium concentrations. We examined the temporal changes in radiocesium concentration following the nuclear accident and compared the levels among year-classes (ycs).

The radiocesium concentration of Pacific cod was always higher in the year classes of 2009 and earlier (≤2009 yc) than in the 2010 yc (Fig. 10.1). The radiocesium concentrations measured from April 2012 to March 2013 ranged from

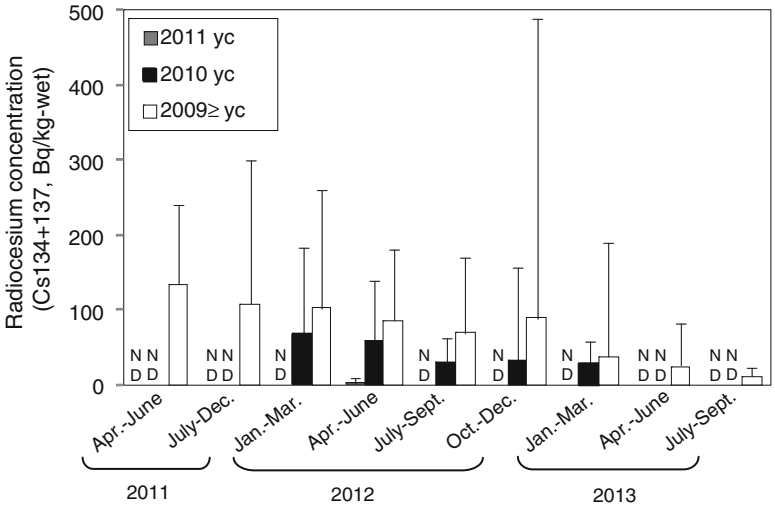

Fig. 10.1 Temporal changes in radiocesium (^{134}Cs + ^{137}Cs) concentration in the 2011, 2010, and ≤2009 year-classes of Pacific cod. *Boxes* and *bars* represent the average and maximum values, respectively. *ND* no data

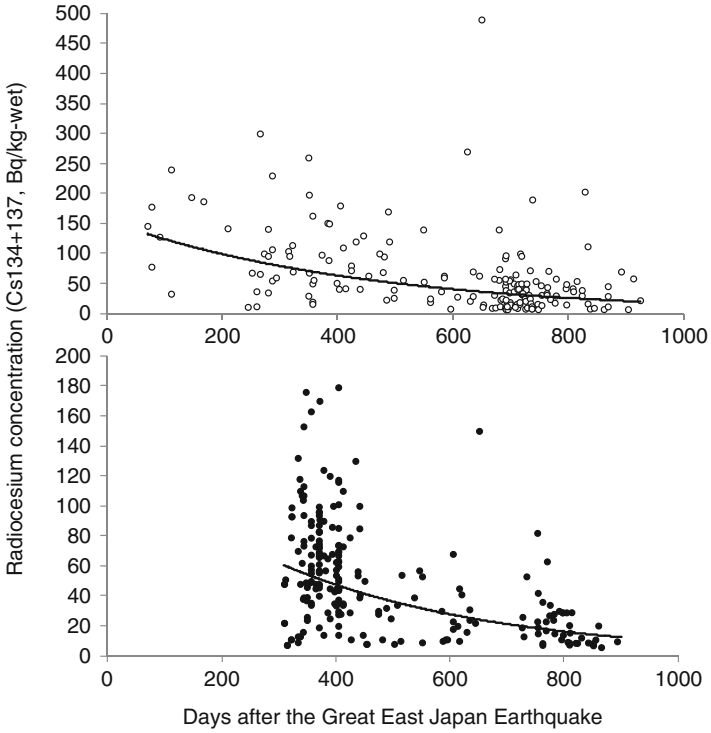

Fig. 10.2 Decay process of radiocesium in ≤2009 (*upper*) and 2010 (*lower*) year-classes of Pacific cod. The relationships were fitted for exponential function, expressed by the curved lines

0.37 to 0.75 times (average ± SD = 0.57 ± 0.16) lower in the 2010 yc than in the year-classes from 2009 and earlier. The concentration of radiocesium has decreased temporally since the nuclear plant accidents in both year-classes (Fig. 10.1). Interestingly, radiocesium was rarely detected, or detected at very low levels, in the 2011 yc.

The ecological half-life (Morita and Yoshida 2005; Iwata et al. 2013) was calculated using the exponential regression for surveyed concentrations of radiocesium and used to estimate the half-lives of radiocesium. This value can be used to predict future radiocesium concentrations. The regressions suggest that the ecological half-time of radiocesium was 309 and 258 days in the ≤2009 and 2010 year classes, respectively (Fig. 10.2). These results suggest that older and larger individuals concentrated higher levels of radiocesium and/or excreted radiocesium at a slower rate than younger and smaller Pacific cod individuals. The factors affecting age-related difference are examined in the subsequent sections.

10.3 Seasonal Change in Distribution

We conducted benthic trawl surveys from 2004 to 2013 in the northern Pacific off Honshu Island, Japan (Tohoku area) and in Sendai Bay using two research vessels (Table 10.1). Surveys off Tohoku area were conducted in April and in October–November at depths between 150 and 900 m (Fig. 10.3, Table 10.1). Surveys in Sendai Bay were conducted in January, February, April, June, July, and November at depths between 30 and 122 m. The details of the benthic trawl survey

Table 10.1 List of trawl survey cruises conducted in the present study by the research vessels *Dai-nana Kaiyo-maru* (D), or *Wakataka-maru* (W) in Sendai Bay (S) or offshore of Tohoku (T) giving the duration of the survey and number of benthic trawl tows (*N*)

Cruise	Vessel	Area	Duration	*N*
200407	W	S	28 Jun–2 Jul 2004	12
201006	W	S	20–23 Jun 2010	12
201202	D	S	2–6 Feb 2012	6
201204	W	S&T	17–25 Feb 2012	19
201210	W	S&T	20 Oct–21 Nov 2012	31
201304	W	S&T	16–23 Apr 2013	20
201310	W	S&T	15 Oct–25 Nov 2013	38

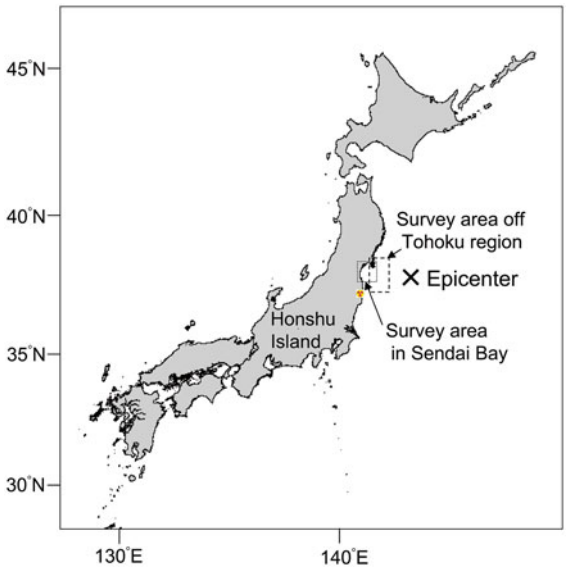

Fig. 10.3 Location of the study site and the epicenter of the Great East Japan Earthquake. Surveys were conducted at depths of 38–650 m in Sendai Bay and offshore of Tohoku

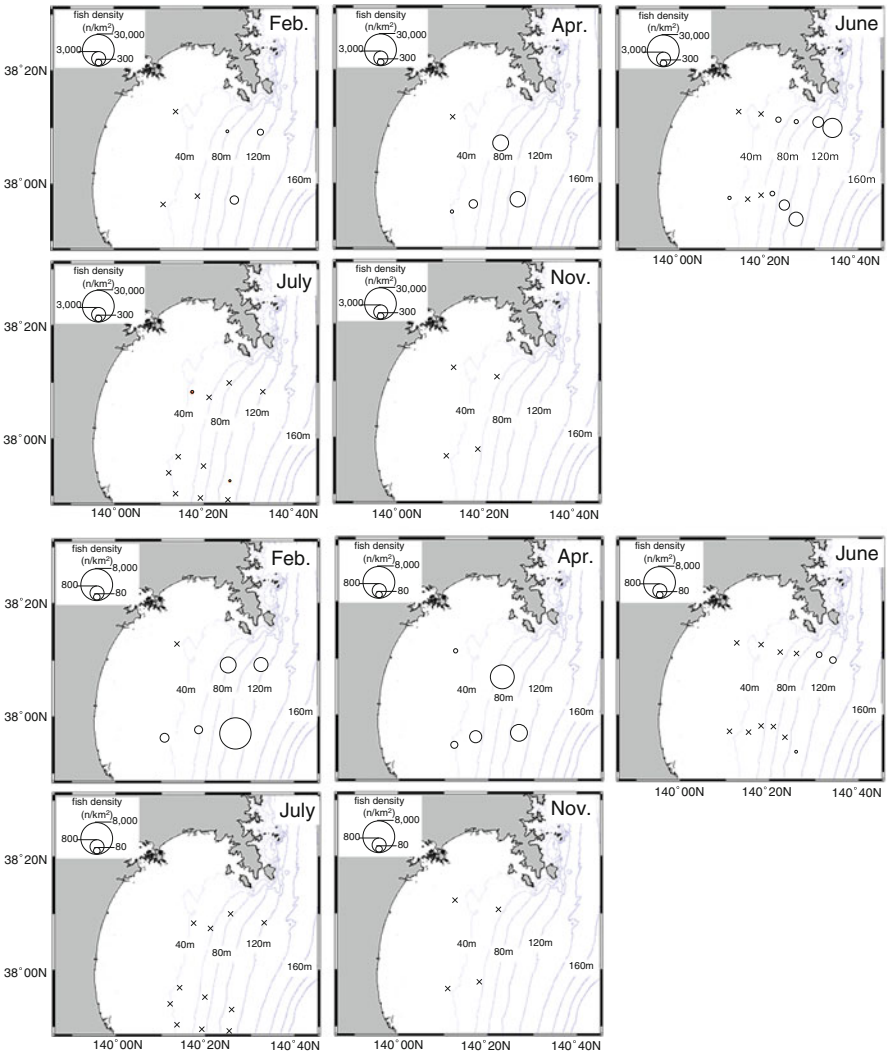

Fig. 10.4 Seasonal changes in the distribution of age 1+ (*upper*) and age ≥2+ (*lower*) Pacific cod in and off Sendai Bay. The timing of the surveys is described in Table 10.1

methodology are described by Hattori et al. (2008). We counted the number of age 1+ and 2+ Pacific cod caught in the net and estimated fish density (numbers/km^2) by dividing the number of fish captured by the trawl area.

Pacific cod aged 1+ year old were captured in shallow areas in Sendai Bay from February to June, but not in July and November (Fig. 10.4). In February and June, the majority of age 1+ cod were captured at depths >80 m, whereas in April they

were captured in shallower waters. Pacific cod of age ≥2+ were also captured in Sendai Bay from February to June, with peak catches occurring in February and April. Only a few individuals remained in the Bay in June, and none was captured in the area shallower than 120 m in July and November.

Based on the results of this long-term trawl survey, Pacific cod appear to be widely distributed offshore of Tohoku in the spring and autumn (Fig. 10.5). In April, 1+-year-old Pacific cod tend to occupy the 100 to 400 m depth zone off Tohoku, but the density is highest at 100–200 m and very low at ≥300 m. In October–November, age 1+ cod occupied the depth zone from 200 to 500 m, with density peaking at 200–400 m. Cod were not captured in areas shallower than 200 m during these months. Age ≥2+ cod were captured at depths of 100–600 m and 200–600 m in April and October, respectively. The distribution of Pacific cod differed between months. The cod occupied depths that are about 100 m shallower in April (300–400 m) than in October.

The density of fish was compared between Sendai Bay and Tohoku for samples collected in April and in October–November. The density of 1+-year-old individuals was high at depths of 50–200 m, and particularly at 80–150 m (Fig. 10.5). Fish were seldom captured deeper than 300 m. The density of age 1+ Pacific cod was about four times higher at the 38–100 m depth than at 120–450 m in April. The age ≥2+ individuals were widely distributed, from 50 to 500 m. In contrast, in autumn, Pacific cod of both age classes were distributed from 200 to 600 m, but were most

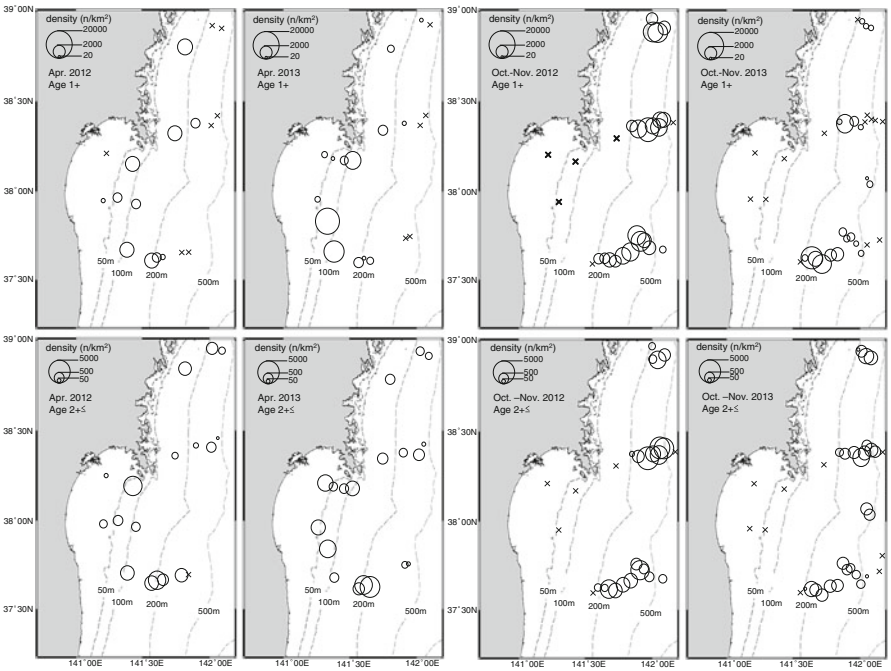

Fig. 10.5 Comparison of the distribution of age 1+ (*upper*) and age ≥2+ (*lower*) Pacific cod between spring and autumn. The timing of the surveys is described in Table 10.1

abundant at 200 to 500 m. The density of age ≥2+ Pacific cod was about two times higher at 38–100 m than at 120–450 m in April. These observations suggest that Pacific cod could inhabit the area near the FNPP at high density in April, during the time when cold water flows into Sendai Bay and offshore areas (Ito et al. 2004), but these fish migrate to the continental slope in July and remain there for several months.

Trawl surveys conducted off Tohoku throughout the year revealed that age 1+ and older Pacific cod were distributed at depths of 200–600 m in autumn, consistent with a previous report (Kitagawa et al. 2002), indicating that Pacific cod only inhabit the upper-continental slope during the autumn. In contrast, Pacific cod were distributed over both the upper continental slope and the continental shelf from winter to early summer. In Sendai Bay, age 1+ and ≥2+ individuals were represented in the catch from February to June. The older cod migrated into Sendai Bay and moved offshore slightly earlier than the younger individuals. In April, Pacific cod aged 1+ and ≥2+ years old were distributed throughout Sendai Bay, and their density was highest at the bay mouth (80–200 m deep). A large amount of radiocesium was released into the ocean after the FNPP accident in mid-March 2011, at a time when Pacific cod had likely moved into the shallower area. After occupying this area for a maximum of 3 or 4 months, the cod migrated off the continental shelf in July and did not return to the bay until February of the next year. Cod were distributed at depths similar to those of bighand thornyhead, *Sebastolobus macrochir* (Hattori et al. 2008), and threadfin hakeling, *Laemonema longipes* (Narimatsu et al. 2014), in offshore areas. The concentration of radiocesium in these two species remained very low or was nondetectable (Wada et al. 2013; MAFF 2014). Taking into consideration the pattern of seasonal migration, the rate of decline of radiocesium levels in Pacific cod, and the concentration of radiocesium in other species that occupy the upper continental slope, we conclude that contamination of Pacific cod with radiocesium occurred soon after the nuclear plant accident, from March to June in 2011.

10.4 Ontogenetic and Seasonal Diet Shift of Pacific Cod

Age 1+ and 2+ Pacific cod caught in Sendai Bay and off the Tohoku area, which is located off FNPP with a depth of 250 m, were used to evaluate their diet. Samples of fish were collected in April, June, and November in Sendai Bay, and in April and November off Tohoku. Fish were frozen soon after capture, their standard length and body weight were recorded, and they were dissected in the laboratory. The stomach was cut open and food items were sorted to the lowest possible taxon. Prey items were weighed to nearest 1 mg (wet weight). The percent contribution of each prey item to the diet of each age class was calculated. We compared the seasonal and spatial variation and ontogenetic shifts in the diet of Pacific cod.

A total of 247 fish stomachs were examined yielding 36 taxon or species of prey items. The primary prey items (>1 % of the total wet weight) differed among seasons, habitat types, and the body size of cod. In Sendai Bay, age 1+ Pacific cod

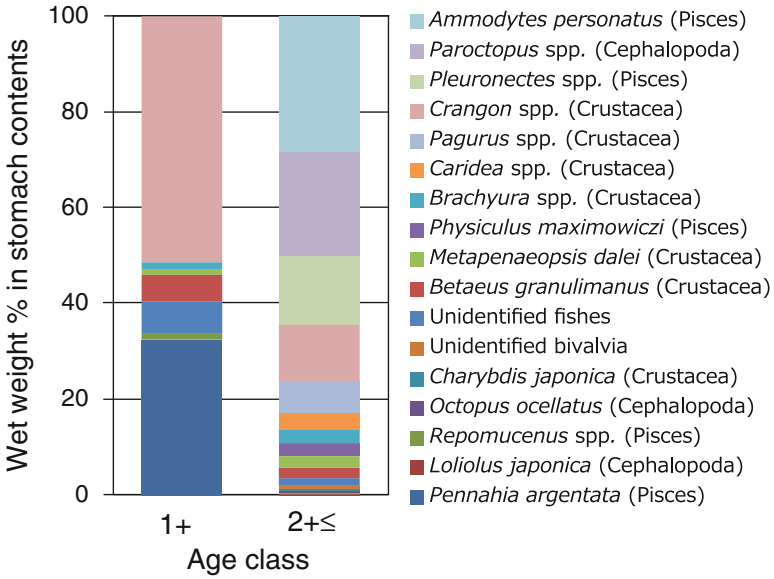

Fig. 10.6 Ontogenetic shift in diet for Pacific cod in Sendai Bay from April to June in 2012 and 2013

preyed primarily on *Crangon* spp. (Crustacea) such as *Crangon affinis* and *C. dalli*, followed by white croaker (*Pennahia argentata*, Pisces; Fig. 10.6). These two prey items accounted for 84 % of the total diet. Unidentified Pisces (6.9 %) and *Betaeus granulimanus* (Decapoda) were the next most common prey items. Age ≥2+ Pacific cod consumed a wider range of organisms compared with younger fish. In Sendai Bay, the older cod most commonly preyed on sand lance (*Ammodytes personatus*), followed by *Paroctopus* spp. (*P. dofleini and P. conispadiceus*), *Pleuronectes* spp. (*P. herzensteini and P. yokohamae*), and *Crangon* spp. A number of other fish and invertebrates were observed in the stomachs of age 2+ Pacific cod captured from April to June in Sendai Bay.

Age 1+ Pacific cod fed on the small pelagic invertebrates *Euphausia pacifica*, *Watasenia scintillans*, and *Themisto japonica* in April and June on the upper continental slope off Tohoku (Fig. 10.7). Age ≥2+ Pacific cod preyed primarily on flathead flounder *Hippoglossoids dubius*, followed by *Euphausia pacifica.* In October and November, benthic shrimp *Pandalus eous* were the most abundant (wet-weight) prey item of 1-year-old Pacific cod, followed by myctophid fish *Diaphus watasei* and unidentified fishes (Fig. 10.7). Older cod frequently fed on unidentifiable fishes, as well as *Diaphus watasei* and horsehair crab *Erimacrus isenbeckii*. These observations suggest that Pacific cod shift food items not only ontogenetically but also spatiotemporally.

Age 1+ cod fed on benthic *Natantia* euphausiids, small decapod cephalopods, small fishes, and cephalopod octopi whereas age ≥2+ individuals fed on Cephalopoda

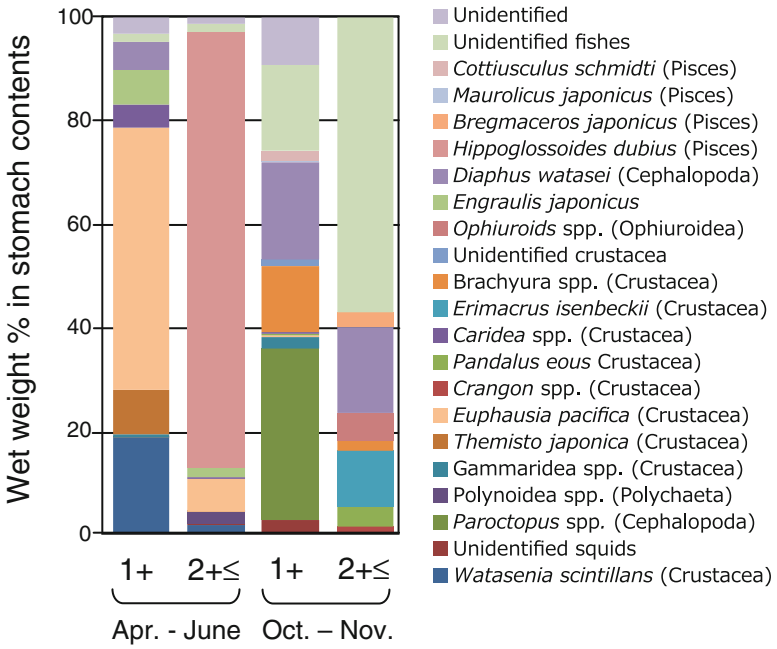

Fig. 10.7 Ontogenetic and temporal changes in diet for Pacific cod off Tohoku from October to November in 2012 and 2013

(octopods), benthic *Natantia*, *Brachyura*, and fish, including flatfish. Prior studies have documented a diet shift in Pacific cod distributed in areas deeper than 100 m (Hashimoto 1974; Yamamura 1994; Fujita et al. 1995). Cod smaller than 30 cm SL (corresponding to 1+-year-old individuals) primarily consume planktonic organisms. Cod in the range 30–40 cm SL (1+ to 2+ years old) also depend on Euphausiids, but the contribution to their diet is lower than for 30 cm fish, and they also feed on demersal organisms. Fish larger than 40 cm SL (≥2+ years old) primarily prey on fish and macrobenthos and rarely on planktonic invertebrates. Seasonal changes in diet were also observed in this population. Pelagic organisms such as euphasiids and mesopelagic fishes were the main prey items in the spring, whereas benthic species were the dominant prey item in autumn. Such variability in the type of prey items consumed by Pacific cod may reflect the general feeding characteristics of this species and seasonal changes in the biotic environment. Our observations suggest that large Pacific cod (age ≥2+) also consume mesopelagic invertebrates and that small individuals (age 1+) feed on similar items. However, Pacific cod basically shift their feeding habit from small plankton to macrobenthos with growth, and macrobenthic organisms such as large octopi and flatfishes can be prey items only for large cod because of the gape limitation of Pacific cod. The demersal fish such as sand lance and flatfish tended to accumulate radiocesium in their body and are only preyed on by large Pacific cod. The ontogenetic niche shift and species-specific difference in

radiocesium concentration may result in the size-dependent difference in radiocesium concentrations observed in Pacific cod.

10.5 Radiocesium Concentration of Prey Items

A part of the species that occurred in the stomachs of Pacific cod were caught in the trawl surveys. The radiocesium concentrations of them and a part of prey items were measured by same method as the fish samples. The concentrations of the rest organisms were referred from the previous reports, respectively (MAFF 2014; Sohtome et al. 2014).

The radiocesium concentrations were analyzed for 17 species or taxon, which are the main prey items of Pacific cod in Sendai Bay and Tohoku (Fig. 10.8). The

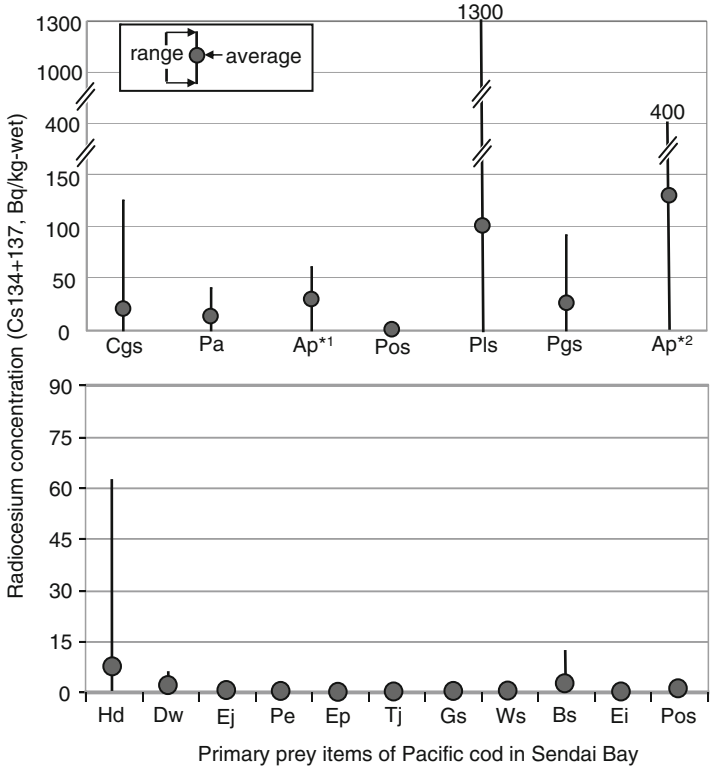

Fig. 10.8 Radiocesium concentrations in the primary prey items of Pacific cod in Sendai Bay (*upper*) and off Tohoku (*lower*). Species or taxon are shown by abbreviations: Cgs *Crangon* spp., Pa *Pennahia argentata*, Ap *Ammodytes personatus*, Pos *Paroctopus* spp., Pls *Pleuronectes* spp., Pgs *Pagurus* spp., Hd *Hippoglossoides dubius*, Dw *Diaphus watasei*, Ej *Engraulis japonicus*, Pe *Pandalus eous*, Ep *Euphausia pacifica*, Tj *Themisto japonica*, Gs Gammaridea spp., Ws *Watasenia scintillans*, Bs *Brachyura* spp., Ei *Erimacrus isenbeckii*. The indicators *1 and *2 indicate specimens caught from April 2011 to March 2012 and from April 2012 to December 2012, respectively

concentration of radiocesium in *Crangon* spp. and white croaker (*Pennahia argentata*, Pisces) ranged from below the detection limit (DL) to 126.3 Bq/kg-wet weight (mean ± SD =19.5 ± 24.3) and below the DL to 41.0 Bq/kg-wet (12.5 ± 16.3), respectively. The concentration of radiocesium was higher within 1 year after the accident (134.5 ± 102.7) than 1 year after the accident (29.0 ± 21.8) in the sand lance *Ammodytes personatus,* the dominant prey item of age ≥2+ cod. Although the radiocesium concentrations in all *Paraoctopus* spp. and hermit crab *Pagurus* spp. (*Anomura*) were below the DL or relatively low (24.4 ± 24.3), high levels were detected in some *Pleuronectes* spp. specimens (102.5 ± 169.2). Almost all the prey items consumed on the upper continental slope had levels below the DL, except for the flathead flounder *Hippoglossoids dubius* (7.7 ± 14.7) and crabs (*Tymolus japonicus*, *Carcinoplax vestiva*: 2.8 ± 4.9). These results suggest that the concentrations of radiocesium were very low in the prey of Pacific cod (all age groups) off the FNPP at a depth of 250 m. In Sendai Bay, organisms consumed by age 1+ Pacific cod had relatively low radiocesium levels. However, some prey items observed in the stomach of age ≥2+ cod had relatively high radiocesium levels.

As described here, the timing of the migration from offshore to inshore and vice versa was similar between age classes, suggesting that the exposure to radiocesium was similar regardless of age and body size. However, the concentration of radiocesium was always higher in older and larger fish than in younger and smaller fish.

A number of marine organisms, including seaweeds, invertebrates, and fish, were contaminated by the radiocesium released from FNPP. The concentration and rate of decrease varied among species, likely because of differences in their biological characteristics (Wada et al. 2013). The levels of radiocesium were highest soon after the FNNP accident in all taxon (Wada et al. 2013). This pattern suggests that radiocesium contamination of all organisms primarily occurred in the first few months after the accident. Organisms that were distributed near the FNPP accumulated radiocesium from the seawater and prey items. The concentration of radiocesium in Pacific cod was variable, likely dependent on the initial intake of radiocesium, rate of decrease speed of radiocesium, the amount of additional intake of radiocesium from seawater, and the rate of growth (BW) during the first few months. However, additional intake of radiocesium only occurred via prey because radiocesium concentration in seawater was rapidly diluted/transported out of the area within a year, except for that in the port of FNPP (Buesseler et al. 2011; Aoyama et al. 2013; Kaeriyama et al. 2013, 2014); those levels in pelagic fish rapidly decreased (Iwata et al. 2013; Wada et al. 2013), and Pacific cod seldom inhabit and stay in the intertidal zone.

Pacific cod grow very rapidly (Hattori et al. 1992), resulting in dilution of the radiocesium in their body (dilution effect). Age 1+ cod are about 0.5 kg BW but grow to 1.5 kg BW in 1 year. Similarly, cod that are 1.0 kg BW (age 2+) grow to 2.3 kg BW in a year. A 0.5-kg BW individual has a 1.30 times higher dilution effect for radiocesium than does a 1.0-kg BW cod. The ecological half-time of radiocesium was estimated to be 258 and 309 days in the 2010 and the ≤2009 year-classes, respectively. Taking into consideration both the dilution effect and the age-specific decrease in concentrations, the level of radiocesium in the 2010 year-class is

expected to decrease 1.56 times earlier than in the ≤2009 year-classes. The mean concentration of radiocesium in the ≤2009 year-classes was 1.75 times higher than in the 2010 year-class during the period January 2012 to March 2013. Assuming the initial concentrations were similar between year-classes, the difference between observed values and estimated values (based on dilution and age-specific effects) may be explained by the ontogenetic differences in prey items and their radiocesium concentration.

10.6 Conclusion

Large numbers of marine organisms were contaminated by radiocesium following the FNPP accident in March 2011. In some demersal fishes that inhabit the coastal regions, the rate of decrease in tissue radiocesium levels was lower than for other pelagic fishes and invertebrates, suggesting that additional radiocesium was taken up from the benthic ecosystem. This finding delayed the reopening of fisheries in the region. The estimated ecological half-life of radiocesium in Pacific cod was from 258 to 309 days; this value is consistent with values in other demersal fishes caught off Fukushima Prefecture (Wada et al. 2013). The half-life was longer in old and larger individuals than in young and small individuals, probably a result of differences in metabolic rate and growth rates between age and body size classes (Doi et al. 2012). Radiocesium concentrations decreased to low levels soon after the accident in seawater and prey items (Buesseler et al. 2011; Aoyama et al. 2013) and have continued to decease in the period up to 2014 (Sohtome et al. 2014). Thus, the potential for intake of radiocesium from the benthic ecosystem is very low in and after 2014. Additionally, radiocesium was rarely detected in the 2011 year-class. Pacific cod hatch during January to February in Sendai Bay (Narimatsu et al., unpublished data) and live a pelagic life for 3–4 months in the coastal zone. Some individuals of the 2011 year-class took in radiocesium via seawater and diet. However, the concentration of radiocesium in their body was diluted by growth, and the fish were only exposed to very low levels of radiocesium after settlement to benthic life. The Pacific cod of the following year-classes had already recruited into the ecosystem of the upper continental slope and were commercially caught in the Tohoku region. This population is primarily composed of young fish, and the generation cycle alters quickly (Narimatsu et al. 2010). We observed a decrease in radiocesium concentrations in the 2010 and ≥2009 year classes and an increase in the proportion of individuals born after the accident at the Nuclear Power Plant. Both these factors reduce the radiocesium concentrations at the population level and suggest the risk of restarting fisheries is minimal.

Acknowledgments We are grateful to the crews of R/Vs *Wakataka maru* and *Dai-nana Kaiyo maru* for assistance in obtaining samples. We also thank Drs. T. Wada and M. Ito for comments on the manuscript, and the staff of Hachinohe Laboratory, Tohoku National Fisheries Research Institute, for help in preparing samples. This work was financially supported by the Fisheries Agency, Japan.

References

Aoyama M, Uematsu M, Tsumune D, Hamajima Y (2013) Surface pathway of radioactive plume of TEPCO Fukushima NPP1 released ^{134}Cs and ^{137}Cs. Biogeosci Discuss 10:265–285

Buesseler KO, Aoyama M, Fukasawa M (2011) Impacts of the Fukushima nuclear power plants on marine radioactivity. Environ Sci Technol 45:9931–9935

Buesseler KO (2012) Fishing for answers off Fukushima. Science 388:480–482

Doi H, Takahara T, Tanaka K (2012) Trophic position and metabolic rate predict the long-term decay process of radiocesium in fish: a meta-analysis. PLoS ONE 7:e29295. doi:10. 1371/journal.pone.0029295

Fujita T, Kitagawa D, Okuyama Y, Ishito Y, Inada T, Jin Y (1995) Diets of the demersal fishes on the shelf off Iwate, northern Japan. Mar Biol 123:219–233

Hashimoto R (1974) Investigation of feeding habits and variation of inhabiting depths with cod (Gadus macrocephalus) distributed on the northeastern fishing ground in Japan. Bull Tohoku Reg Fish Res Lab 33:51–67

Hattori T, Narimatsu Y, Ito M, Ueda Y, Kitagawa D (2008) Annual changes in distribution depths of bighand thornyhead *Sebastolobus macrochir* off the Pacific coast of northern Honshu Japan. Fish Sci 74:594–602

Hattori T, Sakurai Y, Shimazaki K (1992) Age determination by sectioning of otoliths and growth pattern of Pacific cod. Nippon Suisan Gakkaishi 58:1203–1210 (In Japanese with English abstract)

Ito S, Uehara K, Miyao T, Miyake H, Yasuda I, Watanabe T, Shimizu Y (2004) Characteristics of SSH anomaly based on TOPEX/POSEIDON altimetry and *in situ* measured velocity and transport of Oyashio on OICE. J Oceanogr 60:425–438

Iwata K, Tagami K, Uchida S (2013) Ecological half-lives of radiocesium in 16 species in marine biota after the TEPCO's Fukushima Daiichi Nuclear Power Plant accident. Environ Sci Technol 47:7696–7703

Kaeriyama H, Ambe D, Shimizu Y, Fujimoto K, Ono T, Yonezaki S, Kato Y, Matsunaga H, Minami H, Nakatsuka S, Watanabe T (2013) Direct observation of ^{134}Cs and ^{137}Cs in the western and central North Pacific after the Fukushima Dai-ichi Nuclear Power Plant accident. Biogeosciences 10:4287–7295

Kaeriyama H, Shimizu Y, Ambe D, Masujima M, Shigenobu Y, Fujimoto K, Ono T, Nishiuchi K, Taneda T, Kurogi H, Setou T, Sugisaki H, Ichikawa T, Hidaka K, Hiroe Y, Kusaka A, Kodama T, Kuriyama M, Morita H, Nakata K, Morinaga K, Morita T, Watanabe T (2014) Southwest intrusion of ^{134}Cs and ^{137}Cs derived from the Fukushima Dai-ichi Nuclear Power Plant accident in the western North Pacific. Environ Sci Technol 48:3120–3127

Kitagawa D, Hattori T, Narimatsu Y (2002) Monitoring on the demersal fish resources in the Tohoku area. Kaiyo Mon 34:793–798 (in Japanese)

MAFF (Japan Ministry of Agriculture, Forestry and Fisheries) (2014) Results of the inspection on radioactivity materials in fisheries products. http://www.jfa.maff.go.jp/e/inspection/index.html. Accesssed 31 July 2014

Morita T, Yoshida K (2005) Effective ecological half-lives of Cs-137 for fishes controlled by their surrounding sea-waters. Radioprotection 40(Suppl, 1):S635–S640

Narimatsu Y, Ito M, Hattori T, Inagawa R (2014) Stock assessment and evaluation for the threadfin hakeling stock of the north Pacific, Japan (fiscal year 2013). In: Marine fisheries stock assessment and evaluation for Japanese waters (fiscal year 2013/2014), Fishries Agency and Fisheries Research Agency of Japan, pp 851–867

Narimatsu Y, Ueda Y, Okuda T, Hattori T, Fujiwara K, Ito M (2010) The effect of temporal changes in life-history traits on reproductive potential in an exploited population of Pacific cod, Gadus macrocephalus. ICES J Mar Sci 67:1659–1666

Sohtome T, Wada T, Mizuno T, Nemoto Y, Igarashi S, Nishimune A, Aono T, Ito Y, Kanda J, Ishimaru T (2014) Radiological impact of TEPCO's Fukushima Dai-ichi Nuclear Power Plant accident on invertebrates in the coastal benthic food web. J Environ Radioact 138:106–115

Tsumune D, Tsubono T, Aoyama M, Hirose K (2012) Distribution of oceanic 137Cs from the Fukushima dai-ichi Nuclear Power Plant simulated numerically by a regional ocean model. J Environ Radioact 111:100–108

Wada T, Nemoto Y, Shimamura S, Fujita T, Mizuno T, Sohtome T, Kamiyama K, Morita T, Igarashi S (2013) Effects of the nuclear disaster on marine products in Fukushima. J Environ Radioact 124:246–254

Yamamura O (1994) Ecological study on demersal fish community off Sendai Bay, northern Japan, with special reference to niche dynamics among dominant fishes. Doctoral dissertation, Hokkaido University

Chapter 11
Radiocesium Contamination Histories of Japanese Flounder (*Paralichthys olivaceus*) After the 2011 Fukushima Nuclear Power Plant Accident

Yutaka Kurita, Yuya Shigenobu, Toru Sakuma, and Shin-ichi Ito

Abstract Radiocesium (Cs) contamination histories of the Japanese flounder, *Paralichthys olivaceus*, after the 2011 Fukushima Nuclear Power Plant (FNPP) accident were examined by analysis of the spatiotemporal changes in observed Cs concentrations, by comparison of the dynamics of the Cs concentrations in several year-classes of fish, and by simulation studies. Two contamination histories were revealed: (1) severe contamination by water that was directly released from the FNPP with extremely high Cs concentrations for a few months after the accident, which had a highly variable spatial distribution; and (2) long-duration contamination at relatively low concentrations resulting from consumption of contaminated food. These two histories were supported by three observations. First, high Cs concentrations with high variability were observed in the first year after the accident. Second, the highest values of the minimum Cs concentrations were observed in the autumn of 2011. Third, Cs concentrations were lower with smaller variation for fish from the 2011 year-class and younger, which were not exposed to the highly contaminated directly released water, than for fish from the 2010 year-class and older. Simulation studies also indicated that the Cs concentrations in some individuals that were exposed to the directly released water might not be in an equilibrium state even at 3 years after the accident. On the basis of these contamination histories, it can be expected that the Cs concentrations in most Japanese flounder will continue to decrease.

Y. Kurita (✉) • S.-i. Ito
Tohoku National Fisheries Research Institute, Fisheries Research Agency,
3-27-5, Shinhama-cho, Shiogama, Miyagi 985-0001, Japan
e-mail: kurita@affrc.go.jp

Y. Shigenobu
National Research Institute of Fisheries Sciences, Fisheries Research Agency,
2-12-4, Fukuura, Kanazawa, Yokohama, Kanagawa 236-8648, Japan

T. Sakuma
Fukushima Prefectural Fisheries Experimental Station,
13-2, Matsushita, Onahamashimokajiro, Iwaki, Fukushima 970-0316, Japan

K. Nakata, H. Sugisaki (eds.), *Impacts of the Fukushima Nuclear Accident on Fish and Fishing Grounds*, DOI 10.1007/978-4-431-55537-7_11

Keywords Radiocesium • Contamination history • *Paralichthys olivaceus* • Simulation • Fukushima Nuclear Power Plant • Directly released water • Food • Year-class • Equilibrium

11.1 Introduction

The marine environment and animals living in it have been severely contaminated by radionuclides, including radiocesium (Cs; $^{134}Cs + ^{137}Cs$), released from the Fukushima Nuclear Power Plant (FNPP) after the accident on 11 March 2011. The Japanese provisional regulatory limit for Cs in fish products was set at 500 Bq/kg-wet starting immediately after the accident and was enforced until March 2012; a limit of 100 Bq/kg-wet has been enforced since April 2012. After the accident, the landing of many commercially important fish species in Fukushima and neighboring prefectures was legally banned or voluntarily suspended, and the landing of many species in Fukushima Prefecture is still banned (Wada et al. 2013).

Marine fish take up Cs from seawater and food. The rate of intake is related to the Cs concentrations in seawater and food sources. Excretion from the body is related to the Cs concentration in the fish body. It has been suggested that the impact of contamination resulting from the FNPP accident has been temporally and spatially heterogeneous (Tateda et al. 2013; Wada et al. 2013). Marine animals are likely to have been severely contaminated for a few months after the accident, as a consequence of the direct release from the FNPP of massive amounts of water with extremely high Cs concentrations between 26 March and the end of April 2011 and the subsequent consumption of contaminated food (Tsumune et al. 2012; Tateda et al. 2013). The Cs concentrations were higher in the coastal waters south of the FNPP (Wada et al. 2013). An understanding of the contamination histories that produced the observed temporal changes and spatial variation in the intensity of contamination will facilitate prediction of the dynamics of Cs concentrations in fish and will guide decisions regarding the appropriate time to restart fishing operations.

The Japanese flounder *Paralichthys olivaceus*, the studied fish species in this chapter, is a bottom fish inhabiting coastal waters at depths of 150 m or less. They are given birth in summer (June–August). These fish reach 250–300 mm in total length (TL) during their first year, during which time most of them inhabit sandy coasts at depths of less than 20 m and feed on mysids and larval fish. After their first year, they move to deeper waters and feed exclusively on two bait fish, the Japanese anchovy *Engraulis japonicus* and the Japanese sand lance *Ammodytes personatus* (Tomiyama and Kurita 2011). The Japanese flounder is an end-member of the pelagic food chain (from phytoplankton through zooplankton and bait fish to fish feeder). They reach TLs of approximately 400 mm at 2 years and 500 mm at 3 years

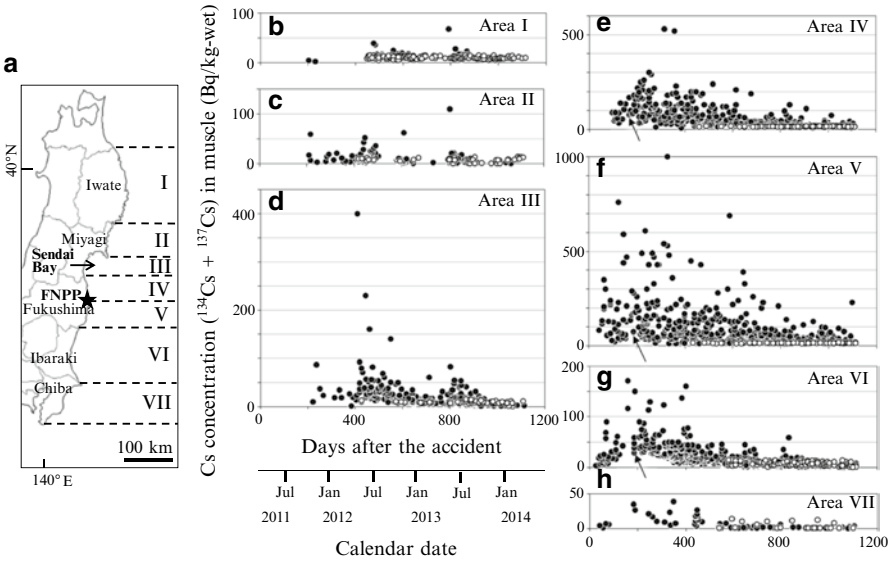

Fig. 11.1 (**a**) Locations of areas I–VII and the Fukushima Nuclear Power Plant (FNPP, *star*) and (**b**–**h**) temporal changes in the concentrations of Cs (^{134}Cs + ^{137}Cs; Bq/kg-wet) in the muscle of the Japanese flounder *Paralichthys olivaceus* collected in the seven areas. Cs concentrations (*circles*) were measured by local governments and published by the Fisheries Agency of the Ministry of Agriculture, Forestry and Fisheries of Japan. *Open circles* indicate Cs concentrations that were less than the detection limit; in these cases, the plotted values correspond to the detection limit. In (**e**–**g**), *arrows* show the peaks in the lowest observed concentration in areas IV–VI, respectively. Cs concentrations of 1,610 Bq/kg-wet at 187 days after the FNPP accident (14 September 2011) in area IV (**e**) and 4,500 Bq/kg-wet at 250 days (16 November 2011) in area V (**f**) were omitted. Note that the *y*-axis scales in **e** and **f** differ from those of the other parts

(Yoneda et al. 2007). The flounder inhabiting the waters off Miyagi, Fukushima, and Ibaraki Prefectures (an area that extends 110 km to the north and 200 km to the south of the FNPP; Fig. 11.1) are considered to be a subpopulation (Kurita et al. 2014), although movement within this area is somewhat limited (Kurita et al., unpublished data).

In this chapter, we examine the temporal changes and spatial variation of Cs concentrations in Japanese flounder in detail and suggest contamination histories that would produce the observed variation. First, we analyzed Cs concentration data collected by local governments and published by the Fisheries Agency of the Ministry of Agriculture, Forestry and Fisheries (2014) to gain a rough understanding of the temporal changes and spatial variation of Cs concentrations (Sect. 11.2). We then investigated temporal changes in Cs concentrations among different year-classes of the flounder, specifically year-classes born before and after the accident, to understand temporal changes in the intensity of contamination (Sect. 11.3). Finally, we simulated the temporal changes in Cs concentration in an effort to understand how the observed Cs contamination distribution was produced (Sect. 11.4).

11.2 Spatiotemporal Distribution of Cs Concentrations in Japanese Flounder

For our analysis, we used Cs concentrations in the flounder monitored by local governments (Fisheries Agency 2014) in the region from 35°45′N to 40°25′N, which was subdivided into seven areas (Fig. 11.1). The sizes and ages of the flounder were not recorded, but almost all the data are expected to be from fish with a TL greater than 300 mm (corresponding to a minimum age of 1–1.5 years; Yoneda et al. 2007), which is the landing size limit for this flounder. The sample sizes for the data points in the figure are not known for certain, but most of the data points represent concentrations from more than three individuals, except in the areas immediately to the north and south of Fukushima Prefecture (areas IV and V; Fig. 11.1e, f); in these areas, most of the data points collected after October 2011 are for individuals.

Examination of the observed concentration data revealed the following features:

- The Cs concentrations clearly differed among the areas (Fig. 11.1). In the far north (areas I and II) and the far south (area VII) from FNPP, the concentrations were low; only 1.1 % of the data exceeded 50 Bq/kg-wet. In contrast, 41.0 % of the data in the area around the FNPP (areas IV and V) exceeded 50 Bq/kg-wet. The average Cs concentrations in the seven areas during the period between 200 and 600 days after the accident decreased in the order V > IV > III = VI > I = II = VII.
- The Cs concentrations were highly variable among individuals (or individual data points) within each area (Fig. 11.1). Some extremely high concentrations were observed, especially during the first year after the accident; for example, concentrations of 1,610 and 4,500 Bq/kg-wet, respectively, were observed on 14 September 2011 (187 days after the accident) in area IV and on 16 November 2011 (250 days) in area V (these two values were omitted in Fig. 11.1). The maximum:minimum ratio during October 2011 and March 2012 in area V was 375 (=4,500/12).
- The dynamic patterns of the higher and lower concentrations differed from each other, especially in area VI (Fig. 11.2). Specifically, examination of the temporal changes in the concentration percentiles in area VI for six consecutive 6-month periods starting in April 2011 revealed that the upper concentration percentiles (75 %, 90 %, and 95 %) decreased steadily during the observed periods, and the lower percentiles (5 %, 10 %, 25 %, and 50 %) increased from April–September 2011 to October 2011–March 2012 and then decreased steadily.
- The lowest observed concentrations increased slightly in areas IV, V, and VI (Fig. 11.1); specifically, the lowest observed concentrations peaked at around 200 days after the accident (September–October 2011; arrows in Fig. 11.1e–g) and then decreased. The peak values of the lowest observed concentrations were approximately 80, 80, and 30 Bq/kg-wet in areas IV, V, and VI, respectively. Although these peak values were clearly lower than the values of the higher per-

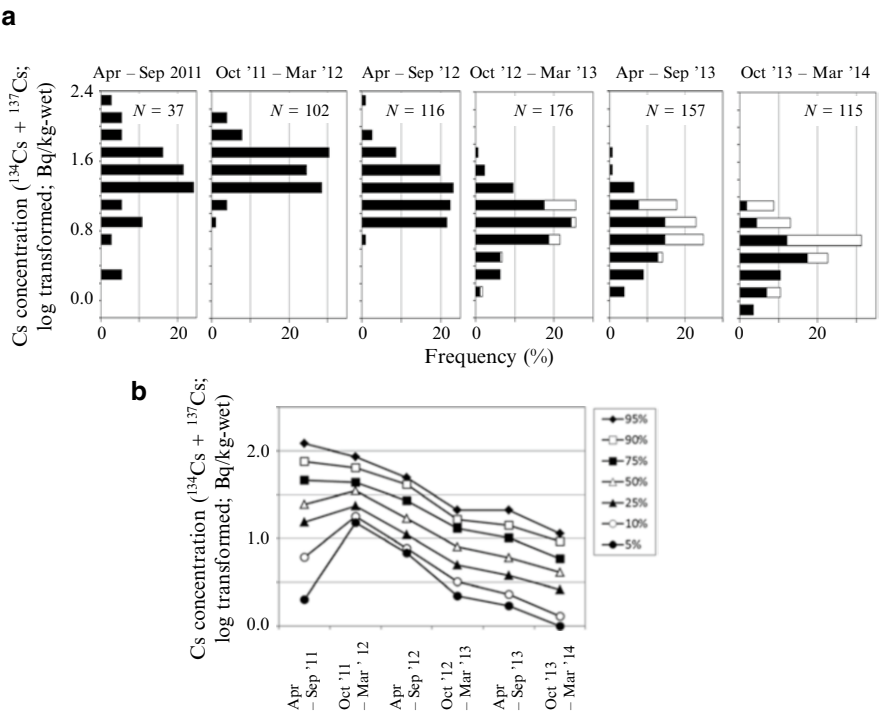

Fig. 11.2 Temporal changes in the (**a**) frequency distribution and (**b**) percentiles of the concentrations of Cs (^{134}Cs+^{137}Cs; Bq/kg-wet) in Japanese flounder *Paralichthys olivaceus* from area VI, April 2011–March 2014. *Open bars* in **a** indicate individuals with concentrations below the detection limit; the value of detection limit was used as the Cs concentration for these individuals. The concentrations of detection limits differ among monitored data. *N* number of samples for each period

centiles, they were still higher than the concentrations before the accident (^{137}Cs, 0.11–0.50 Bq/kg-wet during the period from 1984 to 1995; Kasamatsu and Ishikawa 1997).

These features, along with the results of previous studies of Cs contamination in the environment and in animals (Tsumune et al. 2012; Tateda et al. 2013; Wada et al. 2013), suggest two contamination histories for Japanese flounder. In the first, water released directly from the FNPP, which had extremely high Cs concentrations, contaminated the fish during a short period, probably from March to April 2011 (Tsumune et al. 2012). The spatial variation of the contamination intensity was high; some fish were severely contaminated, whereas others were only slightly contaminated. Second, consumption of bait fish contaminated with relatively low concentrations of Cs led to longer-duration contamination compared to that caused by the directly released water. All flounder can be expected to take up Cs from their food, which indicates that the variation in Cs concentration among individual flounders resulting from Cs in food was smaller than the variation from the Cs in the directly released water.

The first contamination history is supported by the large variation in Cs concentrations, even in the same area, and the occurrence of individuals with extremely high Cs concentrations in 2011 (Figs. 11.1 and 11.2). These individuals apparently were contaminated shortly after the accident, and the amount of additional contamination after that seems to have been relatively low. This history is also supported by the coincidence of the spatial variation of the Cs concentrations in fish bodies and the path of the extremely contaminated water released from the FNPP between 26 March and the end of April 2011; the high Cs concentrations in fish (Wada et al. 2013) and the path of the directly released water (Tsumune et al. 2012) were distributed along the coast to the south of the FNPP.

The second history is supported by the dynamics of the lower Cs concentrations, specifically the temporary increase in the lower percentiles in area VI and the peaking of the lowest concentrations at around 200 days after the accident in areas IV, V, and VI. These features indicate that all the fish were contaminated through the food web because the highly contaminated water was present in the study areas much earlier than the 200th day after the accident (Tsumune et al. 2012) and the contaminated water cannot explain the delayed peak (see also Sect. 11.4).

We validated these histories by comparison of the Cs concentrations in fish from different year-classes, that is, fish born before and after the accident (Sect. 11.3), and by conducting model simulations (Sect. 11.4).

11.3 Difference in Cs Concentrations Among Year-Classes Born Before and After the Accident

On the basis of the contamination histories described in the preceding section, we hypothesized that some of the individuals in the 2010 year-class and older would be heavily contaminated by the directly released water and that, in contrast, all the members of the 2011 year-class and younger would be less contaminated because the latter group of fish has not been exposed to the directly released water, and their main source of Cs contamination would have been their food, which contained Cs at much lower concentrations than the directly released water.

To validate this hypothesis, we compared the Cs concentrations among year-classes during the period from 250 to 950 days after the accident. Fish were collected in Sendai Bay (area III). Total length was measured, age was validated by otolith analysis (Yoneda et al. 2007), and Cs concentrations in the muscle of individual fish were measured individually. The muscle tissue specimens were packed tightly into plastic cylindrical containers, and specific gamma rays emitted from ^{134}Cs (605 and 796 keV) and ^{137}Cs (662 keV) were measured with a high-purity germanium semiconductor detector (ORTEC; GEM30-70-LB-C, 1.85 KeV/1.33 MeV resolution) with a multichannel analyzer. The concentrations of ^{134}Cs and ^{137}Cs were corrected back to the date of sampling for physical decay.

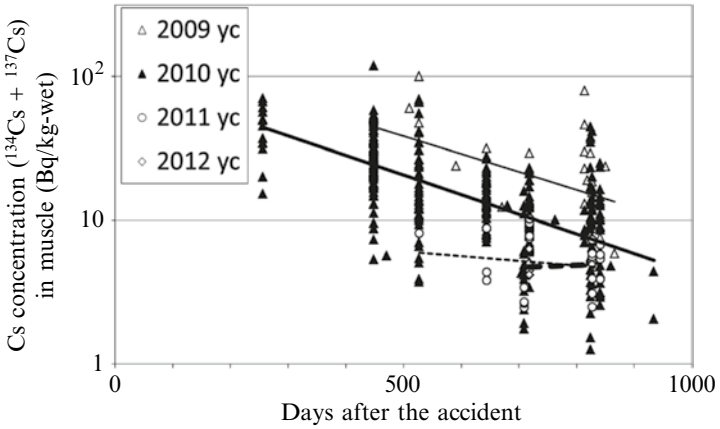

Fig. 11.3 Temporal changes in the concentrations of Cs (^{134}Cs + ^{137}Cs; Bq/kg-wet) in four year-classes of individual Japanese flounder *Paralichthys olivaceus* collected in area III (Sendai Bay). Regression lines for each year-class (yc) excluding outliers (see text) are shown; $p < 0.01$ for *solid lines* [2009 yc (*thin line*) and 2010 yc (*bold line*)] and $p > 0.05$ for *broken lines* [2011 yc (*thin line*) and 2012 yc (*bold line*)]

As expected, the Cs concentrations in the fish from the 2009 and 2010 year-classes varied widely, from 4.8 to 100.2 (0.68–2.00, log transformed) and from 1.3 to 118.8 (0.11–2.07, log transformed) Bq/kg-wet, respectively (Fig. 11.3). There were some sporadic outliers (that is, fish with Cs concentrations outside the values predicted by linear regression ± 2 SD). Except for these outliers, the Cs concentrations of each 2009 and 2010 year-class showed a decreasing tendency. In contrast, the Cs concentrations in the fish from the 2011 and 2012 year-classes were less than 10 (1.0 log transformed) Bq/kg-wet, and there were no outliers (that is, concentrations more than 2 SD from the mean). The Cs concentrations in fish from these year-classes between 644 and 841 days after the accident decreased in the order 2009 > 2010 > 2011 = 2012 year-class (Steel–Dwass test; $p < 0.05$).

Differences in Cs concentrations among the year-classes were likely the result of differing exposures to the highly contaminated environment during the first few months after the accident at the different ages (Fig. 11.4a). Japanese flounder switch from eating mysids during the first year of life to eating bait fish as they age. Therefore, fish from the 2009 year-class experienced the accident when they were 1 year and 9 months old, at which point they were feeding on bait fish. Fish in the 2010 year-class were only 9 months old at the time of the accident, and most of them were inhabiting shallow areas (<20 m deep) and feeding on mysids until summer 2011, at which point they shifted to feeding on bait fish. Fish in the 2011 year-class were not born until 4 months after the accident.

The Cs concentrations in fish caught during the period from December 2012 to June 2013 (644–841 days after the accident) from different year-classes are plotted against TL in Fig. 11.4b; the plot shows clear differences between the 2010 and 2011 year-classes, even in the same size range (344–420 mm TL; *U* test, $p < 0.01$). The major difference was that fish in the 2011 year-class were not exposed to the

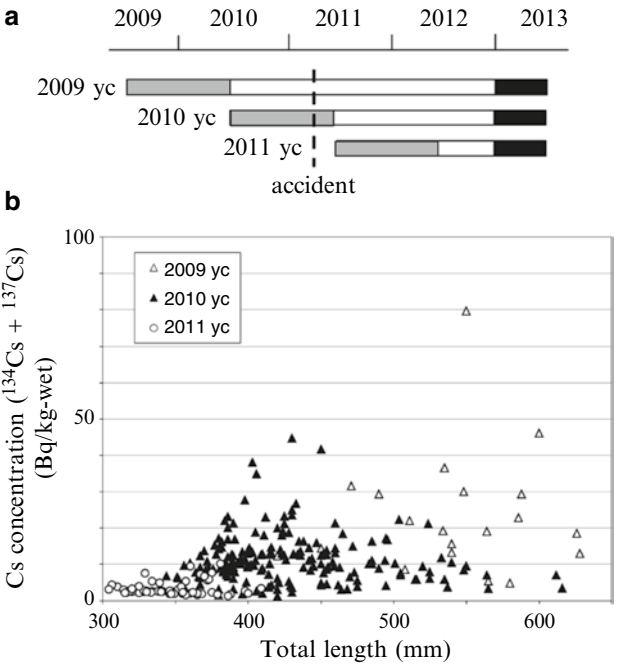

Fig. 11.4 Comparison of the concentrations of Cs (^{134}Cs + ^{137}Cs; Bq/kg-wet) in three year-classes of individual Japanese flounder *Paralichthys olivaceus*. (**a**) Scheme showing the birth time of each year class (yc), the date of the FNPP accident, and the period during which the fish were collected (644–841 days after the accident; *black bars*). Japanese flounder feed on mysids during their first year (*gray bars*) and then on bait fish (*open and black bars*). (**b**) Relationship between Cs concentration and total length of individual Japanese flounder by year-class

directly released water during March–April 2011 and thus were not heavily contaminated. Differences between the 2010 and 2009 year-classes were also observed within the overlapping size range (420–628 mm TL; *U* test, $p < 0.01$). Differences in habitat and growth rate after the accident are the likely causes of these differences.

11.4 Simulation

In the preceding sections, we described two possible contamination histories: short-duration extremely severe contamination caused by directly released water containing extremely high Cs concentrations, and long-duration relatively low-level contamination via the food chain. In this section, these two histories are tested by simulations.

Marine fish take up Cs both from seawater and from food in amounts that are proportional to the Cs concentrations in the seawater and food, respectively. In addition, the amount of Cs excreted from the body of a fish is proportional to the Cs concentration in the body. Therefore, the change in the Cs concentration in the body of a fish can be described by the following equation:

$$dC_b / dt = aC_w + bC_f - cC_b$$

where C_b, C_w, and C_f indicate the Cs concentrations (Bq/kg-wet) in fish muscle (as a proxy for the whole-body concentration), seawater, and food, respectively. The coefficients *a, b,* and *c* designate the constant rates (day^{-1}) of intake and excretion. For simplicity's sake, we ignored the effects of fish growth (Ugedal et al. 1995, 1997) and water temperature (Rowan and Rasmussen 1995), as well as the effect of physical radioactive decay. Coefficients *b* and *c* are given by the following equations:

$$b = DR \times AR$$

$$c = (\ln 2) / BHL$$

where *DR*, *AR*, and *BHL* are daily food ration (kg food/kg body), the proportion of Cs in food absorbed by the gastrointestinal tract, and the biological half-life of the flounder (days), respectively.

In the simulation, we used the following seawater Cs concentrations (Fig. 11.5a): high Cs concentration (seawater A), moderate Cs concentration (seawater B), and

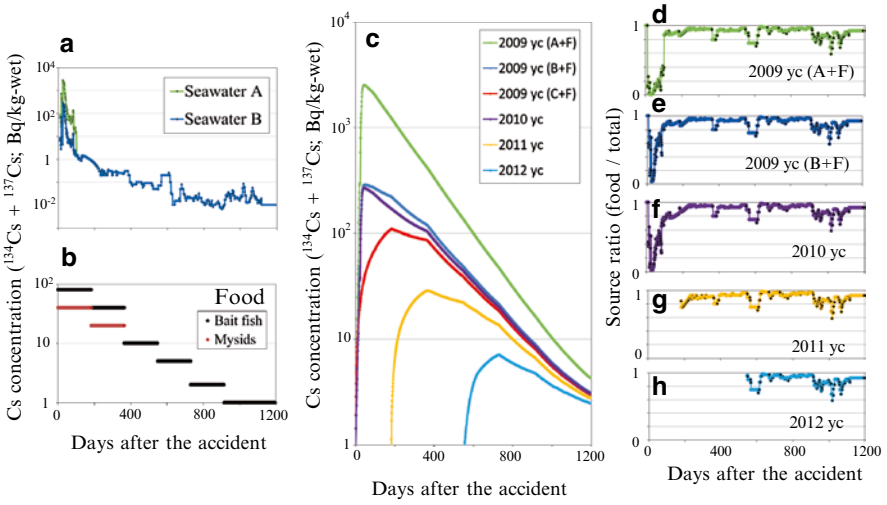

Fig. 11.5 Simulation of the temporal changes in the concentrations of Cs (^{134}Cs + ^{137}Cs; Bq/kg-wet) in Japanese flounder *Paralichthys olivaceus* with different contamination histories and from different year-classes. Temporal changes in Cs concentrations in seawater A and B (**a**) and in food (bait fish and mysids) (**b**). (**c**) Temporal changes in simulated Cs concentrations for fish in the 2009, 2010, 2011, and 2012 year-classes. Also shown are Cs concentrations in fish in the 2009 year-class (yc) that took up Cs from seawater A and food (A + F), seawater B and food (B + F), and seawater C and food (C + F). Ratios of Cs sources (food/total) are shown for the 2009 yc that took up Cs from seawater A and food (A + F) (**d**) and from seawater B and food (B + F) (**e**), and for the 2010 (**f**), 2011 (**g**), and 2012 (**h**) year-classes

Cs concentration of zero (seawater C) during the first 100 days after the accident and a moderate Cs concentration after the first 100 days that is common to all seawaters. The high Cs concentration for the initial 100 days was taken from the coastal monitoring data off Iwasawa, which is 16 km south of the FNPP (Tsumune et al. 2012; TEPCO 2014). As a proxy for moderately contaminated water, we used a value that was 1/10 of the high concentration (see Fig. 3 in Tateda et al. 2013). For the Cs concentrations in food consumed by fish ≥1 year old for six 6-month periods from March 2011 to February 2014, we used values of 80, 40, 10, 5, 2, and 1 Bq/kg-wet, which were based on monitoring data for Japanese sand lance and Japanese anchovy (bait fish) in the coastal waters off northern Fukushima Prefecture (northern half of area IV) (Fisheries Agency 2014) (Fig. 11.5b). For fish younger than 1 year old, we used food concentrations of 40, 20, 10, 5, 2, and 1 Bq/kg-wet for the same 6-month periods; these values were based on data for mysids in the same area (Sohtome et al. 2014). Fish in the 2009 year-class fed on bait fish throughout the simulation period; the fish in the 2010 year-class fed on mysids from March to August 2011 and then shifted to bait fish; and fish in the 2011 and 2012 year-classes fed on mysids during their first 12 months (Fig. 11.4). The coefficient for Cs intake from seawater (a) was set at 0.1 (approximately equal to the value of 0.11 reported by Tateda et al. 2013). DR and AR were set at 0.02 (Kurita et al., unpublished data) and 0.6 (between the value of 0.5 reported by Tateda et al. 2013 and the value of 0.78 reported by Kasamatsu et al. 2001), respectively. BHL was set at 104 days so that the saturated Cs concentration in the fish body was twice the Cs concentration in the food, which was the observed relationship between the concentrations in fish body and food in the equilibrium state before the accident (Kasamatsu and Ishikawa 1997).

In the simulations, we focused on three issues: variation of the Cs concentrations among individuals, the influence of the contamination history during the initial 100 days, and differences in Cs concentrations among the year-classes.

First, the effect of Cs concentration in the seawater was evaluated (Fig. 11.5c–e). The Cs concentrations in the fish body were simulated for fish in the 2009 year-class, which fed on bait fish and were exposed to seawater categories A, B, or C. Differences in the Cs intake levels from seawater during the initial 100 days after the accident produced large variations in the maximum Cs concentrations (Fig. 11.5c): 109 Bq/kg-wet (2.04 log transformed; sources of Cs were seawater C + food), 286 Bq/kg-wet (2.46 log transformed; seawater B + food), and 2,504 Bq/kg-wet (3.40 log transformed; seawater A + food). For fish that were exposed to directly released water (seawater A or B), the body Cs concentration peaked shortly after the accident, at 43 days (23 April 2011) and at 50 days (30 April 2011) for seawaters A and B, respectively, and then decreased rapidly. Even if fish did not take up Cs from seawater during the initial 100 days (seawater C), the body Cs concentration increased to 109 Bq/kg-wet at 184 days (11 September 2011), which corresponds to the peak period of the lowest observed concentrations (as described in Sect. 11.2). High individual variation and a gradual increase in the lowest concentrations until September were observed in the monitored data (Figs. 11.1 and 11.2). Contamination from seawater A was greater than contamination from food during

the first 100 days after the accident and from seawater B during the first 50 days after the accident (Fig. 11.5d, e). The actual observed maximum value, 4,500 Bq/kg-wet, was comparable to the value obtained from the simulation.

Second, different exposures to contaminated seawater during the initial 100 days after the accident influenced the Cs concentration in the fish body for a long time after the accident. Specifically, the Cs concentrations in the bodies of fish that were exposed to seawaters A, B, and C for the initial 100 days (until the middle of June 2011) were 47.6, 21.5, and 18.6 Bq/kg-wet, respectively, at 2 years after the accident and 6.5, 4.2, and 4.0, respectively, at 3 years after the accident (Fig. 11.5c). These results indicate that the Cs concentrations in fish exposed to the directly released seawater, especially seawater A, have not been in the equilibrium state for more than 3 years.

Third, differences between year-classes were evaluated (Fig. 11.5c, f–h). Cs concentrations in fish bodies were simulated for the 2010, 2011, and 2012 year-classes on the assumption that the fish fed on prey and were exposed to seawater B. Fish in the 2010 year-class (purple line), which fed on mysids for the first 4 months after the accident and then shifted to bait fish, showed a temporal variation in Cs concentration that was similar to that for the 2009 year-class (dark blue line). In contrast, the Cs concentrations in the 2011 year-class (yellow line) and 2012 year-class (light blue line) were clearly lower than those in the older fish. The maximum values were 32 (1.51 log transformed) and 8 (0.90 log transformed) Bq/kg-wet for the 2011 and 2012 year-class, respectively, and peak concentrations occurred at 254 days old for both year-classes. Food was the greatest source of Cs for the 2011 and 2012 year-classes throughout their lives (Fig. 11.5g, h), which indicates less individual variation than in the older fish that were exposed to directly released water. The observed data for the year-classes (Fig. 11.3) were in agreement with the simulated results; that is, lower concentrations and less variability were observed for the 2011 and 2012 year-classes than for the older year-classes.

The observed features were reproduced by the simulations under the condition of the two possible contamination histories: fish were contaminated both by exposure to directly released seawater containing extremely high Cs concentrations, that showed high spatial variability and drastically decreased after May 2011, and by exposure via food, in which the Cs concentration was much lower than that in seawater and decreased slowly. The values of additional parameters should be evaluated in future quantitative studies. In particular, the effects of fish size and water temperature, as well as the effects of growth on the accumulation or dilution of Cs (growth accumulation/dilution), are critical because Japanese flounder grow fast and inhabit water with a wide range of temperatures.

11.5 Conclusions

Observed Cs concentration data showed high variation among individual fish, peaks in the lowest concentrations in autumn 2011 for the 2010 year-class and older fish, and lower concentrations with less variation for the 2011 year-class and younger

fish. We suggest two major Cs contamination histories. The first involved contamination by directly released highly contaminated water during March and April in 2011. The Cs concentrations in this water showed high spatial variability, and the effects of seawater decreased drastically after the first few months following the FNPP accident. The other history involved contamination from food: mysids for fish younger than 1 year and bait fish for older fish. The maximum Cs concentrations in food were very low compared to those in the directly released water and decreased slowly. The existence of these two contamination histories was supported by simulation studies. These histories seem to be common to many other fish species (Tateda et al. 2013; Wada et al. 2013; Narimatsu et al. 2014).

The observation of major effects resulting from directly released seawater during the initial few months after the accident is characteristic of the FNPP accident. Most fish that showed high Cs concentrations in 2012 and later were likely to have taken up Cs in the initial few months after the accident but are currently taking up little Cs from food and are excreting Cs continuously. Therefore, it is important to recognize that the observed high Cs concentrations in some individuals may not have reached an equilibrium state, and the Cs concentrations in these individuals do not necessarily indicate the current intensity of contamination from the environment, but rather reflect contamination during the first few months after the accident.

On the basis of the proposed histories of contamination, the intensity of contamination should be low after the first few months following the accident. Even old fish that were exposed to the directly released water currently show low Cs concentrations, below the regulatory value for fish products, 100 Bq/kg-wet. In addition, the abundance of fish in the 2010 year-class and older is decreasing as these fish age and die. Therefore, the Cs concentrations in most fish will continue to decrease to less than 20 Bq/kg-wet, which is the present concentration (as of March 2014) in most of the 2010 year-class and older fish and all of the 2012 year-class and younger fish. The only potential problem is that individuals inhabiting the port in front of the FNPP still show higher Cs concentrations than those of fish inhabiting outside the port (Shigenobu et al. 2014; TEPCO 2014), which indicates that intense contamination is still occurring in the port, although the number of these fish is negligible relative to the overall stock in this area.

Acknowledgments We are grateful to Kaoru Nakata and Adriaan Rijnsdorp for their valuable comments on an earlier version of this manuscript. We also thank Takami Morita, Yoji Narimatsu, Takuji Mizuno, and Tadahiro Sohtome for discussions and useful information. Thanks are also due to Hiroyuki Togashi, Yukinori Nakane, Yosuke Amano, and Tsuyoshi Tamate for their assistance in sampling fish and discussions. The crew of the *R/V Wakataka-maru* and the fishing vessels *Seiko-maru* and *Daiei-maru* are appreciated for assistance with fish sampling.

References

Fisheries Agency, Ministry of Agriculture, Forestry and Fisheries (2014) Results of the inspection on radioactivity materials in fisheries products. http://www.jfa.maff.go.jp/e/inspection/index.html. Accessed on 31 May 2014

Kasamatsu F, Ishikawa Y (1997) Natural variation of radionuclide ^{137}Cs concentration in marine organisms with special reference to the effect of food habits and trophic level. Mar Ecol Prog Ser 160:109–120

Kasamatsu F, Nakamura M, Nakamura R, Suzuki Y, Kitagawa D (2001) Estimation of daily feeding rate of Japanese flounder *Paralichthys olivaceus* taken off Pacific coast of Aomori Prefecture by a radioisotope method. Nippon Suisan Gakkaishi 67:500–502

Kurita Y, Tamate T, Ito M (2014) Stock assessment and evaluation for Japanese flounder, north Pacific stock (fiscal year 2013). In: Marine fisheries stock assessment and evaluation for Japanese waters (fiscal year 2013/2014). Fisheries Agency and Fisheries Research Agency of Japan, Tokyo, pp 1373–1398 (in Japanese)

Narimatsu Y, Sohtome T, Yamada M, Shigenobu Y, Kurita Y, Hattori T, Inagawa R (2014) Why do the radionuclide concentrations of Pacific cod depend on the body size? In: Nakata K, Sugisaki H (eds) Impact of the Fukushima nuclear accident on fish and fishing grounds. Springer, Berlin (chapter 10 in this volume)

Rowan DJ, Rasmussen JB (1995) Bioaccumulation of radiocesium by fish: the influence of physicochemical factors and trophic structure. Can J Fish Aquat Sci 51:2388–2410

Shigenobu Y, Fujimoto K, Ambe D, Kaeriyama H, Ono T, Morinaga K, Nakata K, Morita T, Watanabe T (2014) Radiocesium contamination of greenlings (*Hexagrammos otakii*) off the coast of Fukushima. Sci Rep 4:6851

Sohtome T, Wada T, Mizuno T, Nemoto Y, Igarashi S, Nishimune A, Aono T, Ito Y, Kanda J, Ishimaru T (2014) Radiological impact of TEPCO's Fukushima Dai-ichi Nuclear Power Plant accident on invertebrates in the coastal benthic food web. J Environ Radioact 138:106–115

Tateda Y, Tsumune D, Tsubono T (2013) Simulation of radioactive cesium transfer in the southern Fukushima coastal biota using a dynamic food chain transfer model. J Environ Radioact 124:1–12

TEPCO (2014) Monitoring by sampling. http://www.tepco.co.jp/en/nu/fukushima-np/f1/smp/index-e.html. Accessed on 30 May 2014

Tomiyama T, Kurita Y (2011) Seasonal and spatial variations in prey utilization and condition of a piscivorous flatfish *Paralichthys olivaceus*. Aquat Biol 11:279–288

Tsumune D, Tsubono T, Aoyama M, Hirose K (2012) Distribution of oceanic ^{137}Cs from the Fukushima Dai-ichi Nuclear Power Plant simulated numerically by a regional ocean model. J Environ Radioact 111:100–108

Ugedal O, Forseth T, Jonsson B, Njåstad O (1995) Sources of variation in radiocaesium levels between individual fish from a Chernobyl contaminated Norwegian lake. J Appl Ecol 32:352–361

Ugedal O, Forseth T, Jonsson B (1997) A functional model of radiocesium turnover in brown trout. Ecol Appl 7:1002–1016

Wada T, Nemoto Y, Shimamura S, Fujita T, Mizuno T, Sohtaome T, Kamiayama K, Morita T, Igarashi S (2013) Effects of the nuclear disaster on marine products in Fukushima. J Environ Radioact 124:246–254

Yoneda M, Kurita Y, Kitagawa D, Ito M, Tomiyama T, Goto T, Takahashi K (2007) Age validation and growth variability of Japanese flounder *Paralichthys olivaceus* off the Pacific coast of northern Japan. Fish Sci 73:585–592

Part IV
Mechanisms of Severe Contamination in Fish

Chapter 12
Evaluating the Probability of Catching Fat Greenlings (*Hexagrammos otakii*) Highly Contaminated with Radiocesium off the Coast of Fukushima

Yuya Shigenobu, Ken Fujimoto, Daisuke Ambe, Hideki Kaeriyama, Tsuneo Ono, Takami Morita, and Tomowo Watanabe

Abstract On 1 August 2012, a total of 25,800 Bq/kg-wet of radiocesium (^{134}Cs = 9,800 Bq/kg-wet, ^{137}Cs = 16,000 Bq/kg-wet) was detected in the muscle tissue of two fat greenlings (*Hexagrammos otakii*) caught approximately 20 km north of the Fukushima Dai-ichi Nuclear Power Plant (FNPP). To estimate the contamination level of this fish species off the coast of Fukushima, we measured the radiocesium concentration in the muscle tissue of individual fat greenlings in 2012 and 2013. Radiocesium concentration of fat greenlings caught in southern coastal waters from the FNPP was significantly higher than that of fat greenlings collected in other waters off the coast of Fukushima. However, fat greenlings with a radiocesium concentration greater than 10,000 Bq/kg-wet were not detected, not even from highly contaminated areas. In addition, data obtained from specimens collected off the coast of Fukushima from April to December 2012 suggested that the probability of catching fat greenlings with a concentration greater than 16,000 Bq/kg-wet of ^{137}Cs was exceedingly low (less than 2.794×10^{-6}). In contrast, highly contaminated fat greenlings were frequently caught within the FNPP port. The geometric mean of ^{137}Cs was 55,400 Bq/kg-wet, as calculated from specimens obtained during December 2012 to May 2013. Our investigation suggests that fat greenlings with an extremely high concentration of radiocesium were contaminated within the FNPP port and then migrated offshore.

Keywords Fat greenling • Marine products • High contamination • Radiocesium • Probability

Y. Shigenobu (✉) • K. Fujimoto • D. Ambe • H. Kaeriyama • T. Ono • T. Morita
National Research Institute of Fisheries Sciences, Fisheries Research Agency,
2-12-4, Fukuura, Kanazawa, Yokohama, Kanagawa 236-8648, Japan
e-mail: yshig@affrc.go.jp

T. Watanabe
Tohoku National Fisheries Research Institute, Fisheries Research Agency,
3-27-5, Shinhama, Shiogama, Miyagi 985-0001, Japan
e-mail: wattom@affrc.go.jp

K. Nakata, H. Sugisaki (eds.), *Impacts of the Fukushima Nuclear Accident on Fish and Fishing Grounds*, DOI 10.1007/978-4-431-55537-7_12

12.1 Introduction

Immediately after the Fukushima Dai-ichi Nuclear Power Plant (FNPP) accident in March 2011, high concentrations of radiocesium (^{134}Cs and ^{137}Cs) were detected in several specimens of marine products off the coast of Fukushima (Ministry of Agriculture, Forestry and Fisheries 2014). In April 2011, a concentration of 12,500 Bq/kg-wet and 14,400 Bq/kg-wet of radiocesium was detected in whole-fish specimens of Japanese sand lance (*Ammodytes personatus*) collected approximately 30 km south of the FNPP. These extremely high concentrations in coastal pelagic fish species were caused from their direct exposure to highly contaminated seawater (Bailly et al. 2012; Oikawa et al. 2013). It is known that cesium absorbed by marine organisms is excreted by their potassium ion transport system during osmoregulation (Furukawa et al. 2012; Kaneko et al. 2013). Therefore, a rapid decrease in the radiocesium concentration of seawater would reduce contamination of marine organisms, especially for pelagic fish species (Buesseler 2012; Wada et al. 2013). Temporal trends in radiocesium concentration of marine organisms off the coast of Fukushima gradually declined after the summer of 2011 (Wada et al. 2013). Marine organisms with a radiocesium concentration greater than 10,000 Bq/kg-wet were not reported until 1.5 years after April 2011. On 1 August 2012, however, a total of 25,800 Bq/kg-wet of radiocesium (^{134}Cs = 9,800 Bq/kg-wet; ^{137}Cs = 16,000 Bq/kg-wet) was detected in the muscle tissue of two fat greenlings (*Hexagrammos otakii*) caught approximately 20 km north of the FNPP (Tokyo Electric Power Corporation 2012a). Although Tokyo Electric Power Corporation (2012b) had carried out an intensive investigation within the 20-km radius from the FNPP port, such a highly contaminated fish had not been caught until that point, and the reason for this extremely high level of contamination remains unclear.

Fat greenling is a coastal demersal fish species that lives by preying on benthic organisms. A previous tagging study suggested that the migration distance of fat greenling was restricted within an area of approximately 30-km radius (Fukushima Prefectural Fisheries Experimental Station FPFES 1974). It is assumed that in highly contaminated areas, as is the zone within and around the FNPP port, sedentary demersal fish species continuously receive radiocesium through the benthic food web more constantly than migratory demersal fish species such as Japanese flounder (see Chap. 11) and Pacific cod (see Chap. 10). In this section, we measured radiocesium concentration in the muscle tissue of individual fat greenlings caught off the coast of Fukushima to estimate the contamination level in this fish species. In addition, we attempted to calculate the probability that ^{137}Cs concentration exceeds 16,000 Bq/kg-wet in fat greenlings collected off the coast of Fukushima from April 2012 to March 2013, using our original data in combination with datasets published by the Ministry of Agriculture, Forestry and Fisheries (MAFF) and TEPCO (2014).

12.2 Radiocesium Contamination of Fat Greenlings off the Coast of Fukushima

From May 2012 to March 2013, we collected 236 fat greenlings in northern (approximately 50 km north of the FNPP) and southern (approximately 40 km south of the FNPP) waters (Fig. 12.1). Radiocesium concentration was measured as described by Shigenobu et al. (2014). Fat greenlings caught from the northern waters had a relatively lower radiocesium concentration than those collected from the southern waters (Table. 12.1). In the southern waters, the level of contamination was significantly higher ($p < 0.001$) in coastal waters, at depth less than 30 m (geometric mean, 128 Bq/kg-wet) than in offshore waters, at depth greater than 50 m (geometric mean, 28.4 Bq/kg-wet). The highest radiocesium concentration detected was 1,070 Bq/kg-wet in a fat greenling collected from the southern coastal waters on 20 May 2012. In this study, none of the fish specimens had a radiocesium concentration higher than 10,000 Bq/kg-wet weight.

Figure 12.2 shows the time-series trend of radiocesium concentration of fat greenlings caught within the FNPP port and off the coast of Fukushima from May

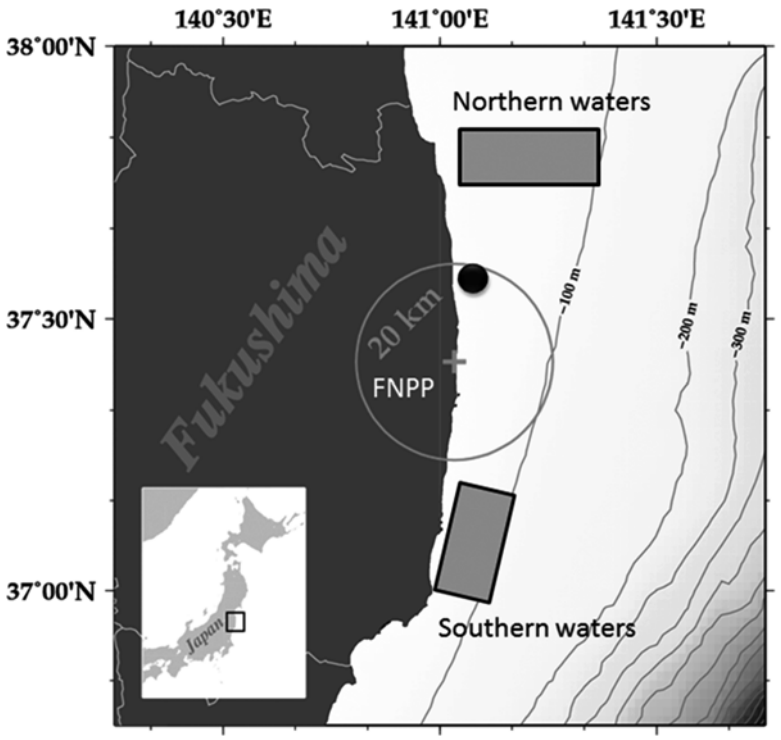

Fig. 12.1 Fat greenlings were collected from several sampling locations. The *gray circle* indicates a sampling area of approximately 20-km radius around the Fukushima Dai-ichi Nuclear Power Plant (FNPP), and the *black spot* indicates the sampling point, where fat greenlings with a 25,800 Bq/kg-wet radiocesium concentration were caught on 1 August 2012

Table 12.1 Radiocesium concentrations in individual fat greenlings off the coast of Fukushima

Sampling area	Number of individuals	$^{134}Cs + ^{137}Cs$ concentration (Bq/kg-wet)		
		Range		
		Min.	Max.	Geometric mean[a]
Northern coastal waters (at depth less than 30 m)	30	4.46	39.2	13.1
Northern offshore waters (at depth more than 50 m)	54	n.d. (<4.24)	193	21.9
Southern coastal waters (at depth less than 30 m)	68	n.d. (<5.31)	1,070	128
Southern offshore waters (at depth more than 50 m)	84	n.d. (<3.28)	987	28.4

[a]Detection limit was used for the calculation of geometric mean in samples in which radiocesium was not detected (n.d.)

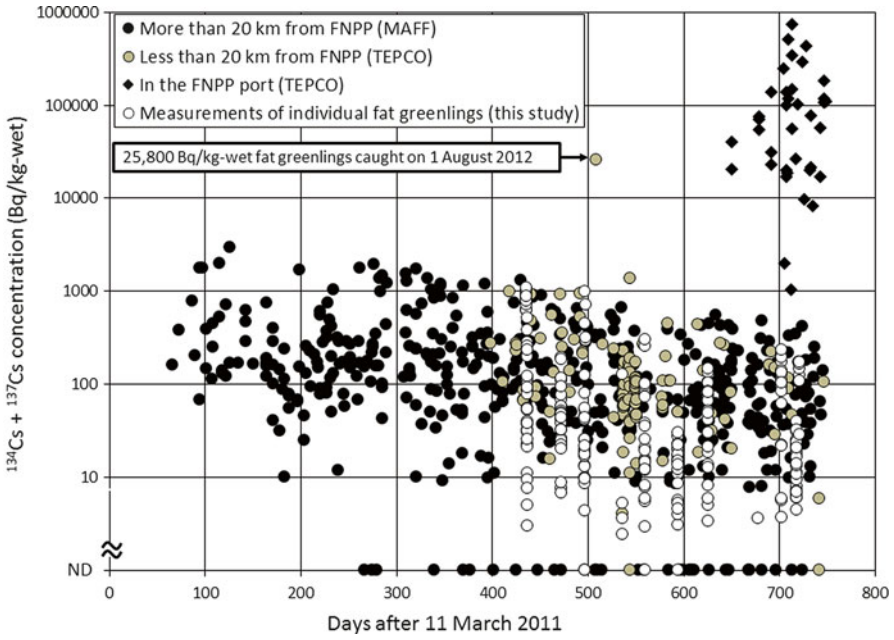

Fig. 12.2 Temporal trend of radiocesium concentration ($^{134}Cs + ^{137}Cs$) in fat greenlings caught within and outside an area of approximately 20-km radius around the Fukushima Dai-ichi Nuclear Power Plant (FNPP). Tokyo Electric Power Corporation (2012b) has been monitoring marine organisms within an area of 20-km radius around FNPP since April 2012

2011 to May 2013, using our original data and datasets published from MAFF and TEPCO. Radiocesium concentration of fat greenlings caught off the coast of Fukushima gradually declined over time. Except for the datasets of fat greenlings collected within the FNPP port, radiocesium concentration exceeded the Japanese threshold (100 Bq/kg-wet) in 76.3 % and 41.2 % of specimens caught off the coast of Fukushima in 2011 and 2012, respectively. In particular, geometric means were 209 Bq/kg-wet in specimens collected from April to December 2011 and 77.2 Bq/kg-wet in those collected from April to December 2012.

Previous studies have reported that radiocesium concentration in marine organisms (Wada et al. 2013) and sediments (Ambe et al. 2014) within the southern coastal area of FNPP was comparatively higher than those in other areas. However, according to our data and published datasets from MAFF and TEPCO, fat greenlings with a radiocesium concentration greater than 10,000 Bq/kg-wet were not identified, not even in specimens collected from highly contaminated areas. This circumstantial evidence suggests a low probability of catching extremely highly contaminated fat greenling off the coast of Fukushima. Our field investigation and laboratory-rearing experiments of a benthic polychaete in highly contaminated sediment suggests that radiocesium intake from contaminated sediments is limited for benthic organisms and demersal fish species (see Chap. 7). Progressive simulation analysis of the contamination mechanism in fat greenling off the coast of Fukushima is presented in Chap. 13.

12.3 Site of Contamination of the Highly Contaminated Fat Greenling

Data of ^{137}Cs concentration in fat greenling specimens collected off the coast of Fukushima from April to December 2012 were log-transformed. A normal distribution curve of log-transformed values was used to calculate the probability of catching fat greenlings with a ^{137}Cs concentration greater than 16,000 Bq/kg-wet (log-transformed value of 4.204) as shown in Fig. 12.3. Values below the detection limit of ^{137}Cs were excluded from this analysis to obtain a more conservative estimate. Normality of the log-transformed values from the combined datasets was confirmed. Arithmetic mean ± standard deviation of log-transformed ^{137}Cs concentration was 1.676 ± 0.5567. The calculated probability of catching fat greenlings with a concentration greater than 16,000 Bq/kg-wet of ^{137}Cs was below 2.794×10^{-6}. This very low value strongly suggests that fat greenlings off the coast of Fukushima from April to December 2012 did not include any highly contaminated individuals.

In contrast, the level of radiocesium contamination in fat greenlings caught in the FNPP port from December 2012 to May 2013 was extremely high. The geometric mean was 55,400 Bq/kg-wet and ranged from 1,030 to 740,000 Bq/kg-wet. Kanda (2013) reported that the average values of ^{137}Cs concentration in seawater samples collected from the intake canal area of Units 1–4 of the FNPP from June to August 2011 ranged between 305 and 1,650 Bq/l. Concentration ratio (CR) of the 25,800 Bq/

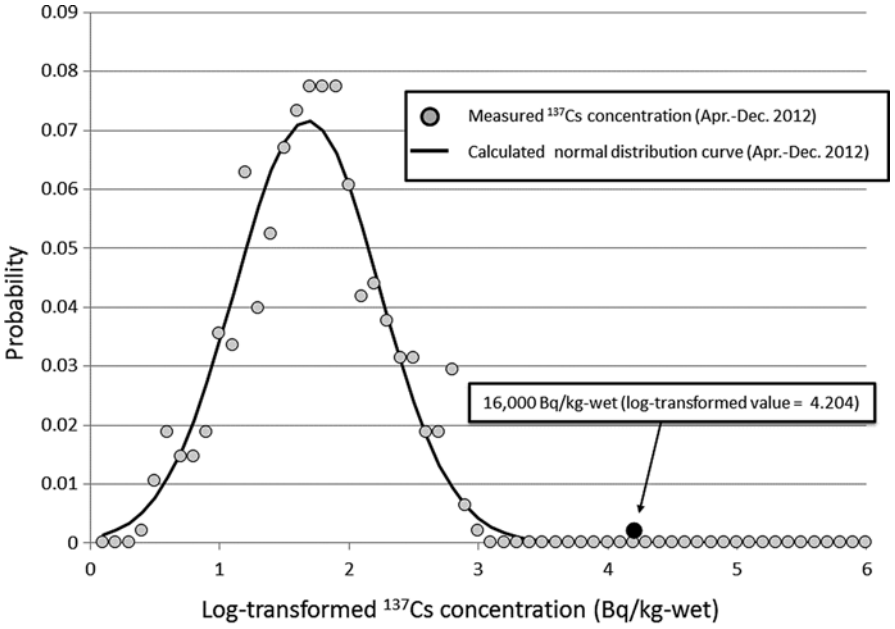

Fig. 12.3 Probability of catching contaminated fat greenlings off the coast of Fukushima. The normal distribution curve was constructed using log-transformed ^{137}Cs concentration in specimens collected from April to December 2012. *Black spot* indicates the 16,000 Bq/kg-wet ^{137}Cs concentration. The probability of catching fat greenlings with a ^{137}Cs concentration greater than 16,000 Bq/kg-wet was less than approximately 2.794×10^{-6}

kg-wet (^{137}Cs of 16,000 Bq/kg-wet) fish specimens to the seawater from the intake canal area of Units 1–4 was between 9.70 and 52.5 for the period of June to August 2011. These results were consistent with previous findings that CR of ^{137}Cs between demersal fish species and seawater around Japan ranged from 15 to 54 (Tagami and Uchida 2013). The results also indicated that the contamination level within the FNPP was much higher immediately after the FNPP accident. Accordingly, for a period of several months after the FNPP accident, the radiocesium contamination level of fat greenlings within the FNPP port was never less than 25,800 Bq/kg-wet. Although the site where the extremely contaminated fat greenlings were caught was 20-km away from FNPP, this distance is within the possible migration distance for this species (FPFES 1974). Therefore, it is assumed that the extremely contaminated fat greenlings had been exposed to highly contaminated seawater over a certain period of time after the accident within or near the FNPP port before they migrated offshore.

Acknowledgments This section is based on the article entitled "Radiocesium contamination of greenlings (*Hexagrammos otakii*) off the coast of Fukushima" published in the open access journal of *Scientific Reports* (doi: 10.1038/srep06851). The authors wish to thank all the fishery workers in

Fukushima Prefecture who collected the greenlings for this study. We also thank all the members of our research group for their assistance with specimen preparation. This study was supported by the Fisheries Agency, the Ministry of Agriculture, and the Forestry and Fisheries of Japan.

References

Ambe D, Kaeriyama H, Shigenobu Y, Fujimoto K, Ono T, Sawada H, Saito H, Miki S, Setou T, Morita T, Watanabe T (2014) Five-minute resolved spatial distribution of radiocesium in sea sediment derived from the Fukushima Dai-ichi Nuclear Power Plant. J Environ Radioact 138:264–275

Bailly du Bois P, Laguionie P, Korsakissok I, Didier D, Fiévet B (2012) Estimation of marine source-term following Fukushima Daiichi accident. J Environ Radioact 114:2–9

Buesseler KO (2012) Fishing for answers off Fukushima. Science 338:480–482

Fukushima Prefectural Fisheries Experimental Station (FPFES) (1974) Research report of resource ecology and fisheries for selected three rockfish species (*Hexagrammos otakii, Sebastes inermis and Sebastes vulpes*) in North Pacific waters of Japan (in Japanese)

Furukawa F, Watanabe S, Kaneko T (2012) Excretion of cesium and rubidium via the branchial potassium-transporting pathway in Mozambique tilapia. Fish Sci 78:597–602

Kanda J (2013) Continuing ^{137}Cs release to the sea from the Fukushima Daiichi Nuclear Power Plant through 2012. Biogeosciences 10:6107–6113

Kaneko T, Furukawa F, Watanabe S (2013) Excretion of cesium through potassium transport pathway in the gills of a marine teleost. In: Nakanishi TM, Tanoi K (eds) Agricultural implications of the Fukushima nuclear accident. Springer Japan, Tokyo, pp 105–118

Ministry of Agriculture, Forestry and Fisheries (2014) http://www.jfa.maff.go.jp/e/inspectio n/index.html. Accessed 12 June 2014

Oikawa S, Takata H, Watabe T, Misonoo J, Kusakabe M (2013) Distribution of the Fukushima-derived radionuclides in seawater in the Pacific off the coast of Miyagi, Fukushima, and Ibaraki Prefectures, Japan. Biogeosciences 10:5031–5047

Shigenobu Y, Fujimoto K, Ambe D, Kaeriyama H, Ono T, Morinaga K, Nakata K, Morita T, Watanabe T (2014) Radiocesium contamination of greenlings (*Hexagrammos otakii*) off the coast of Fukushima. Sci Rep 4. doi:10.1038/srep06851

Tagami K, Uchida S (2013) Marine and freshwater concentration ratios ($CR_{wo\text{-}water}$): review of Japanese data. J Environ Radioact 126:420–436

Tokyo Electric Power Corporation (2012a) Result of radioactive nuclide analysis (fat greenling). http://photo.tepco.co.jp/date/2012/201208-j/120821-01j.html. Accessed 12 June 2014 (in Japanese)

Tokyo Electric Power Corporation (2012b) Handouts at press conference | Archives. http://www.tepco.co.jp/en/nu/fukushima-np/handouts/indexold-e.html. Accessed 12 June 2014

Wada T, Nemoto Y, Shimamura S, Fujita T, Mizuno T, Sohtome T, Kamiyama K, Morita T, Igarashi S (2013) Effects of the nuclear disaster on marine products in Fukushima. J Environ Radioact 124:246–254

Chapter 13
Analysis of the Contamination Process of the Extremely Contaminated Fat Greenling by Fukushima-Derived Radioactive Material

Tomowo Watanabe, Ken Fujimoto, Yuya Shigenobu, Hideki Kaeriyama, and Takami Morita

Abstract We analyzed the contamination process by which the fat greenling, which was caught in the area off the mouth of the Ota River of Fukushima prefecture on August 1, 2012, concentrated radiocesium (^{134}Cs + ^{137}Cs) to the level of 25,800 Bq/kg-wet. The radioactivity environment of the area was insufficient to maintain or increase the radiocesium concentration in the fish at the time. Distribution of the radioactive materials in the otolith of the fat greenling estimated by beta-ray emissions suggested that the fat greenling was in a highly contaminated environment during the period immediately following the Fukushima Dai-ichi Nuclear Power Plant (FNPP) accident. We used a biokinetic simulation of the ^{137}Cs concentration to demonstrate that the fat greenling had to have been exposed to radioactivity from the FNPP to achieve such a high radiocesium concentration. Thus, the extremely contaminated fat greenling originated in the heavily contaminated environment of the FNPP port or the adjoining area in the period just after the accident.

Keywords Fat greenling • Contamination • Radiocesium • Autoradiography

13.1 Introduction

Radioactive nuclides leaked from the Fukushima Dai-ichi Nuclear Power Plant (FNPP), operated by Tokyo Electric Power Company (TEPCO), when it was damaged by the tsunami following the Tohoku Earthquake on March 11, 2011. The United Nations Scientific Committee on the Effects of Atomic Radiation

T. Watanabe (✉)
Tohoku National Fisheries Research Institute, Fisheries Research Agency,
3-27-5, Shinhama, Shiogama, Miyagi 985-0001, Japan
e-mail: wattom@affrc.go.jp

K. Fujimoto • Y. Shigenobu • H. Kaeriyama • T. Morita
National Research Institute of Fisheries Sciences, Fisheries Research Agency,
2-12-4, Fukuura, Kanazawa, Yokohama, Kanagawa 236-8648, Japan

K. Nakata, H. Sugisaki (eds.), *Impacts of the Fukushima Nuclear Accident on Fish and Fishing Grounds*, DOI 10.1007/978-4-431-55537-7_13

(UNSCEAR 2013) estimated the scale of the release of several radioactive nuclides: the range for radioactive iodine (^{131}I) was from 100 to 500 petabecquerel (PBq) and the range for radiocesium (^{137}Cs) was from 6 to 20 PBq. The committee noted that the amounts of released radioactive nuclides were much lower than that which occurred after the Chernobyl accident (the FNPP accident released 20 % of the ^{137}Cs levels released after Chernobyl). The remarkable feature of the FNPP accident was the swift and direct release of highly polluted water to the ocean. Coastal area of Fukushima and adjacent prefectures were covered with seawater bearing high concentrations of ^{131}I and radiocesium (^{134}Cs and ^{137}Cs) after the accident. The direct leakage of ^{137}Cs was estimated as 3.5 PBq and the highest seawater concentration ($>6\times10^4$ Bq/l) was observed at the coast near the FNPP (Tsumune et al. 2012). This value was seven orders of magnitude higher than the pre-accident levels.

The Ministry of Agriculture, Forestry and Fisheries (MAFF) and local government initiated emergency monitoring of radioactivity in marine products immediately after the accident to ensure food safety. Their findings were published on the websites of MAFF (2014) and of the Ministry of Health, Labor and Welfare (MHLW 2014). The Fisheries Research Agency (FRA) supported the measurement of radioactivity in marine products. In April 2011, extremely high levels of ^{131}I and radiocesium (^{134}Cs + ^{137}Cs; $>1.0\times10^4$ Bq/kg-wet) were reported in sand lance larvae. Such high contamination levels were confined to larvae of pelagic fish in the area south of the FNPP and were thought to result from the spread of contaminated water after the accident (Tateda et al. 2013). After that, ^{131}I contamination levels decreased rapidly, consistent with its short half-life (about 8.02 days), and returned to the levels below the limit of detection (hereinafter referred to as ND) after August 2011 (Wada et al. 2013). The relatively longer half-life of ^{134}Cs (about 2.07 years) and ^{137}C (about 30.1 years) caused them to remain in the marine environment for much longer; monitoring of radiocesium in the marine environment and marine products has continued.

Cesium is an alkali metal that is metabolized by the same pathway that metabolizes potassium, which is an essential mineral (Kaneko et al. 2013). As are other alkali metals, radiocesium is exchanged between the environment and body of marine teleost fish by their osmoregulatory systems, which maintain electrolyte balance (Evans 2010). Thus, radiocesium concentrations in the fish depend on the concentrations in the surrounding seawater. Wada et al. (2013) showed continuous reduction in radiocesium concentrations in marine products obtained off the coast of Fukushima Prefecture; the ecological half-life of radiocesium is much shorter than the physical half-lives of ^{134}Cs and ^{137}Cs.

TEPCO began to monitor radioactivity in marine fishes within a 20-km radius of FNPP (hereinafter referred to as the 20-km area) in March 2012. Against the decreasing trend of radiocesium in marine products, extremely high radiocesium concentrations were detected in *Hexagrammos otakii* (fat greenling) in the summer of 2012. The fat greenlings were caught about 1 km offshore near the mouth of the Ota River on August 1, 2012 (Chap. 12). The reported radiocesium (^{134}Cs + ^{137}Cs) level was 25,800 Bq/kg-wet (TEPCO 2012a), the highest radiocesium concentration found in marine fishes at the time. An additional survey of fat greenlings in the area was conducted by TEPCO from September to October 2012, during which time 57 samples were examined (TEPCO 2012b). Most of the surveyed greenlings

showed radiocesium concentrations two orders of magnitude lower than that of the fat greenling caught in the area off the mouth of the Ota River on August 1, 2012. Radiocesium concentrations ranged from ND to 1,350 Bq/kg-wet (median, 77 Bq/kg-wet), equivalent to the levels found in samples taken outside the 20-km area. TEPCO's research on marine fish in the port of FNPP beginning in October 2012 showed highly contaminated fish species, including fat greenlings, with radiocesium concentrations exceeding 10,000 Bq/kg-wet (TEPCO 2014a). Statistical analysis of the data from fat greenlings showed that the probability of finding fat greenlings with ^{137}Cs concentrations exceeding 16,000 Bq/kg-wet was below 3.0×10^{-6}, suggesting their radioactive exposure history was similar to that of the population in the port of FNPP (Shigenobu et al. 2014, Chap. 12).

The purpose of this study was to determine the contamination process of fat greenling by performing a quantitative analysis. We evaluated the radioactivity of the marine environment and the potential for generating highly contaminated fat greenlings. Analysis of fat greenling otoliths revealed the radioactive exposure history of the fish, the progress of which was examined by biokinetic model simulations.

13.2 ^{137}Cs Concentrations in Coastal Seawater and Marine Fish off the Coast of Fukushima Prefecture

Daily observed ^{137}Cs concentrations in seawater sampled at TEPCO's monitoring stations around FNPP and the Fukushima Dai-ni Nuclear Power Plant (TEPCO 2014b) were used to evaluate radioactivity in the coastal areas of Fukushima Prefecture. Station locations are indicated in Fig. 13.1. The station at the shallow draft quay in the port of FNPP (hereinafter referred to as site-FP) was selected for the FNPP port; the northern side of the discharge channel for units 5–6 of FNPP (T-1) and the south discharge channel of FNPP, including stations T-2 and T-2-1, were selected to represent areas outside the FNPP port. The station at the north discharge channel of the Fukushima Dai-ni Nuclear Power Plant (T-3) and stations south thereof, around the Iwasawa shore (T-4), the north side of the Asami River (T-4-1), and the south side of the Kitasako River (T-4-2), were also chosen. To represent the average ^{137}Cs concentration in the area outside the FNPP port (site-F1), data were averaged from T-1, T-2, and T-2-1. Averages were also generated for T-3, T-4, T-4-1, and T-4-2 to represent seawater around the Fukushima Dai-ni Nuclear Power Plant (site-F2). Thus, three daily time-series of ^{137}Cs concentrations were generated for the period from March 21, 2011 to August 31, 2014. These values were used for the simulation of ^{137}Cs concentrations in fat greenling.

Data points of ND were interpolated to produce continuous daily data. ND data during several days at site-FP were interpolated by using the minimum values obtained in the 15 days around the target day; longer consecutive ND periods were filled with values calculated from data obtained at other station in the port by regression analysis. ND data in the site-F1 and site-F2 time-series were filled in the same way.

Figure 13.2 shows the variations in seawater ^{137}Cs concentration at the three sites. High ^{137}Cs concentrations were simultaneously detected at all three stations

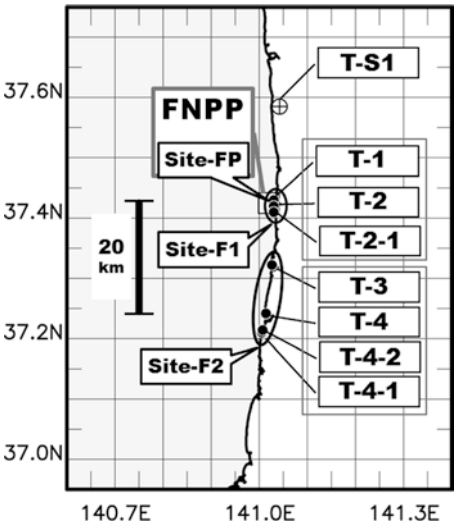

Fig. 13.1 Locations of radiocesium monitoring stations along the coast of Fukushima prefecture. *Site-FP* represents the station at the shallow draft quay in the Fukushima Dai-ichi Nuclear Power Plant (FNPP) port. Stations T-1, T-2, and T-2-1 are adjacent to the FNPP port and are referred to as *site-F1*. Stations T-3, T-4, T-4-1, and T-4-2 are located around the Fukushima Dai-ichi Nuclear Power Plant and southward, referred to as *site-F2*. Station T-S1 is the collection point for the extremely contaminated fat greenling exhibiting 25,800 Bq/kg-wet radiocesium ($^{134}Cs + ^{137}Cs$)

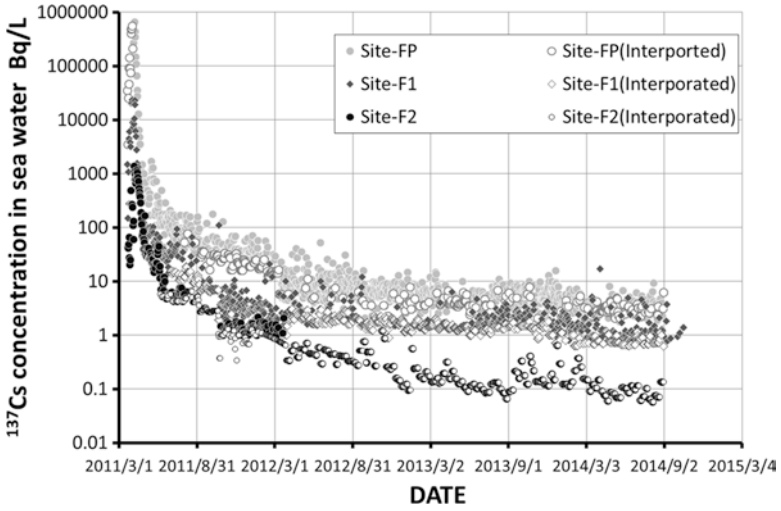

Fig. 13.2 Combined time-series of observed and interpolated daily ^{137}Cs concentration data at site-FP, site-F1, and site-F2 from March 21, 2011, to August 31, 2014

from late March to the beginning of April 2011. Peak values were 6.6×10^5 Bq/l at site-FP, 2.4×10^4 Bq/l at site-F1, and 1.4×10^3 Bq/l at site-F2; values this high have never before been observed in the marine environment (Tsumune et al. 2012; Baxter and Camplin 1993; IAEA 2005; HELCOM 2009). Accumulated values for the period from March 21, 2011 to July 31, 2012, when the fat greenling was thought to be affected by contamination off the coast of Fukushima Prefecture, were as high as 5.4×10^6 Bq/l at site-FP, 2.2×10^5 Bq/l at site-F1, and 1.8×10^4 Bq/l at site-F2. These accumulated values were indicative of the direct load of radioactivity in the ecosystem at each site. In addition, accumulation curves of ^{137}Cs concentrations of each sites indicated sharp increase during the early days and reached 90 % of accumulated values of July 31, 2012 in first 20 (site-FP), 21 (site-F1), and 45 (site-F2) days.

^{137}Cs concentration data for fat greenlings in the coastal waters of Fukushima Prefecture were extracted from the dataset published by MHLW (2014) and from TEPCO data reports for the 20-km area and the FNPP port (TEPCO 2014a). Time-series for fat greenlings in the coastal waters of Fukushima and for the 20-km area indicate similar decreasing trends beginning in the spring of 2012 (Fig. 13.3). The median and the 95th percentile values were calculated from the combined data set of both for each 6-month period beginning March 1, 2011. Ecological half-lives calculated from these values for the period from March 2012 to August 2014 were 175 days for 95th percentile and 194 days for median. The values were slightly lower than the results for fat greenlings (217 days) collected from the southern area off the coast of Fukushima Prefecture between August 2011 and September 2012 (Tateda et al. 2013). The difference reflected the variation in analytical period.

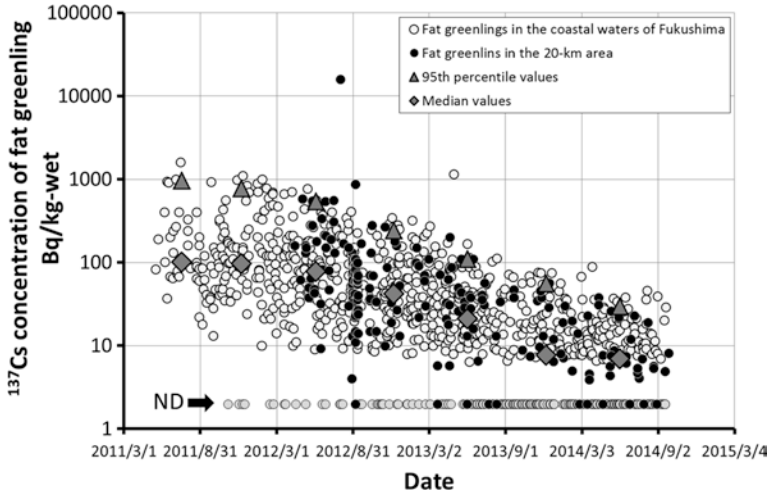

Fig. 13.3 Temporal trends of observed ^{137}Cs concentrations in fat greenlings caught in the coastal waters of Fukushima Prefecture, except the 20-km area and in the 20-km area with median values and 95th percentile values calculated from combined data of both for each 6-month period. The first term includes data from March 1, 2011 to August 31, 2011

13.3 The Marine Environment as a Source of Radioactive Contamination of the Fat Greenling

We sought to determine whether the observed radioactivity in the environment in the summer of 2012 could maintain radiocesium ($^{134}Cs + {}^{137}Cs$) concentrations of 25,800 Bq/kg-wet in the fat greenling. Marine fish obtain radiocesium from the environment via uptake of food and water. ^{137}Cs concentrations in marine fish directly correlate with the concentrations in seawater under stable conditions (Kasamatsu 1999; IAEA 2004), expressed as the concentration factor (CF). Kasamatsu (1999) summarized the CFs of ^{137}Cs for 27 species of marine teleost fish around Japan. The CFs were calculated from data obtained between 1984 and 1996; the average CF value for each fish species ranged from 22 to 122. The IAEA-recommended CF value of 100 for marine fish lies within this range (IAEA 2004). We estimated the CF for fat greenling off the coast of Fukushima prefecture from 29 measures obtained in 1982–2010, archived, and published by the NRA (Nuclear Regulation Authority 2014). The average CF was 67 ± 29, also within the range described by Kasamatsu (1999).

The CF value for fat greenling off the coast of Fukushima suggested that the surrounding seawater should contain ^{137}Cs concentrations of 240 Bq/l to maintain a ^{137}Cs concentration of 16,000 Bq/kg-wet (25,800 Bq/kg-wet for $^{134}Cs + {}^{137}Cs$) in the fish. In August 2012, the ^{137}Cs concentration of seawater was less than 0.1 Bq/l off the coast of Fukushima Prefecture; the highest values observed in the FNPP port were also less than 100 Bq/l (TEPCO 2014b). TEPCO (2012b) also reported values much lower than 0.1 Bq/l in samples obtained around the Ota River.

We also considered the possibility that excretion of ^{137}Cs from the fish was compensated for by ingestion of prey. Assuming a biological half-life of 100 days (World Health Organization and Food and Agriculture Organization of the United Nations 2011), the daily excretion rate was calculated as 0.0069 day^{-1} and the daily amount of ^{137}Cs excreted from the fat greenling was 110 Bq/kg-wet. Assuming an ingestion rate of 0.03 day^{-1} and assimilation rate of 0.5 (Tateda 1997), the fat greenling would have to consume more than 7,300 Bq/kg-wet ^{137}Cs daily to compensate for excretion. The ^{137}Cs concentrations in the marine biota within the 20-km area were ND to 1,000 Bq/kg-wet (TEPCO 2014a), far below the required level.

Thus, the status of environmental ^{137}Cs contamination in the area off the Ota River and in the 20-km area were insufficient to maintain the 16,000 Bq/kg-wet ^{137}Cs concentration observed in the fat greenling, which were then assumed to be excreting excess radiocesium.

13.4 Radioactivity in the Otolith of Contaminated Fat Greenling

The fish otolith is a hard tissue that retains information on the age of the fish and the history of its environment, including temperature, salinity, and chemical composition (Campana 1999). The fish otolith consists mostly of calcium carbonate and

other elements that indicate environmental exposure. For example, strontium is often used as an indicator of environmental salinity (Tsukamoto et al. 1998). Radioactive materials absorbed in the otolith are also used as indicators of environmental conditions. Baker and Wilson (2001) showed that the otolith core of red snapper from the Gulf of Mexico contains ^{14}C produced by nuclear testing. We analyzed the radioactive nuclides contained in the otolith of the fat greenling to characterize its history of radioactive exposure.

Contaminated fat greenling with radiocesium ($^{134}Cs + ^{137}Cs$) concentrations of 25,800 Bq/kg-wet were caught from the area off the mouth of the Ota River and inspected for radioactivity by TEPCO, which provided the fish remnants from which the otoliths were extracted (Fig. 13.4). Radiation emitted from the otolith was measured with a germanium semiconductor detector for gamma-emitting nuclides and with a gas flow radiation counter for beta-emitting nuclides. Significant beta-ray emission was detected and gamma-ray emission was not detected (Fujimoto et al. 2013). Autoradiography was performed with imaging plates (IP) to visualize the distribution of radiation scatter from the sample materials.

We mounted a thin slice of the otolith on a glass slide and placed it on an IP (BAS-MS 2025; Fuji Film) for 13 days. The reaction strength to beta-ray emission

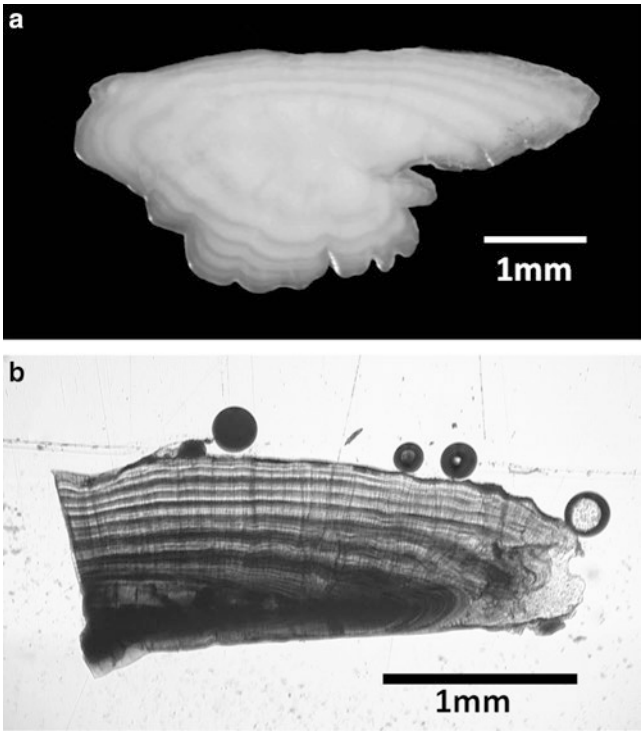

Fig. 13.4 Otolith of the fat greenling (**a**) and its slice (**b**). The otolith in this figure was extracted from the *right side* of the fat greenling's head. The slice was cut from the *left-hand* otolith

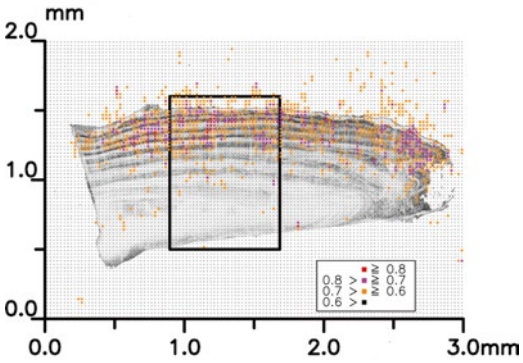

Fig. 13.5 Image of the otolith slice and distribution of cumulative strength of incident radiation on an imaging plate (IP). Dense (*light*) shading areas of the otolith slice correspond to the transparent (opaque) zone. *Colors* indicate the cumulative strength normalized to the highest value. The *rectangle* encloses the area of detailed analysis where the zonal patterns of the annulus were obvious and the one-dimensional analysis along the *vertical* direction could be applied

was recorded on the IP and retrieved by an image analyzer (Typhoon 9400; GE Healthcare) with 25-μm resolution. Beta rays were randomly emitted from the otolith and absorbed by the stimulatable phosphor layer of the IP. The reaction strength reflects the accumulated number or energy of the beta rays. The distribution of the reaction strength on the IP was compared to digital images of the slice obtained by microscopy after careful justification of the pixel positions of both data. Figure 13.5 shows the distribution of reaction strength relative to the highest value on the image of the otolith slice. Higher reactions of the IP were observed around the area corresponding to the outer peripheral region of the slice. The relationship between the two images was quantified in the area indicated by the rectangle in Fig. 13.5, where the annulus had a clear zonal pattern and allowed one-dimensional analysis in the vertical direction. Thirty vertical rows of IP pixel data were included in the area. Relative reaction strength data in each vertical row were reconstructed by using the peak position of the second transparent zone as the origin. We compared the distribution of reaction strength detected by the IP with the vertical pattern consisting of opaque zones and transparent zones of the slice. The higher reaction of the IP corresponded to the area around the second transparent-opaque zone from outer edge of the slice (Fig. 13.6). We fitted a curve that had a form proportional to $1/(h^2 + r^2)$ to the vertical distribution of the reaction strength. h is the distance from the otolith slice to the stimulatable phosphor layer of the IP and r is the distance on the IP surface from the peak of the second transparent zone of the slice to each pixel position along the vertical axis. The formula approximated the distribution of incident radiation on a flat plane from a point source. The proportional coefficient and parameter h were estimated by the least-squares method using Solver in Excel. The statistical significance of the fitted curve in Fig. 13.6 was checked in a form of single regression analysis obtained by variable conversion. The fitted curve indirectly indicated that the position of the source of the radiation was located around the peak of the second transparent zone of the otolith slice. Considering an assumed error of

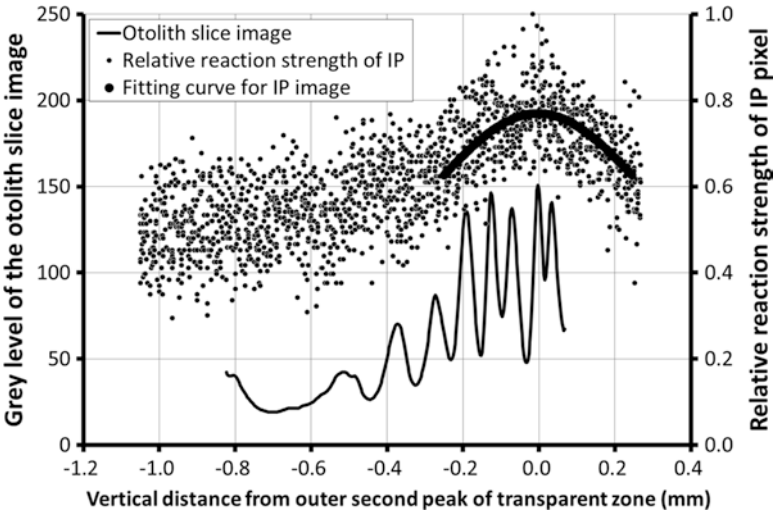

Fig. 13.6 Comparison between the *grey level* of the otolith slice and the relative reaction strength of the IP for the enclosed area in Fig. 13.5. Thirty *vertical rows* of IP pixel data were included. Relative reaction strength data for each *vertical row* were reconstructed by using the peak position of the second transparent zone as the origin. The *vertical* distribution of the zonally averaged *grey level* of the otolith slice is shown by a *solid thin line*. Lower (higher) *grey levels* in the otolith slice correspond to the opaque (transparent) zone. The relative reaction strength of each pixel of the IP is shown with a *full circle*. The fitted *curve* for the IP pixel data in the area around the peak of the second transparent zone is shown by a sequence of *large full circles. Upward arrow* indicates the center of the second transparent zone

±1 pixel (0.025 μm) in justifying the slice and IP images, the probability of containing more radioactive materials was high in the area from the second to the third opaque zones of the otolith slice.

The opaque zone of the otolith was formed in the summer season (Sekigawa et al. 2002); the first transparent-opaque zone on the slice from the fat greenling caught in the summer of 2012 was thought to correspond to the period from autumn 2011 to summer 2012. Thus, the second zone containing the most beta ray-emitting radionuclides corresponded to the period from autumn 2010 to summer 2011. These results strongly suggested that the fat greenling was in an environment rich in beta ray-emitting nuclides between the spring and summer of 2011.

A possible candidate of beta ray-emitting radionuclide contained in the otolith was ^{90}Sr. The beta-ray emissions from the otolith of several fish species collected in the FNPP port were associated with ^{90}Sr concentration in the body, excluding the viscera, and were associated with ^{137}Cs in the muscle tissue (Fujimoto et al. 2013). The amount of ^{90}Sr leakage was estimated at about 3 % of ^{137}Cs (Casacuberta et al. 2012), but it was thought that the ^{90}Sr concentration in seawater rapidly increased, similar to ^{137}Cs from late March to the beginning of April 2011. From these relationships, we hypothesized that the fat greenling absorbed a large amount of radioactive nuclides in the period just after the FNPP accident when contaminated seawater covered the coastal area of Fukushima Prefecture.

13.5 Simulation of ^{137}Cs Concentrations in Fat Greenlings Using a Biokinetic Model

To test our hypothesis, we simulated the contamination of fat greenling in a biokinetic model of ^{137}Cs exchange between environment and biota. Many types of biokinetic model have been used to simulate the concentration of radioactive nuclides in fish (Brown et al. 2006; Kanish and Aust 2013; Tateda et al. 2013). We constructed a simple model of two compartments as shown by Brown et al. (2006). The equation for ^{137}Cs concentration in a fat greenling is expressed as Eq. (13.1). The ^{137}Cs concentrations in marine fish are mediated by uptake through drinking seawater (first term), ingestion of prey (second term), and excretion by the osmoregulation system (last term). Explanations for each variable and parameter are given in Table 13.1. Most values were set according to Tateda (1997). As the fat greenling is thought to be omnivorous (Kasamatsu 1999), we set the ^{137}Cs concentration of prey as a mixture of two groups of marine biota: one group was fish and the other was invertebrates. The ^{137}Cs concentration in prey fish was determined by Eq. (13.1). The ^{137}Cs concentrations in invertebrates were calculated by Eq. (13.2), in which uptake of ^{137}Cs is directly related to the seawater concentration of ^{137}Cs. The parameters of k_{pi} and CF_{pi} empirically determined that the predicted ^{137}Cs values by Eq. (13.2) followed the observed ^{137}Cs values for invertebrates off Fukushima Prefecture. After determining the parameters in Eq. 13.2, we tuned the mixture rate of the prey groups to obtain a simulated CF of fat greenling in the range of 60–70 by using the constant ^{137}Cs concentration value. In addition, the effect of physical disintegration of ^{137}Cs was discarded because it has a 100-fold-longer half-life (about 30.1 years) in comparison to the biological half-life (about 100 days):

Table 13.1 Variables and parameters in the biokinetic equation for a fat greenling

Variable	Value	Unit	Explanation
C_f		Bq/kg-wet	^{137}Cs concentration in fish body
C_{pf}		Bq/kg-wet	^{137}Cs concentration in prey fish body
C_w		Bq/l	^{137}Cs concentration of surrounding seawater
C_{pi}		Bq/kg-wet	^{137}Cs concentration of prey invertebrate
k_w	0.10[a]	(kg/l) day^{-1}	Uptake rate of ^{137}Cs activity from seawater
IR_f	0.030[a]	day^{-1}	Ingestion rate per unit mass of fish
AE_f	0.50[a]	No dimension	Assimilation efficiency for fish
k_f	0.0088[a]	day^{-1}	Excretion rate of ^{137}Cs for fish
CF_{pi}	10[b]	No dimension	Concentration factor for prey invertebrate
k_{pi}	0.0087[b]	day^{-1}	Excretion rate of ^{137}Cs for prey invertebrate
a	0.36[b]	No dimension	Mixing ratio of prey fish

[a]Values were adopted from Tateda (1997)
[b]Values were experimentally determined in this study

$$\frac{dC_f(t)}{dt} = k_w \cdot C_w(t) + IR_f \cdot AE_f \cdot \left[a \cdot C_{pf}(t) + (1-a) \cdot C_{pi}(t)\right] - k_f \cdot C_f(t) \tag{13.1}$$

$$\frac{dC_{pi}(t)}{dt} = CF_{pi} \cdot k_{pi} \cdot C_w(t) - k_{pi} \cdot C_{pi}(t) \tag{13.2}$$

The time course of ^{137}Cs accumulation in the fat greenlings was simulated by using the ^{137}Cs concentration data from seawater at site-FP, site-F1, and site-F2 (shown in Fig. 13.7 with observed data). The derivation curve of ^{137}Cs concentrations for site-F2 (thick solid line) was a good approximation of the envelope curve of observation data. The ^{137}Cs concentration of fat greenling at site-F2 reached maximum in mid-July 2011, then decreased. The simulated ecological half-life for the period after March 2012 is about 208 days, similar to the values calculated from observed data (13.2). An evaluation of the contribution of each term in Eq. (13.1) showed that uptake of ^{137}Cs from the seawater was largely responsible for the increasing ^{137}Cs concentration in the first month, during which time the concentration increased to 80 % of the maximum value. After this point, low but steady uptake via prey contributed to a slow increase toward the maximum ^{137}Cs concentration in mid-July and the slow decrease thereafter. These features are identical to the simulation results for coastal fish indicated by Tateda et al. (2013). We conclude that the simplified model is appropriate for simulating ^{137}Cs concentrations in fat greenling off the coast of Fukushima.

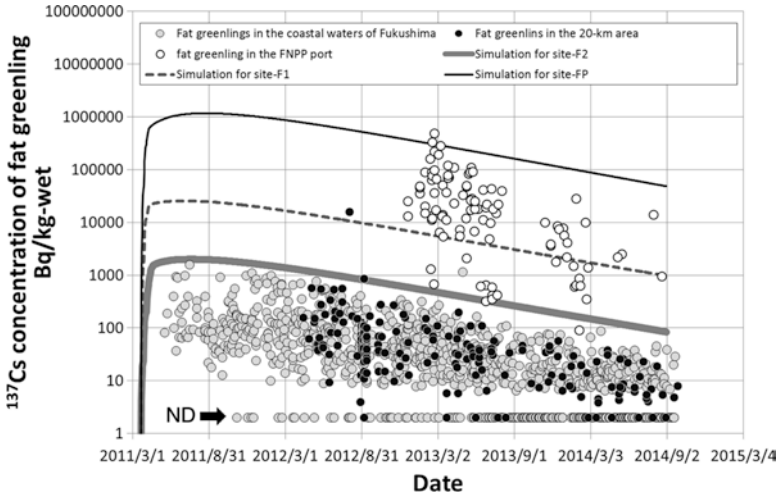

Fig. 13.7 Simulated ^{137}Cs concentration of fat greenlings for site-FP, site-F1, and site-F2 with observed ^{137}Cs concentrations in fat greenling caught in the coastal waters of Fukushima Prefecture, except the 20-km area, in the 20-km area, and in the FNPP port

Simulation results for site-F1 (dashed line) and site-FP (thin solid line) are also shown in Fig. 13.7. The same curve shape was observed, although at a different level. Maximum ^{137}Cs concentration were observed in mid-July and correlated with the integrated values in seawater. The observed ^{137}Cs concentration in fat greenling from the FNPP port was moderately simulated by the model. The ^{137}Cs concentration in the highly contaminated fat greenling was in the range between simulations for site-FP in the FNPP port and site-F1. These model simulations support the hypothesis that the fat greenling collected in the summer of 2012 off the mouth of the Ota River had been exposed to the highly contaminated environment in the FNPP port or adjoining areas.

The range of ^{137}Cs concentrations formed by the large difference between simulations for site-FP and site-F1 bracketed the majority of the distribution of ^{137}Cs concentrations in fat greenlings in the FNPP port. The ^{137}Cs concentration data at site-FP were within the intermediate range compared with other observation points at the initial stage of the radiation leak. Available seawater ^{137}Cs concentration data from April 2011 showed that the averaged value for the observation point in the intake canal south of site-FP was several times higher than the value at site-FP. The minimum values of ^{137}Cs concentrations in the port, where the concentrations were probably no lower than the level found outside the port (site-F1), where the concentration was about one order of magnitude lower than at site-FP. The large variability of observed ^{137}Cs concentrations in fat greenling was partly attributed to the local spatial and temporal distribution of ^{137}Cs in the FNPP port. In additional simulations of a fat greenling entering the FNPP port after the peak period of environmental contamination, highly contaminated fat greenlings were also generated, mainly by prey uptake. This process might also maintain the wider range in the group of highly contaminated fat greenlings in the FNPP port.

As for the extremely contaminated fat greenling caught in the area off the mouth of the Ota River, radioactivity in the otolith and the simulation suggested a generation scenario. The fat greenling were living in the FNPP port or in the adjoining area when contaminated water leaked to the sea and highly contaminated seawater covered the area. The ^{137}Cs concentration of the fat greenling may have reached about 100,000 Bq/kg-wet. The relatively lower concentration compared with other fat greenlings in the FNPP port suggest the habitat was apart from the intake canal of the FNPP port and the fat greenling was able to avoid a direct encounter with the more highly contaminated seawater. After the direct leakage of highly contaminated water to the sea, the fat greenling eventually left the port.

Acknowledgments The authors appreciate the members of the Research Center for Fisheries Oceanography and Marine Ecosystem of the National Research Institute of Fisheries Science for their support. The sliced sample of the otolith was processed by Japan NUS, and the autoradiographic measurement of the otolith slice was performed by BayBioImaging. This study was financially supported by the Fisheries Agency.

References

Baker MS Jr, Wilson CA (2001) Use of bomb radiocarbon to validate otolith section ages of red snapper *Lutjanus campechanus* from the northern Gulf of Mexico. Limnol Oceanogr 46:1819–1824

Baxter AJ, Camplin WC (1993) Measures of dispersion from discharge pipelines at nuclear sites in the UK using caesium-137 in sea water data. Fisheries research data report no. 34. Ministry of Agriculture, Fisheries and Food, Directorate of Fisheries Research, Lowestoft

Brown J, Dowdall M, Gwynn JP, Børretzen P, Selnæs ØG, Kovacs KM, Lydersen C (2006) Probabilistic biokinetic modelling of radiocaesium uptake in Arctic seal species: verification of modelled data with empirical observations. J Environ Radioact 88:289–305

Campana SE (1999) Chemistry and composition of fish otolith: pathways, mechanisms and applications. Mar Ecol Prog Ser 188:263–297

Casacuberta N, Masqué P, Garcia-Orellana J, Garcia-Tenorio R, Buesseler KO (2012) ^{90}Sr and ^{89}Sr in seawater off Japan as a consequence of the Fukushima Dai-ichi nuclear accident. Biogeosciences 10:3649–3659

Evans DH (2010) A brief history of the study of fish osmoregulation: the central role of the Mt. Desert Island Biological Laboratory. Front Physiol 1:13

Fujimoto K, Miki S, Kaeriyama H, Shigenobu Y, Takagi K, Ambe D, Ono T, Watanabe T, Morinaga K, Nakata K, and Morita T (2013) Levels of radioactive cesium contamination in three fish species caught in the main harbor of Fukushima Dai-ichi Nuclear Power Plant, and a trial to estimate strontium-90 from fish otoliths. (submitted to Environ Sci Technol)

HELCOM (2009) Radioactivity in the Baltic Sea, 1999-2006: HELCOM thematic assessment. Baltic Sea environment proceedings no. 117. HELCOM, Helsinki

IAEA (2004) Sediment distribution coefficients and concentration factors for biota in the marine environment. Technical reports series no. 422. IAEA, Vienna

IAEA (2005) Worldwide marine radioactivity studies (WOMARS): radionuclide levels in oceans and seas. IAEA-TECDOC-1429. IAEA, Vienna

Kaneko T, Furukawa F, Watanabe S (2013) Excretion of cesium through potassium transport pathway in the gills of a marine teleost. In: Nakanishi TM, Tanoi K (eds) Agricultural implications of the Fukushima nuclear accident. Springer Japan, Tokyo

Kanish G, Aust M-O (2013) Does the Fukushima NPP disaster affect the caesium activity of North Atlantic Ocean fish? Biogeosciences 10:5399–5410

Kasamatsu F (1999) Marine organisms and radionuclides with special reference to the factors affecting concentrations of ^{137}Cs in marine fish. Radioisotopes 48:266–282 (in Japanese)

MAFF (2014) Results of the monitoring on radioactivity level in fisheries products. http://www.jfa.maff.go.jp/e/inspection/index.html. Date of access: 11 Nov 2014

MHLW (2014) Levels of radioactive contaminants in foods tested in respective prefectures. http://www.mhlw.go.jp/english/topics/2011eq/index_food_radioactive.html. Date of access: 11 Nov 2014

NRA (2014) Environmental radioactivity and radiation in Japan (in Japanese). http://www.kankyo-hoshano.go.jp/. Date of access: 11 Nov 2014

Sekigawa T, Takahashi T, Takatsu T (2002) Age and growth of fat greenling *Hexagrammos otakii* in Kikonai Bay, Hokkaido. Aquat Sci 50:395–400 (in Japanese)

Shigenobu Y, Fujimoto K, Ambe D, Kaeriyama H, Ono T, Morinaga K, Nakata K, Morita T, Watanabe T (2014) Radiocesium contamination of greenlings (*Hexagrammos otakii*) off the coast of Fukushima. Sci Rep 4:6851

Tateda Y (1997) Basic model for the prediction of ^{137}Cs concentration in the organisms of detritus food chain. Abiko Research Laboratory CRIEPI report no. 94056. CRIEPI, Chiba (in Japanese)

Tateda Y, Tsumune D, Tsubono T (2013) Simulation of radioactive cesium transfer in the southern Fukushima coastal biota using a dynamic food chain transfer model. J Environ Radioact 124:1–12

TEPCO (2012a) High cesium density detected in greenling. http://www.tepco.co.jp/en/nu/fukushima-np/images/handouts_120828_02-e.pdf. Date of access: 11 Nov 2014

TEPCO (2012b) Additional survey on high-cesium-level greenling and future countermeasures. http://www.tepco.co.jp/en/nu/fukushima-np/images/handouts_121126_03-e.pdf. Date of access: 11 Nov 2014

TEPCO (2014a) Analysis results of fish and shellfish (The Ocean Area Within 20-km Radius of Fukushima Daiichi NPS). http://www.tepco.co.jp/en/nu/fukushima-np/f1/smp/index-e.html. Date of access: 21 Nov 2014

TEPCO (2014b) Result of radioactive nuclide analysis for the seawater sampled onshore and offshore of the power station. http://www.tepco.co.jp/en/nu/fukushima-np/f1/smp/2014/images/seawater-newest01-e.csv. Date of access: 21 Nov 2014

Tsukamoto K, Nakai I, Tesch W-V (1998) Do all freshwater eels migrate? Nature (Lond) 396:635–636

Tsumune D, Tsubono T, Aoyama M, Hirose K (2012) Distribution of oceanic ^{137}Cs from the Fukushima Daiichi Nuclear Power Plant simulated numerically by a regional ocean model. J Environ Radioact 111:100–108

UNSCEAR (2013) Sources, effects and risks of ionizing radiation (Report to the General Assembly). UNSCEAR, New York

Wada T, Nemoto Y, Shimamura S, Fujita T, Mizuno T, Sohtaome T, Kamiyama K, Morita T, Igarashi S (2013) Effects of the nuclear disaster on marine products in Fukushima. J Environ Radioact 124:246–254

World Health Organization and Food and Agriculture Organization of the United Nations (2011) Impact on seafood safety of the nuclear accident in Japan. http://www.iaea.org/newscenter/focus/fukushima/seafoodsafety0511.pdf

Chapter 14
Contamination Levels of Radioactive Cesium in Fat Greenling Caught at the Main Port of the Fukushima Dai-ichi Nuclear Power Plant

Ken Fujimoto, Shizuho Miki, and Tamaki Morita

Abstract Levels of radioactive cesium (radiocesium, $^{134}Cs + ^{137}Cs$) detected in fish caught at the Fukushima Dai-ichi Nuclear Power Plant (FNPP) Port are summarized. The mean concentration of radiocesium in three fish species (fat greenling, Japanese rockfish, and spotbelly rockfish) was significantly different from that in other fish species studied (brown hakeling, black rockfish, Japanese black porgy, olive flounder, marbled flounder). The levels of radiocesium in fat greenling decreased gradually from 100 kBq/kg-wet in 2013 to several kBq/kg-wet in 2014. A migration of fat greenling into the FNPP Port was assumed to explain the fact that fish containing low radiocesium levels were caught at the port. A low but significant correlation between the total length of the fish and the radiocesium concentration in the muscles was observed in fat greenling caught at the FNPP Port.

Keywords Radiocesium • Fat greenling • Japanese rockfish • Spotbelly rockfish • FNPP Port

14.1 Introduction

The Ministry of Agriculture, Forestry and Fisheries (MAFF), Fukushima Prefecture, and the Fisheries Research Agency (FRA) have been monitoring marine organisms to ensure the safety of fish and fishery products since 2011, immediately after the Fukushima Dai-ichi Nuclear Power Plant (FNPP) accident (MAFF 2013). Although about 40 % of marine organisms collected from the area off the coast of Fukushima Prefecture within a year after the accident contained radiocesium ($^{134}Cs + ^{137}Cs$) at levels exceeding the Japanese safety limit (100 Bq/kg-wet) (Buesseler 2012), the

K. Fujimoto (✉) • S. Miki • T. Morita
National Research Institute of Fisheries Sciences, Fisheries Research Agency, 2-12-4, Fukuura, Kanazawa, Yokohama, Kanagawa 236-8648, Japan
e-mail: fujiken@affrc.go.jp

K. Nakata, H. Sugisaki (eds.), *Impacts of the Fukushima Nuclear Accident on Fish and Fishing Grounds*, DOI 10.1007/978-4-431-55537-7_14

percentage of samples containing radiocesium levels exceeding the allowable limit decreased to 1.9 % by the end of 2013 (MAFF 2013). The contamination levels of radiocesium were gradually decreased even in fish caught in Fukushima Prefecture coastal waters (MAFF 2013). However, an extremely high concentration of radiocesium (25,800 Bq/kg-wet) was detected in fat greenlings caught in the Ota River (20 km north of the FNPP) on August 1, 2012, as reported by the Tokyo Electric Power Company (TEPCO 2014).

In contrast to intensive monitoring of fishery products caught in offshore waters, data for the radionuclide contamination of fish at the FNPP Port were limited because sample collection from this area was difficult. Highly contaminated water was directly discharged from the reactors into the port of FNPP during the early period after the FNPP accident. TEPCO has been monitoring water quality at several stations at the FNPP Port daily, and the results are available on http://www.tepco.co.jp/en/nu/fukushima-np/f1/smp/index-e.html. TEPCO also conducted a Fish Contaminant Monitoring Program at the FNPP Port, and the results were published in 2014. However, the data were focused only on the levels of radiocesium in fish, whereas other related information (e.g., size of the fish) was not made available to the public.

In this section, we summarize the data released from TEPCO relating to radiocesium levels in eight fish species (fat greenling, Japanese rockfish, spotbelly rockfish, brown hakeling, black rockfish, Japanese black porgy, olive flounder, marbled flounder) caught at the FNPP Port, focused on the radiocesium concentration in the muscle tissues of fat greenling (*Hexagrammos otakii*).

In this study, the data of ^{137}Cs concentration in seawater and the concentration of radiocesium in the muscles of fish species caught at the FNPP Port were obtained from the TEPCO website (http://www.tepco.co.jp/en/nu/fukushima-np/f1/smp/index-e.html). Fat greenling samples were collected using small cages and gill nets in a period from February 25, 2013 to May 16, 2014 by TEPCO (Fig. 14.1). After analyzing the data, TEPCO provided the samples to the National Research Institute of Fisheries Science (NRIFS) of FRA. The samples were stored at −20 °C at the TEPCO laboratory near the Hirono Thermal Power Plant (21 km south of the FNPP) before shipment.

14.2 Concentrations of Radiocesium in Seawater and Fish Caught at the Port of FNPP

The concentration of ^{137}Cs in seawater at the unloading deck (station ULD in Fig. 14.1) steeply increased shortly after the beginning of discharge from the reactors. The maximum level of ^{137}Cs (660 kBq/l) was detected on April 6, 2011. The level of ^{137}Cs rapidly decreased to 1 kBq/l at the end of April 2011 and to 100 Bq/l in mid-June 2011 (Fig. 14.2). The concentration factor of ^{137}Cs in fish ranged between 5 and 100 (IAEA 2004). Considering the concentration factor, ^{137}Cs levels

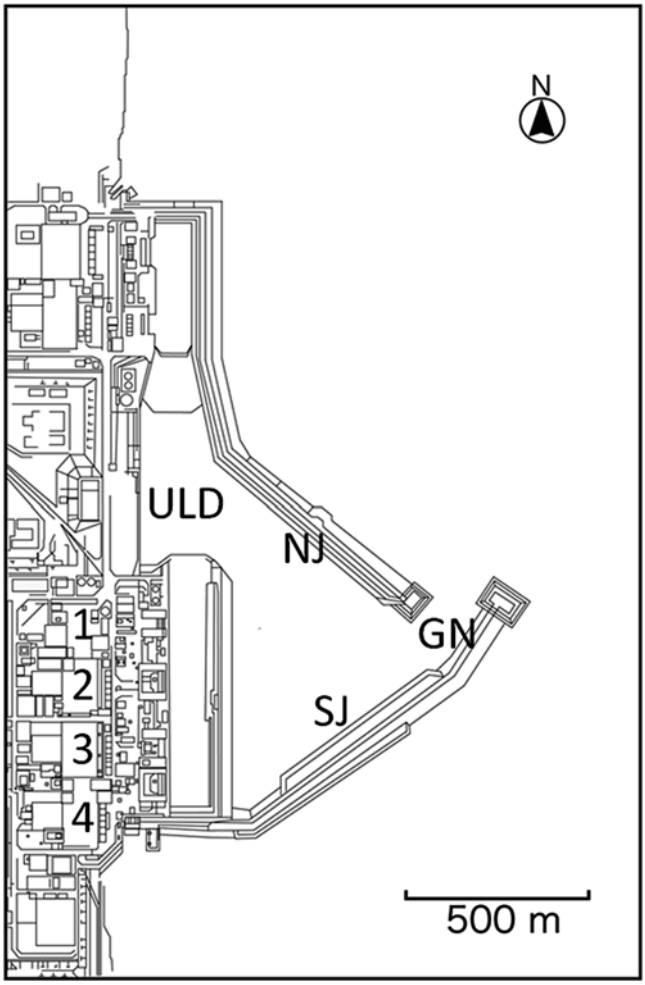

Fig. 14.1 Map of the monitoring sites at the Fukushima Dai-ichi Nuclear Power Plant (FNPP) and Port. *1–4* reactor units 1–4, *ULD* point of cage sampling at the unloading deck, *SJ* point of cage sampling at the north jetty, *NJ* point of cage sampling at the south jetty, *JN* point of gill net sampling at the port entrance

in fish at the FNPP Port could have reached 1,000 kBq/kg-wet between early and mid-April 2011 and 10 kBq/kg-wet in mid-June 2011.

Box plots shown in Fig. 14.3 illustrate the levels of radiocesium in the muscles of eight fish species caught at the FNPP Port. The average radiocesium concentrations of three species (fat greenling, Japanese rockfish, and spotbelly rockfish) were significantly different from those in the other five species (Fig. 14.3; $p<0.05$, Scheffe's test). The inter-quartile range of spotbelly rockfish and Japanese rockfish was narrower than that of fat greenling. Although the 75th quartiles of spotbelly

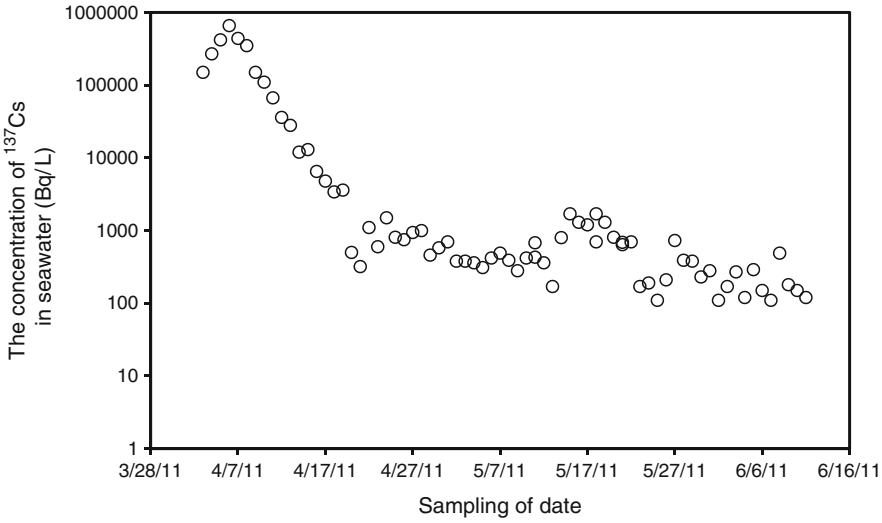

Fig. 14.2 Temporal changes in ^{137}Cs concentration in seawater samples collected at the unloading deck at the FNPP Port. Data were obtained from http://www.tepco.co.jp/en/nu/fukushima-np/f1/smp/index-e.html

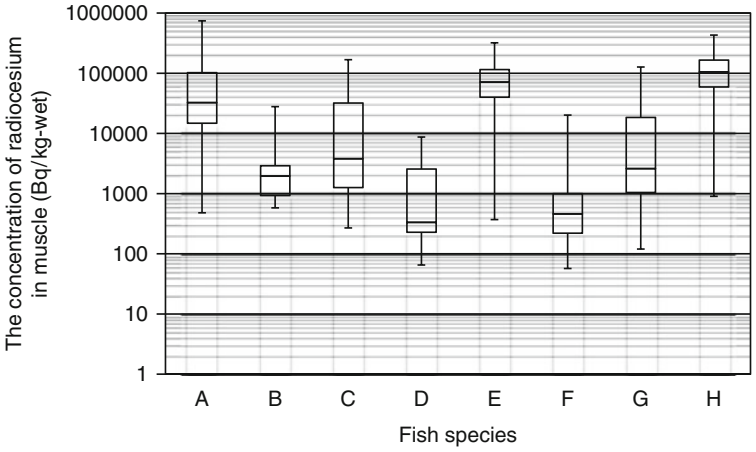

Fig. 14.3 Boxplots of radiocesium concentration in the muscles of fish caught at the FNPP Port from December 20, 2012 to November 19, 2013. Each *box* indicates the inter-quartile range. The *line* inside the box shows the median. The lines extending vertically from the boxes (*whiskers*) show the variability outside the quartiles. Fish species: *A* fat greenling (*Hexagrammos otakii*), *B* brown hakeling (*Physiculus maximowiczi*), *C* black rockfish (*Sebastes schlegeli*), *D* Japanese black porgy (*Acanthopagrus schlegelii*), *E* Japanese rockfish (*Sebastes cheni*), *F* olive flounder (*Paralichthys olivaceus*), *G* marbled flounder (*Pleuronectes yokohamae*), *H* spotbelly rockfish (*Sebastes pachycephalus*)

rockfish and Japanese rockfish were higher than 100 kBq/kg-wet, the median of radiocesium concentration in black rockfish was less than 10 kBq/kg-wet. Furthermore, the inter-quartile range of black rockfish was wider than that of the other two rockfish species, indicating that fluctuations in radiocesium levels in the black rockfish sample population were more intense than those observed in other rockfish. Interestingly, within the flatfish group, the mean radiocesium concentration in marbled flounder was significantly higher than that in olive flounder ($p < 0.001$; Wilcoxon–Mann–Whitney test).

Differences in concentrations of radiocesium among the studied fish species could not be explained only by the changes in radiocesium concentration in seawater. In addition to the direct intake of contaminated water by osmosis via the gills, incorporation of radiocesium through the consumption of prey via the food web might cause variations in radiocesium levels in fish. For example, although the Japanese flounder and marbled flounder live in the same environment, the mean concentrations of radiocesium differ between these two species, probably because their feeding habits are quite different. Japanese flounder prefer fish, whereas marbled flounder prefer worms living on the seabed. Similar to fish, prey organisms (e.g., crustaceans and worms) were labeled with radiocesium at various concentrations. Hence, the kind and amount of prey consumed were key factors influencing the levels of radiocesium within and between fish species living in waters at the FNPP Port.

14.3 Temporal Changes in Radiocesium Levels in Fat Greenling Caught at the FNPP Port

Figure 14.4 shows the temporal changes in radiocesium levels in the muscle tissues of fat greenling caught at the FNPP Port in a period from February 25, 2013 to May 16, 2014. The decreasing trend of radiocesium concentrations confirmed that the fluctuations among individual fish were intense in 2014. The levels of radiocesium were 100 kBq/kg-wet and several kBq/kg-wet at the beginning of 2013 and 2014, respectively. The radiocesium levels in a fish sample collected between June 12 and August 2, 2013 ranged between 0.48 and 0.92 kBq/kg-wet, and the mean value was significantly lower than that of other samples collected within the same period ($p < 0.005$; Student's t test). Additionally, a fat greenling captured on February 3, 2014 had a radiocesium concentration of 0.13 Bq/kg-wet, which was the lowest concentration compared to that in other fat greenling caught at the FNPP Port. Although an explanation of these low radiocesium levels could be that some fat greenling either escaped from contaminated seawater or did not consume organisms containing high concentrations of radiocesium, it is more likely that these fish migrated to the FNPP Port long after the accident. TEPCO constructed barriers made of gill nets at the entrance of the FNPP Port to prevent the escape of fish. However, these barriers were temporarily removed to allow ships to enter and exit

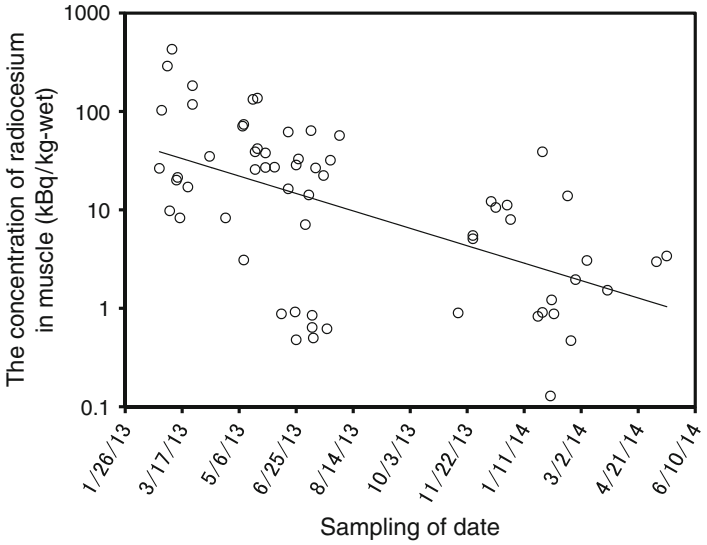

Fig. 14.4 Temporal changes in radiocesium concentration in fat greenling caught at the FNPP Port. Fish samples were collected from February 25, 2013 to May 16, 2014

the port. Therefore, the possibility of fat greenling migrating into the FNPP Port cannot be excluded. The concentration of ^{137}Cs in seawater sampled at the unloading deck (Fig. 14.1, ULD) was below 10 Bq/l in 2014 (TEPCO 2014). Taking into account the concentration factor, which ranged between 5 and 100 (IAEA 2004), ^{137}Cs levels in fat greenling that migrated into the FNPP Port would currently attain a maximum radiocesium concentration of 1 kBq/kg-wet.

14.4 Relationship Between Total Length and Radiocesium Level in the Muscles of Fat Greenling Caught at the FNPP Port

A low but significant correlation ($r = 0.395$, $p < 0.005$) between the total length and radiocesium concentration in the muscles was observed in fat greenling caught at the FNPP Port (Fig. 14.5). Because individuals caught within the experimental period were more than 3 years of age, as deduced from their total length (Fukushima Prefecture Fisheries Experimental Station 1974), all sampled fat greenling would have experienced an extremely high concentration of radiocesium in the seawater shortly after the accident (Fig. 14.2). The "size effect" reported for top fish species (Koulikov and Ryabov 1992) was also observed in fat greenling to some extent. Large-sized fat greenling (e.g., total length >400 mm) contained more radiocesium than did smaller ones because the former were 2 or more years of age and were able

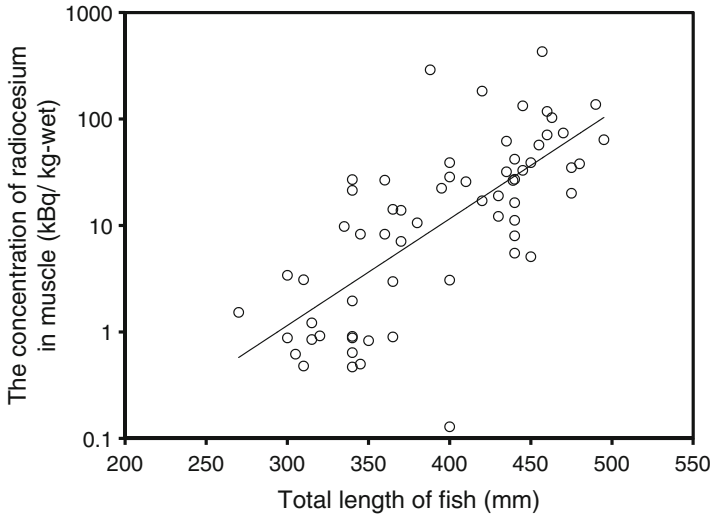

Fig. 14.5 Relationship between the total length of the fish and the concentration of radiocesium in muscles in fat greenling caught at the FNPP Port from February 25, 2013 to May 16, 2014

to catch prey at the time when extremely contaminated water was discharged into the FNPP Port. The amount of radiocesium that was once incorporated into the adult fish has been metabolized and excreted from the body; hence, the levels of radiocesium gradually decreased. In contrast, the concentration of radiocesium in young fish decreased more rapidly as the fish grew and the body mass increased. If the amount of radiocesium remains constant in the fish body, the concentration is reduced by half the initial value when the body mass of the fish doubles. The "growth effect" explains the low levels of radiocesium in small fat greenling (less than 300 mm during the sampling period) because they were very young in March 2011.

Acknowledgments We thank the staff of Tokyo Power Technology Co., Inc. for transporting the samples. This study was supported by the Fisheries Research Agency, Ministry of Agriculture, Forestry and Fisheries of Japan.

References

Buesseler KO (2012) Fishing for answers off Fukushima. Science 338:480–482

Fukushima Prefecture Fisheries Experimental Station (1974) Reports of stocks and habitat for selective fish living in fishing ground around northern part of the Pacific. No. 127 (in Japanese)

International Atomic Energy Agency (IAEA) (2004) Sediment distribution coefficients and concentration factors for biota in the marine environment. Technical report series no. 422. International Atomic Energy Agency, Vienna, p 95

Koulikov AO, Ryabov IN (1992) Specific cesium activity in freshwater fish and the size effect. Sci Total Environ 112:125–142

Ministry of Agriculture, Forestry and Fisheries (MAFF) (2013) Results of the inspection on radioactivity level in fisheries products. http://www.jfa.maff.go.jp/e/inspection/. Accessed 15 Sept 2014

Tokyo Electric Power Company (TEPCO) (2014) Results of radioactive analysis around Fukushima Daiichi Nuclear Power Station. http://www.tepco.co.jp/en/nu/fukushima-np/f1/smp/index-e.html. Accessed 15 Sept 2014

Part V
Freshwater Systems

Chapter 15
Comparison of the Radioactive Cesium Contamination Level of Fish and their Habitat Among Three Lakes in Fukushima Prefecture, Japan, After the Fukushima Fallout

Keishi Matsuda, Kaori Takagi, Atsushi Tomiya, Masahiro Enomoto, Jun-ichi Tsuboi, Hideki Kaeriyama, Daisuke Ambe, Ken Fujimoto, Tsuneo Ono, Kazuo Uchida, and Shoichiro Yamamoto

Abstract Levels of radiocesium ($^{134}Cs + {}^{137}Cs$) contamination in lake water, bottom sediment, plankton, and fish were investigated in three geographically separated lakes in Fukushima Prefecture (Lake Hayama, Lake Akimoto, and Lake Tagokura) between June 2012 and November 2013. Levels of contamination differed among the three lakes, with the highest levels in each measured component found in Lake Hayama, followed by Lake Akimoto, and the least contamination in Lake Tagokura. Among the lakes, the magnitude of contamination decreased with distance from the Fukushima Dai-ichi Nuclear Power Plant. Mean radiocesium concentrations were higher in piscivorous fish than in other fish, possibly reflecting differences in trophic levels. Radiocesium concentrations of the lake water, bottom sediment, plankton, and fish were significantly correlated with surface soil radiocesium content near lake sites.

K. Matsuda (✉) • J. Tsuboi • S. Yamamoto
National Research Institute of Aquaculture, Fisheries Research Agency,
2482-3 Chugushi, Nikko, Tochigi 321-1661, Japan
e-mail: matsukei@affrc.go.jp

K. Takagi
Marine Biological Research Institute of Japan Co., LTD,
4-3-16, Yutaka, Shinagawa, Tokyo 142-0042, Japan

A. Tomiya • M. Enomoto
Fukushima Prefectural Inland Water Fisheries Experimental Station,
3447-1, Inawashiro, Maya, Fukushima 969-3283, Japan

H. Kaeriyama • D. Ambe • K. Fujimoto • T. Ono
National Research Institute of Fisheries Sciences, Fisheries Research Agency,
2-12-4, Fukuura, Kanazawa, Yokohama, Kanagawa 236-8648, Japan

K. Uchida
Fisheries Research Agency, Yokohama, Kanagawa 220-6115, Japan

K. Nakata, H. Sugisaki (eds.), *Impacts of the Fukushima Nuclear Accident on Fish and Fishing Grounds*, DOI 10.1007/978-4-431-55537-7_15

Keywords Lake Hayama • Lake Akimoto • Lake Tagokura • Piscivorous fish • Radiocesium contamination • Trophic level

15.1 Introduction

Radiocesium is one of the major radioactive components of the fallout from the Fukushima Dai-ichi Nuclear Power Plant (FNPP). The total amount of ^{137}Cs discharged into the atmosphere between 12 March and 6 April 2011 was estimated as approximately 1.3×10^{16} Bq (Chino et al. 2011). Before 20 April 2011, 18 % of the total fallout settled on Japanese land (Stohl et al. 2012). Radiocesium monitoring of freshwater organisms (Fisheries Agency 2012) showed that trophic level is an important ecological factor affecting bioaccumulation of ^{137}Cs in fish (Mizuno and Kubo 2013). For example, in the Agano River basin in Fukushima, ^{137}Cs contamination of carnivorous salmonids was roughly twice that of the herbivore ayu *Plecoglossus altivelis* (Mizuno and Kubo 2013). However, levels of radiocesium contamination among individuals within conspecifics have also been found to differ among habitats (Iguchi et al. 2013; Mizuno and Kubo 2013; Yamamoto et al. 2014a), and the causes of these differences are uncertain.

The objective of this study was to investigate factors affecting the differences in concentrations of radiocesium (^{134}Cs + ^{137}Cs) in fish of three geographically separate lakes in Fukushima Prefecture (Fig. 15.1, Table 15.1). These three lakes are located at differing distances from the FNPP and have different air dose rates and radiocesium concentrations in the adjacent surface soil, but have roughly similar retention times (Table 15.1). Sampling of lake water, bottom sediment, plankton, and fish was conducted up to three times per year in spring, summer, and autumn from June 2012 to November 2013.

15.2 Contamination Levels of Lake Water, Bottom Sediment, and Plankton

In each lake, lake water was sampled from one site ($n = 1$), and plankton was sampled one time along a constant distance of the lake surface ($n = 1$) (Fig. 15.1). Bottom sediment samples were collected from one point in each lake during one sampling event ($n = 1$) (Fig. 15.1). Temporal changes in radiocesium concentrations of the lake water, bottom sediment, and plankton are shown in Fig. 15.2. In Lake Tagokura, radiocesium concentrations were not detected in the lake water from November 2012 to October 2013 (detection limits, <2.1 mBq l^{-1}), as was plankton in October 2013 (detection limit, 1,413 Bq kg^{-1} dry mass).

Among these ecosystem components, only the bottom sediment showed significant temporal changes, with a significant decreasing trend in Lake Hayama (Table 15.2; *t* test, $P < 0.05$) and a significant increasing trend in Lake Tagokura (Table 15.2; *t* test, $P < 0.05$). Continuing investigation is necessary to determine the patterns and temporal changes of radiocesium contamination in lake water and plankton.

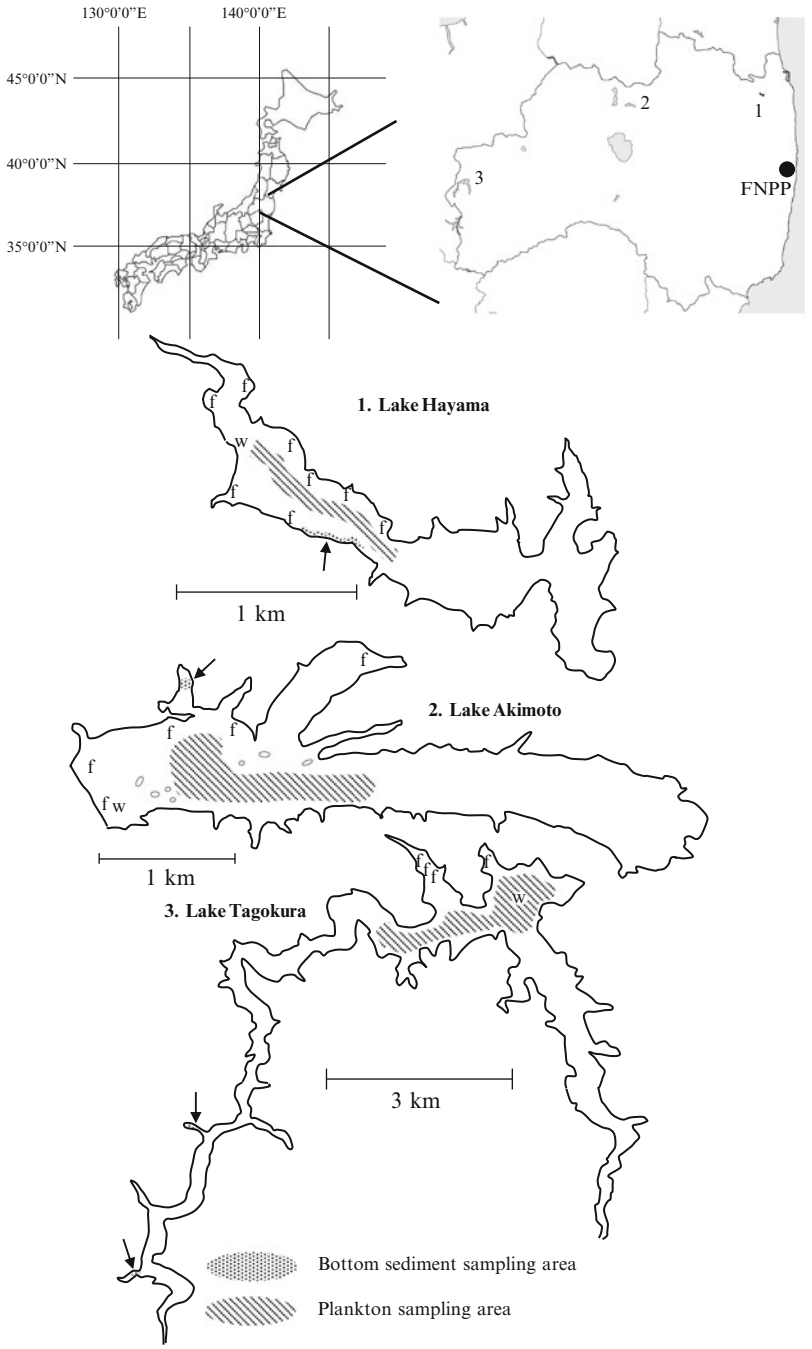

Fig. 15.1 *Upper figure* shows the locations of the study lakes and the Fukushima Dai-ichi Nuclear Power Plant (FNPP) in Fukushima Prefecture. *Lower* figure show the sampling sites in each of the lakes (*w* lake water sampling point, *f* fish sampling point). *Arrows* point to bottom sediment sampling points (Modified from Matsuda et al. 2015)

Table 15.1 Characteristics of the study lakes

	Unit	Hayama	Akimoto	Tagokura
Lake area	(km^2)	1.75	3.6	9.95
Volume	($10^3 \times m^3$)	36,200	32,800	494,000
Max depth	(m)	70	40	80
Altitude	(m)	175	736	515
Linear distance from FNPP[a]	(km)	39	85	157
Retention time[b]	(years)	0.48	0.26	0.31
Lake type		Artificial dam reservoir	Natural	Artificial dam reservoir
Air dose rates at lakeside[c]	($\mu Sv\ h^{-1}$)	2.88	0.57	0.12
Radiocesium contents of surface soil at lakeside[c]	($Bq\ m^{-2}$)	637,663	80,018	16,232

[a]Fukushima Dai-ichi Nuclear Power Plant
[b]Citation from Fukushima and Arai (2014)
[c]Air dose rates at 1-m height from the ground and radiocesium (^{134}Cs + ^{137}Cs) concentrations of surface soil (depth, 0–50 mm) on 6 June 2011 to 8 July 2011 (MEXT 2011) (Cited from Matsuda et al. 2015)

The order of contamination levels of lake water, bottom sediment, and plankton for the study period (2012–2013) in three lakes was Lake Hayama > Lake Akimoto > Lake Tagokura (Table 15.2).

15.3 Radiocesium Concentrations in Fish

Fish from Lake Hayama were analyzed individually, except for Japanese smelt (*Hypomesus nipponensis*); all other fish samples were analyzed from 2 to 103 pooled individuals. Temporal changes in radiocesium concentrations in several fish species in each lake are shown in Fig. 15.3. Significant decreasing trends of radiocesium concentrations in fish from 2012 to 2013 were observed for white-spotted char in Lake Tagokura; smallmouth bass in both Lake Hayama and Lake Akimoto; bluegill, Japanese dace, and crucian carp in Lake Hayama; and Japanese barbell in Lake Akimoto (Table 15.3; *t* tests for parametric groups or Mann–Whitney tests for nonparametric groups, $P < 0.05$). Radiocesium concentrations significantly decreased by 33 % to 65 % between 2012 and 2013 in these fish species (Table 15.3).

Considering only physical decay of radiocesium, the loss of radiocesium concentration in the fish on 20 June 2013 (the first sampling day on 2013) would have been expected to decrease by 9 % of that on 29 November 2012 (the last sampling day on 2012). Therefore, the radiocesium concentrations of crucian carp in Lake Tagokura might increase during the period between 2012 and 2013 without physical decay (Table 15.3). Fukushima and Arai (2014) also found that radiocesium concentrations in channel catfish (*Ictalurus punctatus*) and kokanee (*Oncorhynchus nerka*) increased between 2011 and 2013 in some lakes in northeastern Japan. The order of the contamination level in each fish species for the study period (2012–2013) among the three lakes was also Lake Hayama > Lake Akimoto > Lake Tagokura (Table 15.3).

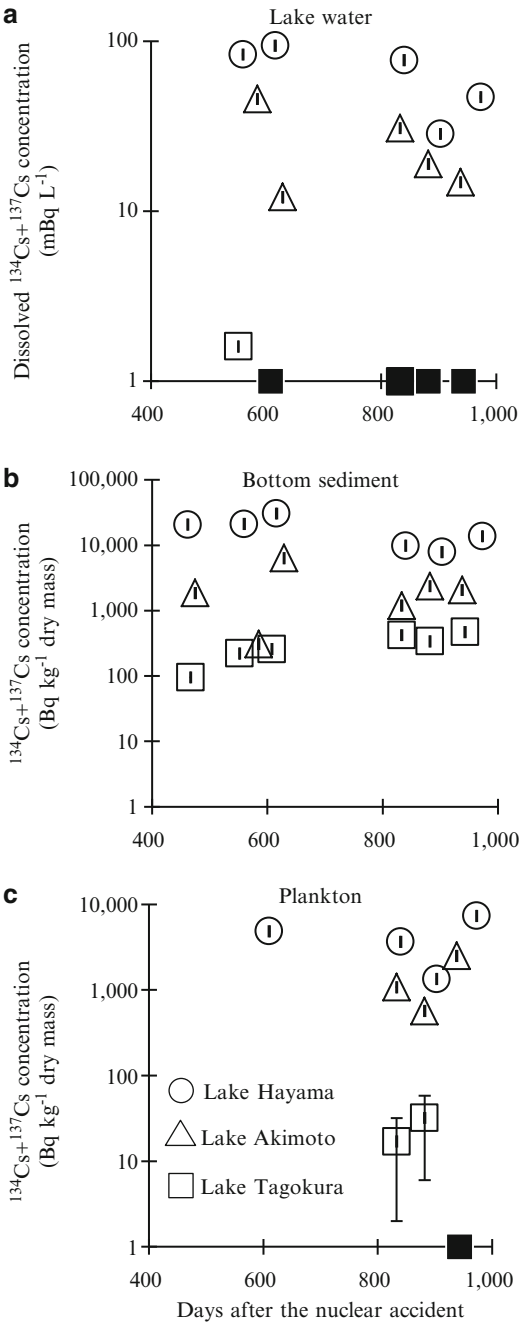

Fig. 15.2 Time-course of radiocesium ($^{134}Cs + ^{137}Cs$) concentrations in samples from each lake: lake water (**a**); bottom sediment (**b**); plankton (**c**). *Vertical bars* indicate 1 SD derived from counting statistics. Samples below detection limits are indicated by *closed squares* on the *x*-axis

Table 15.2 Mean radiocesium ($^{134}Cs + {}^{137}Cs$) concentrations of the water, bottom sediment, and plankton in each lake

Sample	Lake[a]	Mean radiocesium concentration ± SD[b] in 2012–2013	n[c]	(x) Mean radiocesium concentration ± SD[b] in 2012	n[c]	(y) Mean radiocesium concentration ± SD[b] in 2013	n[c]	Loss of radiocesium concentration in 2012–2013: $(1-y/x)\times 100$ (%)
Lake water (mBq l^{-1})	H	66.2 ± 27.4[a]	5	89	2	51 ± 25	3	43
	A	24.5 ± 13.9[b]	5	29	2	22 ± 8.3	3	25
	T	1.6 ± 0.4	1	1.6 ± 0.4	1	ND		
Bottom sediment (Bq kg^{-1} dry mass)	H	17,340 ± 8,519[a]	6	24,189 ± 5,636	3	10,491 ± 2,987	3	57*
	A	2,357 ± 2,091	6	2,841 ± 3,140	3	1,874 ± 607	3	34
	T	301 ± 138[b]	6	191 ± 85	3	410 ± 66	3	−114*
Plankton (Bq kg^{-1} dry mass)	H	4,295 ± 2,495	4	4,852 ± 78	1	4,109 ± 3,021	3	15
	A	1,383 ± 1,004	3			1,383 ± 1,004	3	
	T	25	2			25	2	

Significant difference between the 2012 period and 2013 period was examined by a t test. Asterisk of [Loss of the radiocesium concentration from 2012 to 2013] indicates significant difference between the x and the y ($P < 0.05$). These tests were conducted if there were more than two samples in both or all groups

[a]Lake: H = Hayama, A = Akimoto, T = Tagokura

[b]SD: If $n = 1$, SD is counting error (1 sigma)

[c]n: ND data were excluded. Significant differences among the lakes were examined by a t test (lake water) and by a Kruskal–Wallis test (bottom sediment and plankton). Different small letters following an entry indicates significant difference among the lakes ($P < 0.05$) (Modified from Matsuda et al. 2015)

15.4 Relationship Between Trophic Level and Radiocesium Concentration

Freshwater fish primarily accumulate radiocesium through the food chain rather than directly from the water (Williams and Pickering 1961; Hewett and Jefferies 1976; Yamamoto et al. 2014b). Species-specific food intake and food availability can cause differences in radiocesium concentrations among fish species. Because metals are concentrated in organisms as they are transferred up trophic levels by consumption, the trophic level of a fish is an important ecological factor affecting its concentration of radiocesium (Rowan and Rasmussen 1994). For example, after the Chernobyl accident in 1987, a higher annual mean concentration of ^{137}Cs has been detected in fish from higher trophic levels in some lakes of Finland, including perch (*Perca fluviatilis*) and pike (*Esox lucius*) (Rask et al. 2012).

Okino (2002) showed that fishes classified as piscivorous, including salmonid fishes, the Japanese catfish *Silurus asotus*, and the largemouth bass *Micropterus salmoides*, occupy the top of the food chain in temperate lakes in Japan. We also categorized fish into two groups: (1) piscivorous fish (the white-spotted char *Salvelinus leucomaenis pluvius*, Japanese catfish, the smallmouth bass *Micropterus*

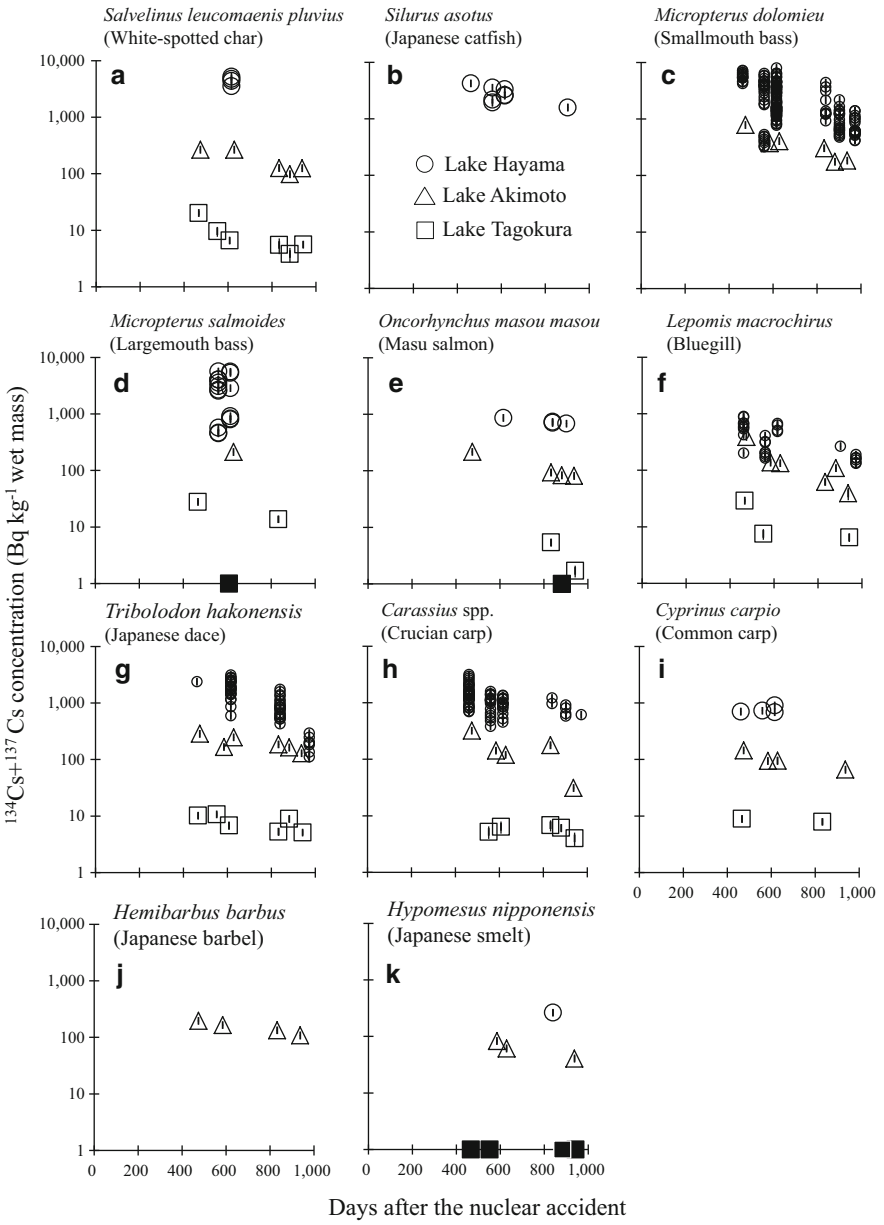

Fig. 15.3 Time-course of radiocesium ($^{134}Cs + {}^{137}Cs$) concentrations in fish from each lake. Concentrations in Lake Hayama are for individual samples except for *Hypomesus nipponensis*; all other values were measured from pooled samples. *Vertical bars* indicate 1 SD. Samples below detection limits are indicated by *closed squares* on the *x*-axis

Table 15.3 Mean radiocesium ($^{134}Cs + {}^{137}Cs$) concentrations of fish in each lake

Species (scientific name)	Lake[a]	Mean total length ± SD[b] (mm)	Mean radiocesium concentration ± SD[b] in 2012–2013	n[c]	(x) Mean radiocesium concentration ± SD[b] in 2012	n[c]	(y) Mean radiocesium concentration ± SD[b] in 2013	n[c]	Loss of the radiocesium concentration in 2012–2013: $(1-y/x)\times 100$ (%)
Salvelinus leucomaenis pluvius (Bq kg^{-1} wet mass)	H	440 ± 48	4,445 ± 704[a]	4	4,445 ± 704	4			
	A	283 ± 55	176 ± 83	5	266	2	116 ± 16	3	56
	T	328 ± 100	8.5 ± 6.0[b]	6	12 ± 7.2	3	5.0 ± 1.0	3	59*
Silurus asotus (Bq kg^{-1} wet mass)	H	491 ± 56	2,745 ± 893	8	2,911 ± 820	7	1,582 ± 18	1	46
	A								
	T								
Micropterus dolomieu (Bq kg^{-1} wet mass)	H	339 ± 77	2,534 ± 1,881[a]	174	3,111 ± 1,885	124	1,104 ± 799	50	65*
	A	298 ± 39	370 ± 223[b]	6	519 ± 228	3	220 ± 71	3	58*
	T								
Micropterus salmoides (Bq kg^{-1} wet mass)	H	375 ± 145	2,708 ± 1,882[a]	16	2,708 ± 1,882	16			
	A	278 ± 18	212 ± 4.2	1	212 ± 4.2	1			
	T	266 ± 65	23[b]	2	29 ± 6.3	1	14 ± 1.0	1	53
Oncorhynchus masou masou (Bq kg^{-1} wet mass)	H	323 ± 62	746 ± 80[a]	4	862 ± 10	1	707 ± 27	3	18
	A	275 ± 31	118 ± 66[b]	4	217 ± 7.8	1	86 ± 6.6	3	60
	T	348 ± 86	3.5[b]	2			3.5	2	
Lepomis macrochirus (Bq kg^{-1} wet mass)	H	123 ± 26	399 ± 236[a]	29	471 ± 227	22	172 ± 46	7	63*
	A	143 ± 36	145 ± 125[b]	6	219 ± 146	3	70 ± 36	3	68
	T	113 ± 45	14 ± 13[b]	3	18	2	6.5 ± 1.1	1	64

Tribolodon hakonensis (Bq kg^{-1} wet mass)	H	258 ± 64	1,338 ± 828[a]	56	1,960 ± 632	28	716 ± 440	28	63*
	A	235 ± 49	196 ± 58[b]	6	232 ± 61	3	159 ± 29	3	31
	T	181 ± 68	7.5 ± 2.7[b]	6	8.7 ± 3.1	3	6.4 ± 2.1	3	26
Carassius spp. (Bq kg^{-1} wet mass)	H	367 ± 62	1,216 ± 556[a]	78	1,255 ± 564	71	817 ± 230	7	35*
	A	161 ± 99	158 ± 106[b]	5	194 ± 110	3	104	2	46
	T	224 ± 57	5.7 ± 1.1[b]	5	5.8	2	5.6 ± 1.5	3	3
Cyprinus carpio (Bq kg^{-1} wet mass)	H	704 ± 52	753 ± 100[a]	4	753 ± 100	4			
	A	433 ± 230	100 ± 33[b]	4	111 ± 29	3	66 ± 3.6	1	41
	T	658 ± 139	8.4[b]	2	8.9 ± 1.2	1	7.9 ± 0.9	1	11
Hemibarbus barbus (Bq kg^{-1} wet mass)	H								
	A	426 ± 73	150 ± 38	4	180	2	121	2	33*
	T								
Hypomesus nipponensis (Bq kg^{-1} wet mass)	H	92 ± 1	263 ± 31	1			263 ± 31	1	
	A	98 ± 12	62 ± 21	3	72	2	41 ± 5.0	1	44
	T	74 ± 10	ND		ND		ND		

Significant difference between the 2012 period and 2013 period was examined by a *t* test or a Mann–Whitney test. *Asterisk* of [Loss of the radiocesium concentration from 2012 to 2013] indicates significant difference between the *x* and the *y* ($P<0.05$). These tests were conducted if there were more than two samples in both or all groups

[a]Lake: *H* Hayama, *A* Akimoto, *T* Tagokura

[b]SD: In $n=1$, *SD* is counting error (1 sigma)

[c]*n ND* data were excluded. Significant differences among the lakes were examined by a Mann–Whitney test (smallmouth bass and largemouth bass), by a one-way ANOVA, or by a Kruskal–Wallis test (white-spotted char, masu salmon, bluegill, Japanese dace, crucian carp, and common carp). Different *small letters* following numbers indicates significant difference among the lakes ($P<0.05$) (Cited from Matsuda et al. 2015)

Table 15.4 Mean radiocesium (^{134}Cs + ^{137}Cs) concentrations of each fish group in each lake during the study period (2012–2013)

	Bq kg^{-1} wet mass ± SD			
	Piscivorous fish	n^a	Other fish	n^a
Lake Hayama	2,636 ± 1,311[a]	5	794 ± 478[b]	5
Lake Akimoto	219 ± 108	4	135 ± 47	6
Lake Tagokura	12 ± 10	3	9.0 ± 3.7	4

[a]*n*: ND data were excluded. Significant differences between piscivorous fish and others were examined by a *t* test. Different small letters after number entries indicates significant difference ($P < 0.05$) (Cited from Matsuda et al. 2015)

dolomieu, largemouth bass, and masu salmon *Oncorhynchus masou*); (2) other fish (the bluegill *Lepomis macrochirus*, the Japanese dace *Tribolodon hakonensis*, the crucian carp *Carassius* spp., the common carp *Cyprinus carpio*, the Japanese barbel *Hemibarbus barbus*, and Japanese smelt). We found that the mean radiocesium concentration in piscivorous fish was significantly higher than in other types of fish only in Lake Hayama during the study period (2012–2013) (Table 15.4; *t* test, $P < 0.01$).

15.5 Geographic Differences in Levels of Radiocesium Contamination

The FNPP fallout was the source of radiocesium in freshwater fish and in lake water, bottom sediment, and plankton. Therefore, correlations between radiocesium concentrations in each of these lake ecosystem components and concentrations in lakeside surface soil were analyzed. Soil samples were taken at a 0- to 50-mm depth on the lakeside of each lake between 6 June and 8 July 2011 (MEXT 2011). The radiocesium concentrations of surface soil on each lakeside (MEXT 2011) are shown in Table 15.1. Significant correlations were found between surface soil radiocesium content and that of lake water ($R^2 = 0.590$, $P < 0.01$), bottom sediment ($R^2 = 0.729$, $P < 0.001$), plankton ($R^2 = 0.555$, $P < 0.01$), and all fish ($R^2 = 0.273$–0.971, $P < 0.01$) (Fig. 15.4).

Thus, the differences in radiocesium concentrations in the lake samples likely reflect the quantity of radiocesium from the FNPP that was deposited at each lake. A previous report found a strong relationship between the distance from the FNPP and the radiocesium concentrations in freshwater fish (Mizuno and Kubo 2013). A similar relationship was observed in the present study, where the quantity of radiocesium deposited in lakeside soil decreased with distance from the FNPP. However, this relationship has not been found in all of northeastern Japan because the pollution did not spread concentrically from the FNPP. For example, Lake Chuzenji (located southwest of the FNPP) and Lake Tagokura are both located roughly 160 km from the FNPP in linear distance, but radiocesium concentrations in the

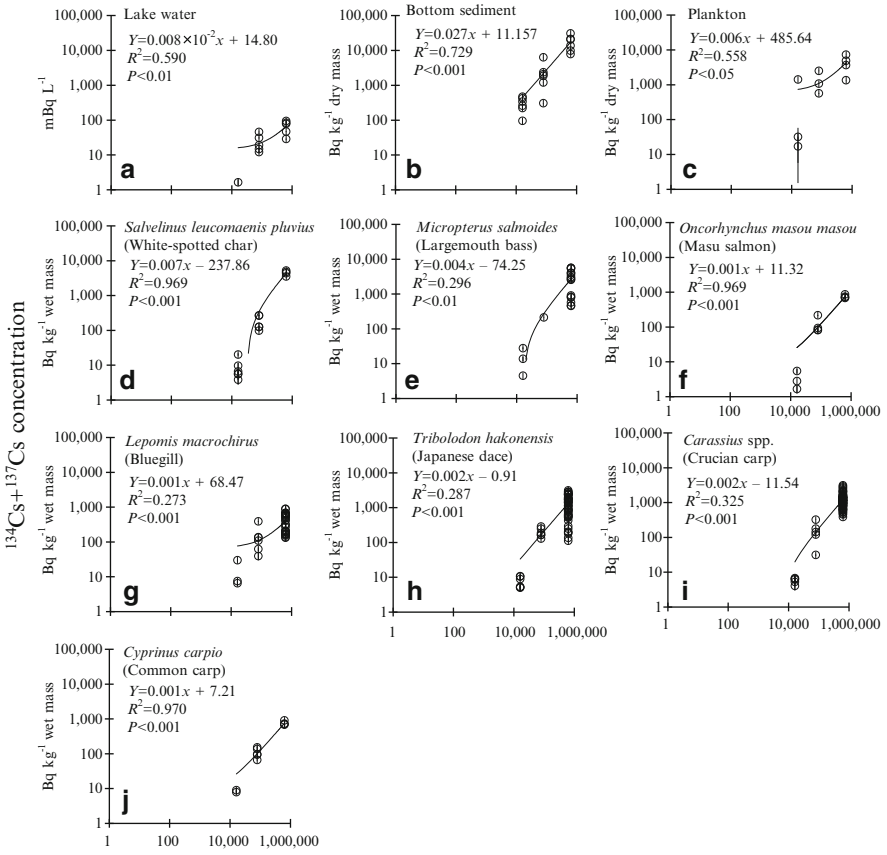

Fig. 15.4 Correlations between the mean radiocesium concentrations ($^{134}Cs + ^{137}Cs$) in each lake sample taken during the study period (2012–2013) and those of the surface soil taken at a 0- to 50-mm depth on each lakeshore between 6 June and 8 July 2011 (MEXT 2011). *Vertical bars* indicate 1 SD. *Solid lines* show significant fitted regression lines (Cited from Matsuda et al. 2015)

muscle of salmonids in 2012 were 142.9–249.2 Bq kg^{-1} wet mass in Lake Chuzenji and only 12 Bq kg^{-1} wet mass in Lake Tagokura (Yamamoto et al. 2014a).

In addition, there is some evidence that different levels of radiocesium contamination of fish among lakes can also be caused by variation in retention time (Fukushima and Arai 2014), depth (Broberg et al. 1995), lake water hardness and conductivity (Hakanson et al. 1992; Särkkä et al. 1995), suspended sediment concentration, and temperature (Rowan and Rasmussen 1994).

In addition to continuing to measure levels of radiocesium contamination in these lakes, future studies are needed to determine the factors underlying continued contamination and the retention of radiocesium in these lakes.

Acknowledgments This chapter was adapted from a paper published by Matsuda et al. (2015). The authors are grateful to Masato Murakami, Tomoko Okazaki, and Maki Yoshida for their assistance with the sample assays and data analyses. They also thank Kaoru Nakata for critical review of the manuscript. This study was supported by the Fisheries Agency, Ministry of Agriculture, Forestry and Fisheries, Japan.

References

Broberg A, Malmgren L, Jansson M (1995) Relations between resuspension and the content of ^{137}Cs in freshwater fish in some Swedish lakes. J Aquat Ecosyst Health 4:285–294

Chino M, Nakayama H, Nagai H, Terada H, Katata G, Yamazawa H (2011) Preliminary estimation of release amounts of ^{131}I and ^{137}Cs accidentally discharged from the Fukushima Daiichi Nuclear Power Plant into the atmosphere. J Nucl Sci Technol 48:1129–1134

Fisheries Agency (2012) Results of the inspection on radioactivity materials in fisheries products. http://www.jfa.maff.go.jp/e/inspection/index.html. Accessed 3 June 2014

Fukushima T, Arai H (2014) Radiocesium contamination of lake sediments and fish following the Fukushima nuclear accident and their partition coefficient. Inland Waters 4:204–214

Hakanson L, Andersson T, Nilsson A (1992) Radioactive caesium in fish in Swedish lakes 1986–1988: general pattern related to fallout and lake characteristics. J Environ Radioact 15:207–229

Hewett CJ, Jefferies DF (1976) The accumulation of radioactive caesium from water by the brown trout (*Salmo trutta*) and its comparison with plaice and rays. J Fish Biol 9:479–489

Iguchi K, Fujimoto K, Kaeriyama H, Tomiya A, Enomoto M, Abe S, Ishida T (2013) Cesium-137 discharge into the freshwater fishery ground of grazing fish, ayu *Plecoglossus altivelis*, after the March 2011 Fukushima nuclear accident. Fish Sci 79:983–988

Matsuda K, Takagi K, Tomiya A, Enomoto M, Tsuboi J, Kaeriyama H, Ambe D, Fujimoto K, Ono T, Uchida K, Morita T, Yamamoto S (2015) Fisheries Science. doi:10.1007/s12562-015-0874-7

Ministry of Education, Culture, Sports, Science and Technology (2011) Nuclide analysis of the soil. http://www.mext.go.jp/b_menu/shingi/chousa/gijyutu/017/shiryo/icsFiles/afieldfile/2011/09/02/1310688_1.pdf. Accessed 3 June 2014 (in Japanese)

Mizuno T, Kubo H (2013) Overview of active cesium contamination of freshwater fish in Fukushima and Eastern Japan. Sci Rep 3:1742

Okino T (2002) Ecosystem of lake. Kyoritsu Shuppan, Tokyo (in Japanese)

Rask M, Saxen R, Ruuhijarvi J, Arvola L, Jarvinen M, Koskelainen U, Outola I, Vuorinen PJ (2012) Short- and long-term patterns of Cs-137 in fish and other aquatic organisms of small forest lakes in southern Finland since the Chernobyl accident. J Environ Radioact 103:41–47

Rowan DJ, Rasmussen JB (1994) Bioaccumulation of radiocesium by fish: the influence of physicochemical factors and trophic structure. Can J Fish Aquat Sci 51:2388–2410

Särkkä J, Jämsä A, Luukko A (1995) Chernobyl-derived radiocaesium in fish as dependent on water quality and lake morphometry. J Fish Biol 46:227–240

Stohl A, Seibert P, Wotawa G, Arnold D, Burkhart JF, Eckhardt S, Tapia C, Vargas A, Yasunari TJ (2012) Xenon-133 and caesium-137 releases into the atmosphere from the Fukushima Dai-ichi nuclear power plant: determination of the source term, atmospheric dispersion, and deposition. Atmos Chem Phys 12:2313–2343

Williams LG, Pickering Q (1961) Direct and food-chain uptake of cesium 137 and strontium 85 in bluegill fingerlings. Ecology 42:205–206

Yamamoto S, Yokoduka T, Fujimoto K, Takagi K, Ono T (2014a) Radiocesium concentrations in the muscle and eggs of salmonids from Lake Chuzenji, Japan, after the Fukushima fallout. J Fish Biol 84:1607–1613

Yamamoto S, Mutou K, Nakamura H, Miyamoto K, Uchida K, Takagi K, Fujimoto K, Kaeriyama H, Ono T (2014b) Assessment of radiocaesium accumulation by hatchery-reared salmonids after the Fukushima nuclear accident. Can J Fish Aquat Sci 71:1772–1775

Chapter 16
Radiocesium Concentrations and Body Size of Freshwater Fish in Lake Hayama 1 Year After the Fukushima Dai-Ichi Nuclear Power Plant Accident

Kaori Takagi, Shoichiro Yamamoto, Keishi Matsuda, Atsushi Tomiya, Masahiro Enomoto, Yuya Shigenobu, Ken Fujimoto, Tsuneo Ono, Takami Morita, Kazuo Uchida, and Tomowo Watanabe

Abstract We measured radiocesium ($^{134}Cs + {}^{137}Cs$) concentrations in five freshwater fish species in Lake Hayama, Fukushima Prefecture, 1 year after the Fukushima Dai-ichi Nuclear Power Plant (FNPP) accident in March 2011. The five species included bluegill (*Lepomis macrochirus*), *Carassius* spp. (*Carassius auratus langsdorfii* and *Carassius cuvieri*), Japanese dace (*Tribolodon hakonensis*), largemouth bass (*Micropterus salmoides*), and smallmouth bass (*Micropterus dolomieu*). We observed a "positive size effect" for radiocesium concentrations in fish muscle, but the coefficient of determination was low for bluegill, *Carassius* spp., and Japanese dace. In contrast, the coefficient of determination was high for the exponential relationship between body size and radiocesium concentrations in largemouth and smallmouth

K. Takagi (✉)
Marine Biological Research Institute of Japan Co., LTD,
4-3-16, Yutaka, Shinagawa, Tokyo 142-0042, Japan

S. Yamamoto • K. Matsuda
National Research Institute of Aquaculture, Fisheries Research Agency,
2482-3 Chugushi, Nikko, Tochigi 321-1661, Japan
e-mail: ysho@affrc.go.jp

A. Tomiya • M. Enomoto
Fukushima Prefectural Inland Water Fisheries Experimental Station,
3447-1, Inawashiro, Maya, Fukushima 969-3283, Japan

Y. Shigenobu • K. Fujimoto • T. Ono • T. Morita
National Research Institute of Fisheries Sciences, Fisheries Research Agency,
2-12-4, Fukuura, Kanazawa, Yokohama, Kanagawa 236-8648, Japan

K. Uchida
Fisheries Research Agency, 2-3-3, Minatomirai, Nishi, Yokohama, Kanagawa 220-6115, Japan

T. Watanabe
Tohoku National Fisheries Research Institute, Fisheries Research Agency,
3-27-5, Shinhama, Shiogama, Miyagi 985-0001, Japan
e-mail: wattom@affrc.go.jp

K. Nakata, H. Sugisaki (eds.), *Impacts of the Fukushima Nuclear Accident on Fish and Fishing Grounds*, DOI 10.1007/978-4-431-55537-7_16

bass. The geometric mean radiocesium concentration in each body size class was generally higher for carnivorous fish than for omnivorous and herbivorous fish.

Keywords Bluegill • *Carassius* spp. • Japanese dace • Largemouth bass • Nuclear accident • Positive size effect • Radiocesium concentration • Smallmouth bass

16.1 Introduction

The Fukushima Dai-ichi Nuclear Power Plant (FNPP) accident released a large concentration of nuclides, including ^{131}I, ^{134}Cs, and ^{137}Cs, into the atmosphere (Butler 2011; Chino et al. 2011). The Tokyo Electric Power Co. (2012) estimated the total amount of ^{131}I, ^{134}Cs, and ^{137}Cs released during March 2011 to be approximately 500 PBq, approximately 10 PBq, and approximately 10 PBq, respectively. Because the half-life of ^{137}Cs is relatively long (30.2 years), contamination of the ecosystem is expected to be long lasting. Following the Chernobyl nuclear power plant accident, research showed that the chemical composition of the water (e.g., potassium levels) and the rate of circulation or turnover of water in freshwater systems affects the bioaccumulation of radiocesium in fish (Elliot et al. 1992; Saxén and Koskelainen 1992; Rask et al. 2012). In addition to these environmental factors, fish body size is often correlated with radiocesium concentrations in fish (Elliot et al. 1992; Koulikov and Ryabov 1992; Smith et al. 2002). Fish body size may be a proxy for age and life stage, with the latter being associated with differences in traits such as feeding ecology and metabolism. The excretion rates for radiocesium are higher in younger age groups than in older age classes. Furthermore, the decrease in radiocesium concentrations in water over time also results in lower radiocesium levels in younger fish (Kryshev and Ryabov 2000). Under these conditions, it is likely that radiocesium levels in fish will be a positive function of size.

As described in Chapter 15, the Fisheries Research Agency has conducted radiocesium monitoring of freshwater fish, lake water, sediment, and plankton in three lakes (Lake Akimoto, Lake Tagokura, and Lake Hayama) in Fukushima Prefecture since 2012. Lake Hayama (Fig. 16.1), the lake nearest to the FNPP among the three lakes, is a small artificially dammed lake (~60 m maximum depth, 36.2×106 m^3 gross capacity of reservoir) in the Mano River system. This lake is located within a 30–50 km radius of the FNPP. The lake is also located in the area that was subject to high levels of radiocesium deposition (~300–600 kBq/m^2) in the period to 28 June 2012 (Ministry of Environment 2012a) as it was in the pathway of the radioactive plume from the FNPP. Indeed, Lake Hayama received the highest deposition of radiocesium among the lakes that are locally important for recreational fishing.

The concentration of radiocesium decreased in the water of Lake Hayama between the accident and 2012 (Chap. 15). Thus, we hypothesized that there would be a positive relationship between radiocesium concentrations in fish and fish body size in Lake Hayama. To test this, we measured radiocesium concentrations in individuals from the five dominant species in Lake Hayama in 2012, including bluegill (*Lepomis macrochirus*), *Carassius* spp. (*Carassius auratus langsdorfii* and *Carassius cuvieri*), Japanese dace (*Tribolodon hakonensis*), largemouth bass (*Micropterus salmoides*), and smallmouth bass (*Micropterus dolomieu*).

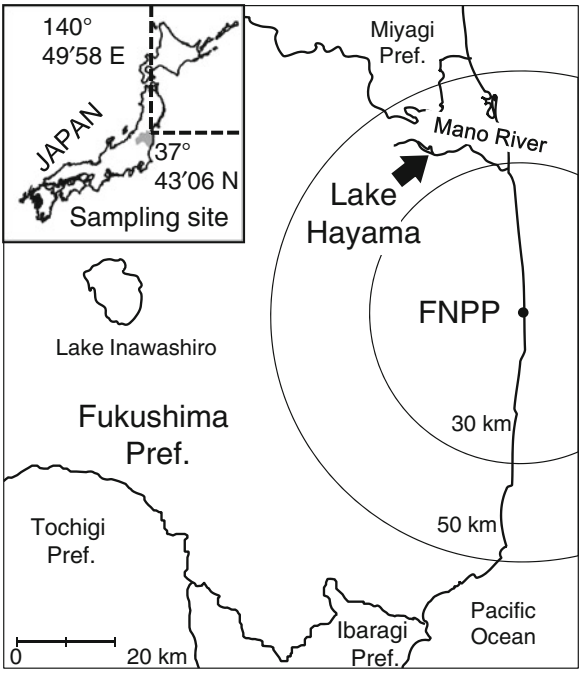

Fig. 16.1 Location of collection sites in Lake Hayama

16.2 Fish Species and Lake Water

The five dominant fish species in Lake Hayama (bluegill, *Carassius* spp., Japanese dace, largemouth bass, and smallmouth bass) were collected by gillnet during 2012 (see Chapter 15). Bluegill, largemouth bass, and smallmouth bass are invasive species. These three species have been observed in lakes and rivers in Fukushima Prefecture since the 1990s. Smallmouth bass were the most dominant species in our surveys in 2012. Largemouth bass and smallmouth bass are carnivorous whereas bluegill, *Carassius* spp., and Japanese dace are omnivorous, and *Carassius* spp. is also herbivorous. Although there are few biological data for Lake Hayama, the five species we collected typically live for several years, so it is likely that some of the fish we collected were exposed to the fallout at the time of the accident in 2011.

The environmental characteristics of Lake Hayama are described in Chapter 15. The concentration of radiocesium in the surface water of Lake Hayama was 89 mBq/l from September to November 2012 (Table 15.2). According to the Ministry of Environment (2011), ^{134}Cs and ^{137}Cs levels had declined to less than 1 Bq/l by September 2011 in the surface water of Lake Hayama whereas levels at the bottom of the lake were 10 and 12 Bq/l, respectively, at this time. From August to November 2012, levels of ^{134}Cs and ^{137}Cs decreased to less than 2 Bq/l and less than 3 Bq/l, respectively, in the water immediately above the lake bed (Ministry of Environment 2012b, 2013a). Thus, radiocesium concentrations decreased rapidly in the water of Lake Hayama during the first year after the fallout.

16.3 "Positive Size Effect" on Radiocesium Concentrations in Five Freshwater Fish Species

The total length (TL) distribution for the five fish species is shown in Fig. 16.2. The TL of bluegill, *Carassius* spp., and Japanese dace ranged from 86 to 163 mm, 217 to 461 mm, and 220 to 374 mm, respectively (Fig. 16.2). Both largemouth and smallmouth bass had a wider range of TL, 80–545 mm and 79–457 mm, respectively (Fig. 16.2). Because we used gill nets to capture fish, it is likely that small *Carassius* spp. and Japanese dace (TL < 200 mm) were not captured. Conversely, small bluegill, smallmouth bass, and largemouth bass have a high body height so are

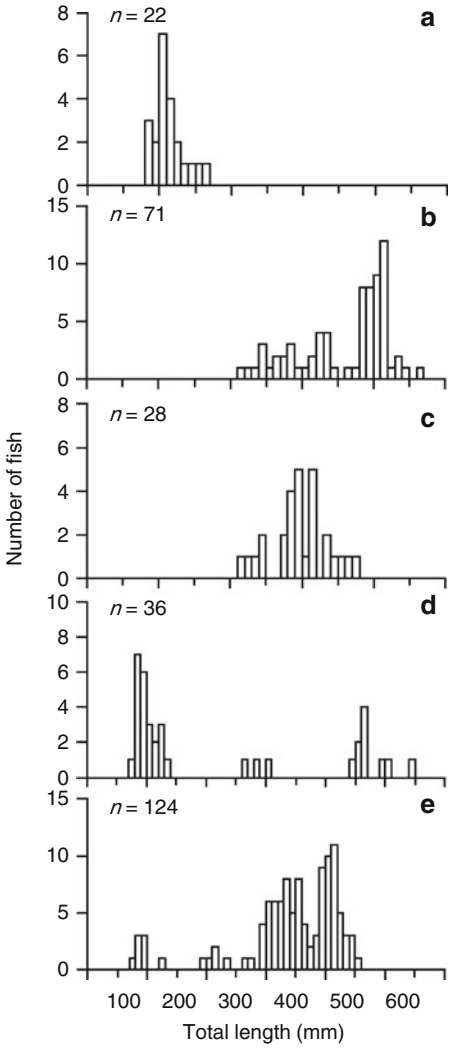

Fig. 16.2 Total length (TL, mm) distribution for bluegill (**a**), *Carassius* spp. (**b**), Japanese dace (**c**), largemouth bass (**d**), and smallmouth bass (**e**)

more susceptible to capture in our gill nets. The small-sized *Carassius* spp. and Japanese dace represent younger fish including age 0 and 1 (Suzuki and Kimura 1977; Liu et al. 1986; Ishizaki et al. 2009).

Judging from our data and the information of age and growth for largemouth and smallmouth bass (Yodo and Kimura 1996; Nakamura et al. 2004), we assume that the samples of these two species included age 0 and older fish. The bluegill we captured were likely older than age 0, although their growth varies considerably with population size structure (Drake et al. 1997; Belk 1995). Taken together, these observations suggest that we obtained both age 0 and older fish only for largemouth and smallmouth bass.

The radiocesium ($^{134}Cs + {}^{137}Cs$) concentrations were generally lower in smaller fish than in larger fish (Fig. 16.3). The natural log of radiocesium concentrations

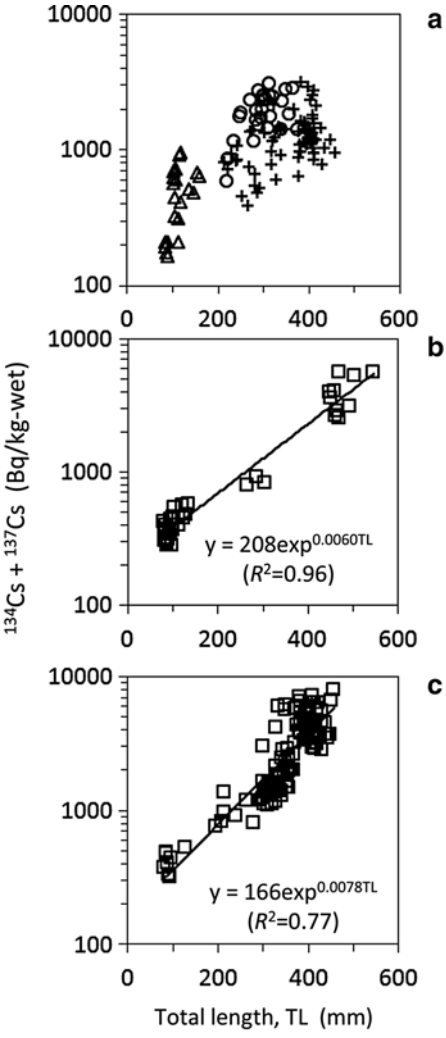

Fig. 16.3 Relationship between total length (TL) of fish and radiocesium ($^{134}Cs + {}^{137}Cs$) concentrations for bluegill (*open triangles*), *Carassius* spp. (*crosses*), and Japanese dace (*open circles*) (**a**), largemouth bass (**b**), and smallmouth bass (**c**). There was an exponential relationship between radiocesium concentrations and TL in largemouth bass (**b**) and smallmouth bass (**c**)

were positively but poorly correlated with TL for bluegill ($R^2 = 0.30$, $p < 0.01$), *Carassius* spp. ($R^2 = 0.23$, $p < 0.01$), and Japanese dace ($R^2 = 0.30$, $p < 0.01$), species for which we were unable to collect younger fish. Conversely, we observed a strong positive exponential correlation between TL and radiocesium concentrations in largemouth bass ($R^2 = 0.96$, $p < 0.01$) and smallmouth bass ($R^2 = 0.77$, $p < 0.01$) (Fig. 16.3).

16.4 Influence of Diet on Radiocesium Concentrations in Freshwater Fish

Both younger and older fish are needed to detect the positive size effect described by Kryshev and Ryabov (2000). We found evidence for a positive size effect in carnivorous bass, the only species for which we were able to obtain both young and old individuals. We compared the radiocesium levels in fish from different trophic positions, although we only collected older individuals from omnivorous and herbivorous species.

The geometric mean radiocesium concentrations by body size class (interval of 100 mm TL) for each species are given in Table 16.1. The geometric mean radiocesium concentration in each size class ($n > 2$) was higher for carnivorous fish than for omnivorous or herbivorous fish, suggesting that trophic position is an important determinant of species-specific concentrations. Only two exceptions to this pattern were observed, in bluegill in the 100 mm < TL ≤ 200 mm size class, and in Japanese dace in the 200 mm < TL ≤ 300 mm size class. Such exceptions may be a function of different life stages; adult (older) omnivorous and herbivorous fish have higher levels than younger carnivorous fish.

We speculate that the larger largemouth and smallmouth bass individuals, which had relatively high radiocesium concentrations, were adults at the time the FNPP accident occurred. These individuals have likely preyed continuously upon radiocesium-contaminated insects and fishes since the time of the accident. Because of their low rate of metabolism, much of the radiocesium was retained within their body during the year following the fallout. In contrast, smaller bass (≤200 mm TL) were likely juveniles (1 year old or younger), larvae, eggs, or did not exist at the time of the FNPP accident. Even if these younger individuals consumed highly contaminated prey items after the fallout from the FNPP, they would still likely have lower radiocesium concentrations than older fish because of their high metabolic rate and dilution resulting from tissue growth.

The radiocesium concentrations in fish were variable, but generally high in the diet items of omnivorous and herbivorous fish, such as bluegill, *Carassius* spp., and Japanese dace in 2012. Radiocesium concentrations in Spirogyra and aquatic insects fluctuated from 94 to 1,870 Bq/kg wet weight and from 92 to 1,100 Bq/kg wet weight, respectively (Ministry of Environment 2012c, 2013b, c, d). Thus, the concentration of radiocesium in Spirogyra was as high as in small fish (≤200 mm TL) in our study (Table 16.1). Given this, even herbivorous *Carassius* spp. are susceptible to radiocesium.

Table 16.1 Geometric mean radiocesium (Cs: $^{134}Cs + ^{137}Cs$) concentration (Bq/kg-wet) ± geometric standard deviation (δ) for each fish species by fish body size class

	Bluegill	*Carassius* spp.	Japanese dace	Largemouth bass	Smallmouth bass
Total length (TL, mm)	Geometric mean Cs (Bq/kg-wet) ± δ (n)	Geometric mean Cs (Bq/kg-wet) ± δ (n)	Geometric mean Cs (Bq/kg-wet) ± δ (n)	Geometric mean Cs (Bq/kg-wet) ± δ (n)	Geometric mean Cs (Bq/kg-wet) ± δ (n)
$0 < TL \leq 100$	188 ± 1.1 (5)	–(0)	–(0)	340 ± 1.2 (14)	404 ± 1.2 (7)
$100 < TL \leq 200$	537 ± 1.5 (17)	–(0)	–(0)	470 ± 1.2 (9)	639 ± 1.3 (2)
$200 < TL \leq 300$	–(0)	730 ± 1.5 (15)	1,670 ± 1.5 (16)	849 ± 1.1 (2)	1,220 ± 1.5 (10)
$300 < TL \leq 400$	–(0)	1,250 ± 1.4 (30)	2,110 ± 1.3 (12)	826 (1)	2,510 ± 1.8 (69)
$400 < TL \leq 500$	–(0)	1,360 ± 1.4 (26)	–(0)	3,440 ± 1.3 (8)	1,360 ± 1.4 (36)
$500 < TL \leq 600$	–(0)	–(0)	–(0)	5,450 ± 1.0 (2)	–(0)
Total	423 ± 1.8 (22)	1,150 ± 1.5 (71)	1,850 ± 1.5 (28)	776 ± 2.8 (36)	1,150 ± 1.5 (124)

Lake Hayama was located in the zone of high radiocesium deposition, so fish are likely exposed to radiocesium from the surrounding forest ecosystem. Compared with European forests, the forests in Japan experience a warmer climate with higher mean annual precipitation. These differences make it likely that Japanese forests will circulate radiocesium deposited by the FNPP accident more rapidly than did the European forests following the Chernobyl accident (Hashimoto et al. 2013). Indeed, the levels of radiocesium in trees dropped rapidly during the first 2 years after the fallout, but radiocesium in the soil surface organic layer and soil surface layer (0–5 cm) components kept the same level during 2012–2013 (Forestry Agency 2014). During this period, fish in Lake Hayama were likely exposed to radiocesium from the organic components of the surrounding forest through the food web. Further monitoring of radiocesium concentrations in fish (including information on body size and age) is needed to predict the long-term dynamics of radiocesium concentrations in fish.

Acknowledgments This chapter was written based on Takagi et al. (accepted).

References

Belk MC (1995) Variation in growth and maturity in bluegill sunfish: genetic or environmental effects? J Fish Biol 47:237–247

Butler D (2011) Radioactivity spreads in Japan. Nature (Lond) 471:555–556

Chino M, Nakayama H, Nagai H, Terada H, Katata G, Yamazawa H (2011) Preliminary estimation of release amounts of ^{131}I and ^{137}Cs accidentally discharged from the Fukushima Daiichi nuclear power plant into the atmosphere. J Nucl Sci Technol 48:1129–1134

Drake MT, Claussen JE, Philipp DP, Pereira DL (1997) A comparison of bluegill reproductive strategies and growth among lakes with different fishing intensities. N Am J Fish Manag 17:496–507

Elliot JM, Hilton J, Rigg E, Tullett PA, Swift DJ, Leonard DRP (1992) Sources of variation in post-Chernobyl radiocaesium in fish from two Cumbrian lakes (northwest England). J Appl Ecol 29:108–119

Forestry Agency (2014) The results of distribution survey of radioactive materials in the forest [fiscal year 2013] (1 Apr 2014). Available via http://www.rinya.maff.go.jp/j/press/ken_sidou/140401.html. Accessed 17 Nov 2014 (in Japanese)

Hashimoto S, Matsuura T, Nakano K, Linkov I, Shaw G, Kaneko S (2013) Predicted spatiotemporal dynamics of radiocesium deposited onto forests following the Fukushima nuclear accident. Sci Rep 3:2564. doi:10.1038/srep02564

Ishizaki D, Otake T, Sato T, Yodo T, Yoshioka M, Kashiwagi M (2009) Use of otolith microchemistry to estimate the migratory history of Japanese dace *Tribolodon hakonensis* in the Kamo River, Mie Prefecture. Nippon Suisan Gakkaishi 75:419–424 (in Japanese)

Koulikov AO, Ryabov IN (1992) Specific cesium activity in freshwater fish and the size effect. Sci Total Environ 112:125–142

Kryshev AI, Ryabov IN (2000) A dynamic model of ^{137}Cs accumulation by fish of different age classes. J Environ Radioact 50:221–233

Liu H, Shimazaki K, Mishima S (1986) Biological studies on Ugui-dace *Tribolodon hakonensis* (Günter) in the Ohno River, Hokkaido, Japan: I. Early development and character of scales different locations. Bull Fac Fish Hokkaido Univ 37:23–29

Ministry of Environment, Government of Japan (2011) The results of radioactive material monitoring of the surface water bodies within Fukushima prefecture (November 15, 2011). Available via http://www.env.go.jp/en/water/rmms/surveys.html. Accessed 7 Nov 2014

Ministry of Environment, Government of Japan (2012a) Extension site of distribution map of radiation dose, etc.,/Digital Japan. Available via http://ramap.jmc.or.jp/map/eng/map.html. Accessed 7 Nov 2014

Ministry of Environment, Government of Japan (2012b) The results of radioactive material monitoring of the surface water bodies within Fukushima prefecture (July–September samples). Available via http://www.env.go.jp/en/water/rmms/surveys.html. Accessed 7 Nov 2014

Ministry of Environment, Government of Japan (2012c) The results of radioactive material monitoring surveys of aquatic organisms (2012 spring samples). Available via http://www.env.go.jp/en/water/rmms/result_ao02-part.html. Accessed 7 Nov 2014

Ministry of Environment, Government of Japan (2013a) The results of radioactive material monitoring of the surface water bodies within Fukushima Prefecture (September–November samples) (January 10, 2013). Available via http://www.env.go.jp/en/water/rmms/surveys.html. Accessed 7 Nov 2014

Ministry of Environment, Government of Japan (2013b) The results of radioactive material monitoring surveys of aquatic organisms (2012 summer samples). Available via http://www.env.go.jp/en/water/rmms/result_ao02-part.html. Accessed 7 Nov 2014

Ministry of Environment, Government of Japan (2013c) The results of radioactive material monitoring surveys of aquatic organisms (2012 fall samples). Available via http://www.env.go.jp/en/water/rmms/result_ao02-part.html. Accessed 7 Nov 2014

Ministry of Environment, Government of Japan (2013d) The results of radioactive material monitoring surveys of aquatic organisms (2012 winter samples). Available via http://www.env.go.jp/en/water/rmms/result_ao02-part.html. Accessed 7 Nov 2014

Nakamura T, Katano O, Yamamoto S (2004) Effect of water flow and water temperature on the growth of smallmouth bass *Micropter duoslomiez* and largemouth bass *M. almoides*. Nippon Suisan Gakkaishi 70:745–749 (in Japanese)

Rask M, Saxén R, Ruuhijärvi J, Arvola L, Järvinen M, Koskelainen U, Outola I, Vuorinen PJ (2012) Short- and long-term patterns of ^{137}Cs in fish and other aquatic organisms of small forest lakes in southern Finland since the Chernobyl accident. J Environ Radioact 103:41–47

Saxén R, Koskelainen U (1992) Radioactivity of surface water and freshwater fish in Finland in 1988–1990. Suppl 6, Ann Rep STUK-A89. Helsinki, pp 1–75

Smith JT, Kudelsky AV, Ryabov IN, Daire SE, Boyer L, Blust RJ, Fernandez JA, Hadderinfh RH, Voitsekhovitch OV (2002) Uptake and elimination of radiocaesium in fish and the "size effect". J Environ Radioact 62:145–164

Suzuki K, Kimura S (1977) Growth of the crucian carps belonging to the genus *Carassius* in the lower reaches of the Nagara River, central Japan. Jpn J Ichthyol 24:199–206

Takagi K, Yamamoto S, Matsuda K, Tomiya A, Enomoto M, Shigenobu Y, Fujimoto K, Ono T, Morita T, Uchida K, Watanabe T (accepted) Radiocesium concentrations and body size of largemouth bass, *Micropterus salmoides*, and smallmouth bass, *M. dolomieu*, in Lake Hayama, Japan. J Appl Ichthyol

Tokyo Electric Power Co., Inc (2012) Press release (May 24, 2012), The estimated amount of radioactive materials released into the air and the ocean caused by Fukushima Daiichi nuclear power station accident due to the Tohoku-Chihou-Taiheiyou-Oki earthquake (As of May 2012). Available via http://www.tepco.co.jp/en/press/corp-com/release/2012/1204659_1870.html. Accessed 2 Apr 2015

Yodo T, Kimura S (1996) Age and growth of the largemouth bass *Micropterus salmoides* in Lakes Shorenji and Nishiko, central Japan. Fish Sci 62:524–528

Chapter 17
Spatiotemporal Monitoring of ^{134}Cs and ^{137}Cs in Ayu, *Plecoglossus altivelis*, a Microalgae-Grazing Fish, and in Their Freshwater Habitats in Fukushima

Jun-ichi Tsuboi, Shin-ichiro Abe, Ken Fujimoto, Hideki Kaeriyama, Daisuke Ambe, Keishi Matsuda, Masahiro Enomoto, Atsushi Tomiya, Takami Morita, Tsuneo Ono, Shoichiro Yamamoto, and Kei'ichiro Iguchi

Abstract Ayu, *Plecoglossus altivelis*, is a herbivorous fish that is an important fishery resource and a key component of the food web in many Japanese streams. After the Fukushima Daiichi Nuclear Power Plant (FNPP) accident in March 2011, ayu were exposed to highly contaminated silt while feeding on benthic microalgae attached to riverbed stones. To understand the effects of radioactive contamination on ayu, radiocesium (^{134}Cs + ^{137}Cs) concentrations were analyzed in riverbed samples (microalgae and silt) and in the internal organs and muscle of ayu in five river systems in the Fukushima Prefecture between summer 2011 and autumn 2013. The concentrations of radiocesium in both the internal organs and the muscles of ayu declined over time. The radiocesium concentrations in the muscle were correlated with, but much lower than, those in the internal organs. The concentrations in the internal organs were correlated with those in the riverbed samples. The concentrations in the muscle were further correlated with ayu body size. Our results suggest

J. Tsuboi (✉) • K. Matsuda • S. Yamamoto
National Research Institute of Aquaculture, Fisheries Research Agency,
2482-3 Chugushi, Nikko, Tochigi 321-1661, Japan
e-mail: tsuboi118@affrc.go.jp

S. Abe
Japan Sea National Fisheries Research Institute, Fisheries Research Agency,
5939-22, 1, Suido-cho, Chuo-ku, Niigata Niigata 951-8121, Japan

K. Fujimoto • H. Kaeriyama • D. Ambe • T. Morita • T. Ono
National Research Institute of Fisheries Sciences, Fisheries Research Agency,
2-12-4, Fukuura, Kanazawa, Yokohama, Kanagawa 236-8648, Japan

M. Enomoto • A. Tomiya
Fukushima Prefectural Inland Water Fisheries Experimental Station,
3447-1, Inawashiro, Maya, Fukushima 969-3283, Japan

K. Iguchi
Faculty of Environmental Studies, Nagasaki University, 1-14 Bunkyo-machi, Nagasaki,
Nagasaki 852-8521, Japan

K. Nakata, H. Sugisaki (eds.), *Impacts of the Fukushima Nuclear Accident on Fish and Fishing Grounds*, DOI 10.1007/978-4-431-55537-7_17

that ayu ingest radiocesium while consuming silt and microalgae from the riverbed, and that a small proportion (about 15 %) is assimilated into the muscle of the fish.

Keywords Bioaccumulation • Soil contamination • Nuclear accident • Radioactive cesium • Ayu

17.1 Introduction

Ayu (*Plecoglossus altivelis*) is a herbivorous fish that is distributed throughout the Japanese Archipelago (Iguchi et al. 1999) (Fig. 17.1). The species exhibits an amphidromous and annual life cycle. After the winter juvenile stage in the sea, young ayu migrate into rivers and graze on benthic microalgae attached to the riverbed (Iguchi and Hino 1996). Ayu are also an important resource for humans and for avian species, such as the great cormorant *Phalacrocorax carbo* (Takahashi et al. 2006); therefore, the radionuclide contamination of ayu may have a significant effect on both humans and aquatic and terrestrial ecosystems. In Fukushima Prefecture, Iguchi et al. (2013) reported high levels of radionuclide contamination in the riverbed sediments. Ayu ingest silt while grazing on benthic microalgae, exposing themselves to the radiation from the contaminated sediments, including the silt component.

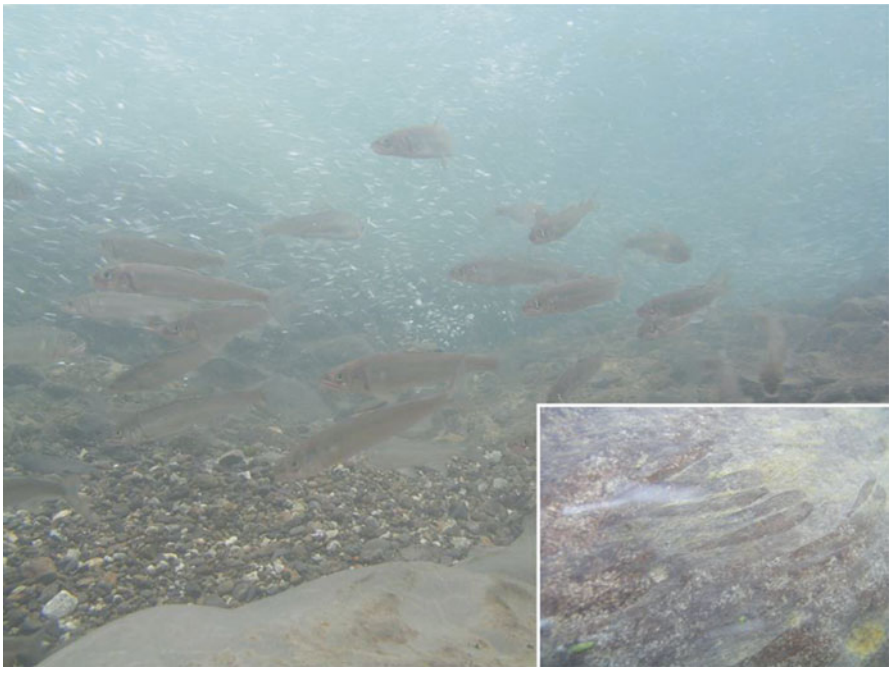

Fig. 17.1 Ayu feed on benthic microalgae attached to the riverbed, grazing it off the rocks with their teeth

The aerosol-bound Cs was deposited on land and became integrated into the surface soil within 2 months after the Fukushima Daiichi Nuclear Power Plant (FNPP) disaster (Masson et al. 2011; Hirose 2012; Yasunari et al. 2011). Radionuclides subsequently spread over central and northern Honshu, Japan. The rivers in Honshu typically have steep gradients and are subject to erosion during snowmelt and typhoons (Yoshimura et al. 2005). As a result, contaminated soils were transported by the rivers from the mountains to the plains in Fukushima Prefecture (Evrard et al. 2013). To understand the route by which herbivorous fish are exposed to radiocesium, we measured radiocesium concentrations in riverbed samples (microalgae and silt) and in the internal organs and muscle of ayu in Fukushima Prefecture.

17.2 Relationship Between the Radiocesium Concentrations in Ayu Internal Organs and Muscle

Ayu ($n = 166$; fork length, 68–206 mm) were collected from five rivers in the Fukushima Prefecture by casting nets (periphery, 16 m; mesh size, 9 mm) between 9 July 2011 and 14 October 2013 (Fig. 17.2). The Niida and Kido Rivers were not

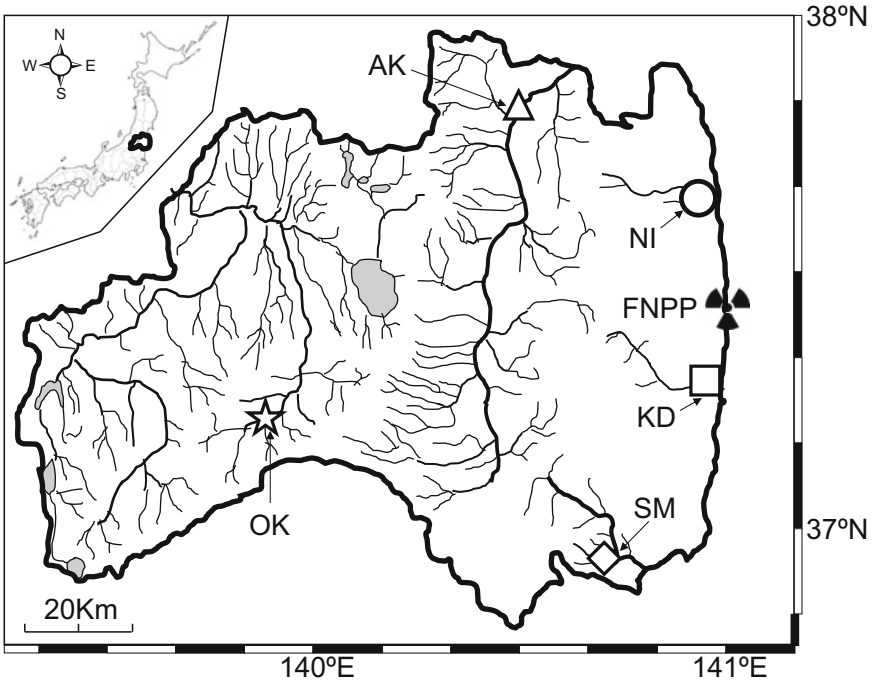

Fig. 17.2 Location of collection sites for ayu and riverbed samples (*NI* Niida River, *KD* Kido River, *AK* Abukuma River, *SM* Same River, *OK* Okawa River). The symbol for each site corresponds to those in Figs. 17.4 and 17.5

Fig. 17.3 *1* River water, *2* muddy sediment, *3* riverbed samples, and *4* ayu were sampled in five rivers between 2011 and 2013

sampled before May 2012 because of concerns about radiation safety in those areas. Collections of water, sediment, and riverbed samples, consisting primarily of benthic microalgae and silt, were made simultaneously at each site (Fig. 17.3) [see Tsuboi et al. (2015) for more details]. Radiocesium was detected in all 36 water and muddy sediment samples, 34 of 36 riverbed samples, and 119 internal organs and 98 muscle samples from 166 fish.

In 2013 the median $^{134}Cs/^{137}Cs$ ratio was 0.46 in all analyzed samples, which is identical to the value 2 years after the fallout from the FNPP. Radiocesium was detected in both the internal organs and the muscle of 84 individuals. Although there was a positive correlation between the concentrations of radiocesium in the internal organs and the muscle of ayu ($r=0.746$, $p=0.006$), the median concentration in the muscle was 14.5 % that of the median concentration in the internal organs ($n=84$, $p<0.001$). Thus, a small proportion (about 15 %) of the radiocesium ingested from the riverbed appears to be transferred to the muscle. Cesium strongly interacts with clay minerals, especially vermiculite and illite minerals (Comans and Hockley 1992). Furthermore, leaching experiments have demonstrated that radiocesium is relatively insoluble in the river suspended sediment in Fukushima, and that the adsorption of radiocesium to the suspended sediment was irreversible (Tanaka et al. 2013). Therefore, most of the radiocesium in the silt ingested by ayu is unlikely to be absorbed but will instead be excreted.

17.3 Biological and Environmental Factors Involved in the Temporal Pattern of Radiocesium Contamination

To evaluate temporal changes in ^{134}Cs and ^{137}Cs concentrations in water, muddy sediment, and ayu, we fitted a generalized linear mixed model (GLMM) with a Gaussian distribution of errors. The GLMM results suggest that the radiocesium concentrations in the muddy sediment but not river water have declined through time (river water: $t=-1.016$, $p=0.318$; muddy sediment: $t=-3.131$, $p=0.004$) (Figs. 17.4 and 17.5). The radiocesium concentrations have declined through time

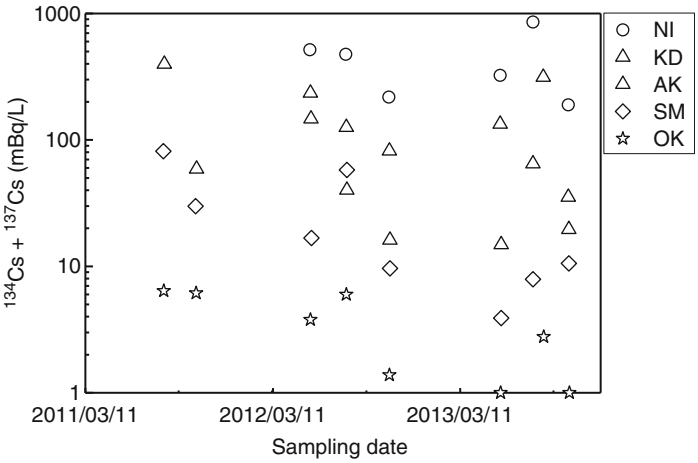

Fig. 17.4 Time-series of radiocesium concentrations in the river water. Symbols correspond to the collection sites in Fig. 17.2 (*NI* Niida River, *KD* Kido River, *AK* Abukuma River, *SM* Same River, *OK* Okawa River)

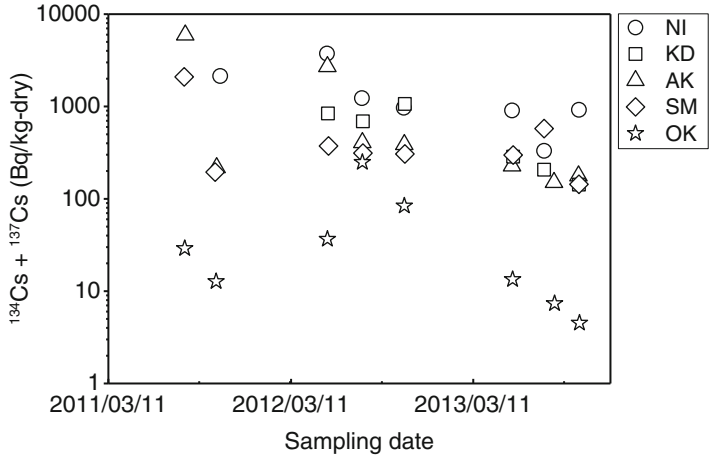

Fig. 17.5 Time-series of radiocesium concentrations in muddy sediment. Symbols correspond to the collection sites in Fig. 17.2 (*NI* Niida River, *KD* Kido River, *AK* Abukuma River, *SM* Same River, *OK* Okawa River)

in both the internal organs and muscle of ayu (internal organs: $t=-3.855$, $p<0.001$; muscle: $t=-2.809$, $p=0.006$) (Fig. 17.6). The concentrations in the internal organs of ayu were positively correlated with those in the riverbed samples (i.e., fish prey) that were collected simultaneously with the ayu ($t=8.197$, $p<0.001$). In contrast, there was no correlation between the concentrations in the ayu muscle and the riverbed samples ($t=-1.202$, $p=0.261$; Fig. 17.6). Thus, we conclude that herbivorous fish assimilate radiocesium from the microalgae and silt on the riverbed stones as they forage. Between 2011 and 2013, the activity concentration of radiocesium in the internal organs and the muscle of ayu declined, mainly because of the half-life of ^{134}Cs (2.07 years), which is considerably shorter than the 30.1 years for ^{137}Cs. However, the concentration of ^{137}Cs in the whole ayu body tended to decrease during 2011 (Iguchi et al. 2013). Therefore, the decrease in the concentration of ^{137}Cs in ayu cannot be explained only by the half-life of ^{134}Cs. The activity concentration of ^{137}Cs in the internal organs, which represented the majority of the ^{137}Cs in ayu, was correlated with that in the riverbed samples. Therefore, the decrease of ^{137}Cs in the riverbed, which may have been caused by flushing out of the contaminated soil from the mountains, would explain the decrease of ^{137}Cs in ayu. In European lakes, ^{137}Cs concentrations in fish muscle peaked a few years after the Chernobyl disaster (Jonsson et al. 1999; Smith et al. 2000). Then, the rate of decrease in muscle ^{137}Cs concentrations was initially rapid, but later slowed. Conversely, in the rivers of Fukushima, the radiocesium contamination levels in ayu peaked immediately after the FNPP accident. The concentrations then decreased slowly, fluctuating with the transport of fresh polluted sediment from the mountains following snowmelt and typhoon events (Figs. 17.5 and 17.6).

Ayu fork length was correlated not with concentrations of radiocesium in the internal organs but with that in the muscle (internal organs: $t=-1.168$, $p=0.246$; muscle: $t=4.329$, $p<0.001$). The concentration of ^{137}Cs in fish increases with fish size according to a power law relationship because of changes in prey items (Smith et al. 2002). For instance, the concentration in northern pike (*Esox lucius*) increased as the trophic level of prey increased from plankton to invertebrates and then to small fish. Indeed, the level of radiocesium contamination in fish at Fukushima increased according to the order herbivores (i.e., ayu) < omnivores < piscivores at Fukushima (Mizuno and Kubo 2013). A positive correlation was also observed for ayu body size relative to the muscle concentration of radiocesium. Thus, in this case, the positive correlation between ayu body size and radiocesium concentrations in their muscle could not be explained by a change in feeding patterns because the prey size and the prey items do not change as the ayu grows. Also, the time (season) of collection had no effect on the activity concentrations of radiocesium in ayu muscle. The activity concentration of radiocesium in fish is a function of uptake and elimination rates. In hatchery-reared ayu, assimilation efficiency decreases as the fish grow (Akutsu et al. 2001). Larger ayu therefore need much more food per unit weight gain than smaller individuals. Thus, at our study site, larger ayu have greater potential to accumulate radiocesium from microalgae on the riverbed stones than smaller ayu.

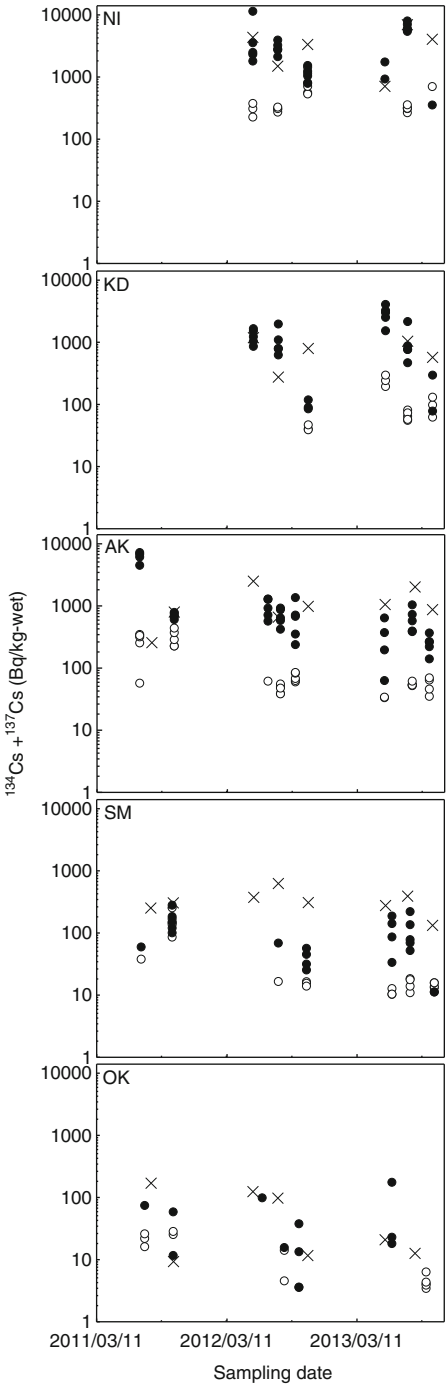

Fig. 17.6 Time-series of radiocesium concentrations in the riverbed samples (i.e., fish dietary items; *cross* symbols) and the internal organs (i.e., stomach contents, stomach, gut contents, gut, liver, spleen, gonad; *solid* symbols) and the muscle (*open* symbols) samples from ayu collected in the five rivers (*NI* Niida River, *KD* Kido River, *AK* Abukuma River, *SM* Same River, *OK* Okawa River)

The overall radiocesium concentrations have declined with time in both the internal organs and muscle of ayu (Fig. 17.6). However, in some rivers surveyed, the radiocesium concentrations in the whole ayu body (i.e., internal organ and muscle) exceeded the Japanese standard limit for radiocesium in foods (100 Bq/kg-wet). Thus, fishing activities were banned in three of the five rivers during the sampling periods of this study (Niida, Kido, and Abukuma Rivers). Spatiotemporal monitoring of the levels of radiocesium in freshwater ecosystems, in areas close to human centers, should continue to increase our understanding of the long-term dynamics of radionuclide contamination and to reveal the effects on the biological and environmental characteristics of each ecosystem.

Acknowledgements This chapter was revised from a paper published by Tsuboi et al. (2015). The authors are grateful to Masato Murakami and Tomoko Okazaki for their assistance with the sample assays and data analyses. They also thank Kaoru Nakata and Kazuo Uchida for critical review of the manuscript. This study was supported by the Fisheries Agency, Ministry of Agriculture, Forestry and Fisheries, Japan.

References

Akutsu M, Sawada M, Ishijima H (2001) A comparative testing among formula feeds on ayu. Bull Tochigi Pref Fish Exp Stat 44:3–4 (in Japanese)

Comans RNJ, Hockley DE (1992) Kinetics of cesium sorption on illite. Geochim Cosmochim Acta 56:1157–1164

Evrard O, Chartin C, Onda Y, Patin J, Lepage H, Lefèvre I, Ayrault S, Ottlé C, Bonté P (2013) Evolution of radioactive dose rates in fresh sediment deposits along coastal rivers draining Fukushima contamination plume. Sci Rep 3:3079

Hirose K (2012) Fukushima Dai-ichi nuclear power plant accident: summary of regional radioactive deposition monitoring results. J Environ Radioact 111:13–17

Iguchi K, Hino T (1996) Effect of competitor abundance on feeding territoriality in a grazing fish, the ayu *Plecoglossus altivelis*. Ecol Res 11:165–173

Iguchi K, Tanimura Y, Takeshima H, Nishida M (1999) Genetic variation and geographic population structure of amphidromous ayu *Plecoglossus altivelis* as examined by mitochondrial DNA sequencing. Fish Sci 65:63–67

Iguchi K, Fujimoto K, Kaeriyama H, Tomiya A, Enomoto M, Abe S, Ishida T (2013) Cesium-137 discharge into the freshwater fishery ground of grazing fish, ayu *Plecoglossus altivelis*, after the March 2011 Fukushima nuclear accident. Fish Sci 79:983–988

Jonsson B, Forseth T, Ugedal O (1999) Chernobyl radioactivity persists in fish. Nature (Lond) 400:417

Masson O, Baeza A, Bieringer J, Brudecki K, Bucci S, Cappai M, Carvalho FP, Connan O, Cosma C, Dalheimer A, Didier D, Depuydt G, De Geer LE, Vismes AD, Gini L, Groppi F, Gudnason K, Gurriaran R, Hainz D, Haldórsson O, Hammond D, Hanley O, Holeý K, Zs H, Ioannidou A, Isajenko K, Jankovic M, Katzlberger C, Kettunen M, Kierepko R, Kontro R, Kwakman PJM, Lecomte M, Leon Vintro L, Leppänen AP, Lind B, Lujaniene G, Ginnity PM, Mahon CM, Malá H, Manenti S, Manolopoulou M, Mattila A, Mauring A, Mietelski JW, Møller B, Nielsen

SP, Nikolic J, Overwater RMW, Pálsson SE, Papastefanou C, Penev I, Pham MK, Povinec PP, Ramebäck H, Reis MC, Ringer W, Rodriguez A, Rulík P, Saey PRJ, Samsonov V, Schlosser C, Sgorbati G, Silobritiene BV, Söderström C, Sogni R, Solier L, Sonck M, Steinhauser G, Steinkopff T, Steinmann P, Stoulos S, Sýkora I, Todorovic D, Tooloutalaie N, Tositti L, Tschiersch J, Ugron A, Vagena E, Vargas A, Wershofen H, Zhukova O (2011) Tracking of airborne radionuclides from the damaged Fukushima Dai-ichi nuclear reactors by European networks. Environ Sci Technol 45:7670–7677

Mizuno T, Kubo H (2013) Overview of active cesium contamination of freshwater fish in Fukushima and eastern Japan. Sci Rep 3:1742

Smith JT, Comans RNJ, Beresford NA, Wright SM, Howard BJ, Camplin WC (2000) Chernobyl's legacy in food and water. Nature (Lond) 405:141

Smith JT, Kudelsky AV, Ryabov IN, Daire SE, Boyer L, Blust RJ, Fernandez JA, Hadderingh RH, Voitsekhovitch OV (2002) Uptake and elimination of radiocaesium in fish and the "size effect". J Environ Radioact 62:145–164

Takahashi T, Kameda K, Kawamura M, Nakajima T (2006) Food habits of great cormorant *Phalacrocorax carbo hanedae* at Lake Biwa, Japan, with special reference to ayu *Plecoglossus altivelis*. Fish Sci 72:477–484

Tanaka K, Sakaguchi A, Kanai Y, Tsuruta H, Shinohara A, Takahashi Y (2013) Heterogeneous distribution of radiocesium in aerosols, soil and particulate matters emitted by the Fukushima Daiichi Nuclear Power Plant accident: retention of micro-scale heterogeneity during the migration of radiocesium from the air into ground and river systems. J Radioanal Nucl Chem 295:1927–1937

Tsuboi J, Abe S, Fujimoto K, Kaeriyama H, Ambe D, Matsuda K, Enomoto M, Tomiya A, Morita T, Ono T, Yamamoto S, Iguchi K (2015) Exposure of a herbivorous fish to ^{134}Cs and ^{137}Cs from the riverbed following the Fukushima disaster. J Environ Radioact 141:32–37

Yasunari TJ, Stohl A, Hayano RS, Burkhart JF, Eckhardt S, Yasunari T (2011) Cesium-137 deposition and contamination of Japanese soils due to the Fukushima nuclear accident. Proc Natl Acad Sci U S A 108:19530–19534

Yoshimura C, Omura T, Furumai H, Tockner K (2005) Present state of rivers and streams in Japan. River Res Appl 21:93–112

Chapter 18
Radiocesium Concentrations in the Muscle and Eggs of Salmonids from Lake Chuzenji, Japan, After the Fukushima Fallout

Shoichiro Yamamoto, Tetsuya Yokoduka, Ken Fujimoto, Kaori Takagi, and Tsuneo Ono

Abstract Approximately 18 months (September–December 2012) after the Fukushima Dai-ichi Nuclear Power Plant accident, elevated radiocesium concentrations were detected in muscle and egg samples from masu salmon (*Oncorhynchus masou*), kokanee (*Oncorhynchus nerka*), brown trout (*Salmo trutta*), and lake trout (*Salvelinus namaycush*) from the Lake Chuzenji system, central Honshu Island, Japan (160 km from the station). Mean muscle concentrations were 142.9–249.2 Bq/kg-wet, and mean egg concentrations were 38.7–79.0 Bq/kg-wet. No relationship between fork length and muscle radiocesium concentration was observed in any of the species, but significant relationships were found between individual muscle and egg radiocesium concentrations from masu salmon, brown trout, and lake trout.

Keywords Brown trout • Kokanee • Lake trout • Masu salmon • Nuclear accident

S. Yamamoto (✉)
National Research Institute of Aquaculture, Fisheries Research Agency,
2482-3 Chugushi, Nikko, Tochigi 321-1661, Japan
e-mail: ysho@affrc.go.jp

T. Yokoduka
Tochigi Prefectural Fisheries Experimental Station,
Sarado, Ohtawara, Tochigi 324-0404, Japan

K. Fujimoto • T. Ono
National Research Institute of Fisheries Sciences, Fisheries Research Agency,
2-12-4, Fukuura, Kanazawa, Yokohama, Kanagawa 236-8648, Japan

K. Takagi
Marine Biological Research Institute of Japan Co., LTD,
4-3-16, Yutaka, Shinagawa, Tokyo 142-0042, Japan
e-mail: takagik@affrc.go.jp

K. Nakata, H. Sugisaki (eds.), *Impacts of the Fukushima Nuclear Accident on Fish and Fishing Grounds*, DOI 10.1007/978-4-431-55537-7_18

18.1 Introduction

A Japanese governmental agency (Fisheries Agency) and local governments initiated monitoring programs soon after the Fukushima fallout to monitor radioactivity contamination in freshwater and marine fish and invertebrates in the affected areas. The results revealed that radiocesium contamination was transferred quickly to freshwater and marine ecosystems, and elevated radiocesium concentrations were detected in many fish and invertebrates (Fisheries Agency 2012). These concentrations decreased over time in most of the epipelagic fish and neustonic organisms (Buesseler 2012). However, some demersal fish off the coast of Fukushima and some freshwater fish in central and northern Honshu Island continue to exhibit higher radiocesium concentrations (Tateda et al. 2013). Freshwater masu salmon (*Oncorhynchus masou*) from the Niida River in Fukushima Prefecture contained the highest measured radiocesium concentrations in March 2012 (18,700 Bq/kg-wet weight; Fisheries Agency 2012). Restrictions have been placed on shipping and consumption of 19 commercially important freshwater fish and invertebrate species as of October 2013 in the extensive deposition area of central and northern Honshu Island.

Because of differences in osmoregulatory physiology, radionuclides usually bioaccumulate at higher concentrations in freshwater compared with marine fish. After the Chernobyl nuclear accident (Ukraine), higher radiocesium concentrations persisted in freshwater fish from several European lakes for 10 years and more (Jonsson et al. 1999; Brittain and Gjerseth 2010; Rask et al. 2012). Lake-dwelling freshwater fish in high deposition areas may also sustain long-standing radionuclide contamination, which results from radionuclide recycling within the aquatic environment (Smith and Comans 1996). In this chapter, we describe radiocesium concentrations in muscle and eggs of masu salmon, kokanee, *O. nerka*; brown trout, *Salmo trutta;* and lake trout, *Salvelinus namaycush*, from the Lake Chuzenji system, central Honshu Island, Japan (Fig. 18.1) to understand the effects of radionuclide contamination on salmonid fish. Although Lake Chuzenji is approximately 160 km from the Fukushima Dai-ichi Nuclear Power Plant (FNPP) in linear distance, the lake watershed area received radiocesium deposits of 8–36 kBq/m^2 after the Fukushima accident (Fisheries Research Agency 2012). Salmonid fish support important recreational and commercial fisheries throughout the Japanese Archipelago. Salmonid eggs (usually raw eggs) are also an important food resource for the Japanese.

Fig. 18.1 A photograph of Lake Chuzenji

18.2 Study Area (Lake Chuzenji)

Lake Chuzenji (36°44′ latitude, 139°27′ longitude) is an oligotrophic, cold-water lake system located in Nikko, Kanto District, Japan (mean surface water quality: pH, 8.2; chemical oxygen demand, 1.4 mg/l; total phosphorus, 0.004 mg/l; total nitrogen, 0.26 μg/l; chlorophyll *a*, 2.4 μg/l) (Tochigi Prefecture Japan 2012). At 1,269 m above sea level, it is the highest major natural lake in Japan. It is approximately 11.5 km^2 in surface area and 163 m in maximum depth (Yokoyama and Yamamoto 2012). The water turnover rate is about 6 years. No fish originally inhabited Lake Chuzenji. However, many freshwater fish, mostly salmonids, have been introduced repeatedly since 1873. The lake system is currently inhabited by four exotic salmonids, namely brook trout, *Salvelinus fontinalis*; lake trout, brown trout, rainbow trout, *O. mykiss*; and three native Japanese salmonids, white-spotted charr, *Salvelinus leucomaenis*; masu salmon, and kokanee. Different masu salmon subspecies (*O. masou masou* and *O. masou* subsp.) were introduced in the 1880s. The current thinking is that the masu salmon in Lake Chuzenji are an admixture of two subspecies or a hybrid between two subspecies and are often referred to as "Honmasu" (Munakata et al. 1999). Detailed descriptions of Lake Chuzenji and its fish fauna are provided in Yamamoto et al. (2010) and Yokoyama and Yamamoto (2012).

18.3 Muscle Radiocesium Concentrations in Salmonid Fish

Mature female masu salmon, kokanee, brown trout, and lake trout were collected from Lake Chuzenji using angling gear and gill nets from October to December 2012. Masu salmon and kokanee that were migrating upstream for spawning during September–October 2012 were collected from a weir located in a Lake Chuzenji inlet stream that passes through Fisheries Research Agency (FRA) property. Stream-dwelling *S. trutta* were also collected using electrofishing equipment from the Toyama Stream, a main Lake Chuzenji inlet stream (Fig. 18.2).

Mean radiocesium concentrations ($^{134}Cs + ^{137}Cs$) in muscle of masu salmon, kokanee, brown trout, and lake trout collected from the lake were 236.5 ± 57.2 [Bq/kg-wet ± standard deviation (SD), $n = 13$], 149.9 ± 19.6 ($n = 13$), 249.2 ± 39.6 ($n = 10$), and 146.9 ± 52.2 ($n = 7$), respectively (Fig. 18.3). The relationship between fork length and radiocesium concentration was not statistically significant for any of the four species ($r = 0.24$–0.59, $P < 0.05$). Mean muscle radiocesium concentration (± SD) in brown trout samples collected from the inlet stream was 36.7 ± 15.6 Bq/kg-wet ($n = 10$). The difference in radiocesium concentration between lake- and stream-dwelling brown trout was statistically significant ($F = 248.93$, *d.f.* = 1,18, $P < 0.001$). A significant difference in muscle radiocesium concentration was observed among the four species collected from the lake ($F = 16.38$, *d.f.* = 3,38, $P < 0.01$). Masu salmon and brown trout had higher radiocesium concentrations than those of kokanee and lake trout (Bonferroni multiple comparisons).

Mean muscle radiocesium concentrations in the four species measured during the study period were 142.9–249.2 Bq/kg. Muscle radiocesium concentrations were also greater than 100 Bq/kg in co-distributed species [rainbow trout, freshwater goby, *Rhinogobius* sp., and smelt (whole body) *Hypomesus nipponensis*; Fisheries Agency 2012; Fisheries Research Agency 2012]. The Ministry of Health, Labor, and Welfare, Japan placed restrictions on shipping fish with more than 100 Bq/kg radiocesium. All salmonid fishing activities, except for catch-and-release, were prohibited in Lake Chuzenji as of June 2014.

Muscle radiocesium concentrations differed among species and between habitats within species. Lake Chuzenji masu salmon and brown trout had higher radiocesium concentrations than those of kokanee and lake trout. Lake-dwelling brown trout had much higher concentrations than those of inlet stream-dwelling brown trout. These differences may be related to differences in species-specific food intake or food availability or both. Radiocesium accumulation in freshwater fish organs results mainly from food intake (Hewett and Jefferies 1976; Forseth et al. 1991; Ugedal et al. 1995; Yamamoto et al. 2014a). Lake Chuzenji kokanee consume mostly zooplankton or chironomid larvae, whereas masu salmon, brown trout, and lake trout are omnivorous (Japan Fisheries Resource Conservation Association 2003, 2008). Higher radiocesium concentrations were found in benthic fish from Lake Chuzenji during September–November 2012 compared with zooplankton species (Fisheries Research Agency 2012). A case study of a Norwegian lake conducted after the Chernobyl reactor accident showed that brown trout feeding mostly on zoobenthos had higher radiocesium concentrations compared with those

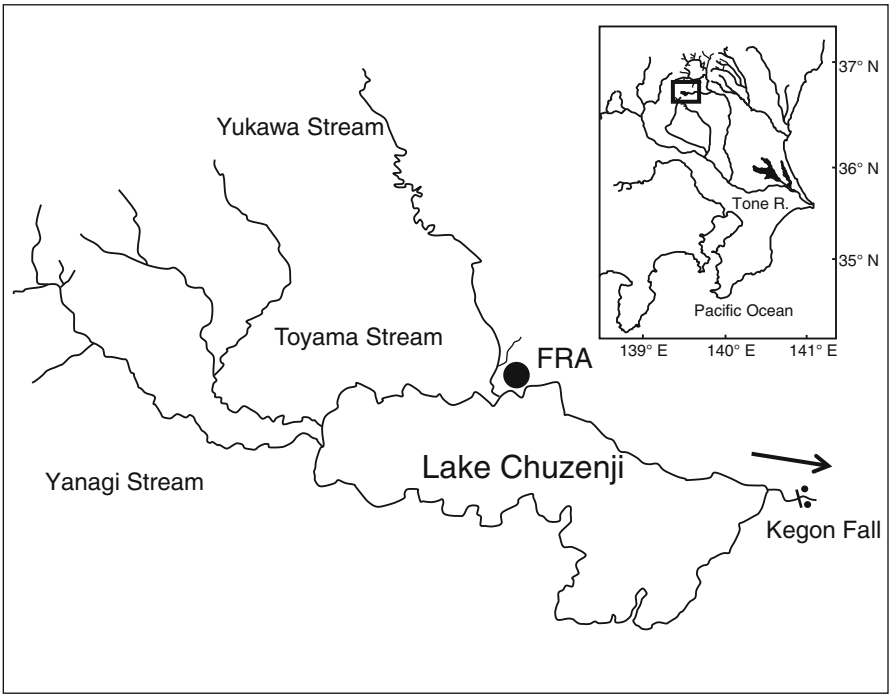

Fig. 18.2 Location of the Lake Chuzenji system, where the study was conducted

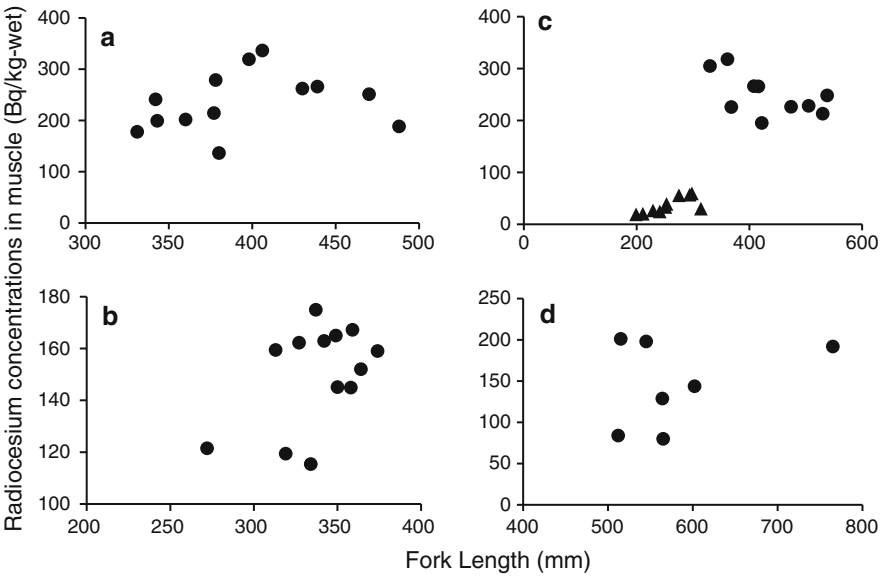

Fig. 18.3 Relationships between fork length and radiocesium concentrations in muscle of masu salmon (**a**), kokanee (**b**), brown trout (**c**), and lake trout (**d**) collected in Lake Chuzenji, Japan, from September to November 2012. *Solid triangles* indicate brown trout collected from the Lake Chuzenji inlet stream

of sympatric Arctic charr (*Salvelinus alpinus*), which are planktonic feeders (Forseth et al. 1991). Segregated habitats with different dominant prey species could also cause differences in radiocesium accumulation in freshwater fish; Lake Chuzenji brown trout mainly prey on benthic gobies and smelt (Japan Fisheries Resource Conservation Association 2003), whereas inlet stream-dwelling brown trout feed on aquatic and terrestrial insects.

Radiocesium concentrations varied individually in the four salmonid species, regardless of body size. The variation was more pronounced in omnivorous masu salmon, brown trout, and lake trout than that in the planktonic kokanee. Radiocesium concentrations also varied within salmonid food items. For example, in October–November 2012, Lake Chuzenji *Ephyra* sp. shrimp contained 128–132 Bq/kg ($^{134}Cs + {}^{137}Cs$), *Palaemon* sp. shrimp contained 47–94 Bq/kg, the freshwater sculpin *Cottus reinii* contained 166–211 Bq/kg, and freshwater goby contained 86–145 Bq/kg (Yamamoto and Yokoduka, unpublished data). These species are major food sources for masu salmon, brown trout, and lake trout. Size-independent individual variations in diet composition may be one of the most important factors affecting variations in radiocesium accumulation, as suggested by Ugedal et al. (1995), who examined Arctic charr and brown trout in a Norwegian lake.

Mean radiocesium concentration in lake trout, which prey mainly on small fish and aquatic insects, was lower than that in masu salmon and lake-dwelling brown trout. Therefore, diet composition does not completely explain the observed radiocesium accumulation patterns. Differences in metabolic rates could also partially explain differences between fish species. Metabolic rate, which is dependent on water temperature, could affect radionuclide intake, retention, and excretion rates (Elliott et al. 1992; Ugedal et al. 1992) and thus predicts ecological half-life (Doi et al. 2012). We did not collect data on the metabolic rates of lake trout or the other co-distributed salmonids in Lake Chuzenji. However, lake trout are larger at maturity than other species, which would affect metabolic rate, food intake, and radiocesium excretion rates.

18.4 Radiocesium Concentrations in Salmonid Eggs

Mean radiocesium concentrations ($^{134}Cs + {}^{137}Cs$) in masu salmon, kokanee, brown trout, and lake trout eggs were 79.0 ± 19.1 (Bq/kg-wet ± SD, $n = 13$), 53.8 ± 6.9 ($n = 13$), 38.7 ± 30.7 ($n = 20$), and 54.5 ± 22.5 ($n = 7$), respectively (Fig. 18.4). The difference was statistically significant among the four species ($F = 8.07$, $d.f. = 3, 49$, $P < 0.001$). In brown trout, mean radiocesium concentration (±SD) in eggs collected from Lake Chuzenji fish was 65.6 ± 17.5 Bq/kg ($n = 10$). Mean radiocesium concentration in eggs collected from fish inhabiting the inlet stream was 11.9 ± 9.2 Bq/kg ($n = 10$). This difference was statistically significant ($F = 73.86$, $d.f. = 1, 18$, $P < 0.001$). There were significant relationships in radiocesium concentration between individual muscle and egg samples from masu salmon ($r = 0.80$, $P < 0.01$), brown trout ($r = 0.96$, $P < 0.0001$), and lake trout ($r = 0.90$, $P < 0.01$). Analysis of covariance, in which egg radiocesium concentration was the dependent variable and

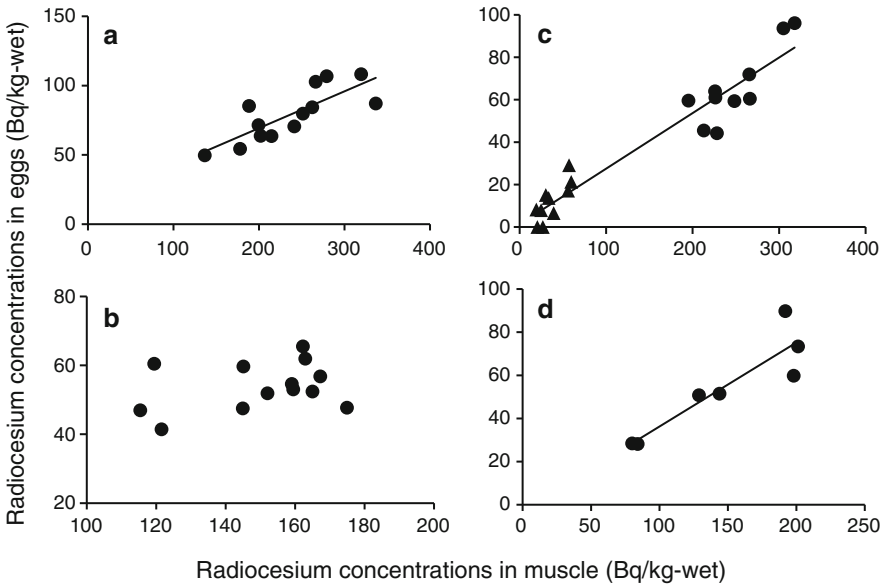

Fig. 18.4 Relationships between radiocesium concentrations in muscle and eggs of masu salmon (**a**), kokanee (**b**), brown trout (**c**), and lake trout (**d**) collected from Lake Chuzenji, Japan, from September to November 2012. *Solid triangles* indicate brown trout collected from the Lake Chuzenji inlet stream

muscle radiocesium concentration was the covariate, revealed that the cesium concentrations between individual muscle and egg was significantly different among the four species ($F = 8.94$, $d.f. = 3, 48$, $P < 0.001$). For brown trout, egg radiocesium concentrations were significantly lower than the concentrations in the other three salmonid fishes (Bonferroni multiple comparisons).

The mean radiocesium concentration ratio in eggs compared with that in muscle were 0.34 for masu salmon, 0.36 for kokanee, 0.28 for brown trout, and 0.37 for lake trout. These ratios were similar to the ratios in co-distributed wild white-spotted charr (0.31) and rainbow trout (0.34; Yamamoto et al., unpublished data). Our analyses also revealed that radiocesium concentrations in masu salmon, brown trout, and lake trout eggs increased proportionally with muscle concentrations. This relationship has not been reported previously and suggests that radiocesium levels in salmonid muscle constitute a convenient surrogate for radiocesium concentrations in eggs. Salmonid eggs are important for hatchery production programs and as food. Release of hatchery-reared fish into many Japanese lakes and rivers, including the Lake Chuzenji system, contribute to immediate resource enhancement and supplement wild fisheries, which are essential components of successful freshwater fisheries management programs (Kitada 2001). Although current radiocesium levels in individual eggs were low, radiocesium turnover studies for each fish species, including elimination rate estimates, and biological and ecological half-lives at each life history stage would be indispensable to further investigate this issue.

Acknowledgments This chapter was revised from a paper published by Yamamoto et al. (2014b). The authors are grateful to Kouji Mutou and the Lake Chuzenji Fishermen's Cooperative for collecting the fish samples and to Masato Murakami, Tomoko Okazaki, Yumiko Watanuki, and Maki Yoshida for their assistance with the sample assays and data analyses. We also thank Hiroyasu Hasegawa, Takami Morita, Kaoru Nakata, Kazuo Uchida, and Hitoshi Kubota for their critical reviews of the manuscript. This study was supported by the Fisheries Agency, Ministry of Agriculture, Forestry, and Fisheries, Japan.

References

Brittain JE, Gjerseth JE (2010) Long-term trends and variation in ^{137}Cs activity concentrations in brown trout (*Salmo trutta*) from Øvre Heimdalsvatn, a Norwegian subalpine lake. Hydrobiologia 642:107–113

Buesseler KO (2012) Fishing for answers off Fukushima. Science 338:480–482

Doi H, Takahara T, Tanaka K (2012) Tropic position and metabolic rate predict the long-term decay process of radioactive cesium in fish: a meta-analysis. PLoS One 7:e29295

Elliott JM, Hilton J, Rigg E, Tullette PA, Swift DJ, Leonard DRP (1992) Sources of variation in post-Chernobyl radiocesium in fish from two Cumbrian lakes (northwest England). J Appl Ecol 29:108–119

Fisheries Agency (2012) Results of the inspection on radioactivity materials in fisheries products. http://www.jfa.maff.go.jp/j/housyanou/kekka.html (in Japanese)

Fisheries Research Agency (2012) The scientific reports of nuclear accident investigations by the Fisheries Research Agency. http://www.fra.affrc.go.jp/eq/Nuclear_accident_effects/index.html (in Japanese)

Forseth T, Ugedal O, Jonsson B, Langeland A, Njåstad O (1991) Radiocesium turnover in Arctic charr (*Salvelinus alpinus*) and brown trout (*Salmo trutta*) in a Norwegian lake. J Appl Ecol 28:1053–1067

Hewett CJ, Jefferies DF (1976) The accumulation of radioactive cesium from water by the brown trout (*Salmo trutta*) and its comparison with plaice and rays. J Fish Biol 9:479–489

Japan Fisheries Resource Conservation Association (2003) Kosho-Kankyou no Kiban-jyouhouseibi-jigyou Houkokusho. Japan Fisheries Resource Conservation Association, Tokyo (in Japanese)

Japan Fisheries Resource Conservation Association (2008). Kosho-Kankyou no Kiban-jyouhouseibi-jigyou Houkokusho. Japan Fisheries Resource Conservation Association, Tokyo (in Japanese)

Jonsson B, Forseth T, Ugedal O (1999) Chernobyl radioactivity persists in fish. Nature (Lond) 400:417

Kitada S (2001) Fish stock enhancement assessment with Japan examples. Kyoritsu, Tokyo (in Japanese)

Munakata A, Amano M, Ikuta K, Kitamura S, Aida K (1999) Growth of wild honmasu salmon parr in a tributary of Lake Chuzenji. Fish Sci 65:965–966

Rask M, Saxén R, Ruuhijärvi J, Arvola L, Järvinen M, Koskelainen U, Outola I, Vuorinen PJ (2012) Short- and long-term patterns of ^{137}Cs in fish and other aquatic organisms of small forest lakes in southern Finland since the Chernobyl accident. J Environ Radioact 103:41–47

Smith JT, Comans RNJ (1996) Modelling the diffusive transport and remobilization of ^{137}Cs in sediments: the effects of sorption kinetics and reversibility. Geochim Cosmochim Acta 60:995–1004

Tateda Y, Tsumune D, Tsubono T (2013) Simulation of radioactive cesium transfer in the southern Fukushima coastal biota using a dynamic food chain transfer model. J Environ Radioact 124:1–12

Tochigi Prefecture, Japan (2012) Tochigi Prefecture water quality chronology [fiscal year] 2012. Available from http://www.pref.tochigi.lg.jp/d03/eco/kankyou/hozen/suisitunenpyou24.html (in Japanese)

Ugedal O, Jonsson B, Njåstad O, Næumanñ R (1992) Effects of temperature and body size on radiocesium retention in brown trout, *Salmo trutta*. Freshw Biol 28:165–171

Ugedal O, Forseth T, Jonsson B, Njåstad O (1995) Sources of variation in radiocesium levels between individual fish from a Chernobyl contaminated Norwegian lake. J Appl Ecol 32:352–361

Yamamoto S, Kitano S, Sakano H, Yagyu M (2010) Differences in longitudinal distribution patterns along a Honshu stream of brown trout *Salmo trutta*, white-spotted charr *Salvelinus leucomaenis*, and masu salmon *Onchorhynchus masou*. Fish Sci 76:275–280

Yamamoto S, Mutou K, Nakamura H, Uchida K, Takagi K, Fujimoto K, Kaeriyama H, Ono T (2014a) Assessment of radiocaesium accumulation by hatchery-reared salmonids after the Fukushima nuclear accident. Can J Fish Aquat Sci 71:1772–1775

Yamamoto S, Yokoduka T, Fujimoto K, Takagi K, Ono T (2014b) Radiocaesium concentrations in the muscle and eggs of salmonids from Lake Chuzenji, Japan, after the Fukushima fallout. J Fish Biol 84:1607–1613

Yokoyama R, Yamamoto S (2012) Freshwater sculpin dwelling in Lake Chuzenji, Nikko, Kanto District, Japan, is identified as Utsusemikajika, *Cottus reinii*, unintentionally introduced from Lake Biwa. Ichthyol Res 59:389–393

Chapter 19
Assessment of Radiocesium Accumulation by Hatchery-Reared Salmonids After the Fukushima Nuclear Accident

Shoichiro Yamamoto, Kouji Mutou, Hidefumi Nakamura, Kouta Miyamoto, Kazuo Uchida, Kaori Takagi, Ken Fujimoto, Hideki Kaeriyama, and Tsuneo Ono

Abstract To understand the process of radiocesium uptake in salmonids after the Fukushima Dai-ichi Nuclear Power Plant (FNPP) accident, a lake caging experiment and two captive-rearing experiments with controlled radiocesium concentrations of water and feed were conducted in and around Lake Chuzenji, central Honshu Island, Japan (160 km from the station). Substantial accumulations of radiocesium were confirmed in muscle of hatchery-reared kokanee (*Oncorhynchus nerka*) and masu salmon (*Oncorhynchus masou*) after release into the cages, indicating that radionuclide contamination of fish is an ongoing process, 1.5 years after the nuclear accident. Two captive experiments, controlling water and feed radiocesium levels, showed that direct radiocesium transfer from water (43 mBq/l) in Lake Chuzenji to muscle tissue was undetected, at least during the approximately 90-day experimental period, whereas a rapid increase in radiocesium levels was observed when fish were cultured using radiocesium-contaminated pellets. The results revealed that radiocesium contamination in salmonids is mainly via the food chain, and that direct intake from water via the skin, gut, or gills has no major direct impact on muscle tissue concentrations.

Keywords Bioaccumulation • Caging experiments • Captive-rearing experiments • Kokanee • Lake Chuzenji • Masu salmon • Radiocesium

S. Yamamoto (✉) • K. Mutou • H. Nakamura • K. Miyamoto • K. Uchida
National Research Institute of Aquaculture, Fisheries Research Agency,
2482-3, Chugushi, Nikko, Tochigi 321-1661, Japan
e-mail: ysho@affrc.go.jp

K. Takagi
Marine Biological Research Institute of Japan Co., LTD,
4-3-16, Yutaka, Shinagawa, Tokyo 142-0042, Japan
e-mail: takagik@affrc.go.jp

K. Fujimoto • H. Kaeriyama • T. Ono
National Research Institute of Fisheries Sciences, Fisheries Research Agency,
2-12-4, Fukuura, Kanazawa, Yokohama, Kanagawa 236-8648, Japan

K. Nakata, H. Sugisaki (eds.), *Impacts of the Fukushima Nuclear Accident on Fish and Fishing Grounds*, DOI 10.1007/978-4-431-55537-7_19

19.1 Introduction

In the preceding chapters, we documented individual radiocesium concentrations in fish from a variety of locations, including in muscle and eggs of several salmonid fishes from the Lake Chuzenji system in central Honshu Island (Chap. 18), in muscle and internal organs of a herbivorous fish, the ayu *Plecoglossus altivelis*, from several rivers in Fukushima Prefecture (Chap. 17), and in muscle of lake-dwelling freshwater fishes from Lake Hayama in Fukushima Prefecture (Chap. 16). There is also a sizeable dataset of radiocesium concentrations in freshwater fishes from northern and central Honshu Island, Japan, an area that was affected by the Fukushima Dai-ichi Nuclear Power Plant (FNPP) accident (Mizuno and Kubo 2013; Arai 2014; Murakami et al. 2014).

Several preceding studies have demonstrated that radionuclide accumulation in freshwater fish results mainly from food intake (Forseth et al. 1991; Ugedal et al. 1995). Experimental studies under controlled laboratory conditions, conversely, have shown that high radiocesium concentrations in water can be transferred into the organs of freshwater fish (Hewett and Jefferies 1976; Man and Kwok 2000). In the recently affected areas of Japan, however, the nature of the processes underlying radionuclide intake by freshwater fish has not yet been explored in detail, despite the economic and biological importance of understanding radionuclide contamination of aquatic biota.

As an urgent investigation into the effects of the FNPP accident on salmonids by the Fisheries Agency of Japan, a caging experiment in Lake Chuzenji (central Honshu Island), and two captive-rearing experiments were conducted using controlled concentrations of radiocesium in water and food to understand radiocesium bioconcentration and bioaccumulation in salmonids. At present (Oct. 2013), most salmonid fishes in Lake Chuzenji still have radiocesium concentrations greater than 100 Bq/kg-wet, which is the Japanese standard limit for radiocesium in foods.

19.2 A Caging Experiment in Lake Chuzenji

To establish the radiocesium uptake rate of hatchery-reared fish released into Lake Chuzenji, two cages about 180 m^3 (6×6×5 m in height) were placed about 50 m from the shore (Fig. 19.1). Each cage was covered on all sides in 4-mm plastic mesh. Five hundred juvenile kokanee (*Oncorhynchus nerka*) and masu salmon (*Oncorhynchus masou*), which were chosen from captive-bred fish in the Fisheries Research Agency (FRA), were selected randomly and released into the respective cages on 22 November 2012. Initial mean fork length and body weight (±SD) of kokanee and masu salmon were 150 ± 13 (mm) and 30.5 ± 8.4 (g), and 93 ± 13 (mm) and 7.2 ± 2.5 (g), respectively. During the experimental period, fish were not given any artificial food. Up until 10 April 2013, 20 fish from each cage were collected randomly at intervals of about 14 days. Sampled fish were frozen immediately, the

Fig. 19.1 Cages set in Lake Chuzenji

fork length and body weight of each fish recorded, and a sample of muscle tissue removed for measurement of radiocesium concentrations. During the experimental period, water temperature in the cages (1-m depth) had a range of 1.4 °C (27 February 2013) to 10.2 °C (29 March 2013).

The kokanee in cages showed little or no growth during the experimental period. Mean fork length and body weight (±SD) at the termination of the experiment (139 days after the start of the experiment) were 149 ± 8 (mm) and 30.0 ± 5.8 (g), respectively. There were no significant differences between initial and final fork lengths and body weights of kokanee (*t* tests; $P > 0.05$). Mean fork length and body weight (±SD) at the termination of the experiment (139 days after the start of the experiment) of masu salmon were 97 ± 11 (mm) and 9.0 ± 3.2 (g), respectively. Mean fork length and body weight of masu salmon at the termination of the experiment were significantly greater than those at the start of the experiment (*t* tests; $P < 0.05$). Substantial radiocesium concentrations ($^{134}Cs + {}^{137}Cs$) in both kokanee and masu salmon muscle tissue from the cages were detected at first sampling (14 days after the start of the experiment), with 2.2 Bq/kg-wet for kokanee and 3.9 Bq/kg-wet for masu salmon (Fig. 19.2). Thereafter, radiocesium levels increased approximately linearly with the duration of the experiment (kokanee: $R^2 = 0.97$, $P < 0.001$; masu salmon: $R^2 = 0.89$, $P < 0.001$). The final radiocesium concentrations in kokanee and masu salmon were 19.2 Bq/kg-wet (ratio of $^{134}Cs/^{137}Cs$, 0.55) and

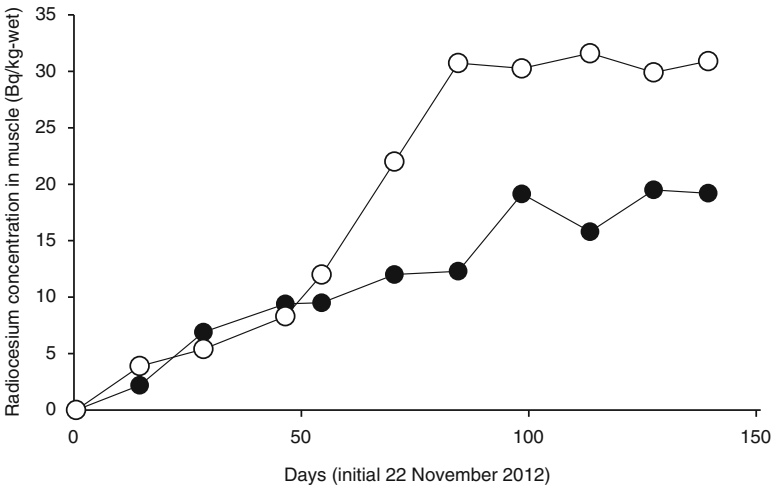

Fig. 19.2 Changes in radiocesium concentrations in kokanee (●) and masu salmon (○) in cages set up in Lake Chuzenji between 22 November 2012 and 10 April 2013

30.9 Bq/kg (^{134}Cs/^{137}Cs, 0.47), respectively. Daily radiocesium accumulation rates were estimated at 0.14 Bq/kg/day in kokanee and 0.22 Bq/kg/day in masu salmon, assuming linear relationships between radiocesium concentrations and experiment duration. During the experimental period, masu salmon had higher radiocesium concentrations than kokanee ($F = 11.3$, $d.f. = 1,21$, $P = 0.007$).

In Lake Chuzenji, mean muscle radiocesium concentrations of wild salmonid fishes [kokanee, masu salmon, brown trout (*Salmo trutta*), and lake trout (*Salvelinus namaycush*)] collected during September to December, 2012, were in the range of 142.9 to 249.2 Bq/kg-wet (Chap. 18). Substantial accumulation of radiocesium was also confirmed in muscle tissue of hatchery-reared salmonids after release into cages set in Lake Chuzenji, indicating that radionuclide contamination of fish was an ongoing process, 1.5 years after the FNPP accident. Both kokanee and masu salmon juveniles in the cages were assumed to have fed mainly on zooplankton entering through the mesh. Radiocesium concentrations in plankton sampled over the same period in Lake Chuzenji (12.6 Bq/kg-dry; Fisheries Research Agency 2015) were much lower than the levels recorded in kokanee and masu salmon muscle tissue within the cages. The result provides strong evidence of in situ radiocesium bioaccumulation from food to fish muscle tissue in a natural lake in Japan. After the Chernobyl nuclear accident, radiocesium concentrations in crustacean zooplankton in Finnish lakes were significantly correlated with those in the water (Rask et al. 2012). During the experimental period of our study, planktivorous kokanee and masu salmon juveniles, with a short food chain, would closely track the environmental contamination of water and zooplankton in Lake Chuzenji.

19.3 Captive-Rearing Experiments with Controlled Radiocesium Concentrations of Water and Feed

To understand the process of radiocesium uptake in freshwater fish, two experiments were conducted on fish in captivity using known concentrations of radiocesium in water and feed. Two fiberglass circular tanks of 0.5 m^3 (1,170 mm in diameter, 770 mm in depth) were set up in the FRA facility at Nikko. Throughout the experimental period, rearing water for this tank was drawn from Lake Chuzenji via an electronic pump. Before influx into the tank, the water was filtered through a 60-μm mesh to remove any particles, including plankton. The discharge rate of filtered water into the tanks was controlled at about 1.24×10^{-4} m^3/s. Into this tank, 200 juvenile kokanee, selected randomly from captive-bred fish in FRA, were released on 7 January 2013, and fed commercial food pellets of approximately 2 % body weight per day. Initial mean fork length and body weight (±SD) were 147 ± 10 (mm) and 27.9 ± 6.3 (g), respectively. Up until 10 April 2013, 20 fish from the tank were collected randomly at intervals of about 14 days. Collected fish were frozen immediately, the fork length and body weight of each fish recorded, and a sample of muscle tissue removed for measurement of radiocesium concentrations. During the experimental period, water temperature in the tank was in the range of 2.0 °C (26 February) to 12.5 °C (5 April). Dissolved radiocesium concentration of the surface water in Lake Chuzenji, collected on 28 November, 2012, was 43 mBq/l (Fisheries Research Agency 2015).

The other tank was filled with spring-fed water upwelling in the FRA facility (Fig. 19.3). Radiocesium concentrations of this water were below the limits of detection. The discharge rate of the spring-fed water into the tank was controlled at about 5.57×10^{-4} m^3/s. Two hundred juveniles of kokanee, selected randomly from captive-bred fish in FRA, were released into the tank on 7 January 2013. Initial mean fork length and body weight (±SD) were 157 ± 10 (mm) and 37.0 ± 7.1 (g), respectively. Fifteen smallmouth bass (*Micropterus salmoides*), collected in Lake Hayama in Fukushima Prefecture (linear distance from the FNPP, ~17 km) in June 2012, were used to prepare food pellets for the experimental fish. Radiocesium concentrations in the muscle of smallmouth bass individuals had a range of 4,213 to 7,188 Bq/kg-wet (mean ± SD, 5,777 ± 891 Bq/kg; median, 5,829 Bq/kg) (Chap. 16). The muscle tissue was carefully homogenized with commercial food pellets, the food pellets having been adjusted to contain an average radiocesium level of 445 Bq/kg-dry. Experimental fish were fed these commercial food pellets with radiocesium material of approximately 2 % body weight per day. Until 10 April 2013, 20 fish from the tank were sampled randomly at intervals of about 14 days. Collected fish were frozen immediately, the fork length and body weight of each fish recorded, and a sample of muscle tissue removed for measurement of radiocesium concentrations. During the experimental period, water temperature in the tank was in the range 8.8 °C (31 January) to 10.1 °C (5 April). All experimental fish used in this study were fed food pellets once or twice a day until used in the experiments but were not acclimated to the experimental tanks before the start of the experiments.

Fig. 19.3 An experimental facility in the Fisheries Research Agency for examining the process of radiocesium intake in salmonid fish

When fish were reared in water from Lake Chuzenji and a diet of commercial pellets, no radiocesium was detected in muscle tissue at any sampling period (detection limits, <1.74 Bq/kg) (Fig. 19.4). Final mean fork length and body weight (±SD) of kokanee in this experiment were 162 ± 12 (mm) and 49.5 ± 11.4 (g), respectively. When fish were reared using spring-fed water and pellets containing radiocesium, radiocesium concentrations in muscle tissue increased rapidly during the experiment. At 93 days after the start of the experiment, the radiocesium concentration increased to 126.2 Bq/kg-wet ($^{134}Cs/^{137}Cs$, 0.51). Final mean fork length (±SD) of kokanee in this experiment were 183 ± 68 (mm) and 67.8 ± 16.6 (g), respectively.

Two captive experiments with controlled water and feed radiocesium concentrations demonstrated that direct radiocesium transfer from water (43 mBq/l) in Lake Chuzenji to fish muscle tissue was undetected, at least during the approximately 90-day experimental period, whereas a rapid increase in radiocesium concentration was observed when fish were cultured using pellets contaminated with high concentrations of radiocesium. The results reinforce the evidence that radiocesium contamination of freshwater fish is mainly via the food chain, and that direct intake from the water via the skin, gut, or gills has little or no effect on muscle tissue levels. Previous experimental studies, however, showed that freshwater fish exposed to water with extremely high concentrations of radionuclides can accumulate the nuclides into their organs (Hewett and Jefferies 1976; Man and Kwok 2000). After the FNPP accident, Japanese governmental agencies initiated detailed sampling

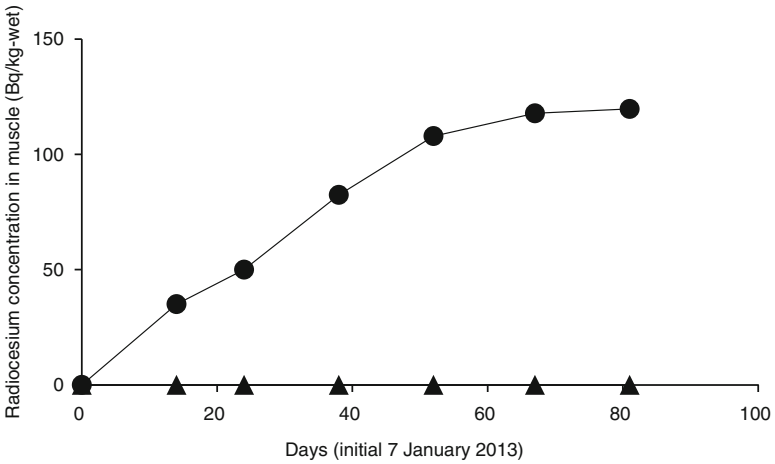

Fig. 19.4 Changes in radiocesium concentrations in kokanee in captivity between 7 January and 10 April 2013. *Circles and triangles* indicate the radiocesium concentrations in kokanee reared using spring-fed water with commercial pellets containing radiocesium material and in kokanee reared using water from Lake Chuzenji and fed with commercial pellets without any radionuclides, respectively

programs to establish the contamination levels of water in the affected area. Monitoring programs did not detect water with radiocesium concentrations greater than 1 Bq/l in any natural rivers or lakes during 2012–2013, with very few exceptions (Ministry of Environment 2015). Water itself, if it should contain radionuclides, is unlikely to have a significant direct impact on levels of radiocesium in fish muscle tissues, at least within current Japanese freshwater systems.

19.4 For Further Study

A meta-analysis of the relevant literature revealed that radiocesium concentrations in fish were a positive function of contamination concentrations in the water, particularly for nonpiscivorous fish species (Rowan and Rasmussen 1994). Although direct radiocesium transfer from water to fish muscle tissue seems to be negligible, water may act as a radiocesium source to planktivorous fish via the food chain (Elliott et al. 1992; Rask et al. 2012; Tuovinen et al. 2013). In many Japanese lakes and rivers, including the Lake Chuzenji system, the release of hatchery-reared fish enhances resources and supplements wild fish stocks, which are essential components of successful freshwater fisheries management programs (Kitada 2001; Yamamoto et al. 2011). Continued monitoring of radiocesium concentrations in water and zooplankton, as well as in fish, is crucial for estimating bioconcentration and bioaccumulation and, thus, for predicting contamination concentrations in released hatchery-reared fish within the affected area.

Acknowledgments This chapter was revised from a paper published by Yamamoto et al (2014). We thank Masato Murakami, Tomoko Okazaki, Yumiko Watanuki, and Maki Yoshida for their assistance with sample assays and data analyses, and the staff of FRA for collecting fish samples. We are grateful to Kaoru Nakata for a critical review of the manuscript, and Hiroyasu Hasegawa and Takami Morita for operational management of the study. This study was supported by the Fisheries Agency, Ministry of Agriculture, Forestry and Fisheries, Japan.

References

Arai T (2014) Radioactive cesium accumulation in freshwater fishes after the Fukushima nuclear accident. SpringerPlus 3:479

Elliott JM, Hilton J, Rigg E, Tullette PA, Swift DJ, Leonard DRP (1992) Sources of variation in post-Chernobyl radiocesium in fish from two Cumbrian lakes (north-west England). J Appl Ecol 29:108–119

Fisheries Research Agency (2015) The scientific reports of nuclear accident investigations by the Fisheries Research Agency. http://www.fra.affrc.go.jp/eq/Nuclear_accident_effects/index.html (in Japanese). Accessed Day Month 2014

Forseth T, Ugedal O, Jonsson B, Langeland A, Njåstad O (1991) Radiocaesium turnover in Arctic charr (*Salvelinus alpinus*) and brown trout (*Salmo trutta*) in a Norwegian lake. J Appl Ecol 28:1053–1067

Hewett CJ, Jefferies DF (1976) The accumulation of radioactive caesium from water by the brown trout (*Salmo trutta*) and its comparison with plaice and rays. J Fish Biol 9:479–489

Kitada S (2001) Fish stock enhancement assessment with Japan examples. Kyoritsu, Tokyo (in Japanese)

Man CK, Kwok YH (2000) Uptake of ^{137}Cs by freshwater fish. Appl Radiat Isot 52:237–241

Ministry of the Environment (2015) The radioactive material measures by the nuclear power plant accident. http://www.env.go.jp/jishin/rmp.html#monitoring (in Japanese) Accessed Day Month 2014

Mizuno T, Kubo H (2013) Overview of active cesium contamination of freshwater fish in Fukushima and eastern Japan. Sci Rep 3:1742

Murakami M, Ohte N, Suzuki T, Ishii N, Igarashi Y, Tanoi K (2014) Biological proliferation of cesium-137 through the detrital food chain in a forest ecosystem in Japan. Sci Rep 4:3599

Rask M, Saxén R, Ruuhijärvi J, Arvola L, Järvinen M, Koskelainen U, Outola I, Vuorinen PJ (2012) Short- and long-term patterns of ^{137}Cs in fish and other aquatic organisms of small forest lakes in southern Finland since the Chernobyl accident. J Environ Radioact 103:41–47

Rowan DJ, Rasmussen JB (1994) Bioaccumulation of radiocesium by fish: the influence of physicochemical factors and trophic structure. Can J Fish Aquat Sci 51:2388–2410

Tuovinen TS, Saengkul C, Ylipieti J, Solatie D, Juutilainen J (2013) Transfer of ^{137}Cs from water to fish is not linear in two northern lakes. Hydrobiologia 700:131–139

Ugedal O, Forseth T, Jonsson B, Njåstad O (1995) Sources of variation in radiocaesium levels between individual fish from a Chernobyl contaminated Norwegian lake. J Appl Ecol 32:352–361

Yamamoto S, Kitamura S, Sakano H, Morita K (2011) Genetic structure and diversity of Japanese kokanee *Oncorhynchus nerka* stocks as revealed by microsatellite and mitochondrial DNA markers. J Fish Biol 79:1340–1349

Yamamoto S, Mutou K, Nakamura H, Miyamoto K, Uchida K, Takagi K, Fujimoto K, Kaeriyama H, Ono T (2014) Assessment of radiocaesium accumulation by hatchery-reared salmonids after the Fukushima nuclear accident. Can J Fish Aquat Sci 71(12):1772–1775